
UNIVERSITY OF LIVERPOOL

# Development and Characterisation of Antiretroviral Drugs Encapsulated in Polymer Stabilised Oil-in-Water Nanoemulsions

Thesis submitted in accordance with requirements of the University of Liverpool for the degree of Doctor of Philosophy

James Joseph Hobson

2014

This thesis is the results of my own work. The material contained within the thesis has not been presented, either wholly or in part, for any other degree or qualification.

James Joseph Hobson

**This research was carried out in the Liverpool HIV Pharmacology Group**

**Department of Molecular and Clinical Pharmacology**

**University of Liverpool**

**UK**

**And**

**The Rannard Research Group**

**Department of Chemistry**

**University of Liverpool**

**UK**

# TABLE OF CONTENTS

**Acknowledgements**

Firstly, I would like to thank Steve and Andrew for giving me the opportunity to carry out a Ph.D. under their expert guidance and mentorship. I have matured so much since that day I walked into Andrew's office wearing an ill fitting suit and a nervous smile, trying my best to seem like a scientist: I'm glad you both saw something in me and wanted to keep me around. I will forever be in your debt.

Secondly, I'd like to thank Neill, not only have you been a most excellent post doc in terms of everything you have taught me and helped me to achieve during my Ph.D., but you have been an awesome friend too. It's been nice having someone who has been there before and knows the stresses and strains that are involved, and someone with such an expert knowledge to help me and guide my project for the better.

And wherever there is a Neill, there is always a Paul close by. Thank you for the philosophical morning chats, the musing out of the window whilst taking in the beautiful views of London road. The three of us combined have a unique (poey) sense of humour, but its something I've enjoyed so much and definitely the one thing that can really keep you going when you're having a bad day.

Mossy and Marco, the 8-bit games nights complete with microwave pasta or dodgy pizza were always fun, but I suppose more importantly thanks for helping me along the way. Its been great being friends with you and see you both progress through Ph.D. to post doc (and lecturer), I hope to follow in your footsteps.

And to Phil, thanks for helping me battle through nerves and getting me to safely and confidently work with HIV in the lab. And to everyone else in Pharmacology, Prof Back, Justin, JT, Dee, Lee, Chris, Rajith, Christina, Nyi, Beth, Megan, Henry, Alessandro, Laura and Sara. Thanks for sharing a lab and office with me and making it fun

To everyone in Chemistry, Sam, Fiona, Andy, Faye, Helen, Maude, thanks for teaching a non-chemist how to do (some) chemistry. Especially to Jane, Tom, Marco, Pierre, Becky and Hannah for showing me how to make polymers and use all those terribly expensive pieces of equipment that we are lucky to have in our labs.

Away from the lab I have to thank my family for all of their support and encouragement throughout my life. Especially Mum, Joe and Nan. You have not only supported me emotionally, mentally and financially for such a long time, but have given me the best upbringing I could ask for. Their tireless support has kept me wanting to always achieve more and work to the very best that I can. And to my Dad, even from a distance you have provided me with encouragement and made me feel like I'm doing something special, and enabled me to keep the heating turned on over winter! I love you all. And Gibbsy, you are my oldest and most loyal friend. Your unconventional scientific theories and unwavering stubbornness have provided some interesting moments over the years, as have all the memories stretch way back to school! I wouldn't change you for the world.

To Louise, my wonderful girlfriend, you have kept me going when things have gotten tough and made me such a happy and confident person. You have put up with me when I've been working late and helped me push through the not so insignificant task of writing a Ph.D. thesis. You are the best thing I could have ever asked for, and I just hope I can be the same for you through your career.

And finally: my granddad. You were my biggest hype man, you always had my back and you always pushed me to do the right thing in life. You were such a role model to me and were quite simply the best man I have ever known. I'm so sorry you never got to see me finish this; I just hope I made you proud. This is for you.

**ABBREVIATIONS**

| | |
|---|---|
| µCi | Microcurie(s) |
| µg | Microgram(s) |
| µl | Microlitre(s) |
| µM | Micromolar |
| µmol | Micromole(s) |
| ºC | Degrees centigrade |
| aa | Amino acids |
| AIDS | Acquired Immunodeficiency syndrome |
| ART | Antiretroviral therapy |
| ATCC | American Tissue Culture Collection |
| ATP | Adenosine Triphosphate |
| AUC | Area under the curve |
| BSA | Bovine Serum Albumin |
| CAR | Cellular Accumulation Ratio |
| cDNA | Complementary DNA |
| CD | Cluster of Differentiation |
| Ci | Curie(s) |
| CNS | Central nervous system |
| $CO_2$ | Carbon dioxide |
| CYP | Cytochrome P450 |
| CYP2B6 | Cytochrome P450 2B6 |
| CYP3A4 | Cytochrome P450 3A4 |

| | |
|---|---|
| Đ | Dispersity |
| DLS | Dynamic Light Scattering |
| DMEM | Dulbecco's Modified Eagles Medium |
| DMSO | Dimethyl sulphoxide |
| EFV | Efavirenz |
| EGDMA | Ethylene glycol dimethacrylate |
| FBS | Fetal Bovine serum |
| g | gram(s) |
| GPC | Gel Permeation Chromatography |
| gp41 | Glycoprotein 41 |
| gp120 | Glycoprotein 120 |
| gp160 | Glycoprotein 160 |
| $^{1}$H NMR | Proton Nuclear Magnetic Resonance |
| HAART | Highly active antiretroviral therapy |
| HBSS | Hanks Balanced Salt Solution |
| HIV | Human Immunodeficiency virus |
| HRP | Horse Radish Peroxidase |
| $IC_{50}$ | Concentration required to produce 50 % inhibition |
| IFNγ | Interferon gamma |
| Ig | Immunoglobulin |
| IL | Interleukin |
| kDa | Kilodalton |
| L | Litre |

| | |
|---|---|
| M | Molar |
| MACS | Magnetic Cell Sorting |
| MDR | Multidrug resistance |
| mg | Milligram(s) |
| $MgCl_2$ | Magnesium chloride |
| MHC | Major Histocompatibility Complex |
| min | Minute(s) |
| MTT | 3-(4,5-Dimethylthiazol-2-yl)-2,5-diphenyltetrazolium bromide |
| ml | Millilitre |
| mM | Millimolar |
| mmol | Millimole(s) |
| $M_n$ | Number average molecular weight |
| mRNA | Messenger RNA |
| MRP | Multidrug resistance-associated protein |
| Mw | Molecular Weight |
| $M_w$ | Weight average molecular weight |
| NaOH | Sodium hydroxide |
| ng | Nanogram(s) |
| nm | Nanometre(s) |
| nM | Nanomolar |
| nmol | Nanomole(s) |
| NNRTI | Non-nucleoside reverse transcriptase inhibitor |

| | |
|---|---|
| NK | Natural Killer |
| NRTI | Nucleoside reverse transcriptase inhibitor |
| NVP | Nevirapine |
| OEGMA | Oligo (ethyleneglycol) methyl ether methacrylate |
| PBMC | Peripheral blood mononuclear cell |
| PBS | Phosphate buffered saline |
| PCR | Polymerase chain reaction |
| PDI | Poly Dispersity Index |
| PE | Phycoerythrin |
| PEG | Polyethylene glycol |
| pg | Picogram(s) |
| PHA | Phytohaemagglutinin |
| PI | Protease inhibitor |
| PIC | Preintegration complex |
| PK | Pharmacokinetic |
| RI | Refractive Index |
| RNA | Ribonucleic acid |
| RT | Reverse transcriptase |
| RTV | Ritonavir |
| s | second(s) |
| SD | Standard deviation |
| SNP | Single nucleotide polymorphism |
| SQV | Saquinavir |

| | |
|---|---|
| TCR | T-cell receptor |
| $T_h$ | T-helper |
| THF | Tetrahydrofuran |
| TNFα | Tumour necrosis factor alpha |
| TLR | Toll like receptor |
| UV | Ultraviolet |
| VBL | Vinblastine |
| *vs.* | Versus |

**Communications**

**Immunological Safety Assessment and Antiviral Activity of Novel Polymer Stabilised Oil-in-Water Nanoemulsions of Efavirenz and Lopinavir**

J. Hobson, N. Liptrott, P. Martin, J. Ford, R. Slater, S. Rannard and A. Owen. Clinical Nanomedicine and Targeted Medicine. The European CLINAM & EPTN Summit, Basel, Switzerland**.** June 2013

**Prediction of Etravirine Pharmacogenetics Using a Physiologically Based Pharmacokinetic Based Approach**

M. Siccardi, A. Olagunju, P. Curley, J. Hobson, S. Khoo, D. Back, and A. Owen. 20th Conference on Retroviruses and Opportunistic Infections, Atlanta, Georgia, USA. March 2013

**Development and Cytotoxic Assessment of Novel "Pickering Like" Stabilisers For Emulsion Based Delivery of Antiretroviral Drugs**

**J. Hobson,** R. Slater, S. Rannard and A. Owen. In Vitro Toxicology Society (IVTS) Winter Meeting, Liverpool, UK. December 2011

**Oil-in-Water Nanoemulsions Stabilised By Branched Pickering Stabilisers: Potential For a Novel Drug Delivery System**

J. Hobson, R. Slater, S. Rannard and A. Owen. PRISM 2011- Postgraduate Researchers in Science and Medicine Meeting, Liverpool, UK. July 2011

**Abstract**

HIV continues to be a global healthcare challenge, with estimates suggesting there are currently 35.5 million infected people globally. To date, there have been an estimated 36 million HIV/AIDS related deaths worldwide. The story is changing however, with the advent of Highly Active Antiretroviral Therapies (HAART), allowing patients to live to normal life expectancies and with increasingly better quality of life. This, coupled with the fact that there has been a 40-fold increase in the number of people with access to antiretroviral therapy, has led to a 29% reduction in AIDS related deaths since 2005.

Despite this encouraging data, there are still numerous limitations of antiviral therapy, including poor bioavailability, poor patient adherence, and emerging resistance. It is hoped that nanomedicine may offer a route to alleviating some of these issues by achieving an equal therapeutic concentration of drug but with a lower dose. The aims of this thesis were to develop a novel nanoemulsion based formulation of EFV and LPV and to assess the suitability of this formulation as dosage form.

Nanoemulsions can be stabilised by surfactants, but often this can have unwanted safety profiles. Stabilisation can also be achieved using amphiphillic polymers that can be synthesised using biocompatible monomers like ethylene glycol. Chapter 2 demonstrates the synthesis of Ethylene Glycol based polymers using both conventional free radical and Atom Transfer Radical Polymerisation techniques. Nanoemulsions have previously been shown in the literature to increase the bioavailability of poorly water-soluble drugs, Chapter 3 shows the development and optimisation of an Oil-in-Water nanoemulsions. The data showed that nanoemulsions synthesised with volatile cosolvents were able to achieve sub 300 nm diameters and have good long-term stability.

Increasing the accumulation and permeation of a poorly water-soluble compound should lead to improvements in bioavailability. Chapter 4 shows that the optimal nanoemulsion had comparable accumulation to aqueous solutions and superior apparent permeability cross Caco-2 cell monolayers. The antiviral activity was equipotent to the aqueous solution, as shown in Chapter 5. This confirms that nanoemulsion did not prevent the API from reaching its sight of action. Finally, all new formulations have the potential for detrimental side effects and immunological responses. It is therefore necessary to conduct pre clinical studies to predict such occurrences. Chapter 6 details the lack of immunological response seen in nanoemulsions, but highlights potential interactions with coagulation.

In conclusion, this study has found that polymer stabilised oil-in-water nanoemulsions based on Castor oil have promising safety and pharmacological profiles. Further *in vivo* and studies are now warranted in order to further predict the suitability of nanoemulsions in man.

# CHAPTER 1

# General Introduction

**Table of Contents**

## 1.1 Scale of the HIV Epidemic

The latest figures form UNAIDS shows that worldwide, there are currently around 35 million (31.4- 35.9 million) people living with Human immunodeficiency Virus (HIV). In 2011 alone, there were 2.5 million (2.2-2.8 million) new HIV infections, and 1.7 million (1.5- 1.9 million) Acquired Immunodeficiency Syndrome (AIDS) related deaths. There has been progress made however, with 25 countries worldwide reporting a decrease in new HIV infections of at least 50%, although this progress is not uniform, and in some places there have been increases in the infection rates [1]. Latest data available on the level of access to antiretroviral therapies (ARVs) shows that in 2012 a total of 9.7 million HIV infected patients had access to ARVs, up by 1.6 million on the previous year. This increase represented the biggest year on year increase ever recorded, and also showed that the number of HIV infected patients in African nations with access to ARVs has risen from 50,000 to 7.5 million over a ten year period [2].

These figures show the vast scale of the epidemic, and importance of research into developing new, and improving existing treatments against the virus all with the key goal of enabling greater access to ARV therapies.

## 1.2 The HIV Virus: Classification and Origins

According to the International Committee on Taxonomy of Viruses, the HIV virus is a Lentivirus, of the Retroviridae family [3]. A schematic of the viral structure is shown in figure 1. There are two major types of HIV virus, HIV-1, which is related to gorillas and chimpanzees found in West Africa [4], and HIV-2, which is related to the Sooty Mangabey, also found is West Africa [5]. The HIV virus is the result of a zoonotic transfer of viruses that infected these primates [6]. Of the two types of HIV virus, HIV-1 is by far the most common, and is found in patients infected all across the globe. HIV-2 on the other hand, is largely restricted to West Africa, with particularly high prevalence in both Senegal and Guinea-Bisssu [7]. However, the overall prevalence rates of HIV-2 infection are decreasing, and there is an increase in HIV-1 infections in West Africa, which may be explained by the lower viral loads and transmission rates that are seen in HIV-2 infected individuals, and the fact that most people infected with HIV-2 virus, do not actually progress to AIDS [8-10]. Thus, the work reported here is focused upon the development of treatments effective against HIV-1.

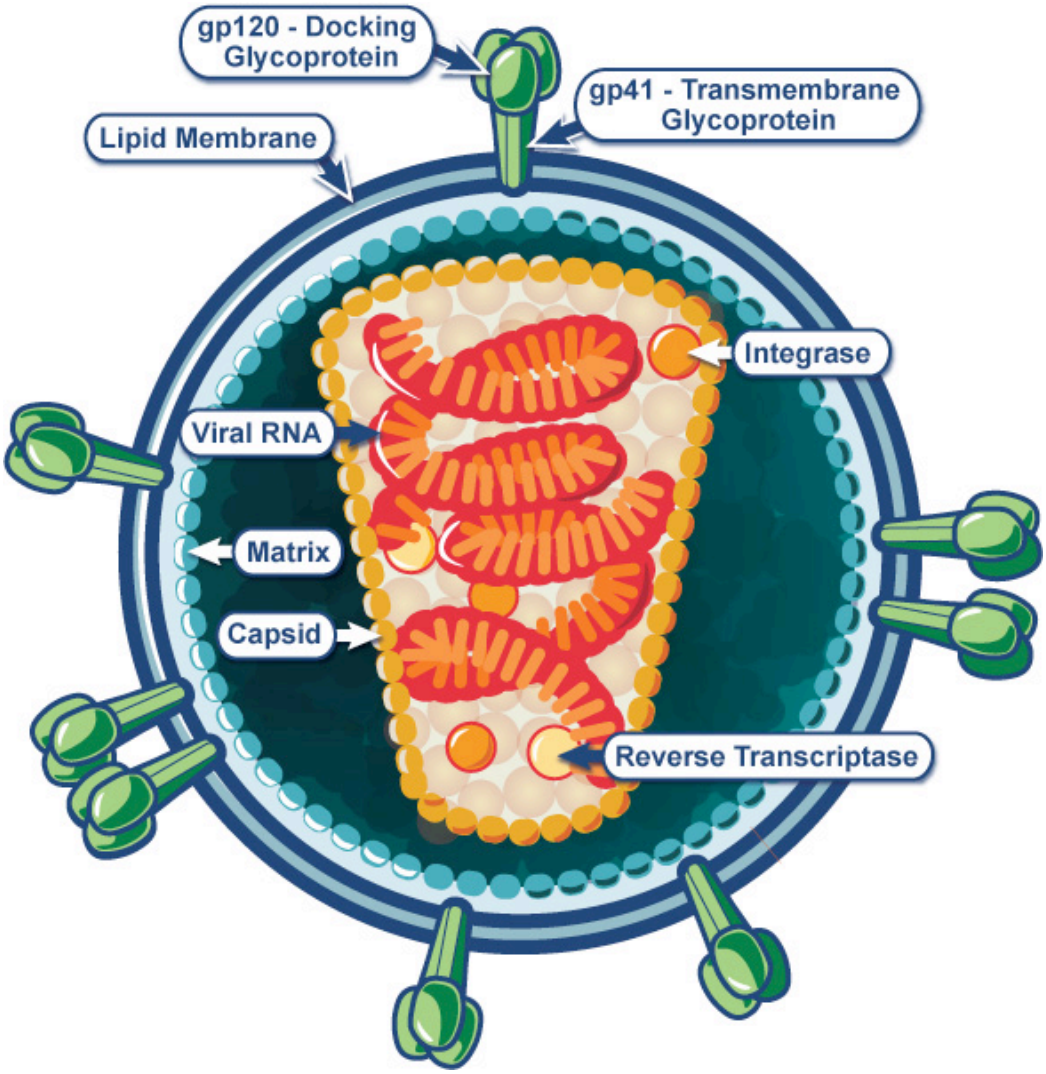


Figure 1.1 Schematic of HIV, showing the essential membrane proteins and viral enzymes needed for replication. Taken from National Institute for Allergy and Infectious Disease

### 1.3 HIV Pathogenesis

HIV is transmitted via contact with infected blood [11], unprotected sex with an infected patient (both heterosexual and homosexual) [12, 13], or by injecting using a needle that has been contaminated by previous use by a infected individual [14]. There is also the possibility of mother to child transfer during childbirth [15] or breast-feeding [16]. The virus initially infects dendritic cells that are found in the mucosal membranes of tissues that line areas of the body such the rectum, penis, vagina, mouth and the gastrointestinal tract. Infected dendritic cells then carry the virus into the lymphatic system, where is it able to infect CD4+ T cells [17].

Infection of these cells causes a dramatic decrease in CD4+ cell count, which along with macrophage and dendritic cells are vital for the working of the human immune system [18]. Loss of these cells due to infection by HIV occurs in a number of ways. The cells can be directly killed by the infection, as the virus hijacks the host genome, using it to generate copies of viral particles and inducing cell cycle arrest [19]. This generation of new particles involves budding out of the host cell, a process that damages and removes parts of the host cell membrane [20, 21], damaging the host cell. The distortion of the cells normal metabolism and genetic machinery, caused by viral replication within the cell, causes apoptosis to occur [22, 23]. Uninfected CD4+ cells can also be killed by the host immune response [24] and this can happen for a number of reasons. When the virus is attached to the healthy cell membrane, it appears to the immune system as if infected. Antibodies bind to the virus, and these

antibodies are then recognised by CD8+ cytotoxic T cells, which kill the cell. This process is known as antibody-dependant cellular cytotoxicity [25].

It is possible for healthy cells to consume HIV fragments [26-28], and these fragments can be expressed on the surface of the healthy host cell. CD8+ T cells can again recognise these fragments as if the cell is infected and set about destroying it [29]. There are also similarities between some of the proteins that are present in the viral envelope and expressed on CD4+ cells. These similarities can sometimes cause the immune system to identify the proteins and damage the cell, ultimately leading to the death of the cell [30, 31].

HIV can infect and reside in cells that are beyond the reach of drugs that enter the systemic circulation. These so-called sanctuary sites include the lymph nodes, brain, testes [32]. HIV can also reside within reservoirs, such as CD4+ cells [33], macrophages and monocytes [34]. The ability of the virus to penetrate and reside inside of these sanctuaries and reservoirs adds to the challenge of trying to treat it, because if the virus is not cleared from these sites, it will constantly reseed the circulation with new viral particles [35, 36]. Sanctuary sites differ to reservoirs in that current drug therapies are unable to penetrate inside, but in the case of reservoirs they can. Thus the strategy of current antiretroviral therapies is to hold back the virus by keeping the number of viral particles in the blood to a minimum. More effective treatments would be able to penetrate these sanctuary sites and clear the virus from within them.

### 1.3.1 HIV Life Cycle

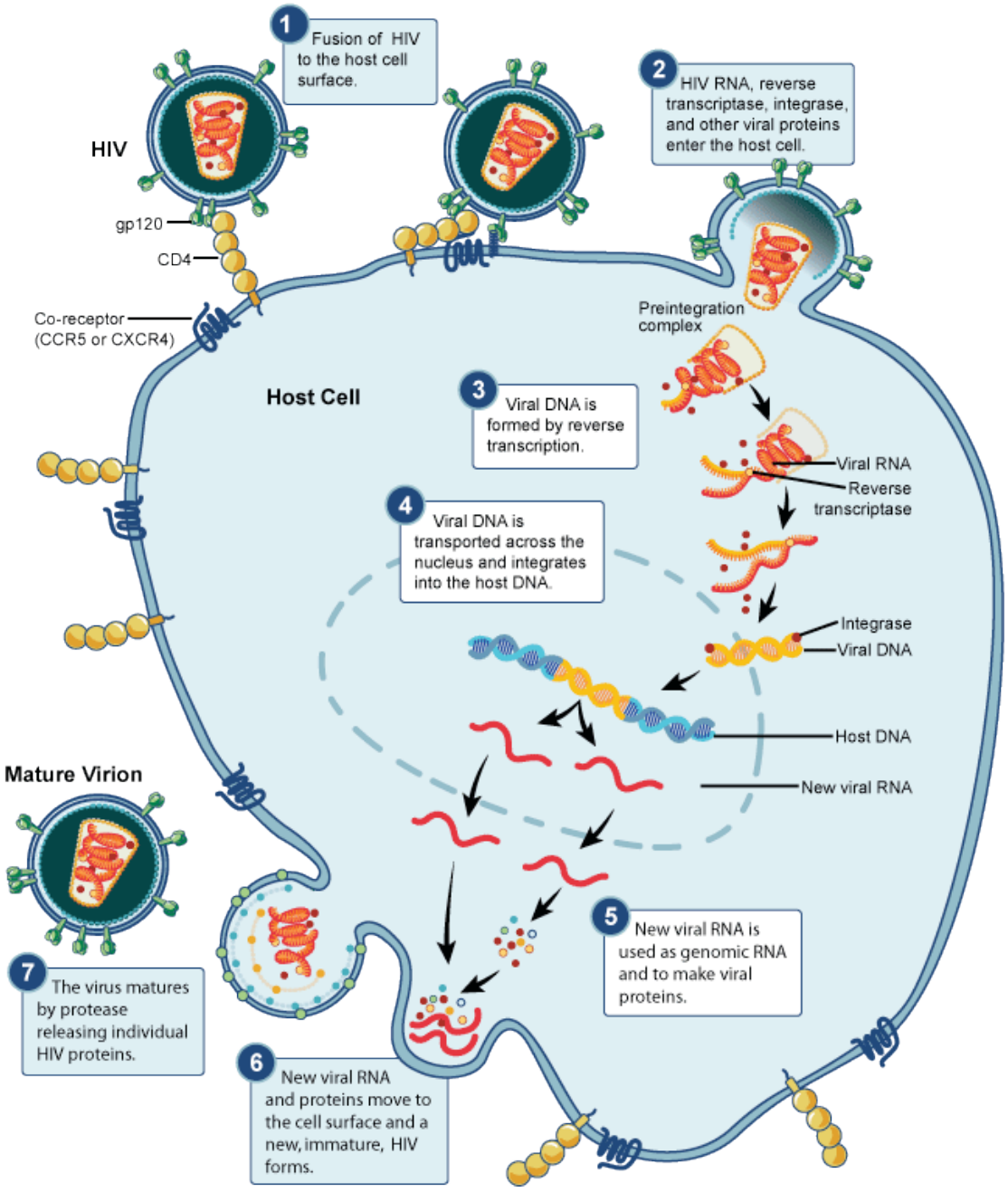


Figure 1.2. HIV life cycle (Picture taken from the National Institute for Allergens and Infectious Disease)

The HIV life cycle can be broken down into 8 distinct stages, Binding and Fusion, insertion of the HIV enzymes into the host cell, Reverse transcription, Integration, Transcription, Assembly, and finally budding / protein maturation. A schematic of this process is shown in figure 2. During the Binding and fusion stage, the HIV binds to CD4 receptors expressed on the surface of CD4+ T cells via two vitally important surface glycoproteins called gp41 and gp120 [37]. However, these receptors alone are not enough for successful binding to take place, as the virus needs to associate with a co-receptor also expressed on the surface of the CD4, namely CCR5 or CXCR4. Thus, different strains of HIV will be referred to as being CCR5 tropic, or CXCR4 tropic, depending upon which of the co-receptors they are able to utilise [38], and there are instances of dual tropic viruses, utilising both co-receptors [39]. The tropism of the virus is of importance as it can influence where in the body and how the virus is able to replicate [40], and also the suitability of therapies that target specific tropisms eg: maraviroc [41]. There are also reports of HIV being able to convert which co-receptor it uses to facilitate entry into CD4+ cells [42], however the majority of new infections use CCR5, with CXCR4 usage emerging later in infection.

Once bound to the surface of the host cell, the viral particle is able to fuse to the membrane and create a pore, into which it then injects its cargo of enzymes and single stranded RNA [43-45]. Inside the host cell, the viral reverse transcriptase enzyme sets about converting the single stranded viral RNA into double stranded viral DNA, in such a way that proof reading does not occur, leading to very high

mutation rates [46-48]. This is essential for the genetic material of the virus to be compatible with the host cell, and thus be able to integrate with the host genome.

During the integration phase of the life cycle, viral DNA that has infiltrated the nucleus of the CD4 cell is inserted into the host genome using the viral integrase enzyme [49]. Once part of the host genome, the genetic material of the virus is able to "hijack" the host cell, and use the cells own enzymes to create more of the viral genetic material [50]. At this stage, the viral DNA that has become part of the host genome is known as a provirus. Activation of the provirus may not happen immediately, and infected cells may lay dormant for many years in infected patients leading to lifelong persistence of HIV [51].

When activation occurs, mediated by the HIV TAT protein [52-54], the virus hijacks the host cell RNA Polymerase [55] and uses it to transcribe the integrated DNA viral genome into viral mRNA. The viral mRNA is then used to create long viral proteins, which are later cleaved during the assembly stage by viral protease enzymes. This cleavage step is vital for the viral material to come together with the viral RNA copies and form mature viral particles, capable of further infection [56].

The final step is for the viral particles to leave the host cell and enter the systemic circulation, this is known as budding [57]. The new viral material associates with the membrane of the host cell, and then leaves by "budding" out of the cell, taking with it part of the host cell membrane, which is used as a container for the newly

synthesised viral material [57]. The host membrane now also contains the glycoproteins that are essential for the virus to bind to new CD4 receptors and co-receptors [57].

### 1.3.2 Disease Progression

There are defined clinical stages of the HIV infection, starting with the initial acute primary infective stage. This is the stage immediately after infection with the virus, where CD4+ cells are rapidly infected. At this stage, the patient will have a very high viral load [58, 59], leading to the virus seeding itself in many organs throughout the body. At this stage the virus can also latently infect CD4+ cells, where the virus will reside only to be activated and replicate at a later time [60]. This is the stage in which the previously mentioned anatomical sanctuary sites are infected with the virus [33, 61]. It is also the stage of infection in which the virus is able to undergo the initial stages of the HIV life cycle, integrating itself into the host genome, preferentially within areas that contain active genes [50], and may lay dormant for a long period of time [51].

During the next stage of infection, which can occur anywhere between two and four weeks post initial infection, the host immune system is able to respond to the infection by utilising antibodies against the virus [62, 63], which are made in B cells. These antibodies associate with the viral particles, making them targets for cytotoxic CD8+ T cells [64-66]. During this period, the levels of virus in the circulation massively decrease and in some cases levels of CD4+ T cells can return to levels

seen before infection. Due to the immune system returning to this normal state, an infected patient would now enter the phase known as HIV latency [67-69], in which no symptoms occur that are related to HIV infection. The most common signs of infection at this stage are symptoms that closely match those of flu, such as fever, aches and fatigue [70]. This stage can last for several years. However, during this stage, the virus continues to replicate in the immune tissues of the lymph nodes, where it initially infiltrated [71].

After the latent phase, the virus activates and begins to continually seed the blood with viral particles infecting more and more CD4+ T cells [72]. This overwhelms the immune system, and it is no longer able to supress the virus. Infected CD4+ cells are destroyed [73], and this compromises the immune system [73], with patients having very low CD4 counts. Such low levels of CD4 cells mean that the immune system is no longer able to protect against other pathogens, and the patient becomes susceptible to opportunistic infections, such as Tuberculosis [74], Influenza [75], and pneumonia [76]. A patient is classed as having progressed to AIDS when they have one or more of these opportunistic infections (AIDS-defining events), and the levels of CD4+ cells in the blood has dropped to levels of less than 200 per cubic millilitre [77].

### 1.4 Antiviral Therapies

The advent of antiretroviral (ARV) therapies, and in particular Highly Active Antiretroviral Therapy (HAART) has led to patients being able to live to much greater life expectancies [78], provided they adhere strictly to the treatment regimen [79]. The quality of life is still not that of a non-infected individual, with multiple doses of pills to be taken each and every day, with undesirable side effects that can impact on patient adherence to HAART regimens [80]. At the time of writing there were 29 different antiretroviral drugs approved by the Federal Drug Administration (FDA), falling into five distinctive types: Nucleoside Reverse Transcriptase Inhibitors (NRTIs), Non-Nucleoside Reverse Transcriptase Inhibitors (NNRTIs), Protease Inhibitors (PIs), entry inhibitors (both fusion and co-receptor antagonists), and Integrase Inhibitors (Table 1).

There are also multiple class combinations of these drugs that are approved by the FDA, these combinations are used in HAART formulations. Fixed dose combinations (FDCs) are also available that consist of two or more types of antiretroviral drugs formulated into the same tablet. This has the effect of reducing pill burden placed upon the patient, but affords less flexibility for personalising therapy to the needs of the patient.

Table 1.1 List of approved drugs for the treatment of HIV infeaction. (Adapted from Federal Drug Adminstraton, http://www.fda.gov/ForConsumers/byAudience/ForPatientAdvocates/HIVandAIDSActivities/ucm118915.htm)

| Class | Drug |
|---|---|
| Nucleoside Reverse Transcriptase Inhibitors | Lamivudine |
| | Zidovudine |
| | Emtricitabine |
| | Abacavir |
| | Zalcitabine |
| | Dideoxycytidine |
| | Azidothymidine |
| | Tenofovir |
| | Didanosine |
| | Stavudine |
| | |
| Non Nucleoside Reverse Transcriptase Inhibitors | Rilpivarine |
| | Etravirine |
| | Delavirdine |
| | Efavirenz |
| | Nevirapine |
| | |
| Protease Inhibitors | Amprenavir |
| | Tipranavir |
| | Saqunavir |
| | Indinavir |
| | Lopinavir |
| | Ritonavir |
| | Fosamprenavir |
| | Darunavir |
| | Atazanavir |
| | Nelfinavir |
| | |
| Fusion Inhibitors | Enfuvirtide |
| | |
| Co-receptor Antagonist | Maraviroc |
| | |
| Integrase Inhibitors | Raltegravir |
| | Dolutegravir |

### 1.4.1 NRTIs

NRTI drugs work by inhibiting the activity of the viral reverse transcriptase enzyme, which is responsible for obtaining copies of the viral single-stranded RNA into double-stranded viral DNA, which is then compatible with the host genome. The inhibition is caused by the NRTIs binding directly to the active site of viral reverse transcriptase in a competitive inhibition, thus rendering it inactive [81]. Figure 1.3 shows the chemical structure of tenofovir, a front line NRTI drug.

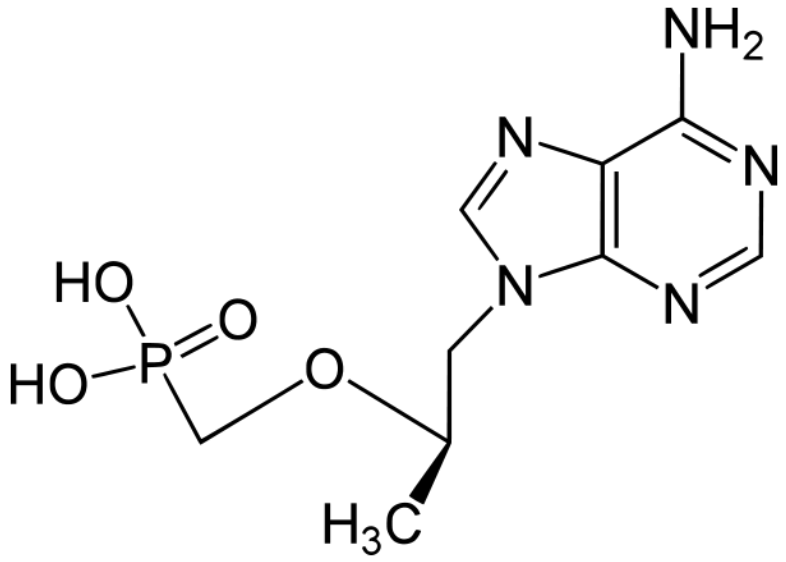


Figure 1.3 The chemical structure of the NRTI drug tenofovir.

### 1.4.2 NNRTIs

NNRTIs work in the same way as NRTIs in that they inhibit the viral reverse transcription enzyme responsible for transcribing viral ribonucleic acid (RNA) into Deoxyribonucleic acid (DNA). Unlike NRTIs though, these drugs act upon a specific site away from the active site of the enzyme, known as the NNRTI pocket [82]. When the drug binds to this site, the enzyme is no longer able to effectively reverse transcribe the viral RNA due to this non-competitive antagonistic action, and so replication is prevented [83]. Examples of NNRTIs include efavirenz, nevirapine and rilpivirine, with rilpivirine being the first HIV drug to be reformulated as a nanoformulation for a long acting parental depot [84]. The chemical structure of efavirenz, one of the two antiretroviral drugs used in the experimental sections of this thesis, is shown in figure 1.4.

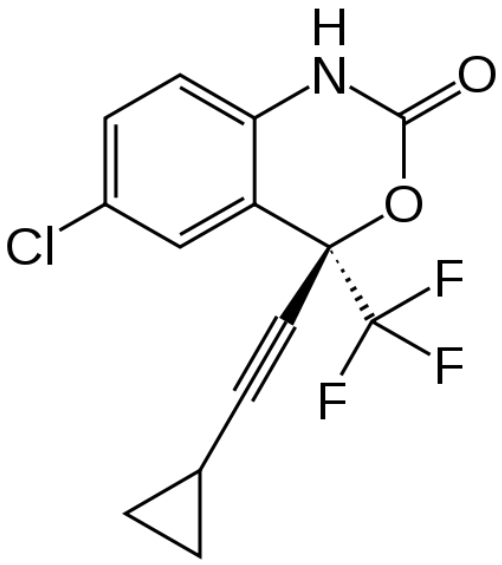


Figure 1.4 The chemical structure of NNRTI drug efavirenz.

### 1.4.3 Integrase Inhibitors

Integrase inhibitors are the most recent class of drug to be approved by the FDA, and prevent the virus from inserting its viral genome into the DNA of the infected host cell [85]. This inhibition is achieved by targeting the viral integrase enzyme, and is effective at preventing the spread of HIV infection to other cells. The first drug of this class to be approved for therapy was raltegravir, developed by Merck and released in 2007 [86]. The second drug in this class, dolutegravir, was approved very recently in August 2013, and has been shown to be effective even in patients who have acquired resistance to raltegravir [87]. A further drug in this class is currently in late stage development and will be a parental long acting nanoformulation, designated GSK744, the drug has shown protection against SIV/HIV in recent primate testing [88]. The chemical structure of raltegravir, a current front line integrase inhibitor is shown in figure 1.5

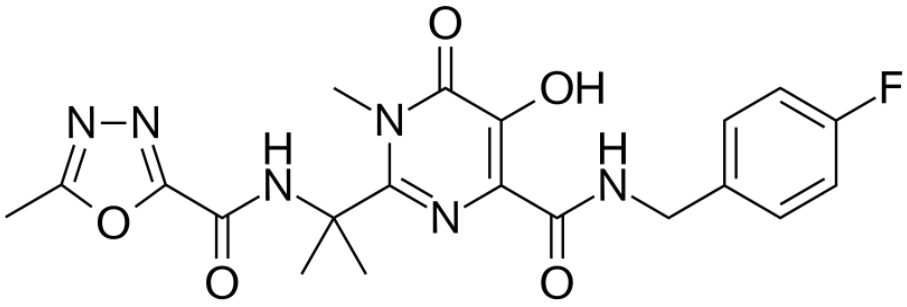


Figure 1.5 The chemical structure of the integrase inhibitor raltegravir

### 1.4.4 Entry Inhibitors

Entry inhibitors such as maraviroc [89] and enfuvirtide [90], have extracellular targets, whereas all other classes of drugs have intracellular targets. As their name suggests, Fusion and Entry inhibitors work by preventing the viral particles from entering healthy cells, and they do this in two distinct ways. Maraviroc, an entry inhibitor, works by binding specifically to the cell surface receptor CCR5 [89]. As previously mentioned this receptor is needed by the virus in order to gain entry into the cell. The viral gp120 associates with the CCR5 receptor, allowing the virus to then fuse with the membrane of the healthy cell and enter. Maraviroc occupies this co-receptor, and thus prevents gp120 from associating with it [89]. However, HIV can utilise other receptors on the cell surface, such as CXCR4, and so maraviroc is only effective against HIV that is CCR5 tropic [91] and thus it is important to determine co-receptor usage prior to initiating therapy. The chemical structure of maraviroc is shown in figure 1.6.

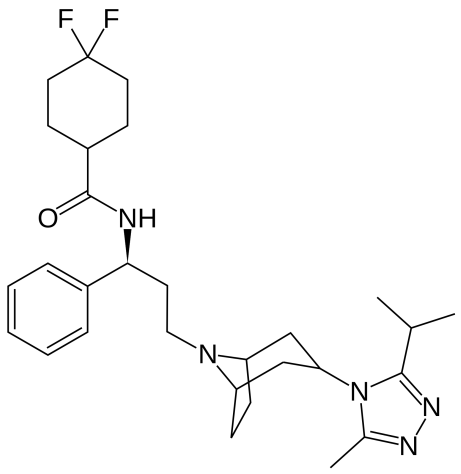


Figure 1.6 The chemical structure of entry inhibitor maraviroc.

Enfuvirtide, also known as T-20 or Fuzeon, prevents the viral particle from fusing with the cell membrane after it has associated with a cell surface receptor. It does this by binding directly to gp41 on the virus [90]. Gp41 undergoes a conformational change during fusion to the cell membrane [92], with enfuvirtide bound to the gp41, this conformational change cannot happen, and so the viral particle is unable to properly fuse with the membrane and create a pore into which it can pass its contents into the healthy cell [93]. Currently there are new generation fusion inhibitors being developed for HIV therapy, but as yet none are approved for use, with major limitations being in their need for daily injections to administer the dose [94]. The chemical structure of enfuvirtide is shown in figure 1.7.

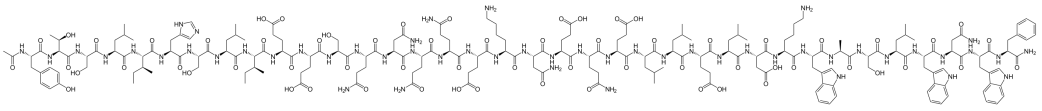

Figure 1.7 The chemical structure of enfuvirtide, a poly peptide consisting of 37 peptide units.

### 1.4.5 Protease Inhibitors

Protease inhibitors (PIs) work by directly inhibiting the viral enzyme that is responsible for the proteolytic cleavage of new viral proteins, this enzyme is essential for the replication of the virus, as it breaks up protein molecules into smaller fragments to be used during replication [95]. Examples of PIs include lopinavir and darunavir, and they are given in combination with another PI called ritonavir. Ritonavir is not administered for its antiviral activity, but instead acts as a

pharmacoenhancer, inhibiting CYP450 3A4 and 2D6, which are the major enzymes involved with the metabolism of PIs [96]. The chemical structure of lopinavir, the second antiretrioviral drug to be used in the experimental sections of this thesis is shown in figure 1.8.

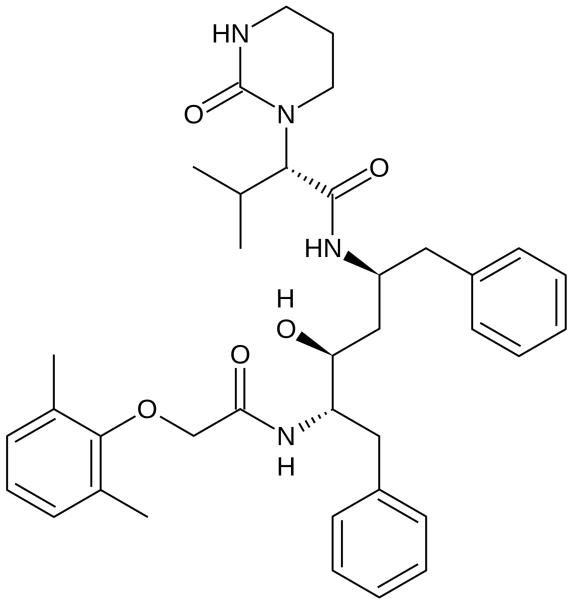


Figure 1.8 The chemical structure of the protease inhibitor lopinavir

### 1.4.6 Limitations of Antiviral Therapies

The main limitation of antiviral therapy is the risk of resistance and treatment failure due to poor patient adherence to treatment regimens [79]. ARV therapies need to be administered multiple times during the day, and at the same time each day, in order to maintain the optimal concentration of drug in the patients' systemic circulation. This can be particularly difficult due to the common toxicities of the drugs and the effect these toxicities have on the patient's quality of life [97, 98].

Many of the drugs suffer from a lack of bioavailability, brought on by the poorly water-soluble nature of the drugs [99]. A lack of bioavailability means that large doses of the drugs are needed in order to achieve a therapeutic concentration in the systemic circulation. This then leads to an exacerbation of the main problem with ARV drugs: side effects, both minor and severe, and many in a dose dependant nature, which then leads to potential reduction in adherence [100]. Common side effects of ARV drugs include, headache, nausea, diarrhoea, fatigue, dizziness, disturbed sleep, and abdominal pain [101]. More serious side effects of ARV drugs can include hyperlipidaemia, anaemia, and liver injury [98].

There are also non-dose dependent side effects that are associated with antiviral therapies such as hypersensitivity reactions, typically associated with abacavir or nevirapine and specific genetic variations in patients [102-105]. Stevens-Johnsons syndrome is a serious hypersensitivity reaction that effects the skin and mucous membranes of the body [106]. It is similar to toxic epidermal necrolysis (TEN) [107].

There are more specific side effects associated with the particular class of ARVs that feature in this thesis, namely the PIs and NNRTIs. For the NNRTI, there is a risk of insomnia, abnormal dreams, teratogenicity and the risk of false positive test results for cannabinoid and benzodiazepine screening, although the later is not due to a toxicity effect from the drug. It is recommend that Efavirenz is taken on an empty stomach, before going to bed [108].

For lopinavir, there is a risk of fatal pancreatitis, myocardial infarction, as well as PR and QT elongation. The PR interval is a measure between the end of a P wave and the beginning of the R wave in an electrocardiogram. Similarly, the QT interval is a measure of the start of the Q wave to the end of the T wave [109]. It is recommend that taking with food will help with tolerating the drug, but there are no specific food restrictions [108]. As the drug is metabolised by cytochrome P450 3A4, there are also a number of significant drug-drug interactions that can occur, specifically with patients who are being treated for other diseases which are associated with HIV infection, such as tuberculosis [110]. Thus, giving larger doses of the drugs, leads to the increased likelihood and increased severity of any side effects, but to limit the amount of drug in an attempt to limit the side effects, would lead to a sub optimal plasma concentrations. There is also the issue of lopinavir being coadministered with ritonavir for its pharmacoenhancing properties, this leads to the inhibition of drug transporters and CYP450 enzymes, which are the cause of many drug-drug interactions [111, 112].

### 1.4.7 Antiviral Resistance

Having a suboptimal concentration of the antiviral drug in the circulation is a particularly dangerous scenario, as it increases the likelihood of resistance to that drug. HIV does not have any proof-reading mechanisms during its replication [113], and so mutations are constantly occurring in the viral genome. Occasionally, these mutations will lead to the virus gaining resistance to one of the ARV drugs [114, 115]. This situation is exacerbated when there is a suboptimal concentration of drug

present in the patient, as it will not effectively prevent the replication of viral particles. Viruses that have gained a resistance mutation will have a greater chance of surviving, and then infecting new cells, releasing more viral particles with the newly acquired resistance [116-120]. Cross-resistance is a particular problem for the NNRTI class of drugs, as many share the same binding pocket on the reverse transcriptase enzyme, and so resistance to one drug can result in class wide resistance [121-124].

As mentioned earlier, HIV has the ability to penetrate into anatomical sanctuary sites within the body. Current formulations of antiretroviral drugs are unable to effectively penetrate into these sites [36]. Complete eradication of the virus from an infected individual is not possible without clearing the virus from all cells in the body.

The cost of the drugs, particularly the most effective frontline therapies can be an issue too, more so in resource-limited settings, where the burden of the disease is higher. This problem is further exacerbated by the fact that many resource-limited nations have high levels of HIV infected individuals.

## 1.5 Nanotechnology and Nanomedicine

It is hoped that many of the limitations discussed above can be addressed by using nanotechnology and nanomedicine approaches, in order to reformulate existing drugs in such a way as to enhance their chemical and biological properties, without altering the chemical structures, and thus retaining the antiretroviral activities while reducing off-target toxicities or improving bioavailability.

Nanotechnology is the use of materials and systems that are in the nanoscale size range. For the purpose of this thesis, a material is defined as being in the nanoscale size range, when its diameter in less than 1 micron (although this definition has been heavily debated in recent years and no single definition has been fully accepted). Nanomedicine refers to the application of different nanotechnologies for the benefit of health. It is a very broad and active field, which includes the use of nanomaterials for synthetic tissues, nano-biologic sensors, cellular imaging, and drug development and delivery [125-128].

Exploiting nanotechnology for the advancement of drug delivery is a major field, and a simple PubMed search for "Nanotechnology and Drug Delivery" conducted in August 2014 delivered 5468 articles. Major aims for nano drug delivery are the reformulation of existing drugs into nanosuspensions [129] or the carrying of drugs either within or upon a nanocarrier. Nanosuspensions have been successfully applied to poorly soluble drugs to enhance dissolution rates and improve their bioavailability. It is estimated (Figure 3) that 90% of new drug candidates in the

pharmaceutical pipeline suffer from poor water solubility [130]. This physical property is preventing many promising candidates from progressing further, and is putting a strain on the pharmaceutical industry in the search for new frontline drugs.

### 1.5.1 Benefits to Research and Development in Pharmaceutical Companies

There are potential cost benefits for some nanotechnologies that target improved bioavailability, as giving a lower physical dose of the drug may reduce the material cost for the therapeutic agent within that particular formulation. This does however need to be balanced with whatever additional cost would be incurred by reformulating the drug in a particular way [131]. There is always a need to keep costs low, not only in terms of profit margins for pharmaceutical companies, but in being able to cheaply supply effective, first line drugs to low income countries, in which the drugs are often needed most [132].

Another benefit to those involved in Research and Development, is that reformulating existing drugs into nanoformulations allows comparisons to be immediately made with the FDA approved formulations. The therapeutic compound will already be approved for use, however when reformulated it will be classed as a new entity, and as such would need to be approved by the FDA [133]. This often still greatly reduces the amount of initial research that is required; nanocarriers are often developed to only enhance the delivery of the therapeutic to its intended target, and not physically alter the drug. If the efficacy of the drug remains at least the same as the standard formulation, new nanocarrier systems still need to be tested for

safety, which is not an easy task due to the inherent difference between nanomaterials and their bulk material counterparts [134]. At present there are a large number of nanomedicine-based approaches being developed in the pharmaceutical industry [135].

Currently there are over 24 FDA approved nanoformulations of drugs, for the treatment of diseases including but not limited to AIDS related Kaposi's scarcoma, Hepatitis B and C, Fungal infections and Rheumatoid Arthritis. Some of these FDA approved formulations are shown in Table 2.

Table 1.2 List of selected FDA approved nanoformulations currently available for prescribing to patients. Adapted from [136]

| Trade Name | Active Ingredient | Indication | Manufacturer | Date of Approval |
|---|---|---|---|---|
| Abelcet | Liposomal amphotericin B | Invasive fungal infections | Sigma Tau | 1995 |
| Abraxane | Albumin protein-bound paclitaxel | Metastatic breast cancer | Celgene | 2005 |
| Adagen | Pegylated adenosine deaminase enzyme | Severe combined immunodeficiency disease | Sigma Tau | 1990 |
| Cimzia | Pegylated Fab′ fragment of a humanized anti–TNF-alpha antibody | Crohn's disease, rheumatoid arthritis | UCB | 2008 |
| Doxil | Pegylated-stabilized liposomal doxorubicin | AIDS-related Kaposi's sarcoma, refractory ovarian cancer, multiple myeloma | Janssen | 1995 |
| Emend | Aprepitant nanocrystal particles | Chemotherapy-related nausea and vomiting | Merck | 2003 |
| Mircera | Methoxy PEG-epoetin beta | Symptomatic anemia associated with CKD | Hoffman La Roche | 2007 |
| Neulasta | Pegfilgrastim | Chemotherapy-associated neutropenia | Amgen | 2002 |
| Pegasys | Peginterferon alpha-2a | Hepatitis B and C | Genentech | 2002 |

Nanomedicine is not always aimed at increasing the bioavailability of a drug. For example, a nanocarrier system may improve a drug by modulating its interaction with the immune system [137-139] or an inorganic nanoparticle (e.g. iron oxide) could be using for medical imaging [140-142]. The following section will highlight the current areas of research in the nanomedicine field, before focusing on nanoemulsions as a nanocarrier drug delivery system (figure 1.9).

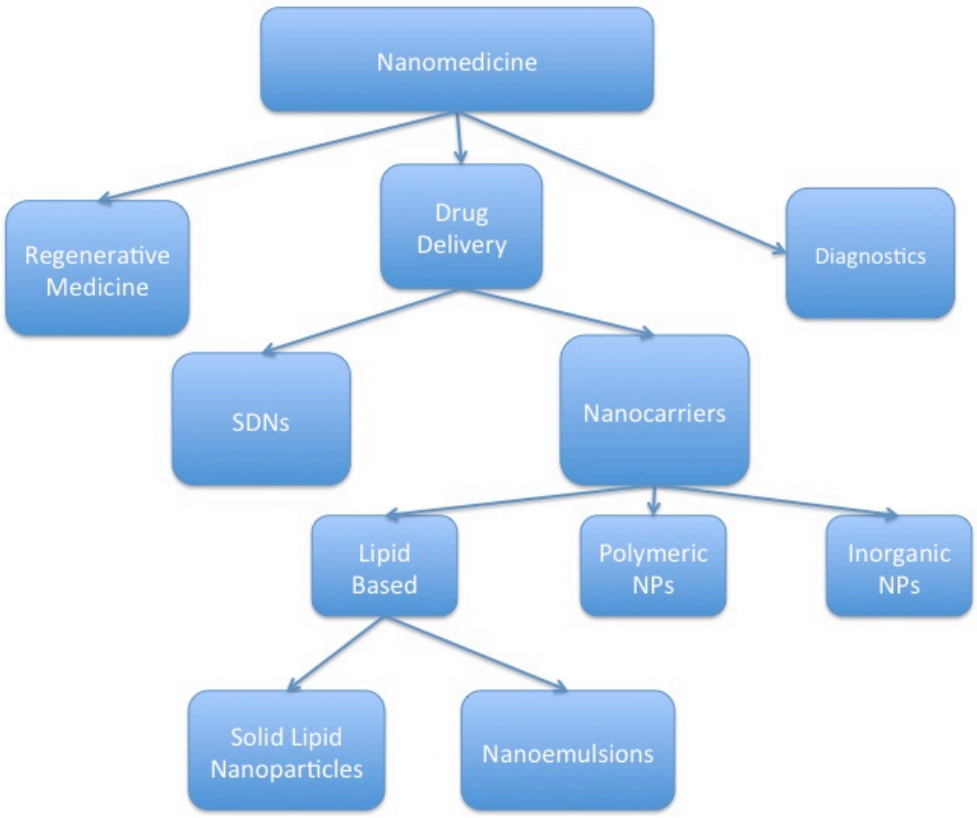


Figure 1.9. Breakdown of the current areas of research that collectively make up the field of nanomedicine.

## 1.6 Current Nanotechnology and Nanomedicine Development

### 1.6.1 Environmental Nanoparticles

For nanotechnology there are still many unanswered questions [143, 144]. In particular, as with all novel materials, there is limited data available regarding the long-term effect on health and the environment caused by nanomaterials, and as there is such a wide range of nanoparticle types, it is important to study the relative effects of each. Most work to date has been carried out with engineered nanoparticles that enter the environment, such as metals and particles within exhaust fumes [145, 146]. Many nanomaterials are present in the environment as a result of manmade actions, an example of which is particulates from diesel fuel [147, 148]. However, there is a difference between persistent nanomaterials such as silver nanoparticles and diesel particulates, and that of biocompatible and biodegradable-engineered nanomaterials, such as those reported in this thesis.

### 1.6.2 Regenerative Medicine

Regenerative nanomedicine is an area of medical research focused on the use of nanoparticles and nanomaterials for the regeneration or reprogramming of cells or organs in the body [149, 150]. The use of nanoparticles is currently being explored for the treatment of Macular Degeneration by Chen *et al*, in which nanoparticles of cerium oxide have been developed as reactive oxygen species scavengers [151]. Reactive oxygen species continually bombard photoreceptor cells, causing a damaging toxic effect and subsequent degeneration of these cells. The data by Chen *et al,* suggests that cerium oxide nanoparticles can reduce levels of reactive oxygen

species in rodent retina models and could potentially have benefits in other reactive oxygen species induced disease states such as diabetes [151].

Gene therapy is another highly active area of research in the regenerative nanomedicine field, with nanoparticles offering the potential of safe and low cost vectors for gene delivery, away from the traditional viral vectors which have associated dangers [152]. There have been many studies performed which show that nanoparticles and in particular DNA conjugated to nanoparticles can be used to deliver genes to desired targets [153-156].

Nanoparticles have also been used in conjunction with stem cell therapies to facilitate regenerative medicine treatments [157], particularly in the use of nanomaterials as scaffolding for the transplantation and growth of stem cells for the regeneration of tissues such as articular cartilage for osteoarthritis [158]. More recently data by Zhou *et al*, has suggested that conductive single walled carbon nanotubes could be used together with hydrogels to scaffold cardiomyocytes, which were then successfully transplanted into a rodent infarct model [159].

### 1.6.3 Diagnostics

Diagnostic nanotechnology refers to areas such as Magnetic Resonance Imaging (MRI) contrast agents, cellular imaging using gold nanoparticles and iron oxide nanoparticles for novel magnetic applications. As they are not therapeutic uses of nanotechnology, they won't be addressed in this work, but have been reviewed elsewhere [160-166].

### 1.6.4 Solid Drug Nanoparticles

Solid drug nanoparticles (SDNs) consist of drug and stabilisers, usually polymers and surfactants, in which the polymer and surfactant is adsorbed directly onto the surface of the nanoparticles of drug in order to increase their dispersability in water. Formulating drugs in this way does have limitations on the amount of drug that can be contained within the total SDN formulation, as compared with the amount of surfactant and polymer, usually in the region of less than 25wt% drug. However, recent advances in SDN technology at the University of Liverpool have shown that it is possible to load SDNs with 70wt% of drug when an emulsion-template freeze drying (or spray drying) design is used. These SDNs also have demonstrated improved transport across gut monolayers, and in rodent models using antiretroviral drugs, were shown to have a four-fold improvement in terms of pharmacokinetic exposure [167].

### 1.6.5 Nanocarriers

Putting a drug inside a nanocarrier allows the drug to be hidden from the aqueous environment. The nanocarrier therefore contains an active ingredient, which can be either hydrophobic [168, 169] or hydrophilic dependent upon the nature of the drug being formulated. For example, recent work by Maity *et al* has demonstrated a graphene-based nanocarrier that is suitable for both hydrophobic and hydrophilic active pharmaceutical agents [170]. Figure 1.10 shows a schematic of a nanocarrier system, specifically a nanoemulsion, in which the active ingredient is dissolved within the carrier system.

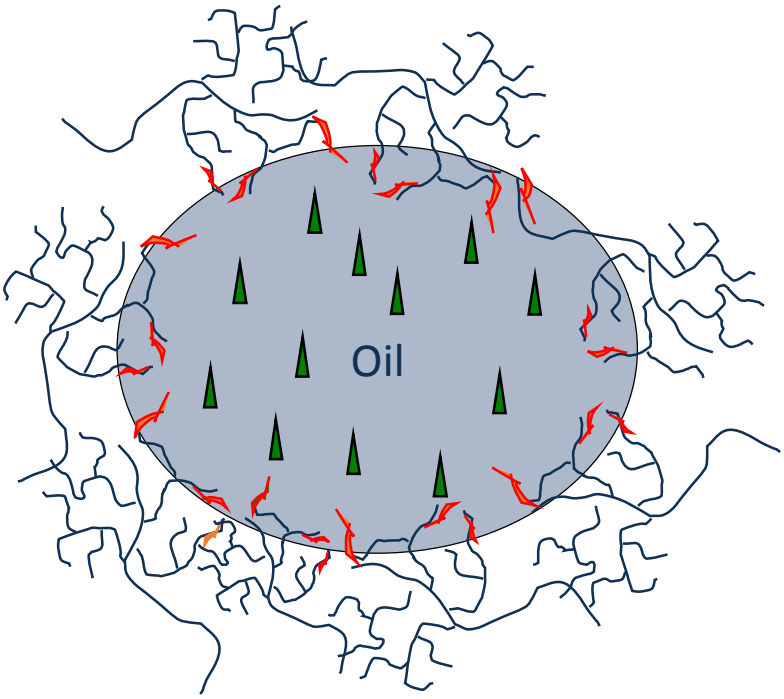


Figure 1.10 Schematic of oil-in-water nanoemulsion nanocarrier system, consisting of an oil phase (grey) stabilised by amphiphilic polymers (red and blue lines). The active pharmaceutical ingredient (green triangles) is dissolved within the oil phase.

The active is hidden from the aqueous environment by the addition of amphiphilic stabilisers that contain (in the case of hydrophobic core structures) hydrophobic sections to anchor to the core, and hydrophilic sections to allow suspension in the aqueous phase. These stabilisers can consist of polymers [171], surfactants [172], amino acids [173] or "Pickering Stabilisers" [174]. With the drug dissolved in the hydrophobic section, it is possible to load high concentrations of therapeutic agent into the nanocarrier, allowing for smaller doses to be given, but yet achieving the same therapeutic concentration [175].

These benefits of nanocarrier systems have multiple implications, particularly in the area of dose-dependent side effects. Lowering the amount of drug without compromising the concentration in the systemic circulation should in theory reduce the likelihood and severity of any side effect. This can be further enhanced if the nanocarrier has been designed to target specific cells or tissues [176]. This can be done by placing a targeting moiety onto the surface of the carrier, such as an antibody or ligand for a cell surface receptor on the target cell [177, 178]. Targeting to just the affected cells would mean that again, in theory, side effects would be reduced due to the healthy cells and tissues not being exposed to the therapeutic or the nanocarrier system.

Preventing the therapeutic from being readily cleared from the systemic circulation is another way in which nanocarriers can improve existing drug formulations [179]. Shielding the encapsulated drug from first pass metabolism and clearance by

immune cells, will have the benefit of allowing the drug to reside in the patient for a longer period of time, potentially increasing the time between doses, and lowering the dose that needs to be administered [180]. As already alluded to, this is highly desirable for drugs that have associated dose dependent side effects or need to be taken on a regular basis, as it increases the likelihood of patient adherence by reducing both side effects and pill burden [80].

### 1.6.6 Inorganic Nanoparticles

Inorganic nanoparticles have been studied extensively for drug delivery applications, due in particular to their wide availability, ability to be functionalised for applications such as cell targeting, and good biocompatibility with cellular systems [181]. Inorganic nanoparticles comprise nanoparticles synthesised from gold [182], silver [183], ceramics [184], silica [185], nanorods [186], quantum dots [187] and metal oxides [188].

Gold nanoparticles have shown promise for the application of gene transfection, due to their amenability to being functionalised with thiolated ligands, allowing for the subsequent attachment of DNA molecules [189]. Work by Jan *et al* has shown that by modifying gold nanoparticles with thiolated oligonucleotides, it is not only possible to improve the stability of the gold nanoparticles in physiologically-relevant fluids, but also to allow use as non-viral DNA delivery vectors [190].

Silica nanoparticles have been used for the passive targeting of cancerous tumours, as evidenced in work by Barbe *et al* [185]. In this study, it was shown that by keeping the particle size between 50 nm and 250 nm, doxorubicin loaded silica nanoparticles were able to release the drug at a steady rate over 20 days, and avoid clearance from the systemic circulation.

### 1.6.7 Polymer Conjugates and Polymeric Nanoparticles

Polymer conjugated drug therapies have been the most successful of the nanomedical approaches to date, with a number of FDA approved formulations in existence, including those mentioned in Table 2 [191-193]. Polymer conjugates consist of the active drug associated with or chemically bound to polymer molecules (such as PEG) that enhance the bioavailability of the drug by shielding it from the aqueous environment.

Dendrimers are polymer nanoparticles that consist of repeating highly branched polymer chains and functional groups, symmetrically arranged around a central core. For the benefit of delivery of poorly water-soluble drugs, this core can be a hydrophobic region, in which the drug can be contained, with the polymer chains that spread out from this core being hydrophilic [194]. Dendrimers have been the subject of much pharmaceutical research since the discovery of a convergent approach to their synthesis in 1990 [195].

Non-dendrimer polymer nanoparticles have been shown to be appropriate for a wide variety of nanomedical applications, including, vaccine development [196], immunotherapy [197], delivery of siRNA for gene therapies [198], aerosol formulations [199] and drug delivery of poorly water soluble drugs [200] and biologics [201].

### 1.6.8 Lipid Based Nanoparticles

There are a number of lipid-based nanoparticles currently being used for development of nanomedical formulations, including liquid based materials such as liposomes and micelles, as well as solid based systems such as solid lipid nanoparticles. Nanoemulsions have been developed for the work featured in this study, and they are classed as a liquid lipid based nanoparticle.

Liposomes are artificially prepared lipid bilayers, assembled such that there is an internal aqueous core, which is surround by the hydrophobic lipid membrane. This arrangement is particularly useful in a drug delivery setting, as both hydrophilic (within the core) and hydrophobic (within the lipid bilayer) compounds can be carried by the liposome. Liposomes can also be functionalised with Polyethylene Glycol (PEG); this prevents the liposomes from being detected by the immune system and increase the circulation time [202, 203].

Micelles, unlike liposomes, do not form lipid bilayers and instead arrange themselves so that the hydrophilic portion of the surfactant is in contact with the

external aqueous solvent, and the hydrophobic portions pack themselves into the centre, thus creating a hydrophobic core. This type of micelle is known as a "Normal Phase" micelle, whereas an "Inverse Phase" micelle refers to one in which the hydrophilic portions are grouped at the core and the hydrophobic portions are arranged around the outside. A reverse phase micelle would occur when a non-polar solvent is present as the continuous phase [204, 205].

### 1.6.9 Solid Lipid Nanoparticles

Unlike traditional lipid nanocarriers, such as the previously mentioned liposomes, micelles, and emulsions (section 1.6.4), solid lipid nanoparticles (SLNs) do not have a liquid lipid core, and instead have a solid lipid core [206]. SLNs first began development in the 1990s [207] and have since been used to process a broad range of drugs into SLN formulations, including, but not limited to, paclitaxel [208-211], clozapine [212] and estradiol [213].

To aid in the production of SLNs, synthesis is usually carried out using elevated temperature homogenisation, typically at temperatures exceeding that of the melting point of the lipid being used, with a subsequent cooling phase to return to solid form, or by using a solvent diffusion approach [214-219]. SLNs can also be formed by the freeze or spray drying of liquid nanosuspensions, in order to produce a solid form.

Solid lipid nanoparticles have been said to be particularly useful for the controlled and sustained release of actives from the particles, as is evidenced by a number of

studies that claim a slow release profile [212, 220-223]. However, these results have been argued as being artificial, due to poor set up of experiments, and the fact that lipid dispersions are harder to assess than the associated solid dosage forms, mainly due to them not disappearing in the experimental media (via dissolution). Their presence can then interrupt analytical readouts [224].

### 1.7 Nanoemulsions

Of most interest to this thesis are oil-in-water nanoemulsions; droplets of oil stabilised in an aqueous environment by surfactants and/or polymers. As with most of the other previously mentioned systems, the benefit of nanoemulsions for drug delivery is obtained by the presence of a hydrophobic oil core [225, 226]. The poorly water-soluble drug can be dissolved into this oil core, and suspended in the aqueous environment by means of the hydrophilic sections of surfactant or polymer.

Nanoemulsions typically have droplet sizes that range between 100 and 500 nm [227], and should not be confused with "Microemulsions", which despite the prefix of "Micro" suggesting sizes in the micron range, actually have droplet sizes of below 100 nm [228]. Previously in the literature, nanoemulsions have also been referred to as "miniemulsions" [229, 230] and "submicron" emulsions [231], thus there is a lack of common nomenclature of emulsions based on particle size, which is likely due to the original definition of a microemulsion being thermodynamically stable, whereas nanoemulsions are referred to as "approaching thermodynamic stability" [232].

Nanoemulsions can occur spontaneously when emulsifiers and surfactant mixes are added to water, due to the arrangement of the amphiphilic molecules so that the hydrophobic sections associate with the oil phase and the hydrophilic sections associate with the water, as this is energetically favourable [232, 233]. However, there are cases in which an input of energy is required to overcome kinetic barriers to self-emulsification [234, 235]. This latter type of oil-in-water nanoemulsion will form the basis of work in this thesis.

Energy can be added to a system in a number of ways, including mixing [236], sonication [237] and high pressure homogenisation [238]. Co-solvents can also be used, as reported in this body of work, to obtain smaller sized emulsion droplets. The co-solvent approach works by addition of a volatile solvent, which is miscible with the chosen oil phase. After the initial emulsion is made, this solvent can be evaporated, causing the oil droplets to shrink whilst surrounded by stabilisers and decreasing the droplet diameters [239]. Smaller diameter particles are of benefit in a drug delivery setting as they should be able to enter into cells and cross the tight membranes of the gut endothelium, a driving factor in oral bioavailability.

Oral delivery of therapeutics is the preferred route for the treatment of chronic diseases as it is simple and removes the need for patients to visit healthcare professionals for infusions or from having to self inject. Oral delivery of poorly water-soluble drugs is not ideal however, and the need for large doses is a serious drawback [240]. This is where nanoemulsions are ideally suited, as they can greatly

improve the solubilisation of such drugs, and increase bioavailability via means of increased permeation across gut endothelium [241-243]. Although there is a lack of clinically available FDA approved nanoemulsion formulations of therapeutics, there is a vast amount of literature in which studies have shown dramatic increases in bioavailability of nanoemulsion formulations, when compared to the standard parent drug (Table 3). This leads to the prediction that nanoemulsion formulations will appear on the market in the years to come.

Table 1.3 Example literature studies showing nanoformulations of poorly water-soluble drugs, with increased bioavailability, in animal models. Adapted from [244].

| **Drug** | **Formulation** | **Particle Size (nm)** | **Animal Model** | **Increase in Bioavailability (%)** |
|---|---|---|---|---|
| Ezetimibe | nanoemulsion | 46.53 ± 8.24 | Wistar Rats | 477.09 |
| Ibuprofen | SEDDS O/W microemulsion | 40 | SD Rats | 800 ± 100 |
| Ketoprofen | SEDDS O/W microemulsion | 19 | SD Rats | 150 ± 23 |
| Tolbutamide | SEDDS O/W microemulsion | 60 | SD Rats | 280 ± 15 |
| Disopyramide | SEDDS O/W microemulsion | 47 | SD Rats | 150 ± 27 |
| Ramipril | Nanoemulsion | 80.9 | Wistar Rats | 229.62 |
| N-4472 | Microemulsion | 17.7 ± 4.8 | SD Rats | 243.11 (Fasted), 393.73 (Non fasted) |
| Biphenyl dimethyl dicarboxylate | Nanoemulsion | 329.98 ± 24.31 | SD Rats | 502.76 |

## 1.8 Aims of this Thesis

The aim of this thesis was to develop a novel nanoemulsion formulation of poorly water-soluble antiretroviral drugs lopinavir and efavirenz [245]. Further to development and final optimisation of chemically stable and biocompatible formulations, the pharmacological properties of the nanoemulsion formulation were tested, in comparison to standard aqueous formulations, in order to assess the potential benefit of nanoemulsion for oral delivery of therapeutic drugs.

- Chapter 2 explores the development of linear and branched polymers consisting of repeat units of oligoethylene glycol methacylate. These polymers were synthesised as emulsifiers for subsequent oil-in-water nanoemulsions. Characterisation of these polymers was performed using NMR spectroscopy, Gel Permeation Chromatography and cell based toxicity assays to determine the biocompatibility of the polymers.

- In Chapter 3 the polymers developed in Chapter 2 are used to stabilise oil-in-water emulsions consisting of castor oil, in which the active pharmaceutical agent (API) was dissolved. These emulsions were characterised for size, surface charge and size distribution using Dynamic Light Scattering and Zeta potential measurements. Long-term stability studies were also performed on the emulsion formulations to assess possible shelf lives, and biocompatibility was assessed using the same cellular toxicity assays performed on the polymer stabilisers in Chapter 2.

- In Chapter 4 the emulsions were assessed for any potential enhanced pharmacological benefit, in terms of permeation through model gut systems (Caco-2 monolayers) and accumulation into a range of relevant cell lines. Quantification of any enhanced effect was determined by the amount of API present in the assay, when comparing emulsion formulation with standard aqueous formulation, using HPLC methods.

- Chapter 5 the emulsions were assessed for their antiviral activity against a laboratory adapted strain of HIV (HIV-1IIIB). In these assays, CD4+ cell lines were exposed to HIV-1IIIB in the presence or absence of various concentrations of aqueous or emulsion formulated antiretroviral.

- Chapter 6 was the final experimental chapter, in which any potential immune interactions were probed. The purpose of these assays was to consider immunological safety, in terms of immune suppression or activation, and any detrimental effects of coagulation times. In all assays the emulsion formulation was compared to current aqueous formulations to assess the relative safety.

- Chapter 7 comprised a final discussion, bringing together the findings of the previous 5 experimental Chapters.

# CHAPTER 2

# Synthesis and Characterisation of Oligo Ethylene Glycol Monomethyl Ether Methacrylate based Polymers (PolyOEGMA) Via Conventional Free Radical and Atom Transfer Radical Polymerisation

**Table of Contents**

## 2.1 Introduction

There are a number of lipid based nanomedicine platforms in development that are particularly suited for the delivery of poorly water soluble and low bioavailability drugs [246-254].

Of these platforms, nanoemulsions provide a system in which a drug can be encapsulated as a payload within the emulsion droplet itself, allowing for the dissolution of that drug to be altered. Emulsions are traditionally stabilised with surfactants [255-259] or solid "Pickering Stabilisers" [260-263], but these can have unwanted cytotoxicity profiles and potential irritant properties [264-266].

Alternatively nanoemulsions can be stabilised with biocompatible polymers, which helps to overcome the problem of persistence of the stabiliser within the body and, dependent upon the structure and chemical properties, can be tuned to prevent cytotoxicity [267, 268]. Polymers containing repeat units of ethylene glycol have been used in many medical settings previously [269-273], and as such have shown the molecule to be safe and effective in a medical setting. Ethylene glycol is also relatively hydrophilic and as such would allow the oil droplets they are stabilising to be freely dispersed in an aqueous environment. There are a number of examples in the literature that demonstrate the synthesis of oil-in-water emulsions stabilised by polymers consisting at least in part of ethylene glycol monomeric units [274-279].

There are a number of methods in which polymers can be synthesised, including controlled radical polymerisation techniques such as reversible addition-fragmentation chain transfer polymerisation (RAFT) [280], nitroxide mediated free radical polymerisation [281] and atom transfer radical polymerisation (ATRP) [282]. Other strategies include utilising "Click" chemistry [283] and photoinitiated polymerisation [284].

Conventional free radical polymerisation is a method of polymer synthesis which imparts little control on the reaction and generates polymers with broad molecular weight distributions and potentially with large variability in structure when undertaking co-polymerisation. Although the simple nature of the method makes it suitable for producing large batches of polymer quickly, the variation in the sample characteristics could potentially lead to issues in reproducibility, especially during scale-up of the polymerisation. This may impact negatively in a drug delivery setting, where it is vital to maintain continuity from batch to batch in order to be certain of the quality and effectiveness of a given formulation. A reaction scheme for the synthesis of linear and branched polymers of oligo ethylene glycol monomethyl ether methacrylate (PolyOEGMA) via conventional free radical polymerisation is shown in Scheme 2.1.

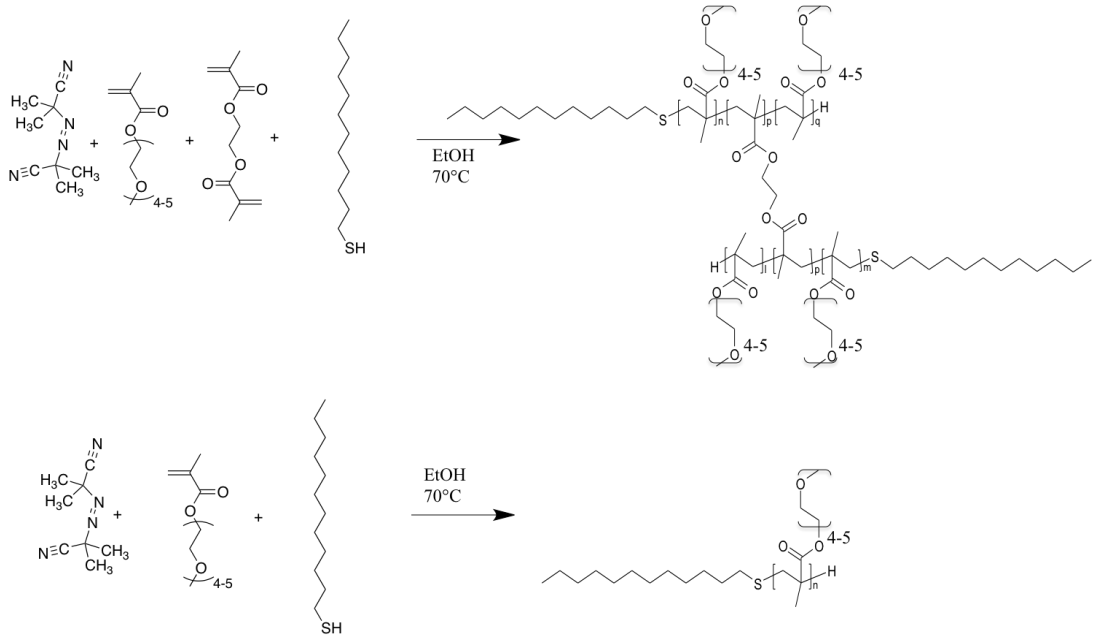


Scheme 2.1 Reaction scheme showing conventional free radical polymerisation initiated by azobisisobutyronitrile (AIBN) and using ethanol as the solvent at 70°C, of branched (using EGDMA) (top) and linear (bottom) PolyOEGMA. Docecane thiol was used as the chain transfer agent.

In contrast, the ATRP process is a more finely controlled method in which the length of polymer chains can be tightly defined by the use of specific initiators and the control of radical concentrations using organometallic catalyst-mediated redox equilibrium. Atom transfer radical polymerisation has been used to synthesise a range of polymers with control of chain length and relatively low dispersity [285-289]. As previously mentioned, having this control enables batches of polymer to be comparable, ensuring that samples are consistent. A reaction scheme for the synthesis of linear and branched polyOEGMA via ATRP is shown in Scheme 2.2.

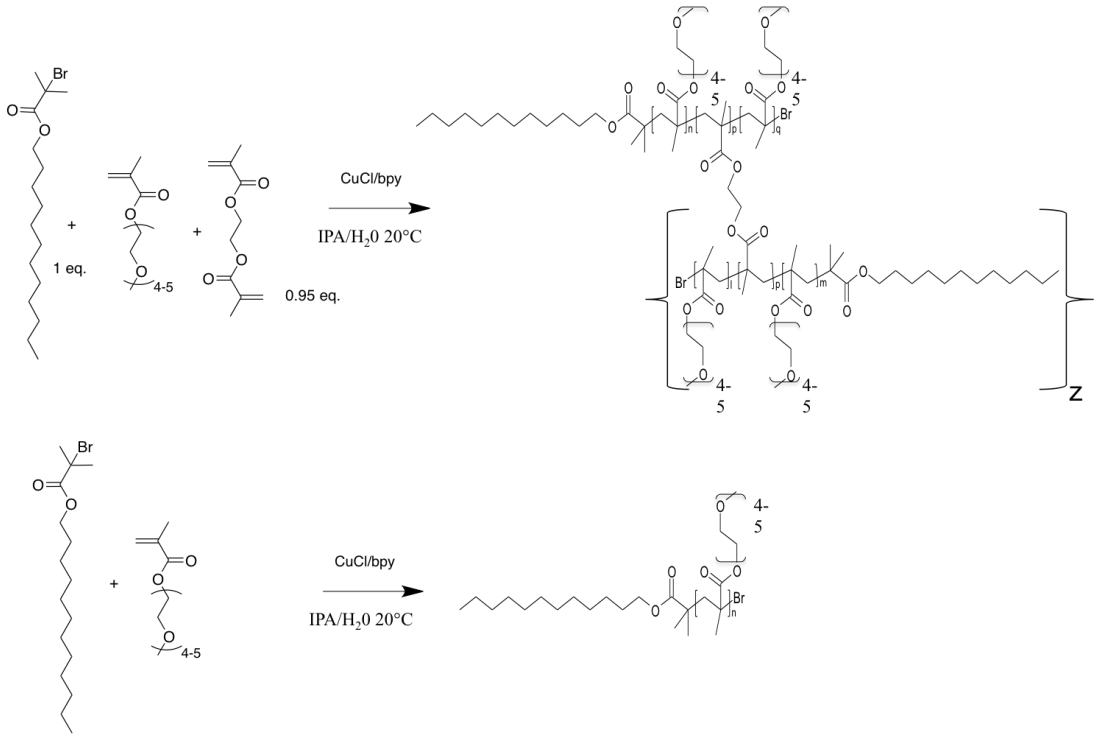


Scheme 2.2 Reaction scheme showing copper catalysed ATRP polymerisation of branched (using EGDMA) (top) and linear (bottom) PolyOEGMA $DP_{80.}$ 2-dodecylbromoisobutyrate was used as the initiator, and 92.5/7.5 IPA/water mix as the solvent at 20°C.

Linear and branched polymers were made by both of the methods described above in order to compare the suitability of each as a stabiliser. Copolymers of OEGMA and methacrylic acid were also synthesised via the conventional free radical route as extensive work by Weaver *et al* has demonstrated the use of conventional free radical polymerisation for the facile synthesis of pH responsive co-polymers [290, 291] and the subsequent formation of pH responsive nanoparticles [292, 293] and nanoemulsions [294, 295]. Incorporation of methacrylic acid into the polymer allows for aggregation to be triggered by exposure to acid, with the droplets redispersing

after returning to a neutral or alkaline pH. This could potentially be used as a strategy to protect pharmaceutical agents from the harsh conditions of the stomach by encapsulation in an aggregated mass of emulsion.

There would also be the issue of determining the cytotoxicity of polymers from each technique. The more uncontrolled nature of the free radical polymerisation would make it more likely to create different sized polymer chains. These chains would contribute at different magnitudes to any observed cytotoxicity and the use of methacrylic acid as a co-polymer could add to the cytotoxic potential, as well as MAA being difficult to incorporate by ATRP methods. As such, pH responsiveness would have to be weighed against potential added cytotoxicity.

The cytotoxicity of the polymers produced in this Chapter was assayed using a Cell TiterGlo® Viability Assay on both Caco-2 and HepG2 cells. These two cell lines were chosen as Caco-2 cells are a model intestinal cell line, and as such provide a good system to look at interactions of orally dosed formulations encountering the intestinal epithelium. HepG2 cells were chosen due to them being a liver cell line, and as such a model for observing the effects a formulation may have if it successfully enters the systemic circulation and enters the liver for metabolism.

The aims of this Chapter were to synthesise biocompatible polymers for subsequent use as emulsifiers, by both conventional free radical polymerisation and ATRP methods. This approach was taken to assess the merits of the simplicity of reaction

using conventional free radical and the controlled nature of ATRP. Cytotoxicity assessments were carried out to determine the biocompatibility of polymers produced and to inform changes to polymer content where necessary. Thus it was hypothesised that polymer stabilisers synthesised via radical polymerisation techniques, and consisting of repeat PEG units would be suitable for stabilising an oil-in-water drug delivery system; both in terms of the physical stability of the system, and the cytotoxic profile.

## 2.2 Materials and Methods

### 2.2.1 Materials

Oligo ethylene glycol monomethyl ether methacrylate (OEGMA), poly(ethylene glycol monomethyl ether methacrylate) (PEGMA), methacrylic acid (MAA), azobisisobutyronitrile (AIBN), 2-dodecylbromoisobutyrate, tetrahydrofuran (THF), ethylene glycol dimethacrylate (EGDMA), dodecanethiol (DDT), copper chloride, 2,2'-bipyridine (BPY), anisole, methanol, isopropyl alcohol, Dowex Marathon MSC acid form beads, aluminium oxide, deuterated methanol (MeOD), acetone, squalene, dodecane, castor oil, peanut oil, soy bean oil, coconut oil, sesame oil, Dulbecco's modified Eagles medium (DMEM), Roswell Park Memorial Institute 1600 medium (RPMI 1600), Hank's balanced saline solution (HBSS), Trypsin-EDTA, (3-(4,5-dimethylthiazol-2-yl)-2,5-diphenyltetrazolium bromide (MTT), glacial acetic acid and dimethylformamide (DMF) were all purchased from Sigma-Aldrich (Dorset, UK). Oxygen-free Nitrogen gas was supplied by BOC Industrial gases (Guildford, UK) and NMR tubes were supplied by Bruker UK (Coventry, UK).

Nuclear Magnetic Resonance spectroscopy analysis was performed using a Bruker Avance III HD 450 MHz NMR spectrometer (Bruker UK, Coventry, UK) or a Bruker Avance 400 MHz spectrometer (Bruker UK, Coventry, UK). Gel permeation/size exclusion chromatography equipment was supplied by Malvern Instruments, (Malvern, UK) fitted with triple detection system of refractive index, differential viscometry, right angle light scattering (90° detection angle) and low

angle light scattering (7° detection angle). THF was used as the eluent at a flow rate of 1 mL/minute. Rotary evaporator was bought from Büchi UK (Oldham, UK)

Fetal bovine serum was supplied by Life Technologies (Paisley, UK), cell culture flasks, cell culture plates, 10 and 25 mL pipettes, pipette tips and isopropyl alcohol were all purchased from Fisher Scientific (Loughborough, UK). Cell TiterGlo® ATP assay was supplied by Promega (Southampton, UK). Caco-2 human epithelial colorectal adenocarcinoma cells and HepG2 hepatocellular carcinoma cells were both purchased from the American Tissue Culture Collection (ATCC) (Manassas, US). 24 well HTS® Transwell plates were supplied by Corning Life Sciences (Amsterdam, The Netherlands).

### 2.2.2 Conventional Free Radical Polymerisation

In a typical experiment OEGMA, MW=300 g/mol (targeted $DP_n$ = 80) (10g, 3.3 x $10^{-2}$ moles) and EGDMA brancher (0.65 g, 3.3 x$10^{-3}$ moles) were weighed into a round bottom flask. For copolymers, methacrylic acid was also added (0.166 moles). The flask was equipped with magnetic stirrer bar, sealed and degassed by bubbling with $N_2$ for 20 minutes and maintained under $N_2$ at ambient temperature. Ethanol (115 mL) was degassed separately and subsequently added to the monomer mixture. Azobisisobutyronitrile initiator (0.113g) was added under a positive nitrogen flow in order to initiate the reaction and the temperature was set to 70°C. Reactions were stopped after 3 days when conversions had reached over 98% determined by $^1$H NMR using the vinyl $CH_2$ peaks and protons of the polymer backbone.

After reactions had completed, excess solvent was removed by rotary evaporation followed by subsequent drying in a vacuum oven for 24 hours. Ice-cold diethyl ether was added to the dried polymers and left in sealed vials in a spark free freezer overnight to ensure precipitation of the polymers and extraction of any residual un-reacted monomer (Please note that use of a non spark-free freezer, or unsealed diethyl ether in a freezer is an explosive hazard). The polymers were kept at -20°C whilst in diethyl ether to prevent them from dissolving. After 24 hours, diethyl ether was decanted and the polymers dried once more in the vacuum oven to ensure all residual solvent had been removed.

### 2.2.3 Atom Transfer Radical Polymerisation and Kinetic Studies

In a typical experiment, dodecylbromoisobutyrate initiator (0.118 g, 3.52 $x10^{-4}$ moles), OEGMA, MW=300 g/mol (targeted $DP_n$ = 80) (9.44 g, 3.15 x $10^{-2}$ moles) and EGDMA brancher (62.5 µL, 3.3 $x10^{-4}$ moles) were weighed into a round bottom flask. The flask was equipped with magnetic stirrer bar, sealed and degassed by bubbling with $N_2$ for 20 minutes and maintained under $N_2$ at ambient temperature. IPA:$H_20$; 92.5:7.5 (12 mL) was degassed separately and subsequently added to the monomer/initiator mixture. The catalytic system; Cu(I)Cl (0.034 g 3.52 $x10^{-4}$ moles) and BPY (0.137 g, 8.8 $x10^{-4}$ moles), were added under a positive nitrogen flow in order to initiate the reaction. The polymerisations were stopped after 8 hours, when conversions had reached over 98 % determined by $^1$H NMR using the vinyl $CH_2$ peaks and protons of the polymer backbone. The polymerisation was stopped by

diluting with a large excess of THF, which caused a colour change from dark brown to a bright green colour.

For each sample taken during a kinetics study, nitrogen was again pumped into the reaction flask, and the sampling needle was purged of oxygen. This prevented addition of oxygen to the polymerisation reaction, which would have quenched the radical species and thus terminated the reaction before it reached completion. The samples taken for kinetics analysis were transferred immediately from the reaction vessel into a glass vial containing MeOD (for NMR spectroscopic analysis) or THF (for GPC analysis) and stirred vigorously. This ensured that the sample was quenched of any radical species and the polymerisation no longer continued, allowing for an accurate determination of percentage conversion and molecular weights to be obtained.

### 2.2.4 NMR Spectroscopy

Polymer samples were dissolved in deuterated methanol overnight and placed into 5 mm Bruker NMR tubes, compatible with both NMR machines available within the Department of Chemistry. $^{1}$H NMR spectroscopy was used as the analysis method, with multiple samples being run in batches using an auto-sampling carousel.

### 2.2.5 Gel Permeation Chromatography

Samples of polymer were dissolved in THF overnight, at a final concentration of 2 mg/mL. Samples were then filtered using 200 nm nylon filters to remove any impurities or contaminants from the sample. Analysis was conducted using a Viscotek GPC machine fitted with Refractive Index (RI), Ultraviolet (UV), Right Angle Light Scattering (RALS) and viscosity detectors.

### 2.2.6 Rotary Evaporation

Residual solvent was removed from polymer batches using rotary evaporation, with vacuum set to 200 mBar and temperature of the water bath at 55°C. Cold tap water was pumped around the condensing vessel and solvent collected in a Wolffe bottle attached to the bottom of the condenser.

### 2.2.7 Polymer Precipitation

Polymer purification was carried out by firstly dissolving the polymer in the minimum volume of THF and adding dropwise to a conical flask containing ice-cold petroleum ether 60-80 in which it precipitated out of solution. To maintain the low temperatures, the conical flask was placed in a crystallisation dish and surrounded by dry ice. After addition of all polymer solution the petroleum ether was decanted and polymer sample dried using rotary evaporation, to remove residual organic solvent.

### 2.2.8 Adherent Cell Culture

All mammalian cell culture was carried out under strict aseptic conditions. Caco-2 and HepG2 cells were cultured by seeding a starter culture vial of approximately 5 million cells in a Nunc T25 flask, containing 10 mL of pre-warmed DMEM supplemented with 15% FBS. The FBS was sterile filtered before addition to media using 0.2 μm syringe filters. Cells were placed at 37°C in an incubator containing 5% $CO_2$ overnight. At this point cell media was changed to remove residual DMSO that came from the starting culture vial. Cells were then grown until they were around 80-90% confluent, as determined by inversion microscopy, at which point they were continually passaged for further growth into larger flasks (T-75 or T-175).

Cell passage was carried out at around 80% confluence. Cells were washed twice with hanks balanced salt solution in order to remove any serum, which would inhibit trypsin activity. 5 mL of trypsin-EDTA was added, and incubated at 37°C for around 5-10 minutes. Cells that were stuck onto the surface of the flask after this time were removed by gently striking the flask. Serum containing media was added to inactivate remaining trypsin, and this cell suspension removed and centrifuged to pellet the cells. Supernatant was aspirated in order to remove trypsin. The cell pellet was re-suspended in an appropriate volume of fresh pre-warmed DMEM supplemented with 10% FBS, and the cells counted in order to determine dilutions for experimental procedures and correct volumes to reseed flasks.

Cells were counted using an Invitrogen Countess® automated cell counter (Invitrogen-Life Technologies, Paisley, UK), as per the manufacturers protocol. In short, 10 μL of trypan blue was added to 10μL of cell suspension and pipetted into the counting slide. The slide was inserted into the Countess reader, and the total numbers of cells, including live and dead cells were derived by automated microscopy based upon trypan blue not entering live cells.

### 2.2.9 Suspension Cell Culture

Suspension cells were raised from frozen stocks in the same way as previously described in 2.2.8. However RPMI 1600 medium supplemented with 10% sterile filtered FBS was used in place of DMEM. Also during the changing of the media after overnight incubation, the cells were pelleted at 2000 RPM for 5 minutes at 4°C, and re-suspended in fresh culture media.

Cell suspension was transferred from culture flasks into 50 mL falcon tubes, and cells pelleted for 5 minutes at 2000 RPM. Cell culture media was aspirated and fresh complete culture media used to re-suspend the cell pellet. The cell suspension was then transferred to fresh culture flasks at a 1 in 4 ratio, such that cells would continue to divide and grow. Cells were passaged in this way every 3 days or sooner if cell culture media had turned from red to orange in colour, due to the phenol red indicator present in the media. Cells were counted in the same way as described in 2.2.8.

### 2.2.10 Cell TiterGlo® Viability Assay

Approximately 10,000 cells per 100 μL were seeded per well in a 96 well tissue culture plate, and left to adhere for 24 hours. After this time, 100 μL of polymer sample was added to each well for a dilution 1:1 series with a maximal of 5% (w/v) and left for 5 days incubation.

Upon completion of the incubation, 180 μL was removed from each well, and 20 μL of ATP reagent was added, leaving each well with a volume of 40 μL. The ATP reagent lysed the cells, and reacted with the ATP of the cells to produce a luminescent signal. After a 10-minute incubation to stabilise the signal, the plates were read using a TECAN GENios plate reader, set to luminescence mode, with 2 seconds of shaking prior to reading.

The CellTiterGlo® assay worked on the principle that metabolic activity of the cells can be used as a proxy for determining cellular viability. The amount of ATP present was directly proportional to the amount of cells, and thus the level of luminescence was directly proportional to the amount of cells. Comparing the luminescent values of sample conditions to the control untreated condition allowed for a direct measure of cellular viability.

### 2.2.11 Data Analysis

NMR spectra were analysed using Spinworks software, GPC data were analysed using OmniSec 4.7 software, DLS data were analysed using Zetasizer software, Mastersizer data were analysed using Mastersizer 2000 software, and all of the above were plotted using Microsoft Excel for Macintosh computers 2011.

Data for cytotoxicity was analysed using Graphpad Prism 6 software, using a Non-Linear Regression Sigmoidal dose response curve analysis, after data had been log transformed. For this, concentrations causing half maximal inhibition ($IC_{50}$ values) were derived. All data were presented as mean ± standard deviation of experiments conducted in quadruplicate.

## 2.3 Results

### 2.3.1 Conventional Free Radical Polymerisation

Initially a conventional free radical polymerisation method was used to generate both homopolymers of oligo ethylene glycol monomethyl ether methacrylate MW = 300 g/mol (OEGMA), poly ethylene glycol monomethylether methacrylate MW = 950 g/mol (PEGMA) and co-polymers of these with methacrylic acid (MAA), all of which were branched using ethylene glycol dimethacrylate (EGDMA). Reactions were left for 72 hours to reach completion and resulted in a range of different molecular weight polymers, based upon the starting composition (Table 2.1). The highest molecular weight achieved was that of polymer 79, which contained both MAA and PEGMA, whereas the lowest molecular weight polymer was 82, which contained MAA and OEGMA.

Table 2.1 Final compositions of branched copolymers that were synthesised using conventional free radical polymerisation method. Both the weight average molecular weight (Mw) and the number average molecular weight (Mn) are shown.

| **Polymer Reference Number** | **Composition** | **$M_w$** | **$M_n$** | **$M_w/M_n$** |
|---|---|---|---|---|
| 79 | $MAA_{96}/PEG_{22}MA_4$-$EGDMA_{10}$-$DDT_{10}$ | 347,500 | 16,616 | 20.9 |
| 80 | $MAA_{92}/PEG_{22}MA_8$-$EGDMA_{10}$-$DDT_{10}$ | 327,528 | 31,827 | 10.3 |
| 81 | $OEG_{4.5}MA_{100}$-$EGDMA_{10}$-$DDT_{10}$ | 16,991 | 6,683 | 2.5 |
| 82 | $MAA_{82}/OEG_{4.5}MA_{18}$-$EGDMA_{10}$-$DDT_{10}$ | 15,312 | 6,369 | 2.4 |
| 83 | $MAA_{69}/OEG_{4.5}MA_{31}$-$EGDMA_{10}$-$DDT_{10}$ | 15,961 | 6,893 | 2.3 |

### 2.3.2 ATRP Polymerisations to Form Branched Polymers

The controlled radical polymerisation ATRP was used to synthesise an analog of polymer 81 to a number average degree of polymerisation of 80 ($DP_{80}$), i.e. there were 80 repeat units of OEGMA within each primary chain of the branched polymer, from now on referred to as PolyOEGMA $DP_{80}$. 2-Dodecyl bromoisobutyrate was used as the reaction initiator, and also acted as the hydrophobic anchor, mirroring the chain ends derived from dodecanethiol that were present in the conventional free radical polymers. The reaction reached >97% (Figure 2.3) completion after 8 hours at ambient temperature, as determined by $^1$H NMR spectroscopy (Figures 2.1 and 2.2). The $M_w$ of the branched PolyOEGMA $DP_{80}$ polymer was 3.59 MDa, $M_n$ was 1.65 MDa and $M_w/M_n$ was 2.170, whereas the linear PolyOEGMA $D0P_{80}$ had $M_w$, $M_n$ and $M_w/M_n$ of 124,526 Da, 79,511 Da and 1.6 respectively (Table 2.2, as determined by gel permeation chromatography (Figure 2.4 and 2.5).

Table 2.2 Summary of final the molecular weights of PolyOEGMA $DP_{80}$ synthesised by ATRP method. Determined by gel permeation chromatography using THF eluent and RI detector, with a sample concentration of 2 mg/mL.

| **ATRP Polymers** | **$M_w$** | **$M_n$** | **$M_w/M_n$** |
|---|---|---|---|
| Linear PolyOEGMA $DP_{80}$ | 124,526 | 79,511 | 1.6 |
| Branched PolyOEGMA $DP_{80}$ | 3,590,000 | 1,650,000 | 2.2 |

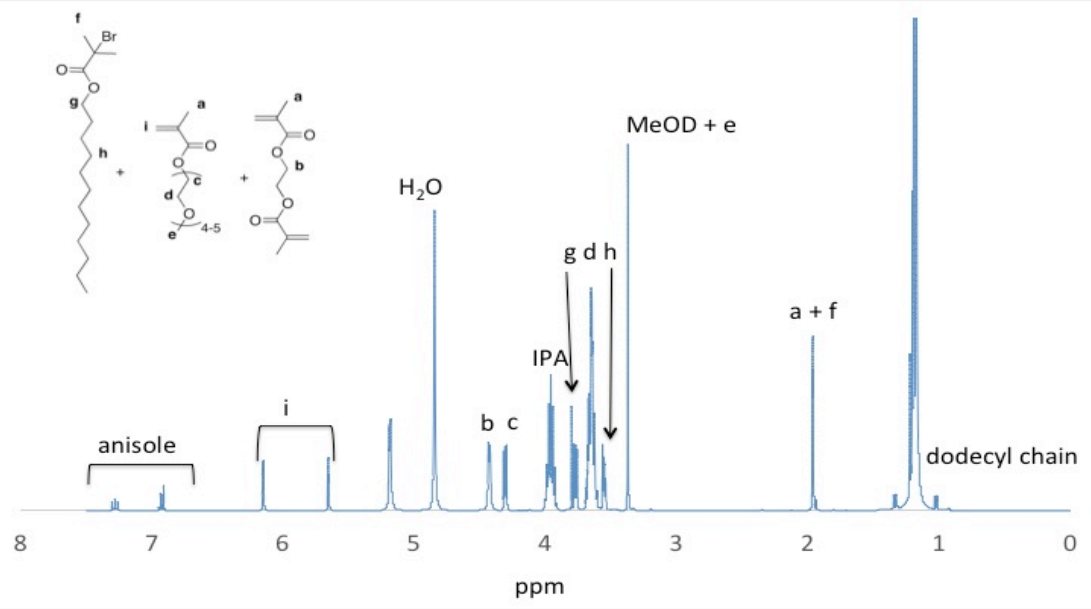


Figure 2.1 $^{1}$H NMR spectrum of PolyOEGMA $DP_{80}$ B at time zero. Determined using a Bruker Avance 400 MHz NMR Spectrometer and MeOD as the solvent. A 15-minute scan was performed.

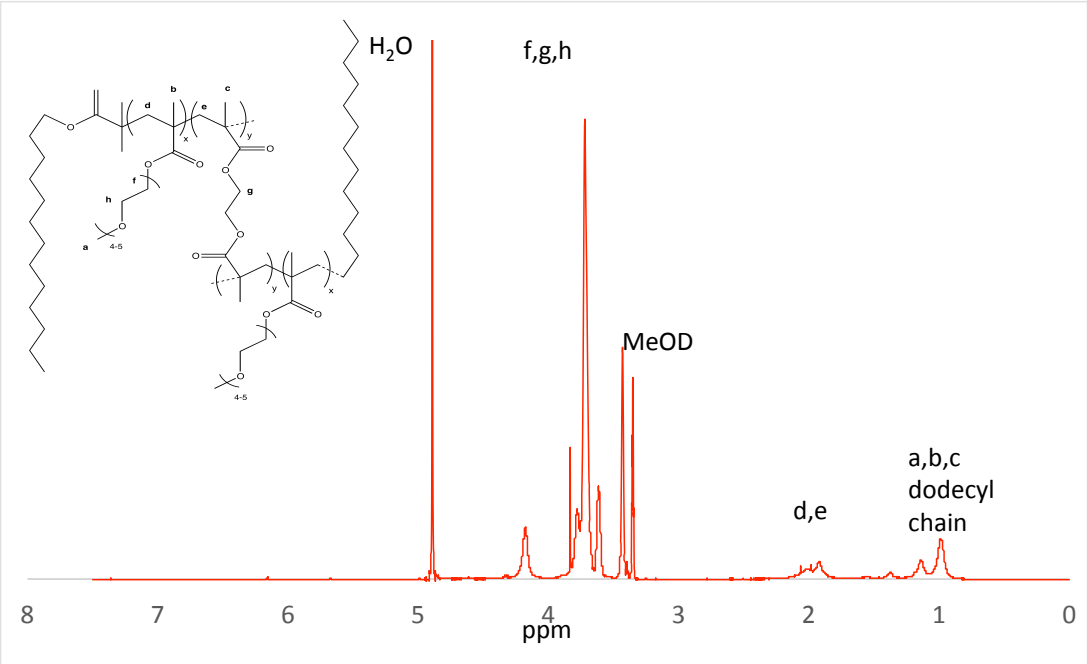


Figure 2.2 $^{1}$H NMR spectrum of PolyOEGMA $DP_{80}$ B at 8 hours. Determined using a Bruker Avance 400 MHz NMR Spectrometer and MeOD as the solvent. A 15-minute scan was performed.

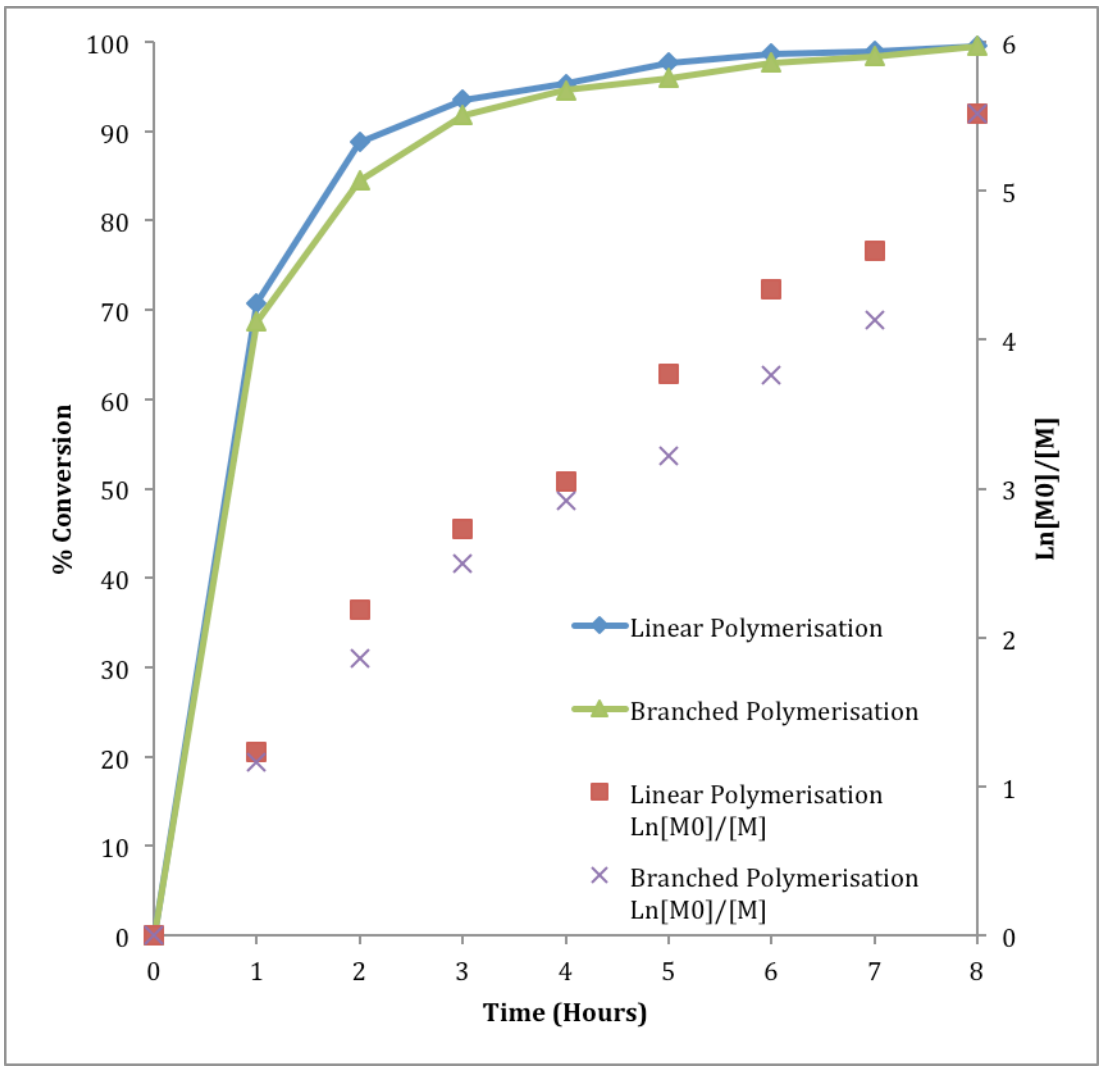


Figure 2.3. Kinetic time course of linear and branched PolyOEGMA $DP_{80}$ polymerised by ATRP at ambient temperature under nitrogen atmosphere. The % conversion was derived from $^{1}H$ NMR spectroscopy by integrating the proton signal of the monomer double bond and deriving the ratio of that to the polymer signal.

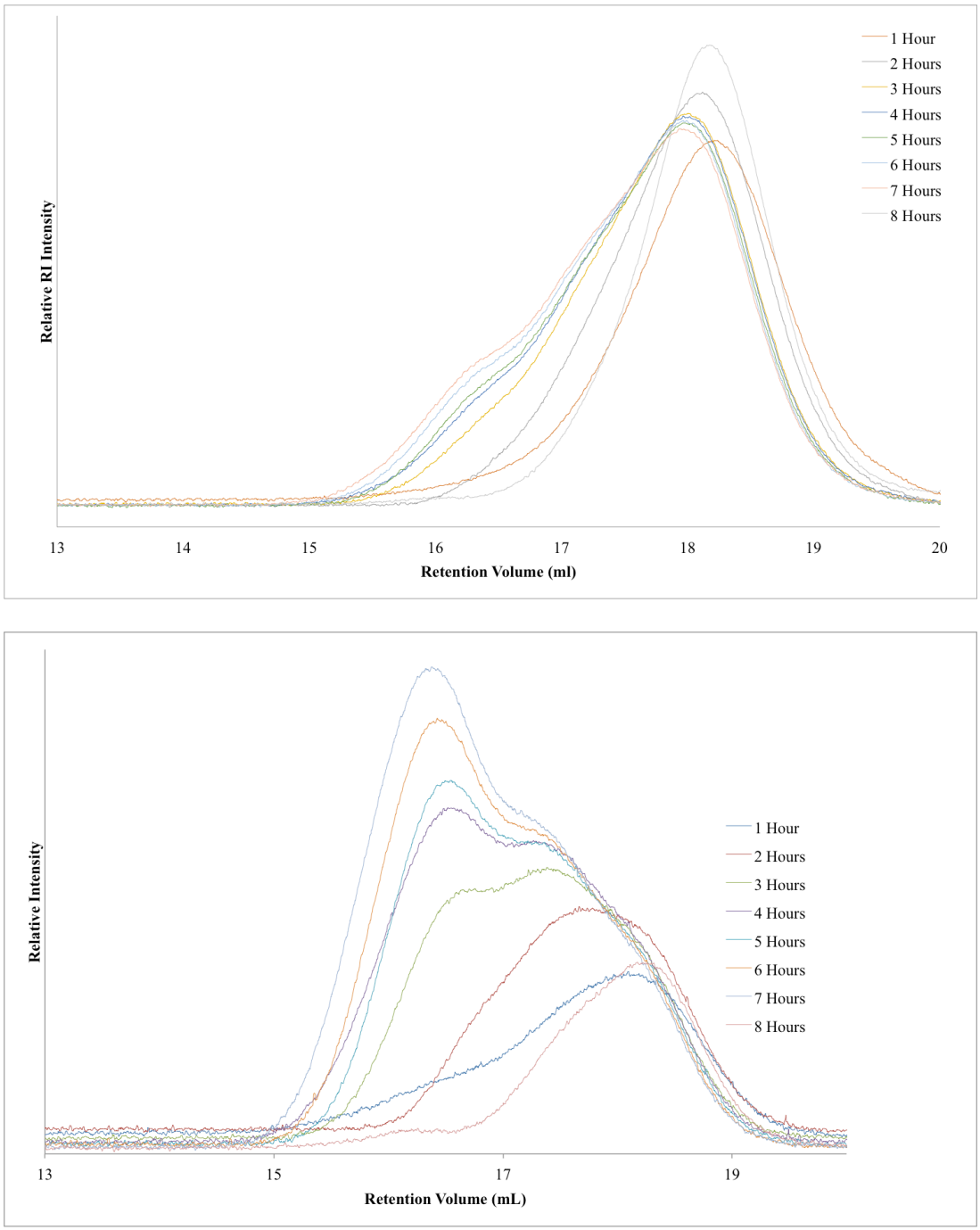


Figure 2.4 GPC Refractive Index (top) and Right Angle Light Scattering (bottom) chromatograms of kinetic time points of linear PolyOEGMA $DP_{80}$ synthesised by ATRP. THF was used as eluent and samples ran for 45 minutes at a flow rate of 1 mL/min. Sample concentration was 2mg/mL.

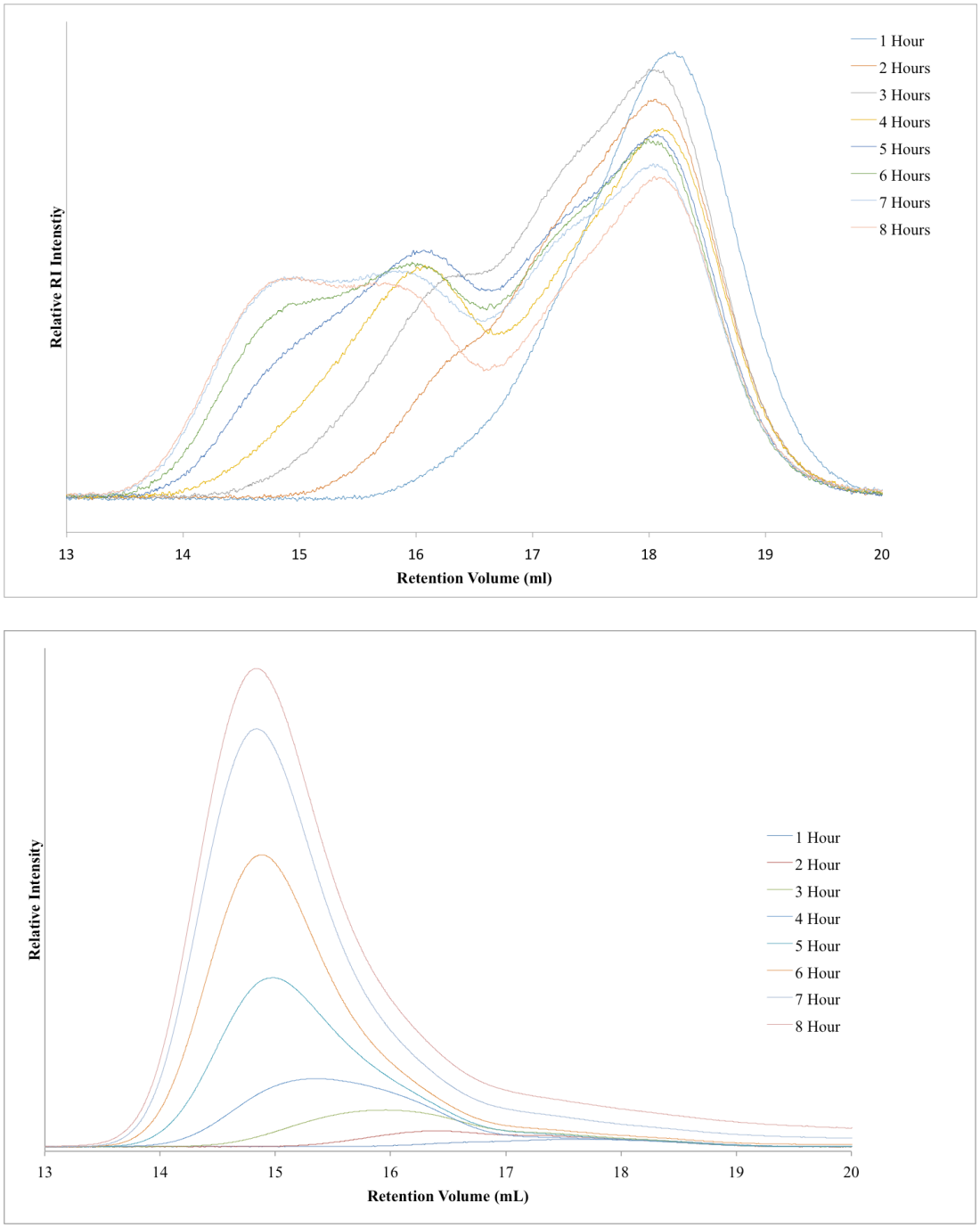


Figure 2.5 GPC Refractive Index (top) and Right Angle Light Scattering (bottom) chromatograms of kinetic time points of branched PolyOEGMA $DP_{80}$ synthesised by ATRP. THF was used as eluent and samples ran for 45 minutes at a flow rate of 1 mL/min. Sample concentration was 2 mg/mL.

### 2.3.3 Free Radical Polymer Cytotoxicity Using CellTiterGlo® ATP Assay

Cytotoxicity of polymers 79-83 (Table 2.1) was assessed using CellTiterGlo® ATP assay in both Caco-2 cell (Figure 2.6) and HepG2 cells (Figure 2.7). $IC_{50}$ values were derived from non-linear regression analysis and are shown in Table 2.3. The polymers were incubated with the cells for 5 days, with the most toxic polymer being 79 in HepG2 cells and 81 in Caco-2 cells, having $IC_{50}$ values of 0.17 % w/v and 0.20 % w/v respectively.

Table 2.3 $IC_{50}$ values of polymers 79-83 after incubation with HepG2 and Caco-2 cell lines for 5 days, at 37°C and 5% $CO_2$. $IC_{50}$ values were determined by CellTiterGlo® ATP assay

| Polymer | HepG2 ($IC_{50}$ %w/v) | Caco-2 ($IC_{50}$ %w/v) |
|---|---|---|
| **79 ($MAA_{96}$/$PEG_{22}MA_4$-$EGDMA_{10}$-$DDT_{10}$)** | 0.17 | 0.39 |
| **80 ($MAA_{92}$/$PEG_{22}MA_8$-$EGDMA_{10}$-$DDT_{10}$)** | 0.52 | 1.15 |
| **81 ($OEG_{4.5}MA_{100}$-$EGDMA_{10}$-$DDT_{10}$)** | 0.40 | 0.20 |
| **82 ($MAA_{82}$/$OEG_{4.5}MA_{18}$-$EGDMA_{10}$-$DDT_{10}$)** | 0.17 | 0.28 |
| **83 ($MAA_{69}$/$OEG_{4.5}MA_{31}$-$EGDMA_{10}$-$DDT_{10}$)** | 0.32 | 0.63 |

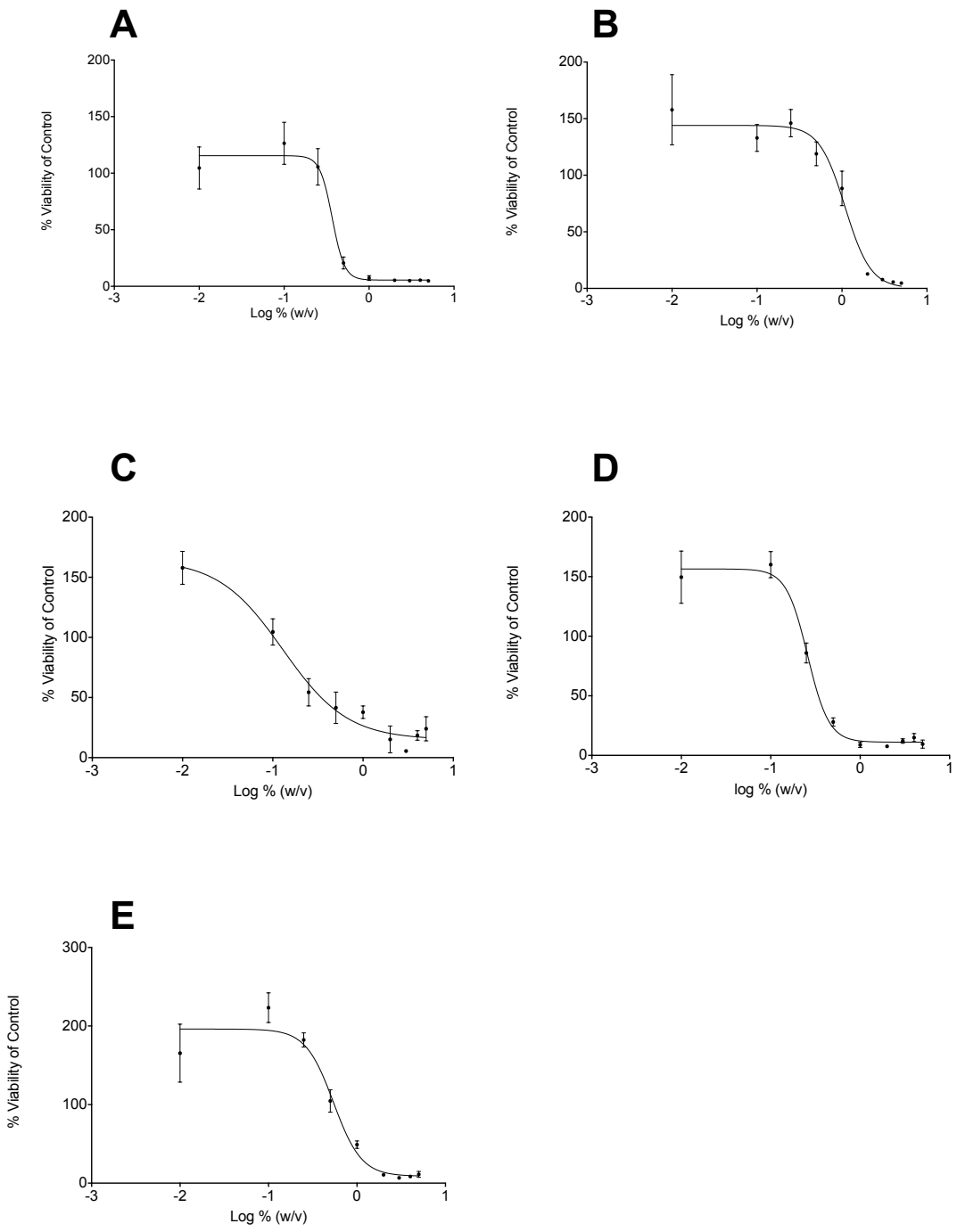


Figure 2.6 Effect of polymers 79-83 (A-E), synthesized by conventional free radical polymerisation, on the metabolic activity of Caco-2 cells determined by ATP assay. As a proxy for cytotoxicity.

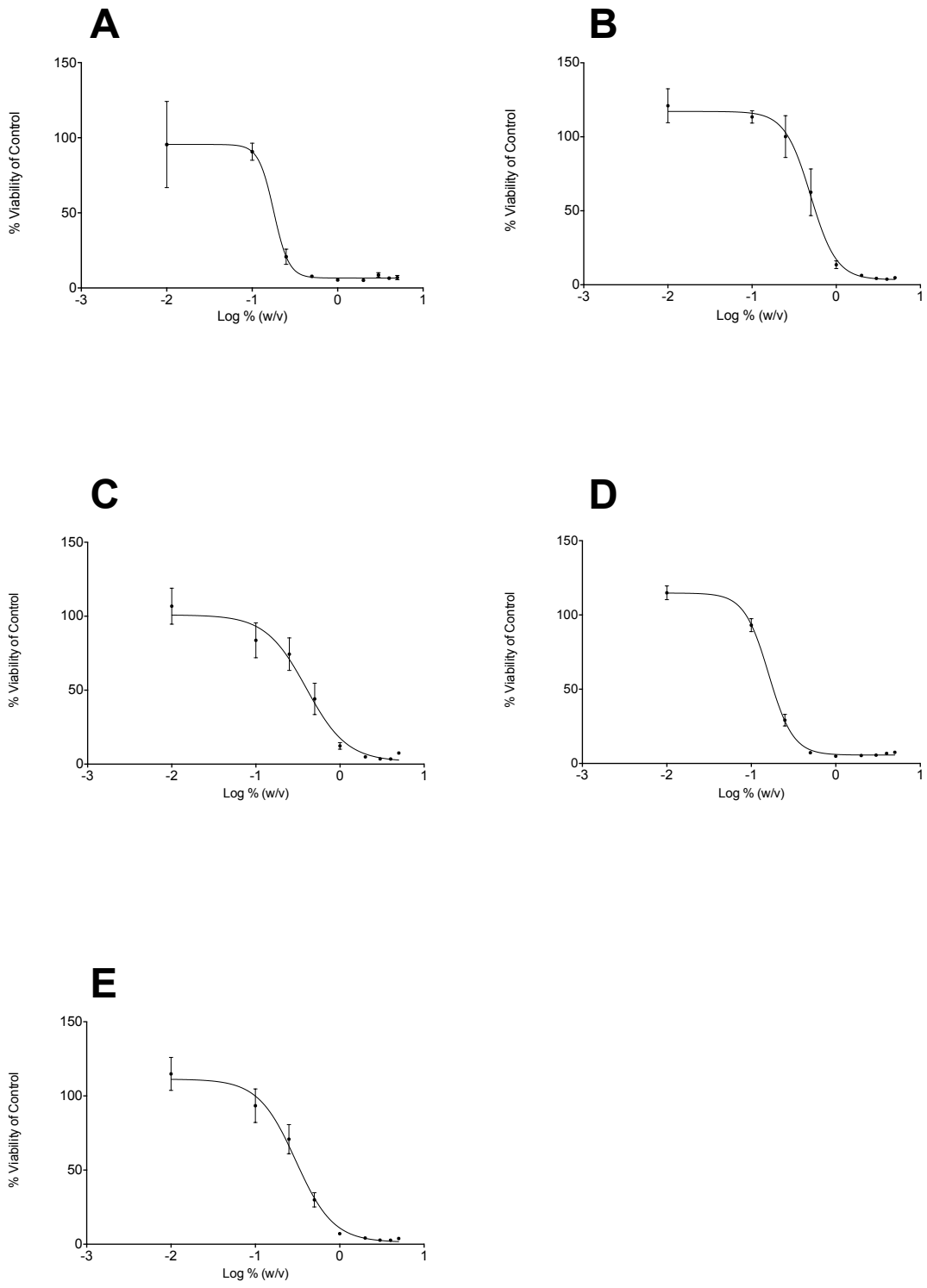


Figure 2.7 Effect of polymers 79-83 (A-E), synthesized by conventional free radical polymerisation, on the metabolic activity of HepG2 cells determined by CellTiterGlo® ATP assay. As a proxy for cytotoxicity

### 2.3.4 ATRP Polymer Cytotoxicity

The cellular cytotoxicity of the optimal branched polymer PolyOEGMA $DP_{80}$, synthesised using ATRP method, was assessed using CellTiterGlo® ATP assay. The results showed that the cytotoxicity shown towards both Caco-2 and HepG2 cells was less than that seen with non ATRP synthesised polymers 79-83, having an $IC_{50}$ value of 0.98 % w/v in HepG2 cells and 2.9 % w/v in Caco-2 cells (Figure 2.8)

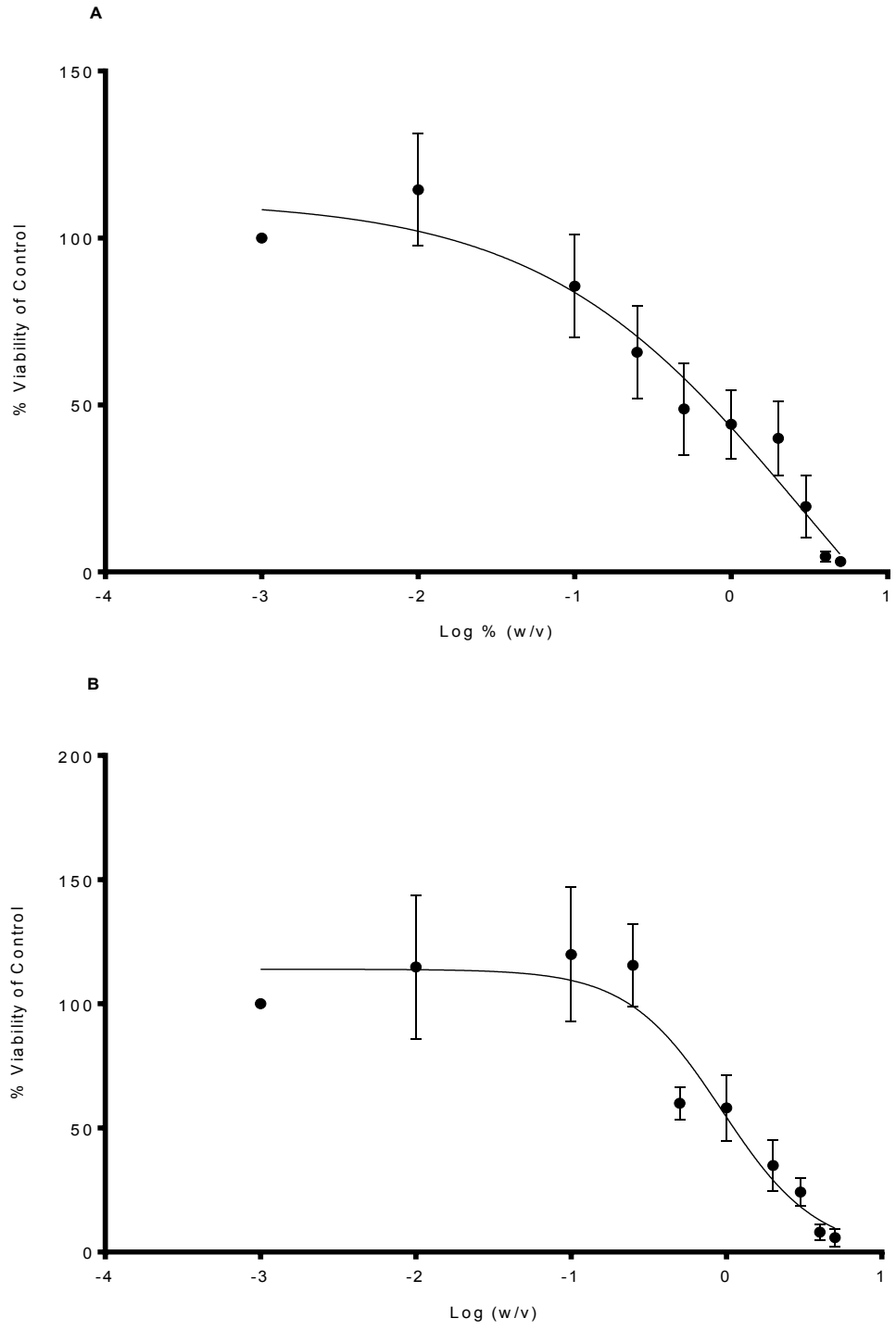


Figure 2.8 Effect of ATRP synthesised Branched PolyOEGMA $DP_{80}$ on the metabolic activity of Caco-2 cells (A) and HepG2 cells (B) as determined by CellTiterGlo® ATP assay. A proxy for cellular cytotoxicity.

## 2.4 Discussion

Initially, conventional free radical polymerisation was used for its facile and one-step approach to synthesising polymer stabilisers. The resultant polymers did, however, vary significantly in their molecular weights, as was to be expected from this type of synthesis. As it was an uncontrolled method, it is not possible to precisely target a desired degree of polymerisation and the dispersity of the polymer samples is high. In a drug delivery setting this is not desirable, as any downstream effects on cellular assays, such as cytotoxicity or membrane integrity, could be variable due to variability in size, charge and amount of polymer present on the nanocarrier. Work by Liu *et al* had shown that these factors influence the cytotoxicity of a nanocarrier system [296], and work conducted by Knetsch *et al* demonstrated a change in polymer cytotoxicity dependent upon amounts of different types of monomer unit present [297]. Therefore having a controlled method that was as reproducible as possible was extremely important. It was for this reason that the uncontrolled free radical approach was abandoned in favour of an ATRP synthesis [298], compounded by cytotoxicity data that was suggestive of non-biocompatible characteristics.

Examining the cytotoxicity of the different conventional free radical polymers used for the stabilisation of emulsions, there was a difference observed between those polymers that were co-polymers of ethylene glycol and methacrylic acid (79, 80, 82 and 83) and those consisting of just poly ethylene glycol repeat units (free radical polymer 81 and ATRP PolyOEGMA $DP_{80}$). This can be put down to the fact that the

methacrylic acid monomer is irritant, toxic and has been shown to be a teratogen [299-301] and even in small quantities, residual unreacted monomer in these polymer mixes would have an effect on cells. Poly(ethylene glycol) on the other hand has a good safety profile and has appeared in many recent publications in the nanomedicine field [302-308].

ATRP allows the primary polymer chain lengths to be tightly controlled, such that a targeted number average degree of polymerisation ($DP_n$) can be used to keep the individual component chain lengths to a desired size. In the case of the final chosen polymer (PolyOEGMA), this was $DP_{80}$, as in 80 repeat units of the monomer per polymer chain [282, 298]. The ATRP method also produced polymers in a much shorter time (8 hours compared to 72 hours), which is beneficial when considering possible scale up issues. For these reasons, PolyOEGMA was chosen as the polymer to stabilise the emulsion droplets. Poly ethylene glycol had also been previously reported in a number of drug formulations [302, 308-319] and appeared in FDA approved formulations [320].

In summary, this work resulted in the selection of branched PolyOEGMA DP80 as a suitable stabiliser for oil-in-water emulsions. The next Chapter will present data that showed that this polymer was also suitable in terms of its effectiveness at stabilising oil-in-water nanoemulsions with desirable physical characteristics, as well as long-term stability.

# CHAPTER 3

# Synthesis and Characterisation of Polymer Stabilised Oil-in-Water Nanoemulsions

**Table of Contents**

## 3.1 Introduction

There are a number of reports in the literature that show a size dependant effect on the cytotoxicity of nanomaterials and nanoformulations [321-326] and, as such, being able to tune the size of a nanoformulation may be highly beneficial. Different sized nanoformulations may also be more or less likely to have specific biological interactions, such as with the immune system [327, 328], uptake into cells [329-331] and permeation across biological barriers [332, 333]

Different methods of synthesis can be employed in order to obtain different sized nanoemulsions, including the use of low energy techniques such as homogenisation and microfluidics [334] or stirring [335], or the use of high energy techniques such as sonication [336] and high pressure homogenisation [337]. The use of low energy techniques has the benefit of being more cost effective, as the equipment needed is less expensive.

A potential drawback of low energy techniques is that the size of the droplets may not be in the desired size range, as the energy put into the system to break up the oil phase into smaller droplets is not as great. To overcome this, it could be possible to use a volatile solvent in combination with the non-volatile oil phase, and subsequently evaporate the volatile solvent component from the emulsion droplets [338]. This would have the effect of reducing the droplet sizes without the need for high power systems.

It is important therefore to select appropriate non-volatile oil and volatile solvent phases that are compatible with each other and also possess a high capacity for drug loading. Castor oil has been used in many cosmetic products and has a full toxicological profile supporting its safety for use in man [339]. It was also shown to be a good solvent for the target antiretroviral drugs efavirenz and lopinavir, with maximum concentrations of 50 mg/mL and 25 mg/mL being achieved, respectively. Castor oil can also be dissolved into ethyl acetate, which is both volatile and has an LD50 in rats of 11.3 g/kg, indicated its low toxicity[340].

As in Chapter 2, Caco-2 and HepG2 cells have been used to assess cytotoxicity of the prepared nanoemulsions, as they are good models for intestinal and liver environments, respectively. In addition to these cells, two immune cell lines have been used to assess cytotoxicity, namely CEM and Raji B cells. These were chosen due to being well established immune cell lines and providing a good starting point for considering the biocompatibility of the candidate nanoemulsions before progressing to *ex vivo* primary human cells (Chapter 6). This is particularly important in the context of HIV, since the target cells reside within the immune system.

Again, as in Chapter 2, CellTiterGlo® assay was used to assess cytotoxicity of nanoemulsions, but here it was also complemented with the 3-(4,5-dimethylthiazol-2-yl)-2,5-diphenyltetrazolium bromide (MTT) assay. Both assays measure cellular viability as function of cell metabolism, but the MTT assay is more widely used and

accepted as a method for assessing cellular viability. Therefore, both assays were employed to facilitate literature comparisons.

Thus, the following Chapter explores the formation and optimisation of an oil-in-water nanoformulation, stabilised with ethylene glycol based amphiphilic polymers. The polymers and their synthesis were previously described in Chapter 2 and were used to make both pH responsive and non-pH responsive emulsion droplets. pH responsive droplets would have the potential benefit of adding a protective effect in the stomach, due to aggregation and shielding of the drug. However, if aggregation was not quickly reversed then the pH responsive emulsions may prove to have no benefit. Nanoemulsions were physically characterised using dynamic light scattering (DLS) techniques to obtain size and surface charge and, for larger emulsions, laser diffraction using a Malvern Mastersizer 2000 was employed.

The aim of this Chapter was to develop a stable nanoemulsion system that was able to be loaded with lopinavir or efavirenz and to assess the cytotoxicity of these nanoemulsions. It was hypothesised that the polymers produced in Chapter 2 would prevent the aggregation of oil droplets, by means of steric stabilisation. Furthermore, it would be expected that methacrylic acid containing polymer stabilisers would produce pH responsive emulsion characteristics, but may have increased cytotoxicity due to the presence of methacrylic acid.

## 3.2 Materials and Methods

### 3.2.1 Materials

In addition to the materials stated in section 2.2.1, the following were also acquired: Acetone, squalene, dodecane, castor oil, peanut oil, soy bean oil, coconut oil, sesame oil, were all purchased from Sigma-Aldrich (Dorset, UK).

TecanGENios 96 well plate reader was supplied by Tecan Group limited (Reading, UK). THP-1 human monocytic cell line, CEM human T Lymphoblast cell line and Raji-B Human Lymphoblastoid cell line were all acquired from stocks stored within the laboratory. 24 well HTS Transwell plates were supplied by Corning Life Sciences (Amsterdam, The Netherlands). Efavirenz and lopinavir were supplied by LGC Pharma (London, UK), and pH meter and refractometer were both obtained from Mettler-Toledo (Greifensee, Switzerland). Zetasizer NanoZS dynamic light scattering equipment and Mastersizer 2000S were supplied by Malvern Instruments, (Malvern, UK). Ultra Turrax T-25 digital homogeniser was bought from IKA Laboratory products (Staufen, Germany) and Sartorius M-Pact balance supplied by Sartorius Lab Products (Epsom, UK).

### 3.2.2 Emulsion Synthesis via Homogenisation

For emulsions prepared using co-polymers of OEGMA or PEGMA with methacrylic acid synthesised via the conventional free radical route (See Section 2.2.1), and not containing a co-solvent, 3 mL of oil phase (squalene, dodecane, or coconut oil) was added to 3 mL of polymer dissolved in water in a 14 mL glass tube. This two-phase mixture was homogenised for 2 minutes using an Ultra Turaxx T-25 digital homogeniser fitted with an S 25 N -10G dispersing element, and set to maximum speed of 25,000 RPM. During the 2 minutes, the vial was rotated clockwise for 30 seconds, anticlockwise for 30 seconds, and then up and down for 1 minute, to achieve a creamy emulsion (figure 3.1). Each emulsion sample was analysed using the Mastersizer 2000.

For emulsions prepared using the cosolvent approach and stabilised using polymers synthesised using the ATRP method, a slightly different methodology was followed before the homogenisation step. Firstly, non-volatile oil and volatile cosolvent were mixed in a desired ratio. A range of ratios (99:1 volatile cosolvent to non-volatile oil, up to 50:50 volatile cosolvent to non volatile oil) was examined in order to find the optimum ratio based on size of nanoemulsion droplets, however, for the experimental data referring to emulsion E65 in the following Chapters of this thesis, a 99:1 volume ratio of volatile cosolvent to non-volatile oil was used. This ratio gave nanoemulsion droplets below 300 nm in diameter. Thus 2.970 mL of volatile cosolvent (ethyl acetate) was added to 30 μL of non-volatile oil (castor oil), to make a total oil/cosolvent phase of 3.00 mL. To this, 3 mL of a 5% w/v concentration of

polymer dissolved in water was added and the homogenisation method detailed previously carried out (figure 3.1). After homogenisation, the cosolvent was evaporated over a period of 24 hours by removing the vial cap and leaving in a fume hood at ambient temperature. These emulsions were analysed for size and charge using Dynamic Light Scattering (DLS).

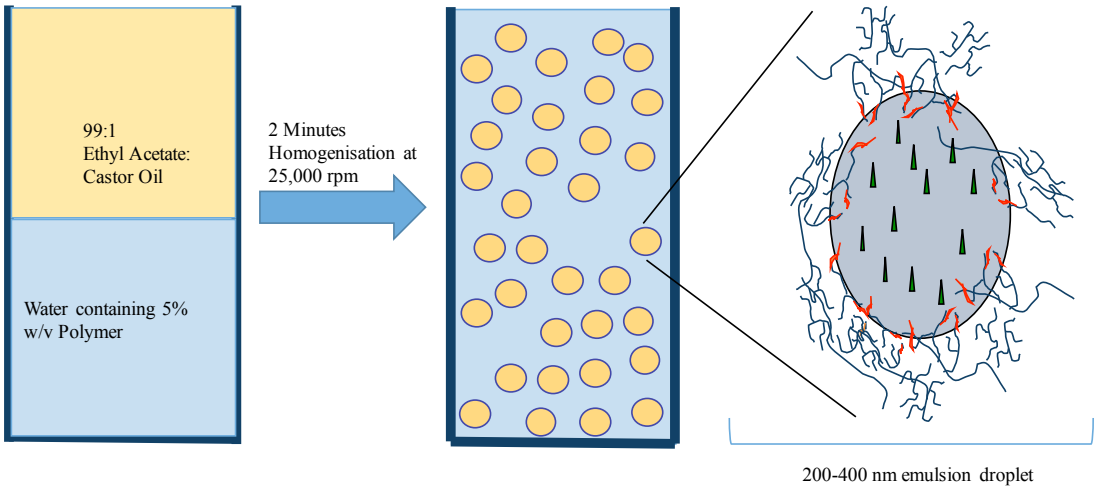


Figure 3.1 Schematic of emulsion formation using homogenisation technique. The active pharmaceutical agent was dissolved in the castor oil and the polymer stabiliser in the water phase. Prior to homogenisation two distinct phases were observed, with a single continuous creamy emulsion phase seen after homogenisation for 2 minutes at 25,000 rpm.

### 3.2.3 Determination of Droplet Diameter using Laser Diffraction

The size of emulsion droplets stabilised with the polymers synthesised by conventional free radical polymerisation (See section 2.3.1) was determined by laser diffraction using a Mastersizer 2000 (Malvern Instruments LTD, Malvern, UK). Briefly, one or two droplets of emulsion were added to the sample dispersion unit until laser obscuration was in the range of 5 and 20%. The unit circulates distilled

water through the laser source and detector, allowing the sample to be continually analysed. The mass moment mean D[4,3] diameter of the emulsion droplets was determined. Five repeat measurements were taken, and the average of those was used to report the D[4,3] diameter of the emulsion droplets. Circulating water was replaced before each new measurement to ensure no contamination.

### 3.2.4 Determination of Droplet Diameter and Surface Charge Using Dynamic Light Scattering

The size of emulsion droplets made using the volatile cosolvent approach and stabilised with polymers synthesised via the ATRP route (see section 2.3.2) were measured using Dynamic Light Scattering (DLS), as they had diameters below that of the Mastersizer lower limit of accurate detection (<1 μm). Samples were measured in plastic 'zeta cells', which allowed for measurement of both z-average diameter and zeta potential (surface charge) Samples were diluted to obtain a laser attenuation of 5 or 6, in order to limit any effects of overly concentrated or dilute samples. Each sample was measured 3 times for both diameter and surface charge, with each measurement having an automated number of scans, as determined by the Zetasizer software, but usually around 12 scans for diameter and 50 scans for zeta potential. The average value from the 3 scans was reported. The temperature within the measurement cell was set to a constant 25 ºC.

### 3.2.5 Adherent Cell Culture

As described in 2.2.8

### 3.2.6 Suspension Cell Culture

As described in 2.2.9

### 3.2.7 Cellular Cytotoxicity using 3-(4,5-dimethylthiazol-2-yl)-2,5-diphenyltetrazolium bromide (MTT) Assay

Approximately 100,000 cells per 100 μL were seeded per well in a 96 well tissue culture plate, leaving 24 hours for cells to adhere to the plate. After this 24-hour period, media was aspirated from all wells and replaced with fresh complete culture media containing appropriate sample concentrations. A maximal drug concentration of 10 μM was used, decreasing in a 1:1 dilution series. For blank emulsion samples were an equivalent volume of nanoemulsion was used to prepare the sample, such that the volume of nanoemulsion was the same as those in the drug loaded nanoemulsion samples.

Plates were left for between 1 and 5 days, after which time 20 μL of 5 mg/mL MTT reagent (3-(4,5-dimethylthiazol-2-yl)-2,5-diphenyltetrazolium bromide) was added to every well and left for 2 hours. At the end of the 2-hour incubation, 100 μL of MTT lysis buffer (50% DMF, 10% SDS, adjusted to pH 3.2 using glacial acetic acid) was added to each well and left for a further 24 hours in order to dissolve formazan crystals. Plates were then read on a Tecan GENios plate reader (Tecan

Group, Manndorf, Switzerland) reader set to absorbance mode, with wavelength at 560 nm.

The assay works on the principle that the mitochondria within the cells being assayed will be able to metabolise the 3-(4,5-dimethylthiazol-2-yl)-2,5-diphenyltetrazolium bromide into formazan. This is provided that the metabolic function of the cells was not affected after exposure to the test compound. The formazan crystals that were formed by this metabolism were dissolved by the lysis buffer and the amount of absorbance was proportional to the metabolic activity of the cells. With all values compared to control wells on each plate that contained only cells and complete cell culture media, it was possible to use the assay as a proxy for cellular viability.

### 3.2.8 Cell TiterGlo® Viability Assay

As described in 2.2.10. A maximal drug concentration of 10 μM was used, decreasing in a 1:1 dilution series. For blank emulsion samples an equivalent volume of nanoemulsion was used to prepare the sample, such that the volume of nanoemulsion was the same as those in the drug loaded nanoemulsion samples.

### 3.3 Results

The following data refers to emulsions stabilised by the polymers described in Chapter 2. They are summarised below in Table 3.1

Table 3.1 Summary of polymer composition and characteristics as determined by GPC analysis. Free radical polymers from are shown as a comparison to the ATRP polymers

| **Polymer Reference Number** | **Conventional Free Radical Branched Polymers** | **$M_w$** | **$M_n$** | **$M_w/M_n$** |
|---|---|---|---|---|
| 79 | $MAA_{96}/PEG_{22}MA_4$-$EGDMA_{10}$-$DDT_{10}$ | 347,500 | 16,616 | 20.9 |
| 80 | $MAA_{92}/PEG_{22}MA_8$-$EGDMA_{10}$-$DDT_{10}$ | 327,528 | 31,827 | 10.3 |
| 81 | $OEG_{4.5}MA_{100}$-$EGDMA_{10}$-$DDT_{10}$ | 16,991 | 6,683 | 2.5 |
| 82 | $MAA_{82}/OEG_{4.5}MA_{18}$-$EGDMA_{10}$-$DDT_{10}$ | 15,312 | 6,369 | 2.4 |
| 83 | $MAA_{69}/OEG_{4.5}MA_{31}$-$EGDMA_{10}$-$DDT_{10}$ | 15,961 | 6,893 | 2.3 |

| **ATRP Polymers** | **$M_w$** | **$M_n$** | **$M_w/M_n$** |
|---|---|---|---|
| Linear PolyOEGMA $DP_{80}$ | 124,526 | 79,511 | 1.6 |
| Branched PolyOEGMA $DP_{80}$ | 3,590,000 | 1,650,000 | 2.2 |

### 3.3.1 Emulsions Stabilised with Polymer prepared by Conventional Free Radical Polymerisation

Two polymers from Table 3.1 (79 and 81) were then used to stabilise oil-in-water emulsions consisting of a squalene oil phase with no volatile cosolvent. The polymer concentration was 5% w/v. In neutral conditions emulsions FR1 (stabilised by polymer 79) and FR2 (stabilised by polymer 81) produced the same average droplet volume moment mean diameter D[4,3] of 9 μm. When the emulsions were placed in acidic conditions, FR1 had a greatly increased average diameter (100 μm) (Figure 3.2), whereas there was very little change in size and distribution for emulsion FR2 (Figure 3.3).

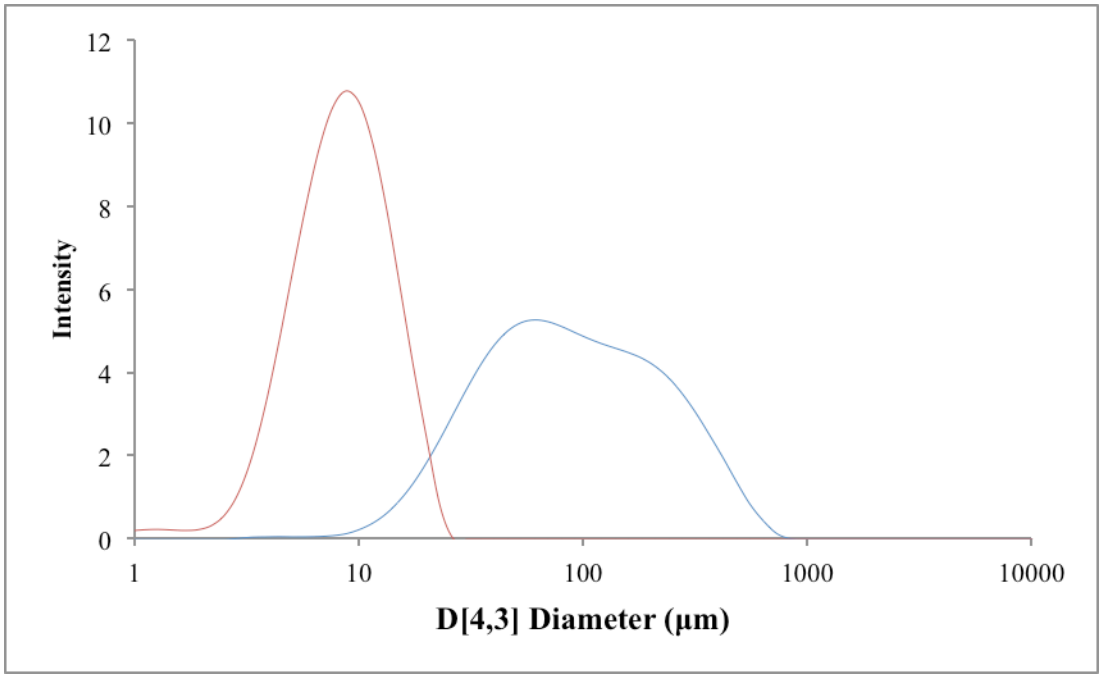


Figure 3.2. Distribution of droplet D[4,3] diameters for emulsion FR1 in pH 7 (red) and pH 2 (blue) as determined by laser diffraction, using a concentration of sample to achieve laser obscuration of between 5 and 20%.

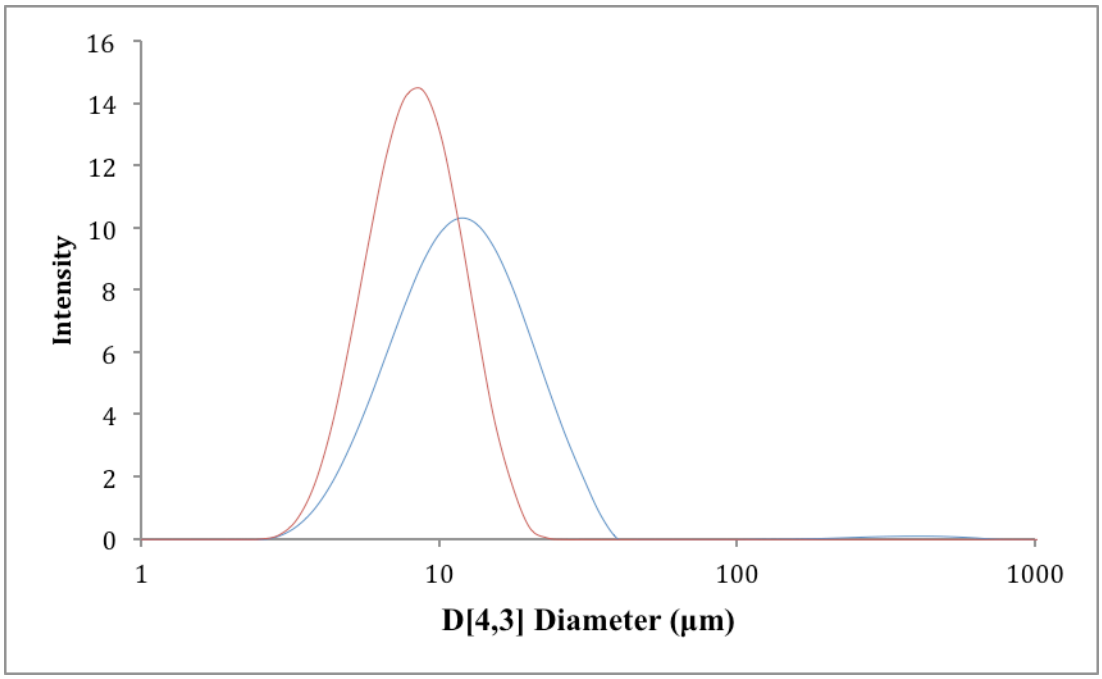


Figure 3.3. Distribution of droplet D[4,3] diameters for emulsion FR2 in pH 7 (red) and pH 2 (blue) as determined by laser diffraction, using a concentration of sample to achieve laser obscuration of between 5 and 20%.

Emulsion FR1 was placed in initial neutral conditions within the Mastersizer and the pH was rapidly dropped to pH 2 by addition of concentrated hydrochloric acid, in order to simulate the conditions upon entering the human digestive tract. The volume moment mean diameter D[4,3] of the droplets was measured every 5 minutes for 150 minutes. At 20 minutes the pH was increased back to pH 7, to simulate the conditions from stomach, through intestine and eventually the systemic circulation. The initial droplet D[4,3] diameter was 9 µm, upon addition of hydrochloric acid this size increased to a maximum of 98 µm. After addition of

sodium hydroxide, to increase the pH back to initial starting conditions, the average droplet D[4,3] diameter slowly began to decrease, eventually reaching a plateau of 22 μm, but not returning to the original droplet size of 9 μm (Figure 3.4).

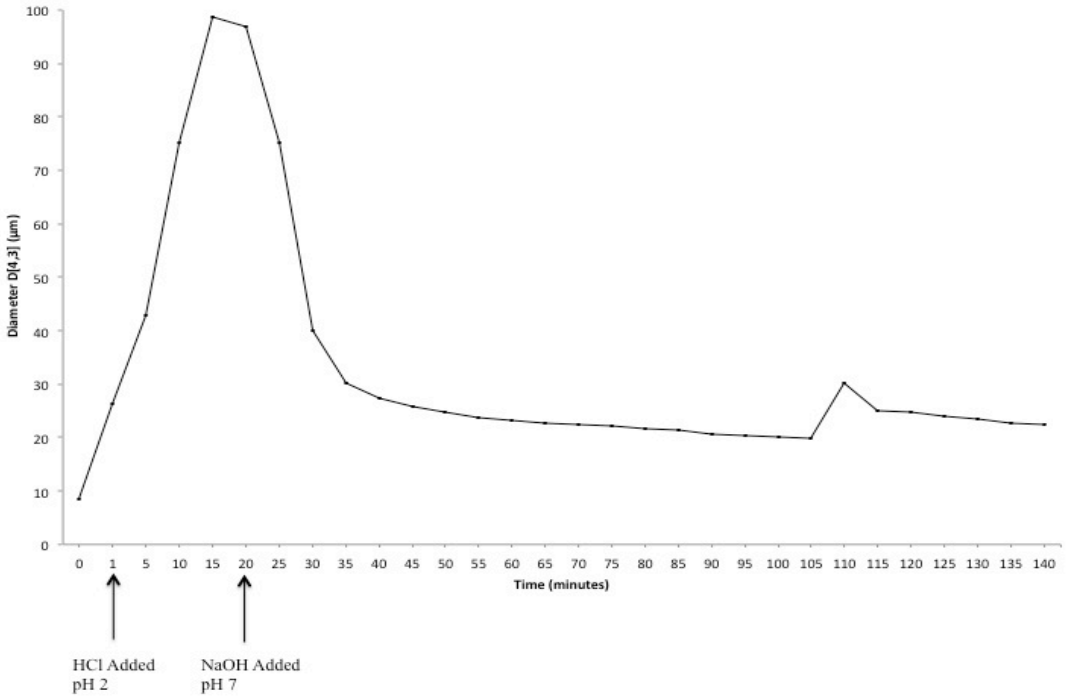


Figure 3.4. Change in average droplet diameter of emulsion 79 after exposure to sudden decrease in pH (pH 10 down to 2) by addition of HCl and subsequent increase in pH back to pH 10 by addition of NaOH. Data obtained by laser diffraction using a concentration of sample to achieve laser obscuration of between 5 and 20%.

### 3.3.2 Nanoemulsions Stabilised by ATRP PolyOEGMA $DP_{80}$ Polymers

A library of nanoemulsions was produced as described in Section 3.2.2 and using the constituents identified in Figure 3.5. This resulted in 74 nanoemulsion samples being produced, which were subsequently assessed for physical characterisation (Figure 3.6 and Tables 3.2 to 3.6). The nanoemulsions were rejected if average diameters exceeded 500 nm, and their stability after emulsification was poor, in terms of particle aggregation over time. There was also a series of experiments conducted to quantify the drug loading capacities of each non-volatile oil phase used, from which castor oil was shown to have the greatest loading capacity at 50 mg/mL of EFV and 25 mg/mL of LPV possible (Data not shown). Based on all of these characteristics, an optimal emulsion formulation was chosen for further studies.

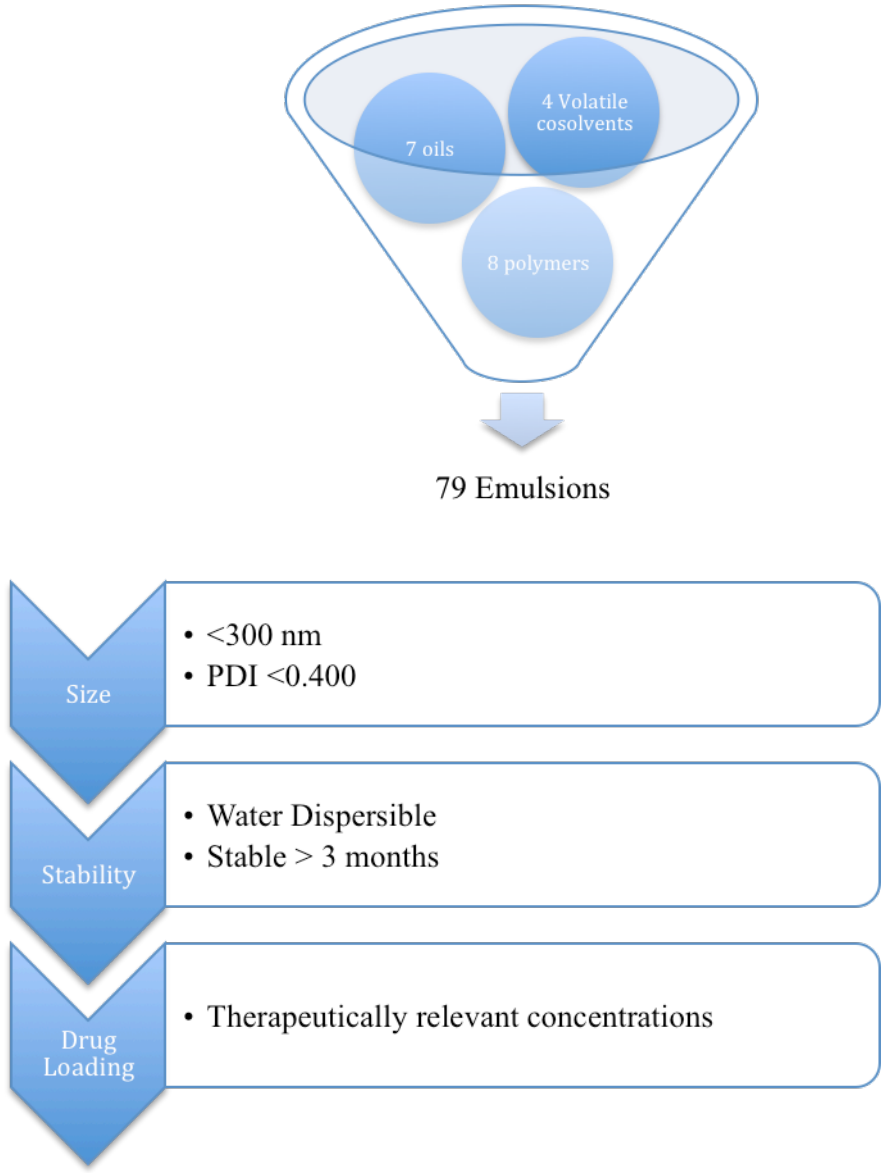


Figure 3.5. Constituent library and Screening protocol for optimisation of drug-loaded nanoemulsions. Oils used were castor oil, peanut oil, soybean oil, sesame oil, squalene, dodecane and coconut oil. 4 volatile co-solvents used were ethyl acetate, hexane, THF and chloroform. Polymers used are described in Table 3.

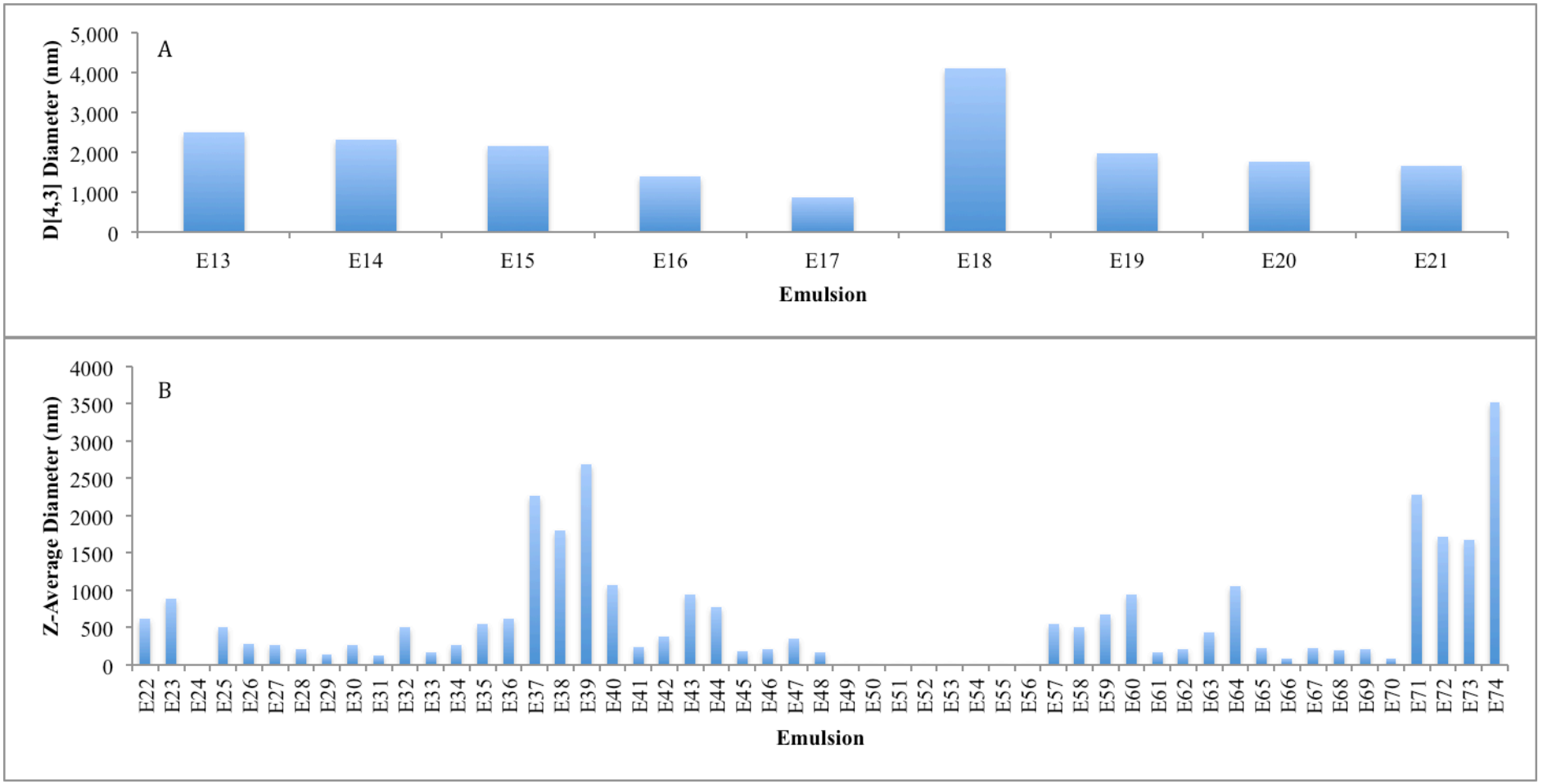


Figure 3.6. Average droplet diameters of the nanoemulsion library as determined by laser diffraction D[4,3] (A) or dynamic light scattering (z-average) (B) (Note: Those with no data bars present had demulsified before the measurement could be taken.

Table 3.2 Composition of emulsions containing coconut oil as the non-volatile oil phase. All polymers are branched unless stated as linear.

| **Identifier** | **Oil** | **Solvent** | **Polymer** |
|---|---|---|---|
| E13 | 100% Coconut Oil | N/A | 5% PolyOEGMA DP50 |
| E14 | 100% Coconut Oil | N/A | 5% PolyOEGMA DP80 |
| E15 | 100% Coconut Oil | N/A | 5% PolyOEGMA FR |
| E16 | 25% Coconut Oil | 75% Hexane | 5% PolyOEGMA DP50 |
| E17 | 25% Coconut Oil | 75% Hexane | 5% PolyOEGMA DP80 |
| E18 | 25% Coconut Oil | 75% Hexane | 5% PolyOEGMA FR |
| E19 | 10% Coconut Oil | 90% Hexane | 5% PolyOEGMA DP50 |
| E20 | 10% Coconut Oil | 90% Hexane | 5% PolyOEGMA DP80 |
| E21 | 10% Coconut Oil | 90% Hexane | 5% PolyOEGMA FR |
| E22 | 1% Coconut Oil | 99% Hexane | 5% PolyOEGMA DP50 |
| E23 | 1% Coconut Oil | 99% Hexane | 5% PolyOEGMA DP80 |
| E24 | 1% Coconut Oil | 99% Hexane | 5% PolyOEGMA FR |
| E41 | 10% Coconut Oil | 90% Ethyl Acetate | 5% PolyOEGMA DP50 |
| E42 | 10% Coconut Oil | 90% Ethyl Acetate | 5% PolyOEGMA DP80 |
| E43 | 10% Coconut Oil | 90% Ethyl Acetate | 5% PolyPEGMA DP50 (Linear) |
| E44 | 10% Coconut Oil | 90% Ethyl Acetate | 5% PolyPEGMA DP50 |
| E45 | 1% Coconut Oil | 99% Ethyl Acetate | 5% PolyOEGMA DP50 |
| E46 | 1% Coconut Oil | 99% Ethyl Acetate | 5% PolyOEGMA DP80 |
| E47 | 1% Coconut Oil | 99% Ethyl Acetate | 5% PolyPEGMA DP50 (Linear) |
| E48 | 1% Coconut Oil | 99% Ethyl Acetate | 5% PolyPEGMA DP50 |

Table 3.3 Composition of emulsions containing 100% volatile solvent phase. All polymers are branched unless stated as linear.

| **Identifier** | **Oil** | **Solvent** | **Polymer** |
|---|---|---|---|
| E27 | N/A | 100% Hexane | 5% PolyOEGMA DP80 |
| E27 | N/A | 100% Hexane | 5% PolyOEGMA DP80 |
| E28 | N/A | 100% Hexane | 5% PolyOEGMA DP50 |
| E29 | N/A | 100% Hexane | 5% PolyPEGMA DP50 (Linear) |
| E30 | N/A | 100% Hexane | 5% PolyPEGMA DP50 |
| E37 | N/A | 100% Ethyl Acetate | 5% PolyOEGMA DP50 |
| E38 | N/A | 100% Ethyl Acetate | 5% PolyOEGMA DP80 |
| E39 | N/A | 100% Ethyl Acetate | 5% PolyPEGMA DP50 (Linear) |
| E40 | N/A | 100% Ethyl Acetate | 5% PolyPEGMA DP50 |

Table 3.4 Composition of emulsions containing dodecanoic acid as the non-volatile oil phase. All polymers are branched unless stated as linear.

| **Identifier** | **Oil** | **Solvent** | **Polymer** |
|---|---|---|---|
| E4 | 50% Dodecanoic Acid | 50% Chloroform | 2% PolyOEGMA DP50 |
| E25 | 10% Dodecanoic Acid | 90% Hexane | 5% PolyOEGMA DP80 |
| E26 | 1% Dodecanoic Acid | 99% Hexane | 5% PolyOEGMA DP80 |
| E49 | 10% Dodecanoic Acid | 90% Ethyl Acetate | 5% PolyOEGMA DP50 |
| E50 | 10% Dodecanoic Acid | 90% Ethyl Acetate | 5% PolyOEGMA DP80 |
| E51 | 10% Dodecanoic Acid | 90% Ethyl Acetate | 5% PolyPEGMA DP50 (Linear) |
| E52 | 10% Dodecanoic Acid | 90% Ethyl Acetate | 5% PolyPEGMA DP50 |
| E53 | 1% Dodecanoic Acid | 99% Ethyl Acetate | 5% PolyOEGMA DP50 |
| E54 | 1% Dodecanoic Acid | 99% Ethyl Acetate | 5% PolyOEGMA DP80 |
| E55 | 1% Dodecanoic Acid | 99% Ethyl Acetate | 5% PolyPEGMA DP50 (Linear) |
| E56 | 1% Dodecanoic Acid | 99% Ethyl Acetate | 5% PolyPEGMA DP50 |

Table 3.5 Composition of emulsions containing squalene as the non-volatile oil phase. All polymers are branched unless stated as linear.

| **Identifier** | **Oil** | **Solvent** | **Polymer** |
|---|---|---|---|
| E31 | 10% Squalene | 90% Hexane | 5% PolyOEGMA DP50 |
| E32 | 10% Squalene | 90% Hexane | 5% PolyPEGMA DP50 (Linear) |
| E33 | 10% Squalene | 90% Hexane | 5% PolyPEGMA DP50 |
| E34 | 1% Squalene | 99% Hexane | 5% PolyPEGMA DP50 (Linear) |
| E35 | 1% Squalene | 99% Hexane | 5% PolyPEGMA DP50 |
| E36 | 1% Squalene | 99% Hexane | 5% PolyOEGMA DP50 |
| E57 | 10% Squalene | 90% Ethyl Acetate | 5% PolyOEGMA DP50 |
| E58 | 10% Squalene | 90% Ethyl Acetate | 5% PolyOEGMA DP80 |
| E59 | 10% Squalene | 90% Ethyl Acetate | 5% PolyPEGMA DP50 (Linear) |
| E60 | 10% Squalene | 90% Ethyl Acetate | 5% PolyPEGMA DP50 |
| E61 | 1% Squalene | 99% Ethyl Acetate | 5% PolyOEGMA DP50 |
| E62 | 1% Squalene | 99% Ethyl Acetate | 5% PolyOEGMA DP80 |
| E63 | 1% Squalene | 99% Ethyl Acetate | 5% PolyPEGMA DP50 (Linear) |
| E64 | 1% Squalene | 99% Ethyl Acetate | 5% PolyPEGMA DP50 |

Table 3.6 Composition of emulsions containing castor oil, sesame oil, peanut oil, soybean oil or O-Xylene as the non-volatile oil phase. All polymers are branched unless stated as linear.

| **Identifier** | **Oil** | **Solvent** | **Polymer** |
|---|---|---|---|
| E65 | 1% Castor Oil | 99% Ethyl Acetate | 5% PolyOEGMA DP80 |
| E66 | 1% Sesame Oil | 99% Ethyl Acetate | 5% PolyOEGMA DP80 |
| E67 | 1% Peanut Oil | 99% Ethyl Acetate | 5% PolyOEGMA DP80 |
| E68 | 1% Soybean Oil | 99% Ethyl Acetate | 5% PolyOEGMA DP80 |
| E69 | 1% O-Xylene | 99% Ethyl Acetate | 5% PolyOEGMA DP80 |
| E70 | 1% Castor Oil | 99% Hexane | 5% PolyOEGMA DP80 |
| E71 | 1% Sesame Oil | 99% Hexane | 5% PolyOEGMA DP80 |
| E72 | 1% Peanut Oil | 99% Hexane | 5% PolyOEGMA DP80 |
| E73 | 1% Soybean Oil | 99% Hexane | 5% PolyOEGMA DP80 |
| E74 | 1% O-Xylene | 99% Hexane | 5% PolyOEGMA DP80 |

### 3.3.3 Nanoemulsion With Optimal Droplet Diameter, Stability and Drug Loading Capacity

The optimal nanoemulsion in terms of its droplet diameter (< 300 nm) and its long-term stability in terms of lack of aggregation over time (> 2 years) was selected from the group of emulsion described in Section 3.3.2. It was stabilised with a 5% w/v solution of PolyOEGMA $DP_{80}$, had a non-volatile oil core consisting of castor oil, and ethyl acetate was used as the volatile cosolvent. This emulsion had a ratio of 99:1 ethyl acetate to castor oil, prior to homogenisation and subsequent evaporation of ethyl acetate and will be referred to from hereon in as E65.

Changing the solvent to oil ratio within the emulsion prior to homogenisation allowed the final size of the droplets to be finely tuned. Increasing the ratio of non volatile castor oil increased the overall droplet size, until at 50:50 ethyl acetate to castor oil, the droplet sizes were in excess of 1 μm (Figure 3.7)

The sizes of the droplets could also be tuned by changing the concentration of branched PolyOEGMA $DP_{80}$, whilst maintaining the ethyl acetate to castor oil ratio at 99:1. An optimal concentration of 5% w/v of PolyOEGMA $DP_{80}$ was found to confer the greatest stability and smallest sizes to the emulsions. Concentration >5% w/v of branched PolyOEGMA $DP_{80}$ did not result in emulsion droplets with smaller z-average diameters, but below 5% w/v, droplet z-average diameters were seen to increase (Figure 3.8). The change in particle size distribution when the concentration of polymer stabiliser was changed is shown in Figure 3.9.

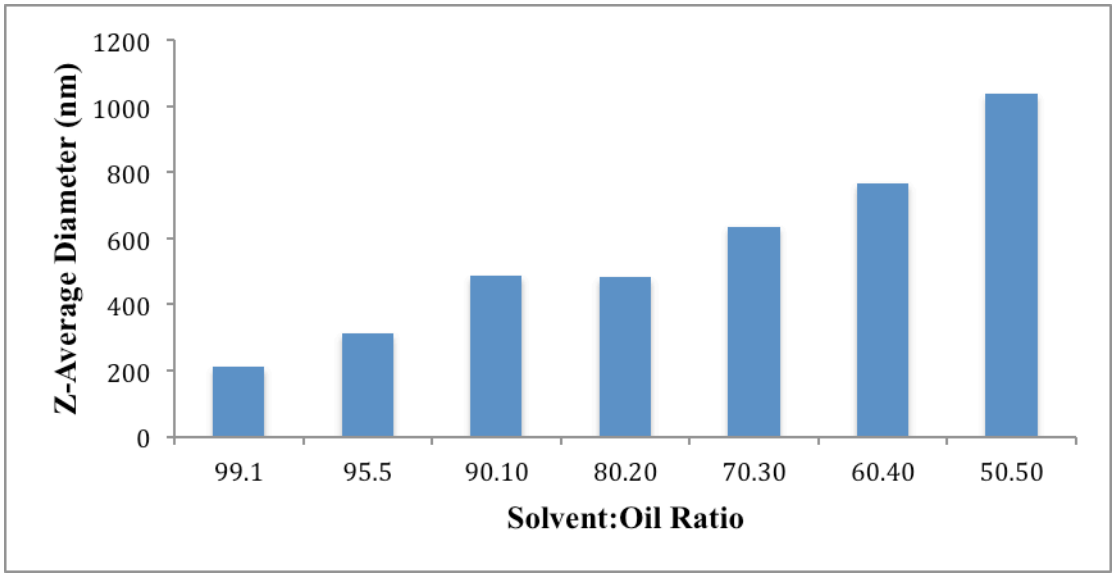


Figure 3.7 Effect on size of changing the ratio of cosolvent to oil prior to homogenisation. Increasing the amount of cosolvent resulted in smaller final droplet diameters, after evaporation for 24 hours. Droplet diameters were determined by dynamic light scattering

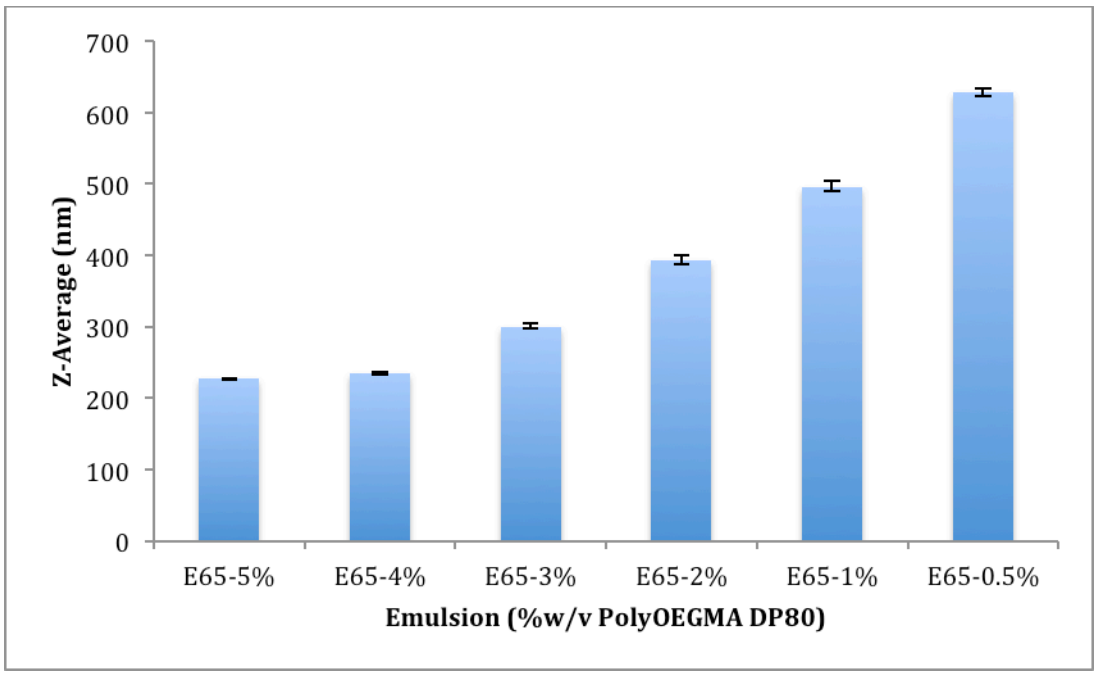


Figure 3.8. Effect on droplet diameter as a result of changing the final concentration of polymer stabiliser from between 0.5% w/v and 5% w/v. The cosolvent to oil ratio was maintained at 99:1. Droplet diameters were determined using dynamic light scattering.

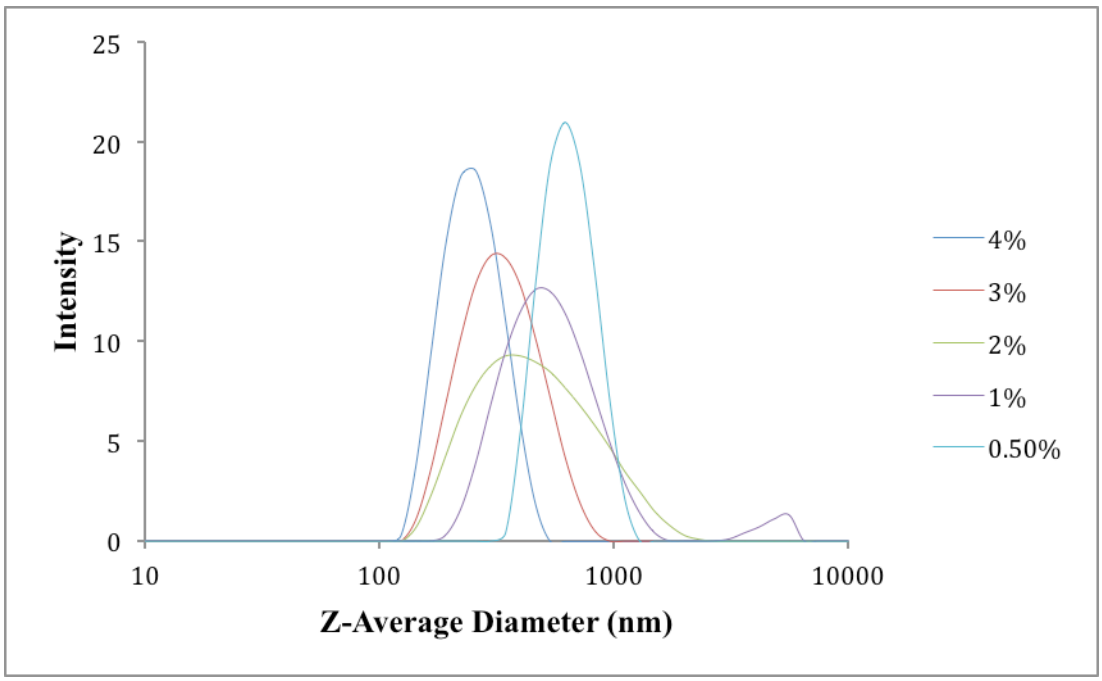


Figure 3.9 Effect on the distribution of droplet diameters as a result of altering the % w/v of polymer stabiliser between 0.5% w/v and 5% w/v. Cosolvent to oil ratio was maintained at 99:1. Droplet diameters were determined using dynamic light scattering.

E65 could be loaded with either EFV or LPV and for comparisons; a blank emulsion containing castor oil without any loaded drug was also produced. The average droplet sizes were the same regardless of which drug was dissolved in the non-volatile oil phase (Figures 3.10 and 3.11), and this was true also for the surface charge (Figure 3.12). The concentration of drug in the final undiluted emulsion was 1.59 mM for EFV and 379 μM for LPV.

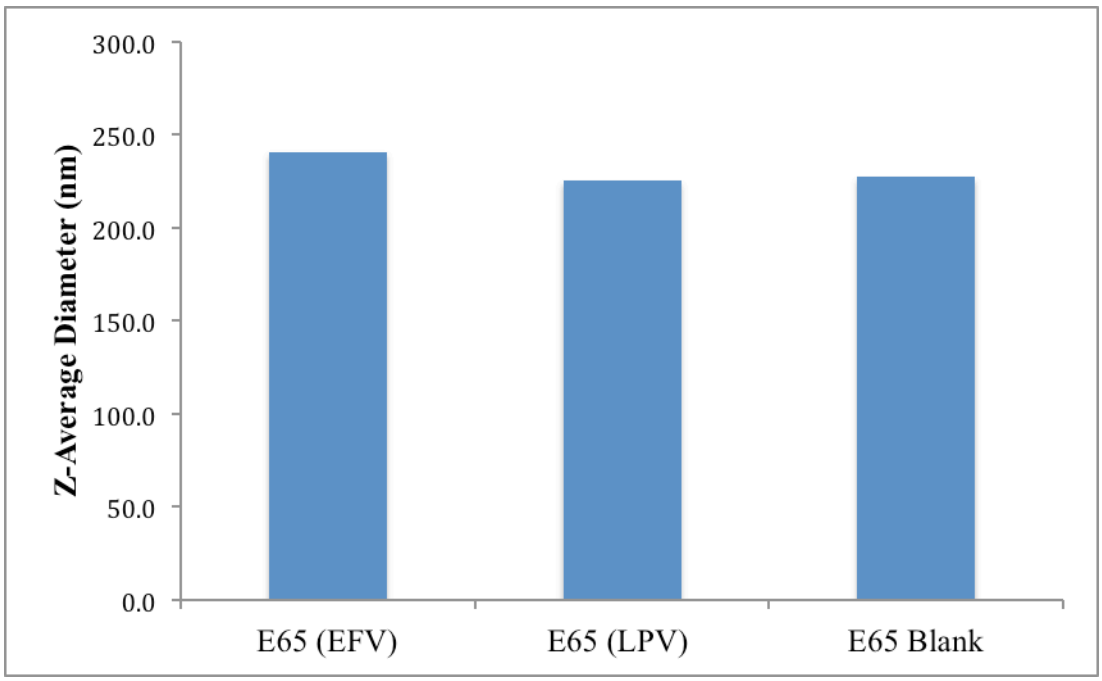


Figure 3.10 Z-average diameters of blank, efavirenz and lopinavir loaded E65 emulsions. Data was obtained using dynamic light scattering, with a 100-fold dilution of neat emulsion sample in order to obtain laser attenuation between 5 and 7.

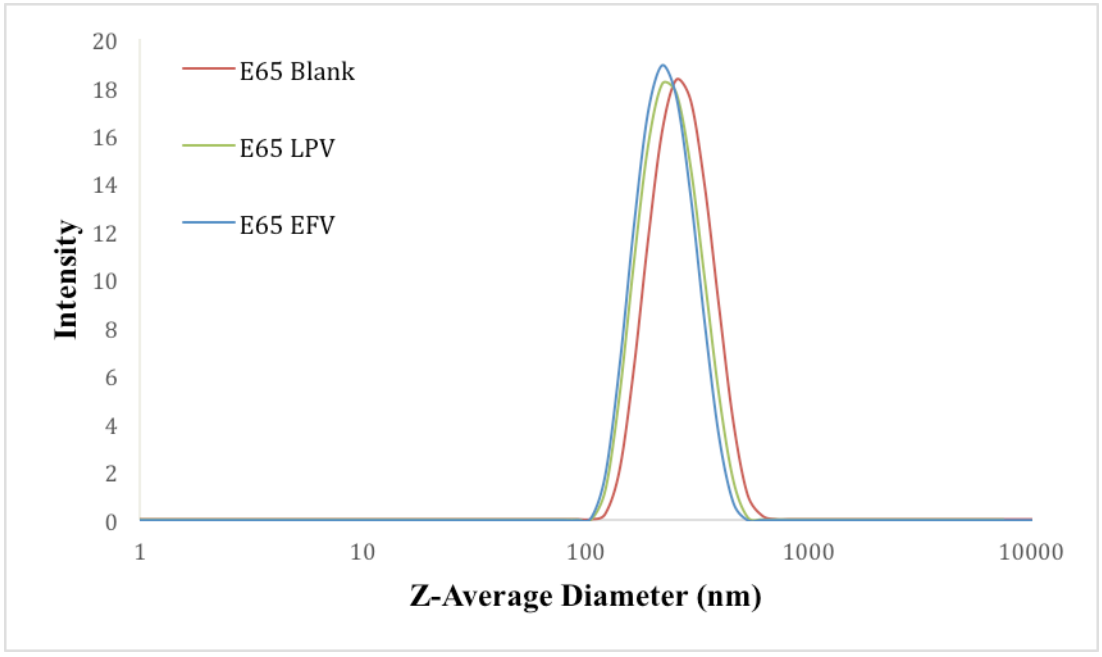


Figure 3.11 Z-Average droplet diameter distribution of E65 nanoemulsion loaded with EFV, LPV or no drug. Data was obtained using dynamic light scattering, with a 100-fold dilution of neat emulsion sample in order to obtain laser attenuation between 5 and 7.

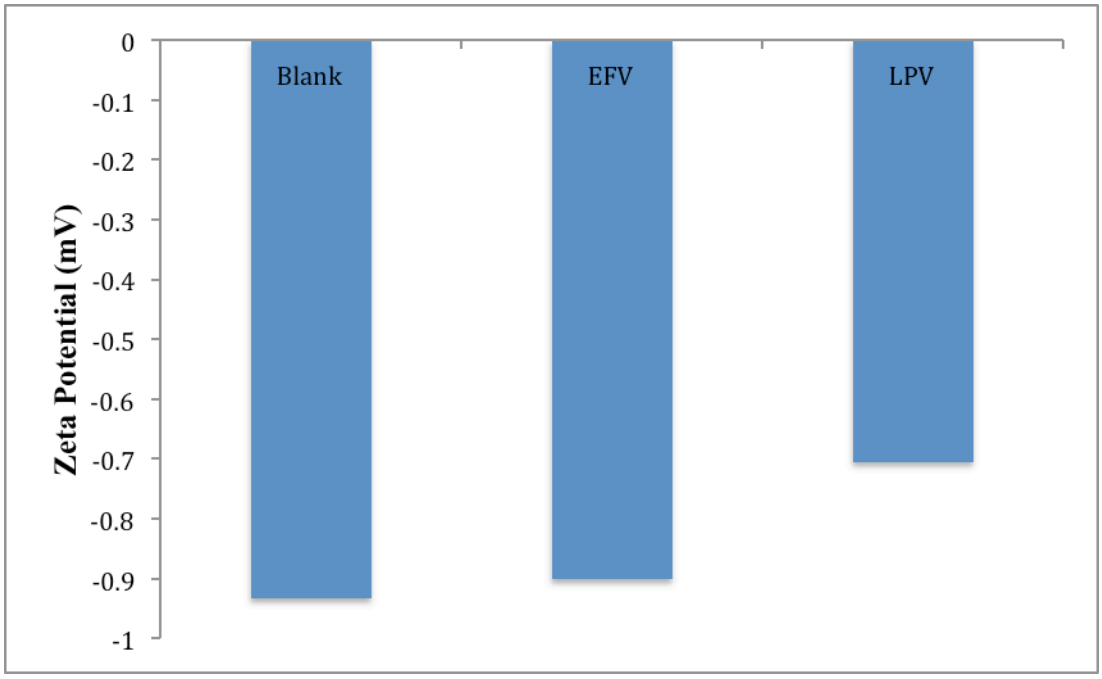


Figure 3.12 Zeta potential of blank, EFV and LPV loaded emulsion E65. Here, Zeta potential refers to the potential difference between the nanoemulsion droplets and the aqueous phase into which they were dispersed (distilled water). Data was obtained using a zeta cell and dynamic light scattering, with a 100-fold dilution of neat emulsion sample in order to obtain laser attenuation between 5 and 7 using a Malvern Zetasizer Nano ZS.

The long-term stability of E65 was shown to be in excess of 2 years in water, whether loaded with EFV, LPV or no drug. This was determined by assessing the nanoemulsion diameter and the distribution of nanoemulsion droplet size over time. A shorter stability study was carried out using E65 dissolved into complete cell culture media (DMEM) and left at 4°C for 3 months. Again emulsions remained stable over this period. However, unlike storage in water, the medium diluted emulsions had slightly smaller average droplet sizes; 194 nm for EFV loaded E65 and 164 nm for Blank E65 compared to 294 nm for the same emulsion in water (Figure 3.13).

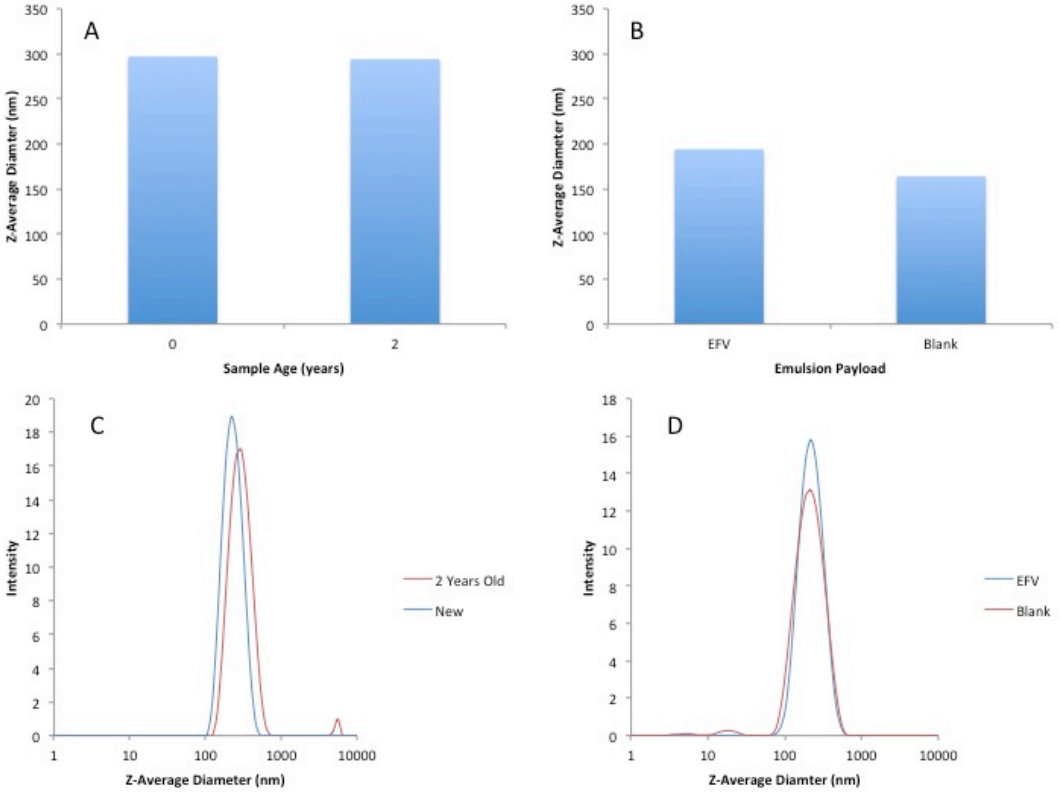


Figure 3.13. Two-year stability of emulsion E65 (A) and stability study of emulsion diluted in biological media after 3 months storage at 4°C (B). Corresponding DLS size distributions for two-year stability study (C) and media stability study (D). Data was obtained using dynamic light scattering, with a 100-fold dilution of neat emulsion sample in order to obtain laser attenuation between 5 and 7.

The stability of emulsion droplets when diluted was also assessed (Figure 3.14). Emulsions were seen to maintain the same droplet size throughout each dilution, to a maximum of 4096 fold dilution. Further dilution past this point rendered the emulsion sample too dilute to be detected and analysed by the DLS instrument. DLS measurements could not be reliably taken until a 4-fold dilution of the neat emulsion was made, due to multiple scattering artefacts affecting the reported z-average diameters.

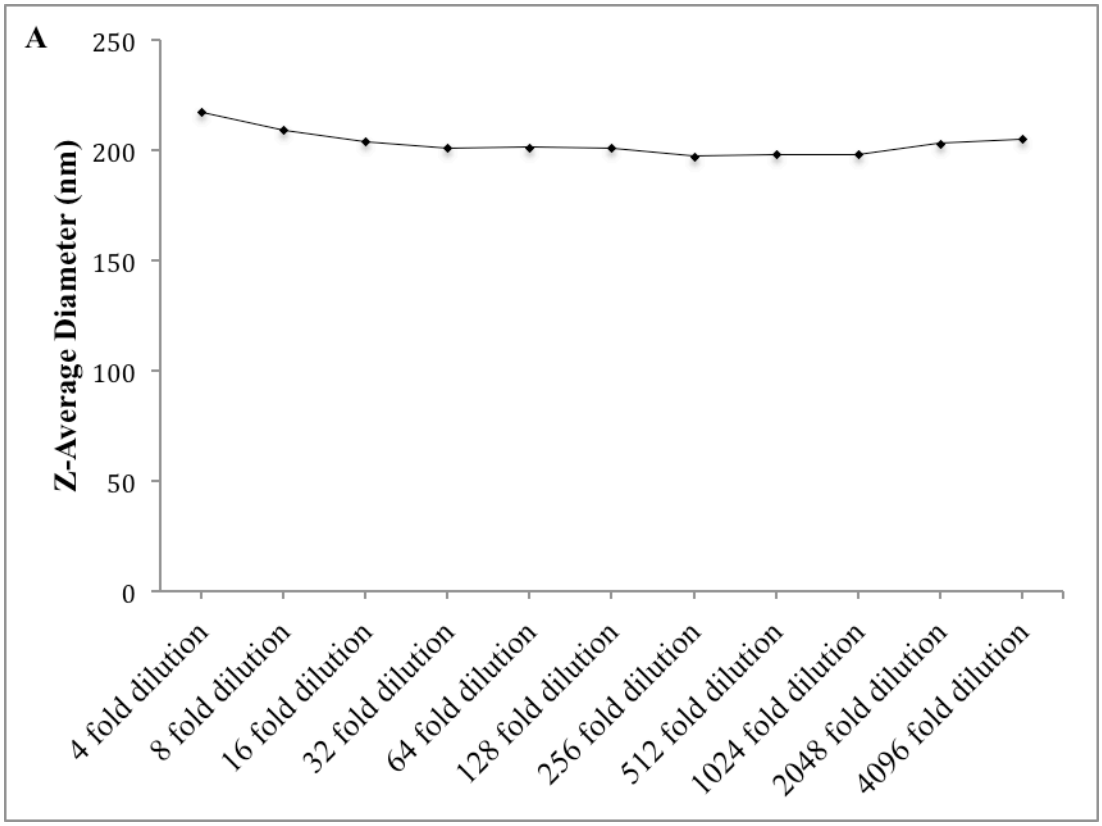


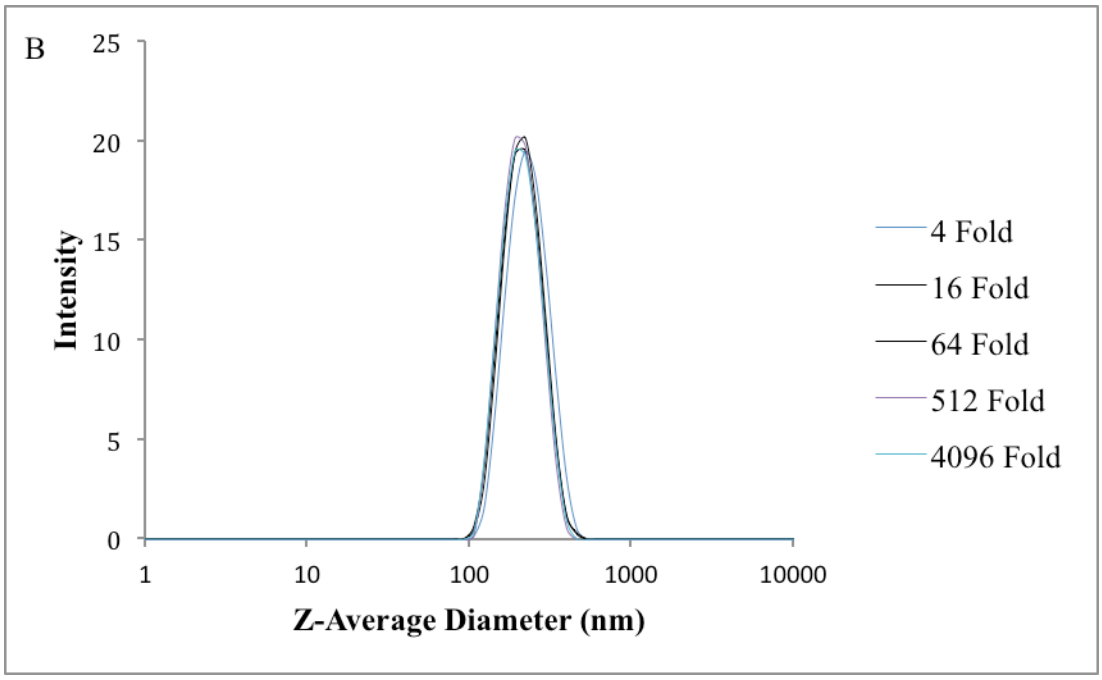


Figure 3.14 Stability of emulsion E65 when diluted in water up to 4096 fold, as determined by no change in z-average diameters (A) and size distributions (B). Data was obtained using dynamic light scattering, with a 100-fold dilution of neat emulsion sample in order to obtain laser attenuation between 5 and 7.

### 3.3.4 Nanoemulsion Cytotoxicity

#### 3.3.4.1 Caco-2 Cells

The final optimised emulsion E65 (3.3.3) was assessed for its cytotoxicity against Caco-2 cells, both as a blank emulsion and having a payload of EFV or LPV. The cytotoxicity of the emulsion was compared to that of an equivalent concentration of an aqueous solution of EFV and LPV. The results for MTT assay showed that the EFV aqueous formulation had an $IC_{50}$ value of 55 μM but that the LPV aqueous solution did not show any overt cytotoxicity at the concentrations tested, as reported by the non-convergence of sigmoidal dose response curves (Figure 3.15). The same was observed for EFV and LPV loaded nanoemulsions, as well blank nanoemulsion in that no convergence occurred (Figure 3.15).

The data from the CellTiterGlo® ATP assay this time showed no convergence for EFV aqueous solution but an $IC_{50}$ value of 31.5 μg/ml for aqueous LPV. There was also no convergence for EFV nanoemulsion (nEFV), LPV nanoemulsion (nLPV), and blank nanoemulsions (Figure 3.16).

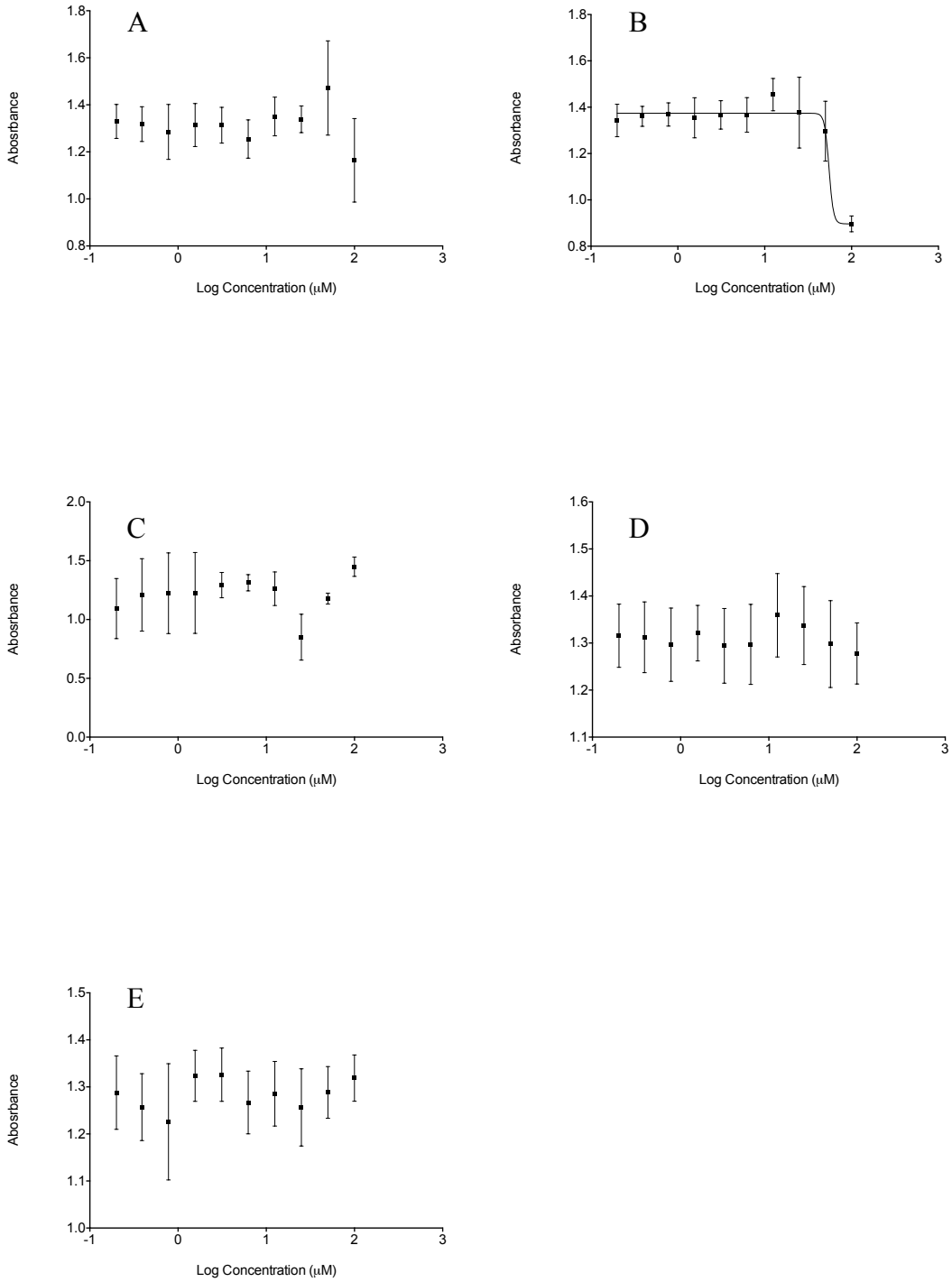


Figure 3.15 Effect of LPV aqueous solution (A), EFV aqueous solution (B), LPV nanoemulsion (C), EFV nanoemulsion (D) and blank nanoemulsion (E), on the metabolic activity of Caco-2 cells determined by MTT assay. Metabolic activity is proportional to absorbance, and used as a proxy for cytotoxicity.

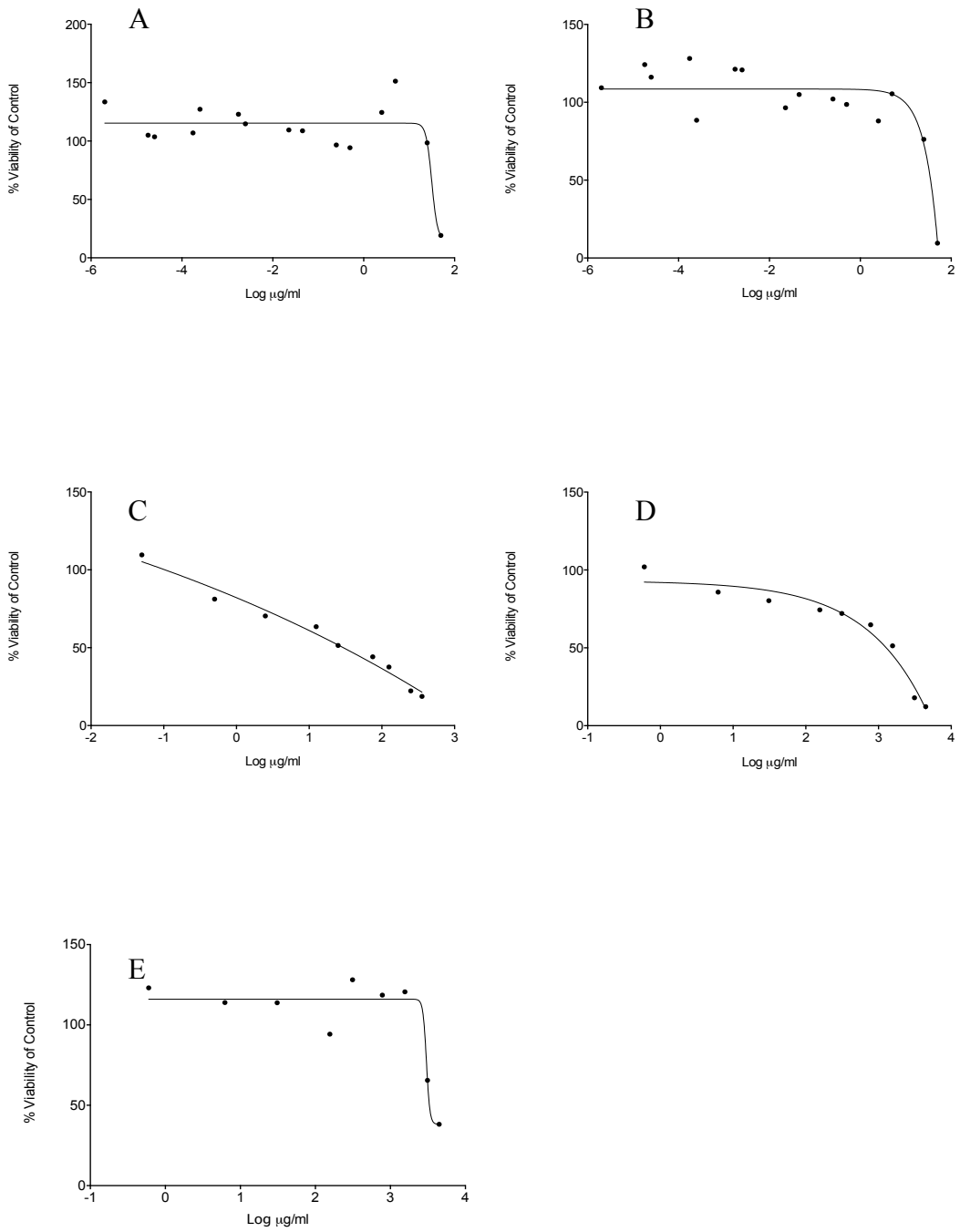


Figure 3.16 Effect of LPV aqueous solution (A), EFV aqueous solution (B), LPV nanoemulsion (C), EFV nanoemulsion (D) and blank nanoemulsion (E), on the metabolic activity of Caco-2 cells determined by ATP assay. Metabolic activity is proportional to luminescence and used as a proxy for cytotoxicity. Data expressed as % viability of control untreated cells.

### 3.3.4.2 HepG2 Cells

The final optimised emulsion E65 (Section 3.3.3) was assessed for its cytotoxicity against HepG2 cells, both as a blank emulsion and having a payload of EFV or LPV. The cytotoxicity of the emulsion was compared to that of an equivalent concentration of EFV and LPV as aqueous solutions. The results for MTT assay showed that the aqueous solutions of LPV and EFV did not show any cytotoxicity at any of the concentrations tested. The same was true for the LPV and EFV nanoemulsions (Figure 3.17)

CellTiterGlo® ATP assay also showed there was no overt cytotoxicity for LPV and EFV aqueous solutions and for LPV and EFV nanoemulsions (Figure 3.18).

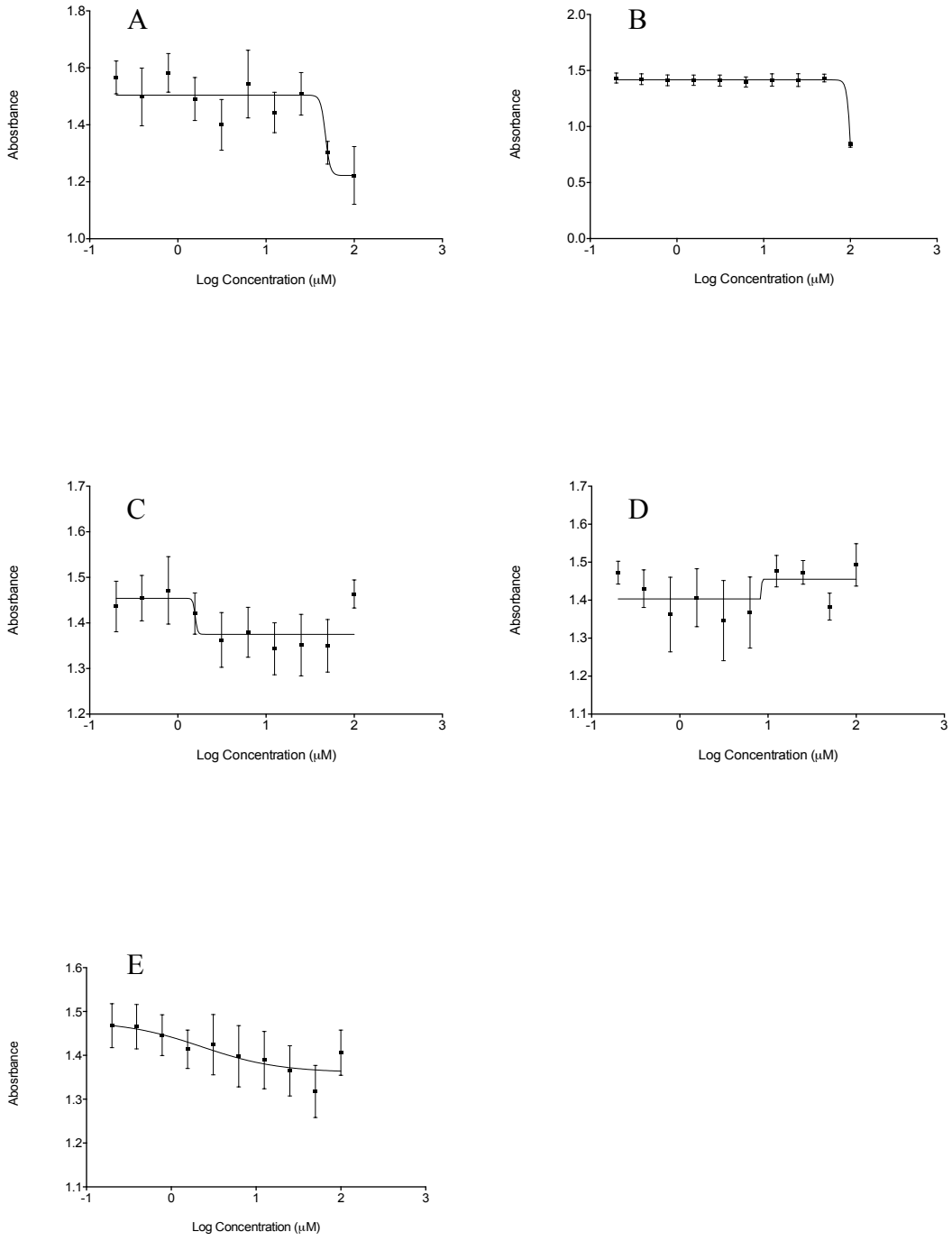


Figure 3.17 Effect of LPV aqueous solution (A), EFV aqueous solution (B), LPV nanoemulsion (C), EFV nanoemulsion (D) and blank nanoemulsion (E), on the metabolic activity of HepG-2 cells determined by MTT assay. As a proxy for cytotoxicity.

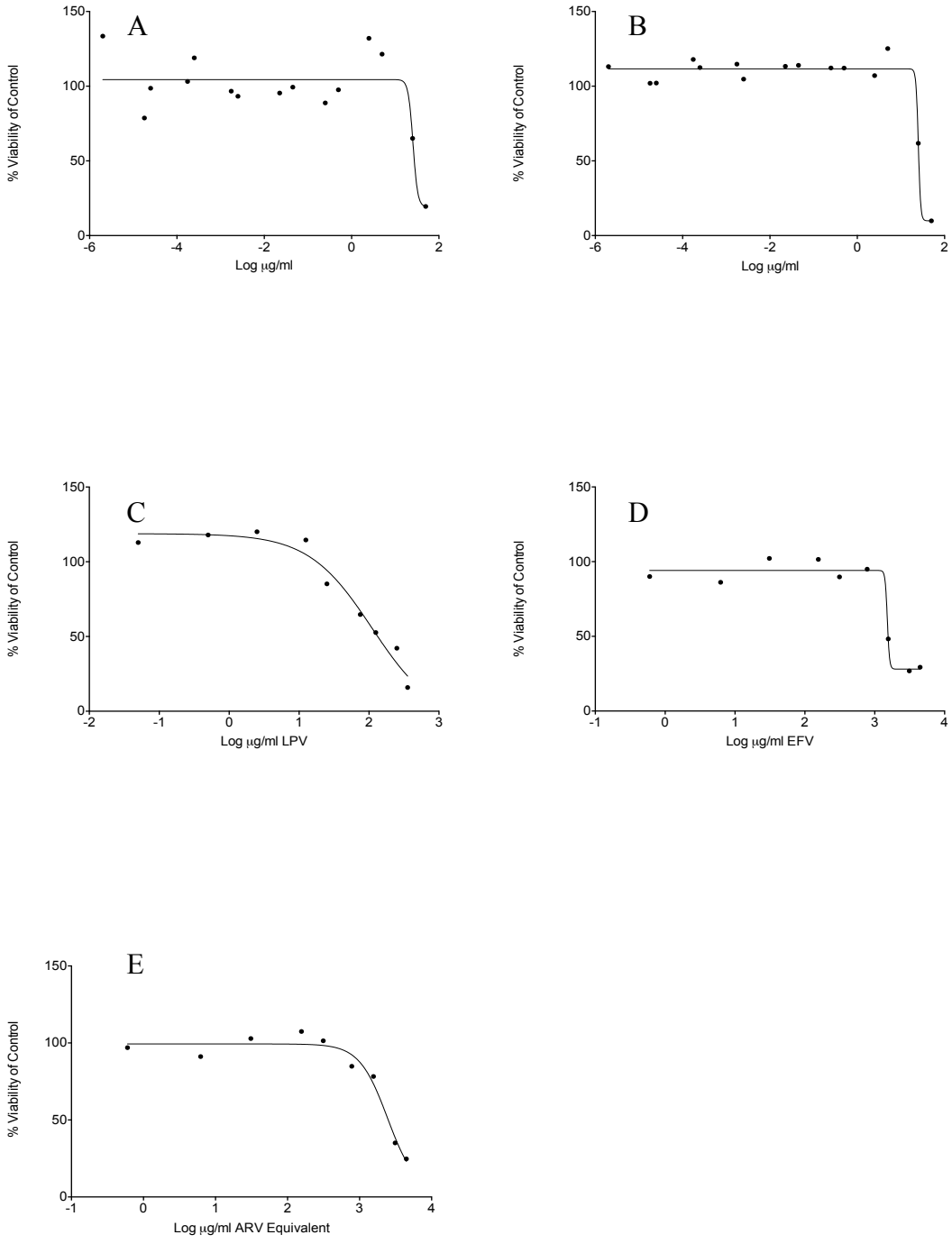


Figure 3.18 Effect of LPV aqueous solution (A), EFV aqueous solution (B), LPV nanoemulsion (C), EFV nanoemulsion (D) and blank nanoemulsion (E), on the metabolic activity of HepG2 cells determined by ATP assay. Metabolic activity is proportional to luminescence and used as a proxy for cytotoxicity. Data expressed as % viability of control untreated cells.

### 3.3.4.3 CEM Cells

The final optimised emulsion E65 (Section 3.3.3) was assessed for its cytotoxicity against CEM cells (T-lymphocyte), both as a blank emulsion and having a payload of EFV or LPV. The cytotoxicity of the emulsion was compared to that of an equivalent concentration of EFV and LPV aqueous solution. The results for MTT assay showed that there was no overt cytotoxicity observed at any of the concentrations other than the highest tested for the aqueous solutions of EFV and LPV (Figure 3.19). The nanoemulsion formulations had $IC_{50}$ values of 4 μM for LPV loaded nanoemulsion; 6 μM for EFV loaded nanoemulsion and 12 μM for blank nanoemulsion (Figure 3.19).

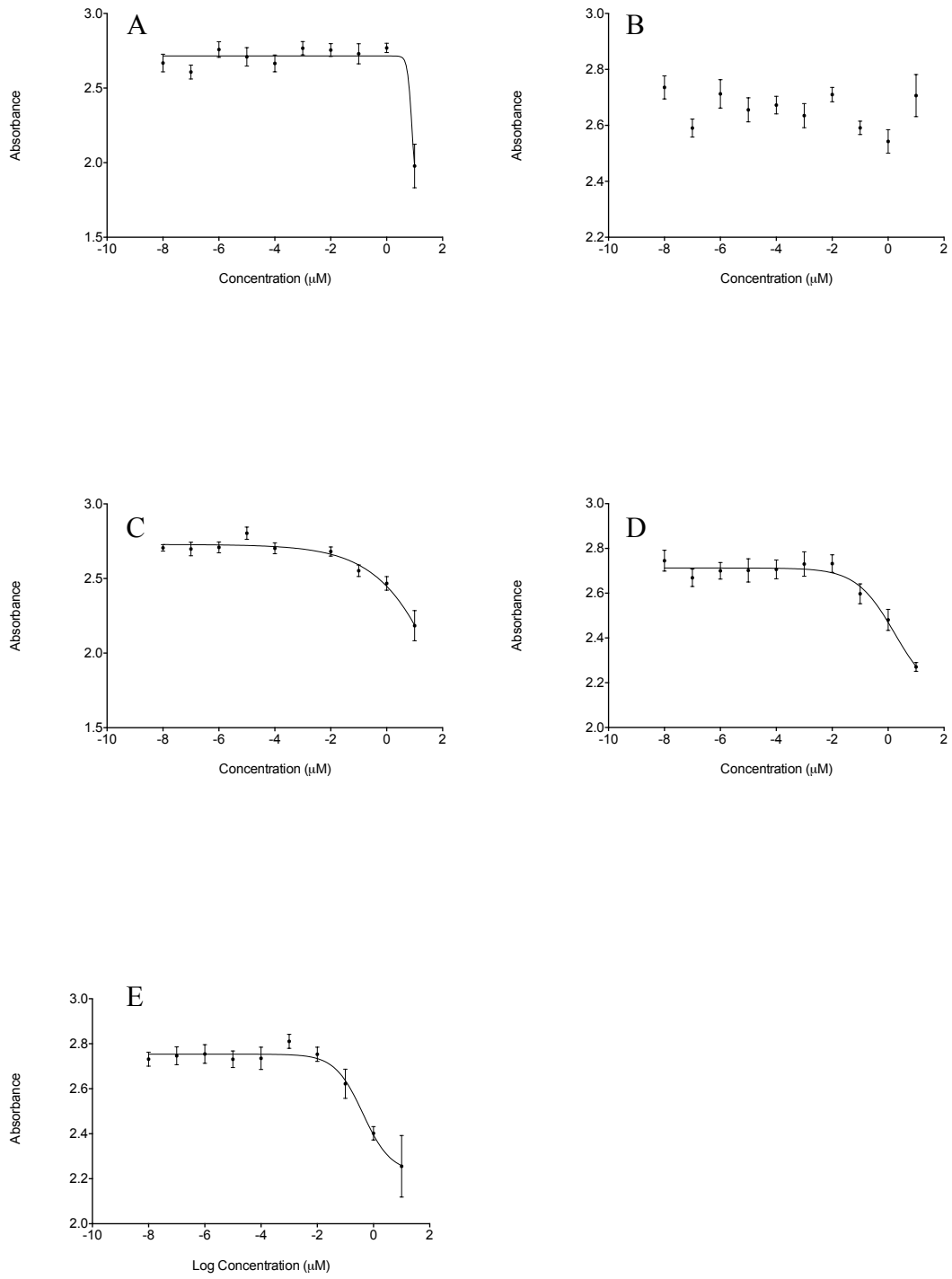


Figure 3.19 Effect of LPV aqueous solution (A), EFV aqueous solution (B), LPV nanoemulsion (C), EFV nanoemulsion (D) and blank nanoemulsion (E), on the metabolic activity of CEM cells determined by MTT assay. As a proxy for cytotoxicity.

### 3.3.4.4 Raji B Cells

The final optimised emulsion E65 (Section 3.3.3) was assessed for its cytotoxicity against Raji B cells (B-lymphocyte), both as a blank emulsion and having a payload of EFV or LPV. The cytotoxicity of the emulsion was compared to that of an equivalent concentration of EFV and LPV aqueous solution. The results for MTT assay showed that the LPV aqueous solution did not show any cytotoxicity other than at the highest concentration tested and EFV aqueous solution had an $IC_{50}$ value of 7.9 μM. LPV nanoemulsion also showed no cytotoxicity other than at the highest concentration, whereas EFV nanoemulsion had an $IC_{50}$ value for 1.7 μM and blank nanoemulsion 0.4 μM (Figure 3.20)

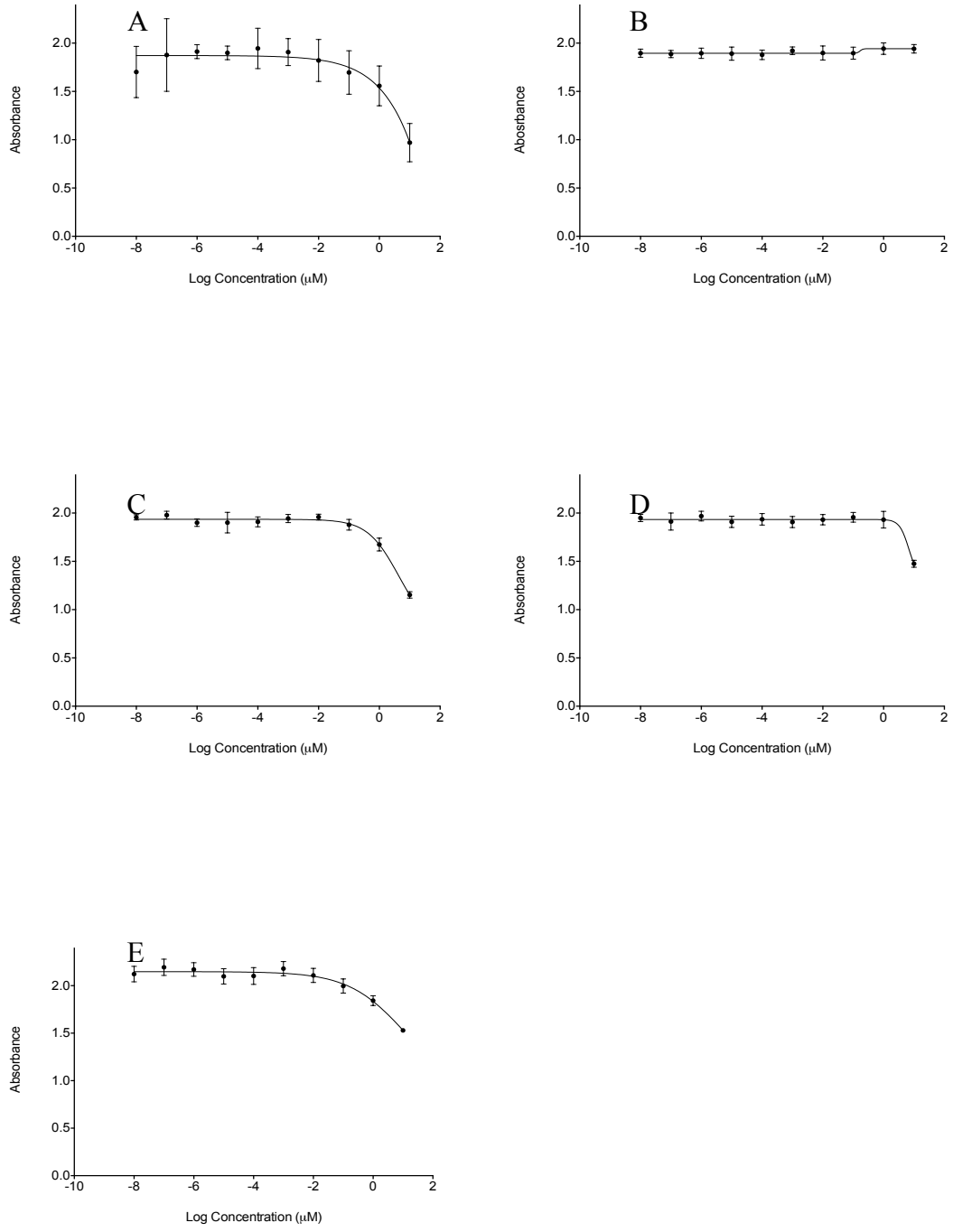


Figure 3.20 Effect of LPV aqueous solution (A), EFV aqueous solution (B), LPV nanoemulsion (C), EFV nanoemulsion (D) and blank nanoemulsion (E), on the metabolic activity of Raji-B cells determined by MTT assay. As a proxy for cytotoxicity.

### 3.4 Discussion

Size is an important factor when considering an emulsion drug delivery vehicle, as the size of the droplets will influence how they interact with the human body, such as ability to cross biological membranes [341] (e.g. intestine [342], placenta [343] or blood brain barrier [344]), interact with the immune system or how the droplets would be cleared from the systemic circulation. A successful oral drug delivery system needs to be able to efficiently cross the intestinal barrier and enter into the systemic circulation. Once there, it needs to avoid interacting with the immune system in such a way that it triggers an adverse immune response, an area of research [345-352] that is receiving much attention as nanomedicine becomes increasingly common (see also Chapter 6). The nanocarrier then needs to deliver the drug payload to its desired site and remain in circulation as long as possible [353].

It is obviously difficult to get all of these attributes perfectly optimised in a single formulation, so the goal of nanomedicine is to target specific areas for improvement, dependent on the drug in question [354]. For EFV and LPV the goal is to make them more bioavailable by increasing their permeation across the gut barrier (increased penetration into target cells is also desirable). It has also been shown that efavirenz has a lower bioavailability in HIV infected patients compared to healthy individuals [355], further showing the importance of developing novel formulations to overcome this.

For increased penetration across the biological barriers, smaller sized droplets have been reported as being more effective [356, 357], as they can pass between cells via paracellular permeation [358], or through cells by endocytosis [359-366]. Thus the droplet sizes of the emulsions stabilised by free radical polymers (FR1 and FR2) were not fit for purpose. Exploration of the pH responsiveness of these emulsions as had previously been shown by Weaver *et al* [292-295], did not lead to any benefits when considering protection from the acid environment in the stomach, as the emulsions did not disperse fully after acid triggered aggregation. The methodology for synthesising the emulsion was therefore changed to a homogenisation with co-solvent evaporation technique. This technique allowed smaller emulsion droplets to be formed, as during the evaporation of the co-solvent, droplets would collapse and be stabilised by the polymer. This change in methodology also coincided with the change from conventional free radical polymer synthesis to ATRP polymer synthesis due to moving away from the use of methacrylic acid, due to its cytotoxicity, its pH responsive nature when in a copolymer with OEGMA and its difficulty to use in ATRP reactions.

The co-solvent evaporation method allowed much smaller droplets to be formed, simply by allowing the volatile solvent ethyl acetate to evaporate after homogenisation of the emulsion. This evaporation caused the oil droplets to collapse whilst maintaining their surfaces coated in the branched PolyOEGMA DP80 polymer, imparting great stability.

Ethyl acetate was chosen as the co-solvent as it was immiscible in water, was able to dissolve the desired oil phase (castor oil) and was volatile enough that evaporation could take place over a 24-hour period at room temperature. Ethyl acetate also has been reported to exhibit low cytotoxicity [340], mitigating concern about residual solvent after evaporation.

The optimal emulsion E65 (99:1 ethyl acetate: castor oil stabilised with 5% w/v branched PolyOEGMA DP80) was chosen from the nanoemulsion library due to both its physical characteristics (size and charge) as well as its initial stability. The long-term stability study showed that the emulsion droplets were stable for in excess of 2 years when left in a sealed glass vial at room temperature, away from direct sources of light. This was in keeping with literature reports of nanoemulsions being stable for long periods of time [367], and that of data presented by Shakeel *et al* in which nanoemulsions were produced with predicted shelf lives of 2.38 years, as determined by accelerated stability studies [368]. The stability of the E65 emulsion was thought to be conferred by the steric repulsion that would be afforded by the large branched polymer anchored to the oil droplet, and the fact that there were multiple anchor points per polymer, due to its branched nature.

The polymers would prevent the surface of the oil droplets coming into contact with each other, and in doing so prevent Ostwald Ripening [369]. This steric repulsion theory was further supported by the neutral surface charge (zeta potential values of between 0 and 10/-10 are considered to be neutral) [370], such that charge

stabilisation was not observed. This would explain the good stability in biological media, as a charge stabilised particle would be subject to destabilisation and possible aggregation due to the presence of charged salts and proteins present in biological media, as previously described [371-373].

Tuning the size of the emulsion droplets was possible by either changing the volatile cosolvent to non-volatile oil ratio, or changing the concentration of branched PolyOEGMA $DP_{80}$ stabiliser. Changing the solvent to oil ratio had the simple effect of increasing the amount of oil present in the final emulsion, and so increasing the overall size of the droplets. Reducing the amount of polymer present had the effect of increasing the size of the droplets due to a lack of stabilisation, and so it was thought that droplets had more chance of coming together to form larger droplets before being covered with polymer [374-376].

An exciting set of data was that of the stability of the emulsion droplets when exposed to a series of dilutions. The data showed that the droplets did not destabilise when diluted, and this is important when considering doses of drug. Having a system that can be diluted easily in water, without detrimental effect on its stability is highly promising for being able to adjust the amount of drug being administered, especially in children or those with special requirements. If given in a liquid form, water would simply need to be added to the stock suspension in order to reduce dose. It would also be much more accurate than extemporaneous formulations, those in which tablets are crushed up to produce a liquid dose [377-380].

The lack of overt cytotoxicity seen throughout the testing of E65 nanoemulsions gives early confidence in the choice of polymer, oil and synthesis procedure. It would have been possible to generate $IC_{50}$ values by using higher starting concentrations of both the aqueous solutions of EFV and LPV, and the equivalent nanoemulsions. However, this would be difficult for two reasons: 1) increasing the concentration would involve ranges that are approaching non therapeutically relevant levels and is limited by the poor aqueous solubility of the drugs without modification [381-383], and 2) increasing the starting concentration of the nanoemulsion formulations would mean a large volume of sample relative to the culture media. This would have the effect of skewing the cytotoxicity data as cytotoxicity could have been caused by lack of nutrients for cell function and growth [384-387], particularly since incubation times were 5 days for cellular cytotoxicity assays, and that the cells would be in a suspension containing a high volume of water relative to complete cell medium.

Further studies of nanoemulsion cytotoxicity by Yu and Huang [388] demonstrated no cytotoxicity against Caco-2 cells as compared with micron sized emulsions, in agreement with the findings reported here. However, there was a difference in cytotoxicity observed against HepG2 cells [388], contrary to the data shown in this report, further validating the biocompatible nature of the polymer stabiliser and emulsion system used in this thesis. Literature reports suggest also that non-lipid based nanomaterials, such as those consisting of metal oxides and silica are considerably more cytotoxic in comparative *in vitro* studies [389-392].

In summary, the assessments carried out in this and the previous Chapter have shown that both the constituents and the final constructed nanoemulsion carrier system are non-cytotoxic at the relevant concentrations for therapeutic usage. Further safety assessment of the nanoemulsions in terms of enhanced therapeutic benefit continues in Chapters 4 and 5, followed by assessment of immune safety in Chapter 6.

# CHAPTER 4

# Pharmacological Assessment of Optimised Oil-in-Water Nanoemulsion (E65)

**Table of Contents**

## 4.1 Introduction

A novel drug formulation not only has to be safe, but also has to have a pharmacological profile equal to or better than the existing formulation or the drug in solution. Poor bioavailability is often the main limiting factor in the effectiveness and efficacy of a drug, particularly for the estimated 70% of new drugs coming though the pharmaceutical pipeline with poor bioavailability classification [130].

Aside from simply increasing the bioavailability of a pharmaceutical compound, it can be beneficial to improve the way in which it can be administered or the chemical environment in which it has to be dissolved. For example, many oral solutions of pharmaceutical compounds rely on a solvent into which the drug is dissolved prior to administration. This can lead to unpleasant tastes and burning sensations in the mouth due to the high percentage of solvent needed which can be particularly problematic in paediatric formulations, and indeed potentially harmful, due to the level of solvent used [393]. Therefore, taking a drug with poor water solubility and formulating it in such a way as to allow for its direct dispersal and dissolution into water is highly attractive. This would also allow for easy manipulation of dosages for patient populations that are not suited to standard tablet sizes, such as children and those with low body weights. It could also be used for personalising dose according to pharmacogenetics, removing the requirement for extemporaneous formulations [378] and additionally allowing patients who have difficulty in swallowing tablets (e.g. dysphagia) to take their medications [394, 395]. It would also remove the need for physically cutting up the standard dosage tablets in an

attempt to modify the amount of drug being administered, a practice that is risky, especially in HIV therapy where a precise therapeutic concentration window needs to be maintained in order to prevent toxicity or viral resistance.

Increasing the amount of the drug that can traverse the intestinal epithelium is also a desirable feature for any drug delivery system. However, it should be noted that increased accumulation and penetration into some cell types is not always beneficial. The liver for example is the main site of metabolism for pharmaceutical compounds, and as such preventing the amount of drug that enters the liver could potentially have a positive impact on bioavailability, in terms of increasing the residence time of the active form of the pharmaceutical or avoiding first pass metabolism. This is also of benefit in situations where the toxicity of a pharmaceutical agent comes not from the drug directly, but from one or more of its subsequent metabolites [396]. In this regard, central nervous system toxicity of EFV has been suggested to involve the 8-Hydroxy EFV metabolite [397].

The aims of the work presented in this Chapter were to assess any pharmacological benefit of having LPV or EFV in a nanoemulsion formulation. The accumulation of drug into cells, as well as the permeation across a model intestinal system was investigated, with the purpose of predicting any potential improvement in bioavailability. It was hypothesised that the formulation of EFV or LPV into a nanoemulsion would increase the apparent permeability and accumulation into cells, as compared with an equivalent aqueous solution.

## 4.2 Materials and Methods

In addition to the materials stated in sections 2.2.1 and 3.2.1, the following were also acquired: HPLC grade acetonitrile and methanol were purchased from Sigma-Aldrich (Dorset, UK). 24 well HTS Transwell plates were supplied by Corning Life Sciences (Amsterdam, The Netherlands). C18 HPLC separation column was purchased from Fortis Technologies LTD (Cheshire, UK)

### 4.2.1 Adherent Cell Culture

As described in 2.2.8

### 4.2.2 Suspension Cell Culture

As described in 2.2.9

### 4.2.3 Assessment of Transcellular Permeation Across Caco-2 Cell Monolayers

Caco-2 cells were seeded at a density of 35,000 cells per well in the apical chamber of a 24 well Corning® HTS® transwell plate, and left to adhere for 24 hours. After this time, culture media was replenished by removal with an aspirator, also removing those cells that had not adhered. Culture media used was DMEM supplemented with 15% FBS, which was continually replenished every other day for a three week period. After three weeks had passed, the formation of an intact caco-2 monolayer was assessed using a trans-epithelial electrical resistance (TEER) probe (Merck Millipore, Billerica, USA), resistance values in excess of 600 ohms indicated that tight caco-2 monolayers were ready for use in the assay [398].

During the assay, culture media was removed from wells and replaced with 15% FBS supplemented DMEM that had a final concentration of 10 µM aqueous solution or nanoemulsion equivalent of LPV or EFV. In different wells the apical or basolateral chambers (donor chambers) were loaded with drug or nanoemulsion containing media, with the opposite chambers (acceptor chambers) of those wells being filled with fresh drug-free media. Samples were taken from both apical and basolateral chambers from all wells at 1, 2, and 24 hour time periods. Samples were then immediately frozen at -40°C for subsequent batch analysis via HPLC. Figure 4.1 shows the set up and layout of the transwell plates.

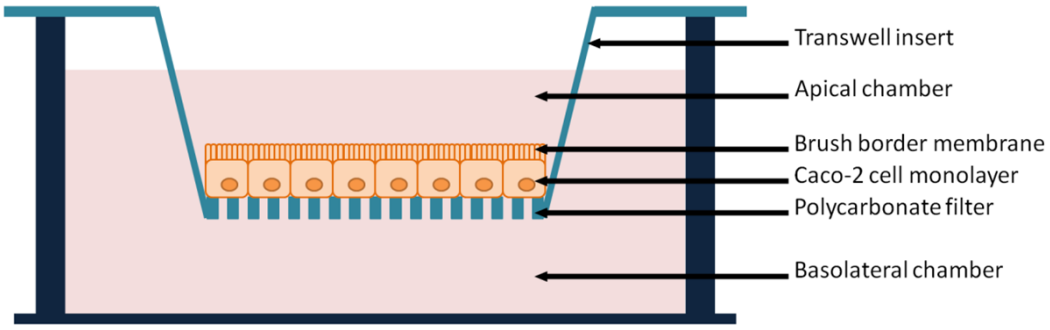


Figure 4.1 Schematic of the Caco-2 transwell system. The cells are allowed to adhere and polarise for 14-21 days, after which test samples are loaded into either the apical or basolateral chamber. Sampling either side of the cell monolayer allows for the level of drug permeation (Papp) to be calculated.

The apparent permeability (Papp) was calculated using the following equation:

$$Papp = \frac{\left(\frac{A}{T}\right) * (V)}{S * 0.3}$$

Where A is the concentration in the sample, T is the time in seconds at which the sample was collected, V is the total volume of sample contained in the chamber being sampled, S is the initial starting concentration of the drug and 0.3 is the surface area in $cm^2$ of the transwell insert on which the Caco-2 cells are grown.

### 4.2.4 Adherent Cellular Accumulation

1 x $10^6$ cells (Caco-2 or HepG2) were seeded per well in 24 well cell culture plates and incubated for 24 hours in order for cells to adhere to culture plastics. After this time the media was removed and replaced with DMEM supplemented with 10% FBS and containing a final concentration of 10 μM of either aqueous solution or nanoemulsion formulation of LPV or EFV. Samples were taken at 4 and 24 hours post incubation with drug or nanoemulsion containing media and both intracellular and extracellular samples were taken. Extracellular samples were taken by simply removing the media and storing in a universal tube at -40°C prior to analysis on HPLC. Intracellular samples were taken by first washing the adherent cells 3 times with ice cold HBSS to remove any free drug. After the final wash an ice-cold solution of 50% methanol and 50% water was pipetted onto the cells and a cell scraper used to remove the cells from the surface of the cell culture plate. The cell lysate was then pipetted into universal tubes and again stored at -40°C prior to analysis.

Cellular accumulation ratio (CAR) was calculated using the following equation:

$$CAR = \left(\frac{intracellular\ concetration}{cell\ volume}\right) / \left(\frac{extracellular\ concentration}{extracellular\ volume}\right)$$

Cell volumes were derived using a Cell Sceptre 2.0 Handheld Automated Cell Counter (Merck Millipore, Billerica, USA).

### 4.2.5 Suspension Cell Cellular Accumulation

1 x $10^6$ cells (Caco-2 or HepG2) were seeded per well in 24 well cell culture plates and DMEM supplemented with 10% FBS and containing a final concentration of 10 μM of either aqueous solution or nanoemulsion formulation of LPV or EFV was added. Samples were taken at 4 and 24 hours post incubation by transferring the samples to deep well plates and centrifuging at 2000 xg for 5 minutes. Supernatant was taken as the extracellular sample, and the pellet washed 3 times with ice cold HBSS to remove any free drug. After the final wash an ice cold solution of 50% methanol and 50% water was added and the cell lysate transferred to universal tubes for storage at -40°C prior to analysis.

### 4.2.6 High Performance Liquid Chromatography

High Performance Liquid Chromatography (HPLC) protocols for the analysis of LPV and EFV were previously developed in house. These protocols were for aqueous forms of LPV and EFV and therefore, the method was further validated to include an appropriate extraction phase (see 4.2.6.3) to remove any nanoemulsion-

associated drug molecules. The method was adapted to also increase the wash phase at the end of the run for each individual sample, so as to remove residual polymer stabiliser that was found to accumulate in the C18 column. This extra wash step was incorporated to extend the life of the column thereby preventing degradation of the C18 beads.

#### 4.2.6.1 HPLC Sample Extraction Protocol

Samples from transwell and accumulation assays first underwent an extraction procedure to remove drug molecules from any remaining intact nanoemulsion droplets as well as to remove any proteins that may have bound to and coated the drug molecules. 200 µL of sample (thawed from -40°C storage) was added to 1 ml of HPLC grade acetonitrile in a universal tube and vortexed for 30 seconds. The universal tubes where then centrifuged for 5 minutes at 4°C at 13,300 rpm, after which the supernatant was transferred to fresh glass tubes. These tubes were placed in a vacuum centrifuge drier and heated to 35°C to remove excess acetonitrile and dry down the sample to a pellet. Pellets were then re-suspended in 200 µL fresh 20% HPLC grade acetonitrile, 80% HPLC grade water, and transferred to 1.8 ml HPLC vials and sealed for HPLC analysis.

#### 4.2.6.2 EFV HPLC Conditions

The mobile phase (C) consisted of 95% water and 5% acetonitrile, with 5mM final concentration of ammonium formate. The elution buffer (D) consisted of 90% acetonitrile and 10% water with no ammonium formate. A calibration curve was

produced using a 1:2 dilution from 20,000 ng/ml to 39 ng/ml, with separate quality control samples at 600 ng/ml, 3000 ng/ml and 15,000 ng/ml.

The initial starting conditions of each run were 100% C, changing to 92% D / 8% C after 30 seconds, holding at this percentage for 5 minutes before raising to 100% D for 1 minute. The final 2 minutes of the run returned the column to 100% of C, ready for the injection of the next sample. The EFV was eluted at around 4.3 minutes into the run.

#### 4.2.6.3 LPV HPLC Conditions

The mobile phase (C) consisted of 10 mM potassium phosphate buffer (pH 3.2 with orthophosphoric acid). The elution buffer (D) consisted of 95% acetonitrile and 5% water with no ammonium formate. A calibration curve was produced using a doubling dilution from 20,000 ng/ml down to 39 ng/ml, with separate quality control samples at 600 ng/ml, 3000 ng/ml and 15,000 ng/ml.

The initial starting conditions of each run were 50% C / 50% D, holding for 2 minutes before changing over the next 2 minutes to 70% D / 30% C. At 4.1 minutes the % of D increased to 80% holding at this percentage for 3 minutes before returning to the initial conditions of 50% C and 50% D for 2 minutes, to prepare the column for the next injection. The LPV was eluted at 5.2 minutes into the run**.**

### 4.2.7 Statistical Analysis of Data

Statistical analysis was performed using SPSS version 21 for Macintosh computers, where data was normally distributed a independent samples t-test was performed to obtain p values. Where data was non normally distributed a non-parametric Mann-Whitney U test was performed. P values are stated throughout.

## 4.3 Results

### 4.3.1 LPV HPLC Quantification and Calibration Curve

Calibration curves were created for the quantification of aqueous and nanoemulsion formulations of LPV. The standard curve produced an $r^2$ value of 0.99 showing a good linearity across the assay concentration range (Figure 4.2).

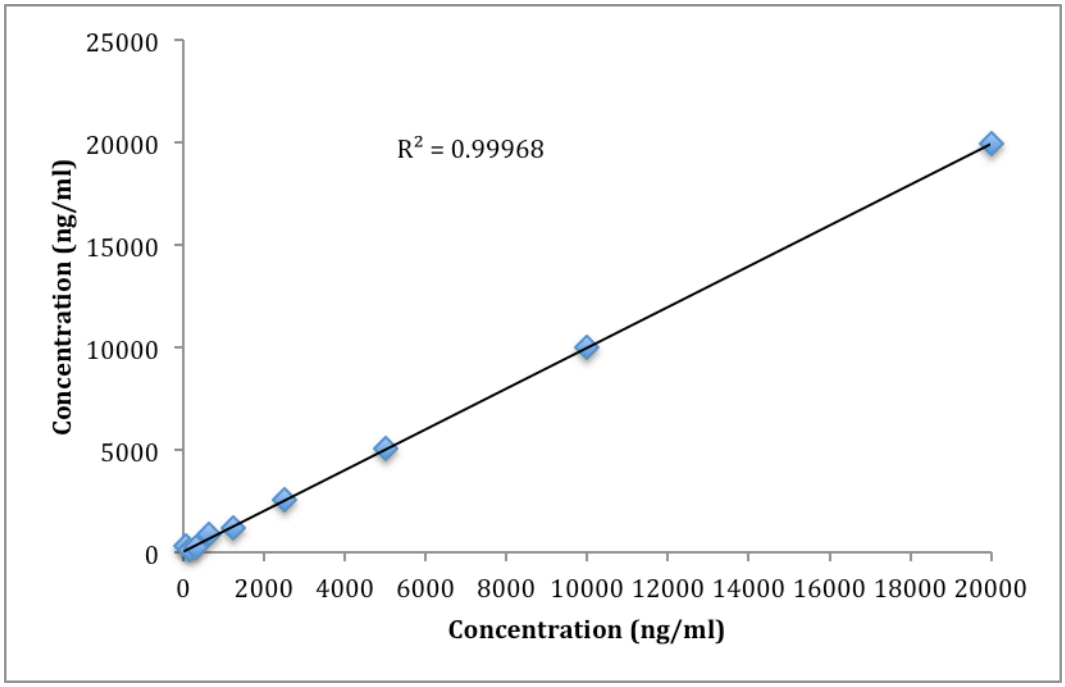


Figure 4.2 Calibration curve for HPLC analysis of LPV. Standards were analysed using a 1:1 dilution ration from 20,000 ng/ml to 39 ng/ml, using a C18 column and flow rate of 1 mL/min.

### 4.3.2 EFV HPLC Quantification and Calibration Curve

Calibration curves were created for the quantification of aqueous and nanoemulsion formulations of EFV. The standard curve produced an $r^2$ value of 0.99 showing a good linearity across the assay concentration range (Figure 4.3)

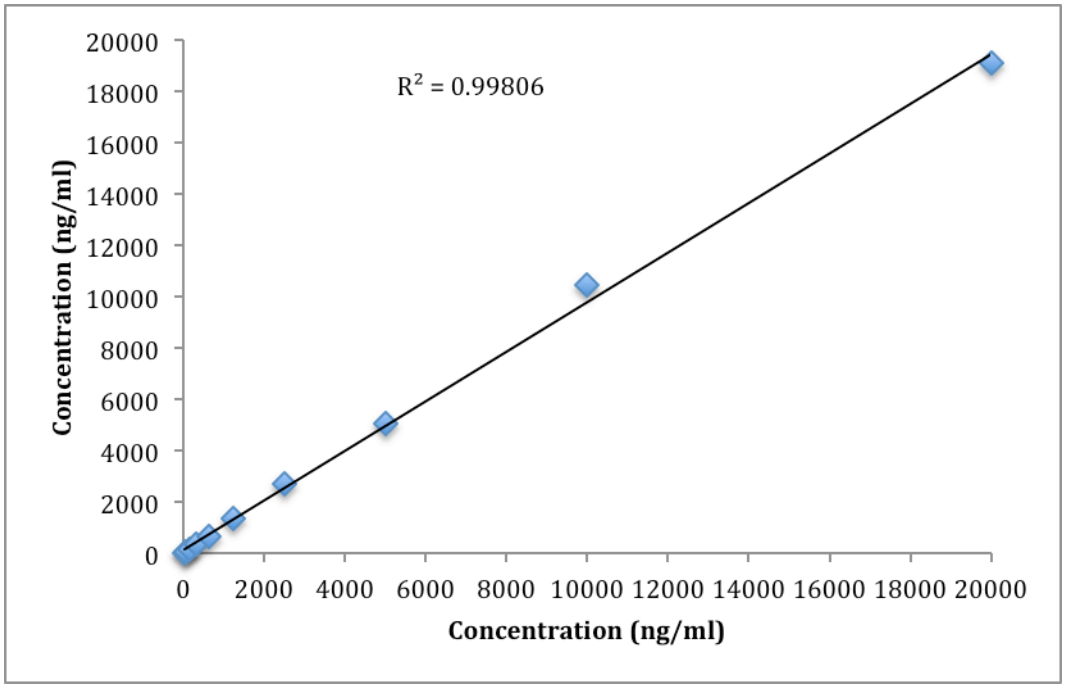


Figure 4.3 Calibration curve for HPLC analysis of EFV. Standards were analysed using a 1:1 dilution ration from 20,000 ng/ml to 39 ng/ml, using a C18 column and flow rate of 1 mL/min.

### 4.3.3 Assessment of Transcellular Permeability of LPV Aqueous Solution and LPV Nanoemulsion in the Apical to Basolateral Direction

For apparent permeability (Papp, apical to basolateral direction; modelling intestine to systemic circulation) there was a significantly greater permeability seen for the nanoemulsion formulation of LPV at both 1 hour and 2 hour time points, with Papp values of 1 x $10^{-4}$ vs. 8.4 x $10^{-6}$ ($p = <0.05$) at 1 hour and 6.4 x $10^{-5}$ vs. 2.7 x $10^{-6}$ ($p = <0.05$) at 2 hours (Figure 4.4). At 24 hours there was a Papp value for the LPV nanoemulsion of 1.8 x $10^{-6}$, compared with a Papp of for LPV aqueous solution of 4.6 x $10^{-6}$ although this was not significant ($p = 0.18$) (Figure 4.4).

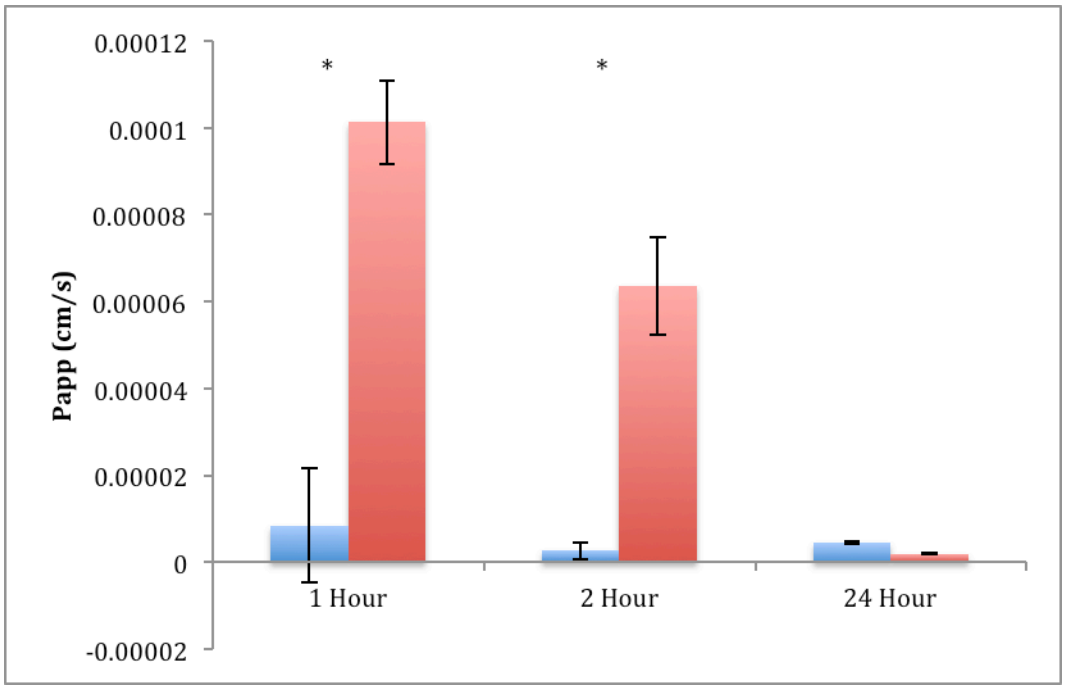


Figure 4.4 Apparent permeability of aqueous (blue) and nanoemulsion (red) formulations of LPV in the direction of apical to basolateral. Samples were incubated for 1, 2 or 24 hours at a concentration of 10 µM LPV, added to the apical chamber. The full volume of media was taken from each chamber, for subsequent HPLC analysis. Data expressed as +/- standard deviation, N=4.

### 4.3.4 Assessment of Transcellular Permeability of LPV Aqueous Solution and LPV Nanoemulsion in the Basolateral to Apical Direction

The apparent permeability (Papp, basolateral to apical direction; systemic circulation to intestine) was significantly greater for the nanoemulsion formulation of LPV at the 1 hour time point, with a Papp value of $6.1 \times 10^{-5}$ compared with $9.3 \times 10^{-6}$ for LPV aqueous solution ($p = <0.05$) (Figure 4.5). This correlated with the Papp values observed in the apical to basolateral direction, suggesting that the nanoemulsion formulation was able to permeate the caco-2 monolayer to a much greater degree than the aqueous formulation, regardless of the direction across the monolayer.

There was no difference in Papp observed at 2 hours between the LPV nanoemulsion and LPV aqueous solution with values of $6.0 \times 10^{-6}$ and $1.3 \times 10^{-5}$ ($p = 0.11$). At the final 24-hour time point the Papp values showed a significantly higher B-A permeability for LPV aqueous solution $5.1 \times 10^{-6}$ compared to $3.5 \times 10^{-6}$ for LPV nanoemulsion ($p = < 0.05$) (Figure 4.5).

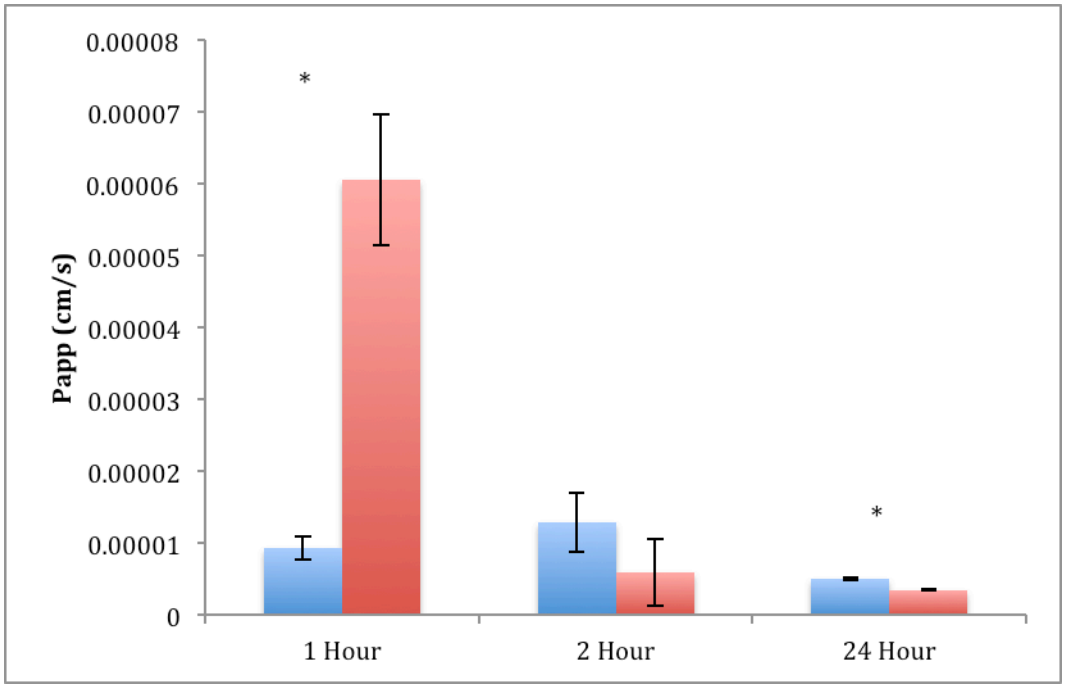


Figure 4.5 Apparent permeability of aqueous (blue) and nanoemulsion (red) formulations of LPV in the direction of basolateral to apical. Samples were incubated for 1, 2 or 24 hours at a concentration of 10 µM LPV, added to the basolateral chamber. The full volume of media was taken from each chamber, for subsequent HPLC analysis. Data expressed as +/- standard deviation, N=4.

### 4.3.5 Assessment of Transcellular Permeability of EFV Aqueous Solution and EFV Nanoemulsion in the Apical to Basolateral Direction

The Papp value for EFV nanoemulsion at the 1-hour time point was 6.5 x $10^{-6}$ compared with 1.7 x $10^{-5}$ for the EFV aqueous solution, which showed no significant difference ($p = 0.20$). For the 2 hour time point, the aqueous solution of EFV had a significantly lower apparent permeability of 8.2 x $10^{-6}$ compared to 1.1 x $10^{-5}$ for EFV nanoemulsion ($p = <0.05$), and the same was observed at the 24 hour time point with EFV aqueous solution having a Papp of 7.0 x $10^{-7}$ compared with 6.4 x $10^{-6}$ for EFV nanoemulsion ($p = <0.05$) (Figure 4.6).

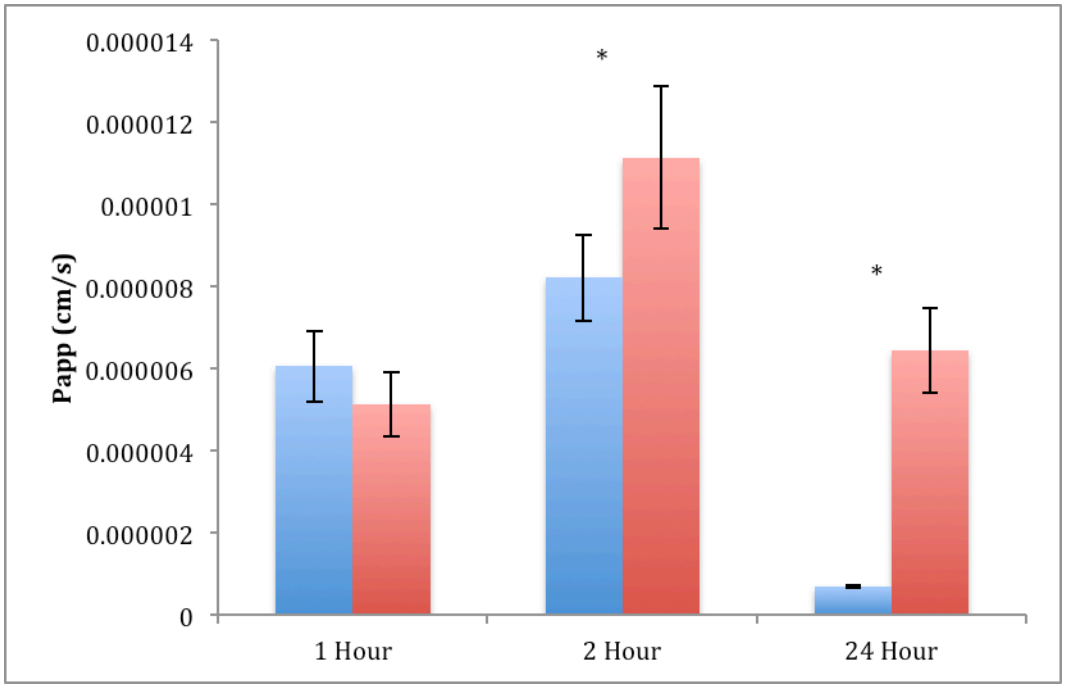


Figure 4.6 Apparent permeability of aqueous (blue) and nanoemulsion (red) formulations of EFV in the direction of apical to basolateral. Samples were incubated for 1, 2 or 24 hours at a concentration of 10 µM EFV, added to the apical chamber. The full volume of media was taken from each chamber, for subsequent HPLC analysis. Data expressed as +/- standard deviation, N=4.

### 4.3.6 Assessment of Transcellular Permeability of EFV Aqueous Solution and LPV Nanoemulsion in the Basolateral to Apical Direction

At the 1-hour time point the EFV aqueous solution had a Papp of 2.4 x $10^{-5}$ which was significantly greater than the Papp of EFV nanoemulsion at 4.2 x $10^{-6}$ ($p = <0.05$). At 2 hours the EFV aqueous solution was again significantly greater than EFV nanoemulsion with Papp values of 2.6 x $10^{-5}$ and 1.2 x $10^{-5}$ respectively ($p = <0.05$). At the final 24-hour time point, the EFV nanoemulsion was shown to be significantly higher when compared to the EFV aqueous solution with Papp values of 8.5 x $10^{-6}$ and 8.4 x $10^{-7}$ respectively ($p = <0.05$) (Figure 4.7).

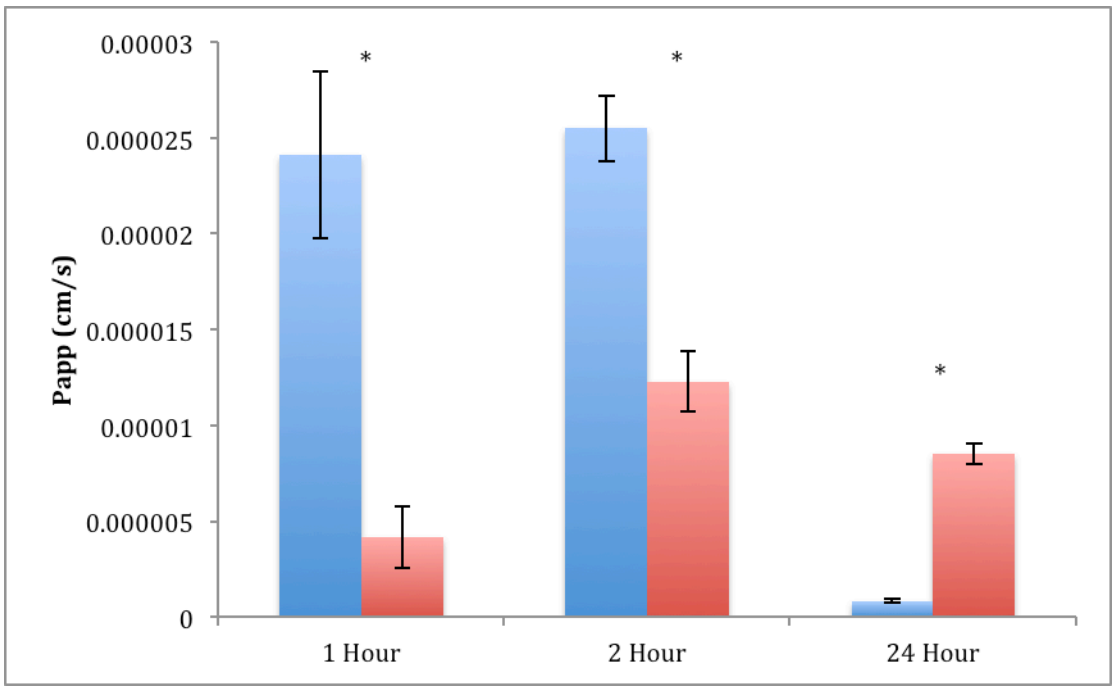


Figure 4.7 Apparent permeability of aqueous (blue) and nanoemulsion (red) formulations of EFV in the direction of basolateral to apical. Samples were incubated for 1, 2 or 24 hours at a concentration of 10 µM EFV, added to the basolateral chamber. The full volume of media was taken from each chamber, for subsequent HPLC analysis. Data expressed as +/- standard deviation, N=4.

### 4.3.7 Monitoring the Apical and Basolateral Concentrations of Transcellular Permeability Studies

10 µM EFV or LPV (aqueous or nanoemulsion) was added to either the apical or basolateral chambers of a transwell plate and then samples taken from both apical and basolateral chambers, regardless to which one the drug had been added. As detailed, in Figures 4.8 to 4.11, when drug was added to the apical chamber of the transwell plate, there was a gradual reduction in concentration of drug as it permeated into the basolateral chamber, regardless of the formulation of the drug.

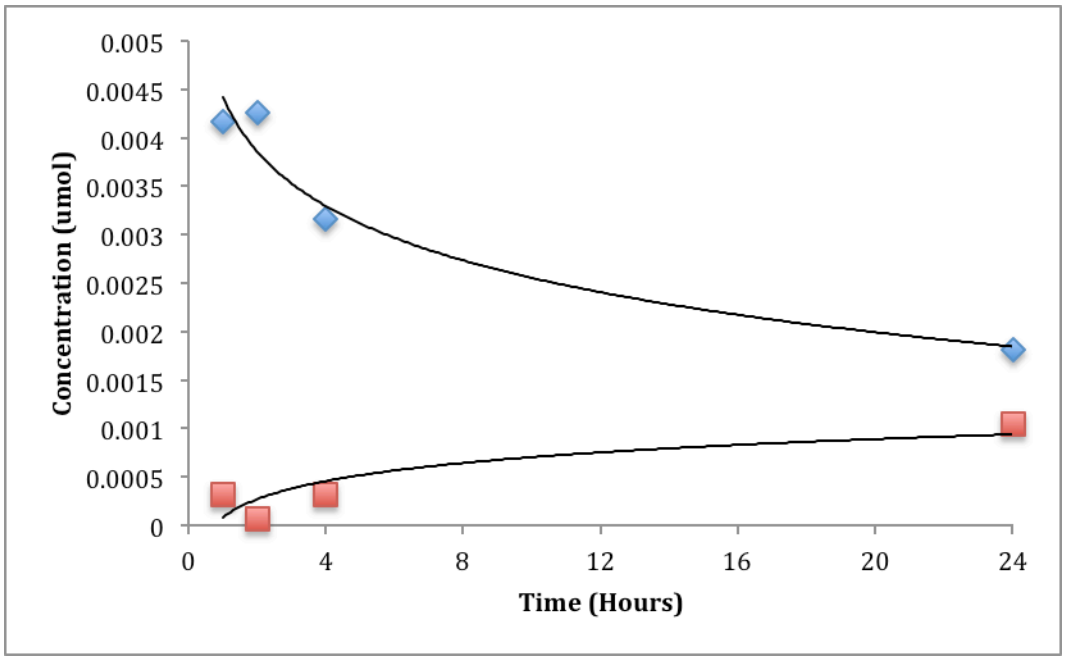


Figure 4.8 Change in apical (blue) and basolateral (red) aqueous LPV concentration measured over the 24-hour period of permeability assay. 10 μM of LPV was added to the apical chamber.

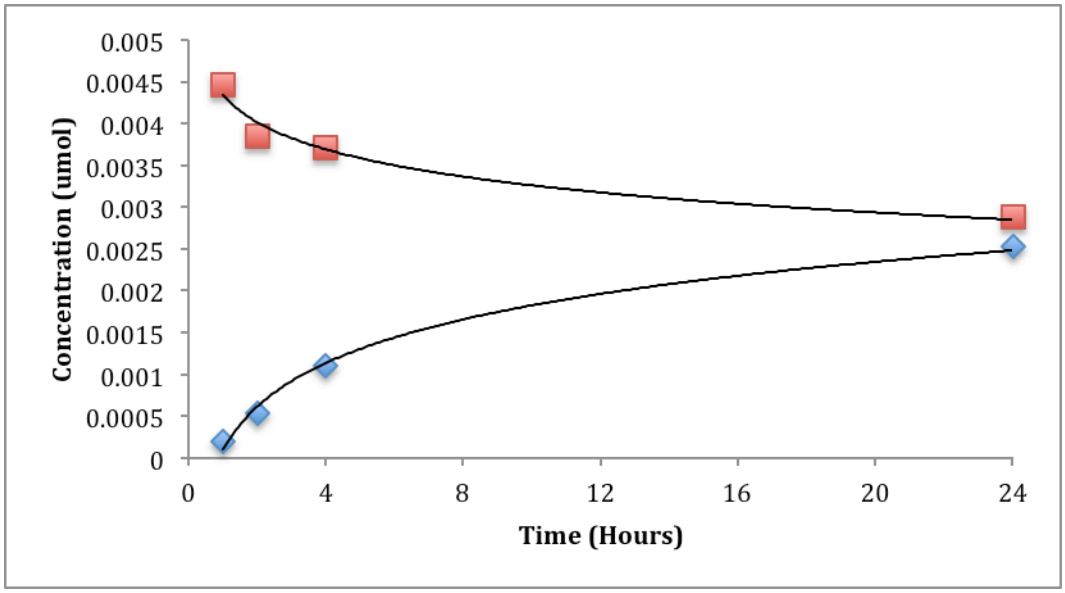


Figure 4.9 Change in apical (blue) and basolateral (red) nanoemulsion LPV concentration measured over the 24-hour period of permeability assay. 10 μM of LPV was added to the apical chamber.

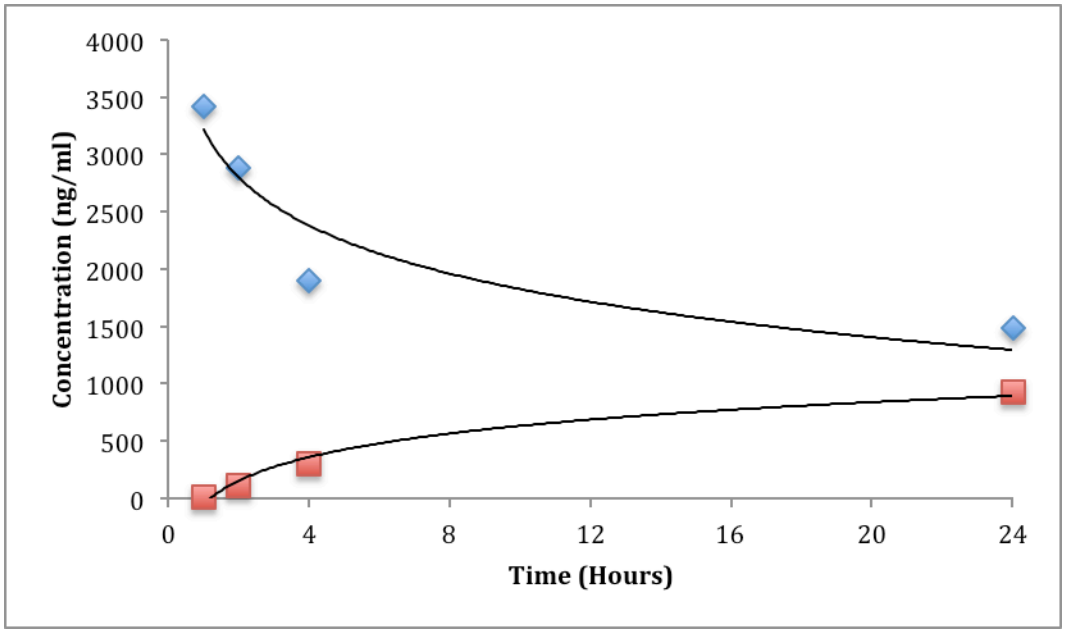


Figure 4.10 Change in apical (blue) and basolateral (red) aqueous EFV concentration measured over the 24-hour period of permeability assay. 10 µM of EFV was added to the apical chamber.

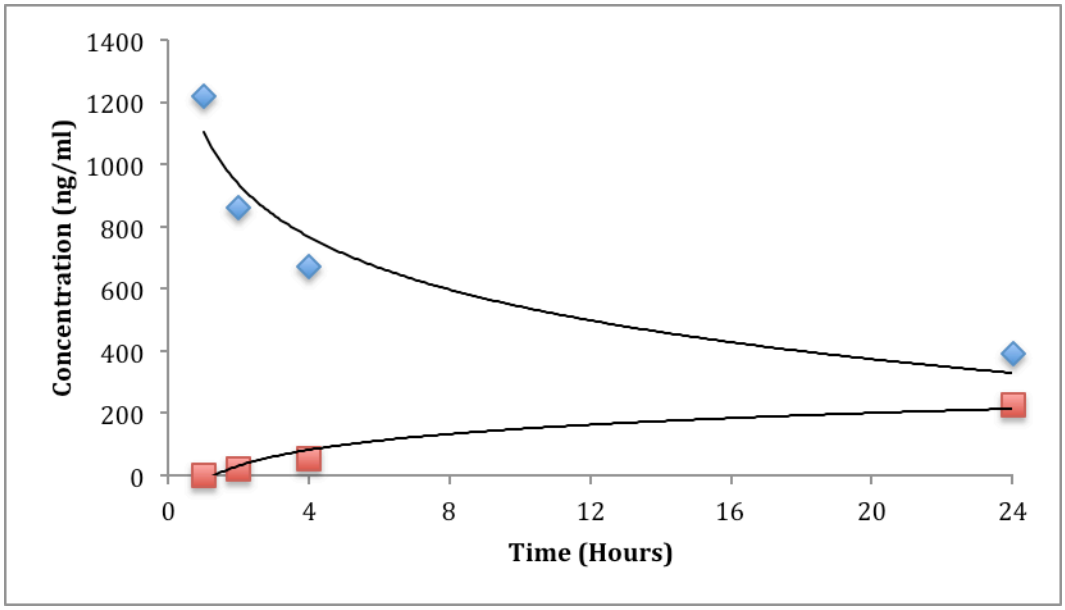


Figure 4.11 Change in apical (blue) and basolateral (red) nanoemulsion EFV concentration measured over the 24-hour period of permeability assay. 10 µM of EFV was added to the apical chamber.

The same was seen when drug was added to the basolateral chamber, again regardless of the formulation of the drug (Figures 4.12 to 4.15). Interestingly, when aqueous EFV was added to the basolateral chamber, the concentrations in both of the chambers did reach equilibrium (Figure 4.14).

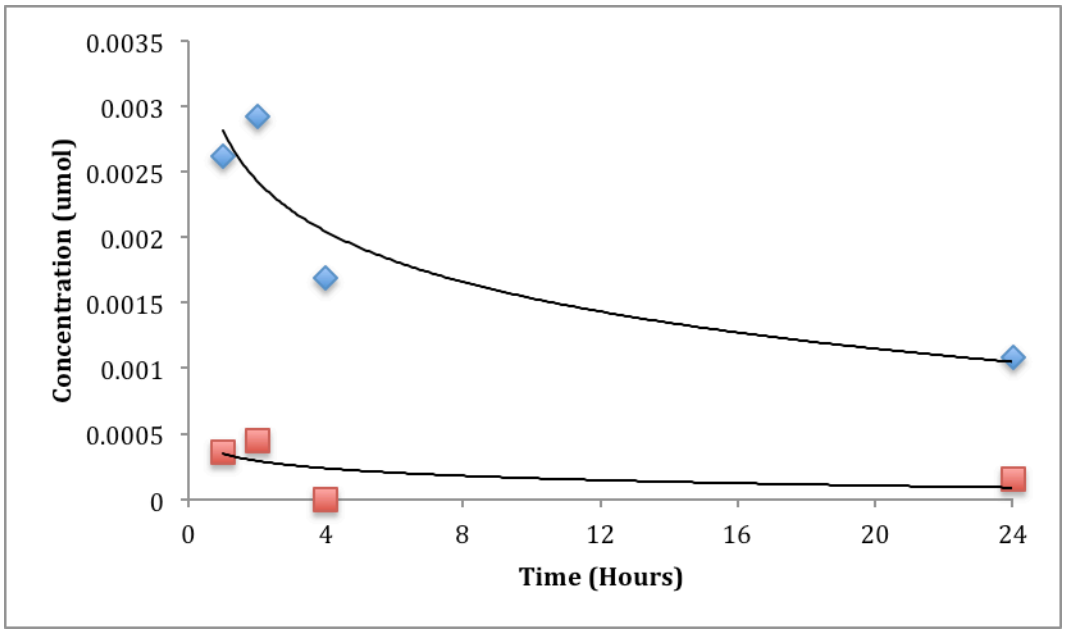


Figure 4.12 Change in apical (blue) and basolateral (red) aqueous LPV concentration measured over the 24-hour period of permeability assay. 10 µM of LPV was added to the basolateral chamber.

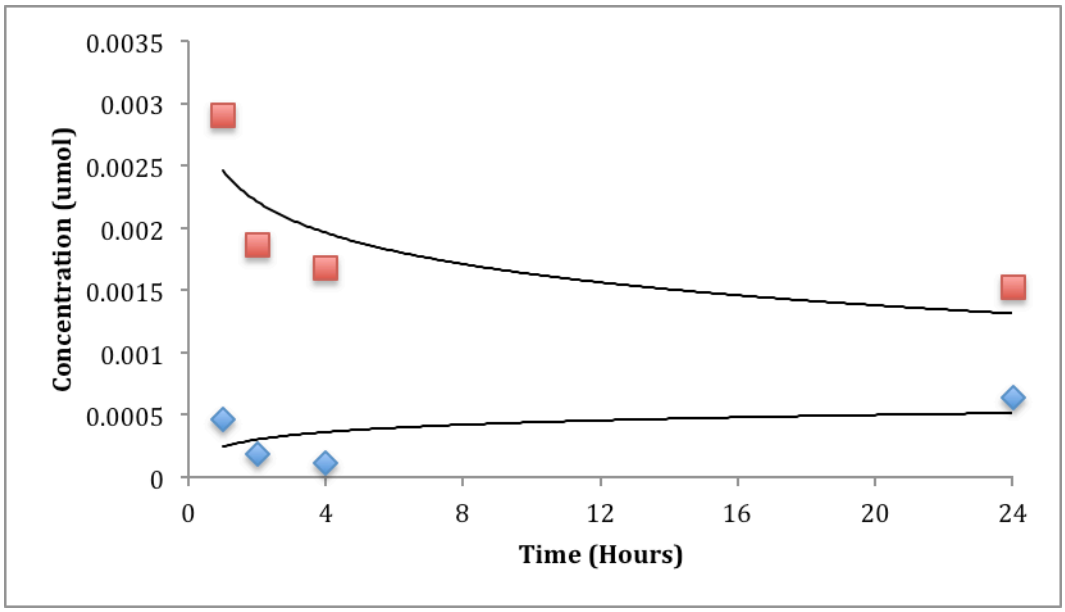


Figure 4.13 Change in apical (blue) and basolateral (red) nanoemulsion LPV concentration measured over the 24-hour period of permeability assay. 10 µM of LPV was added to the basolateral chamber.

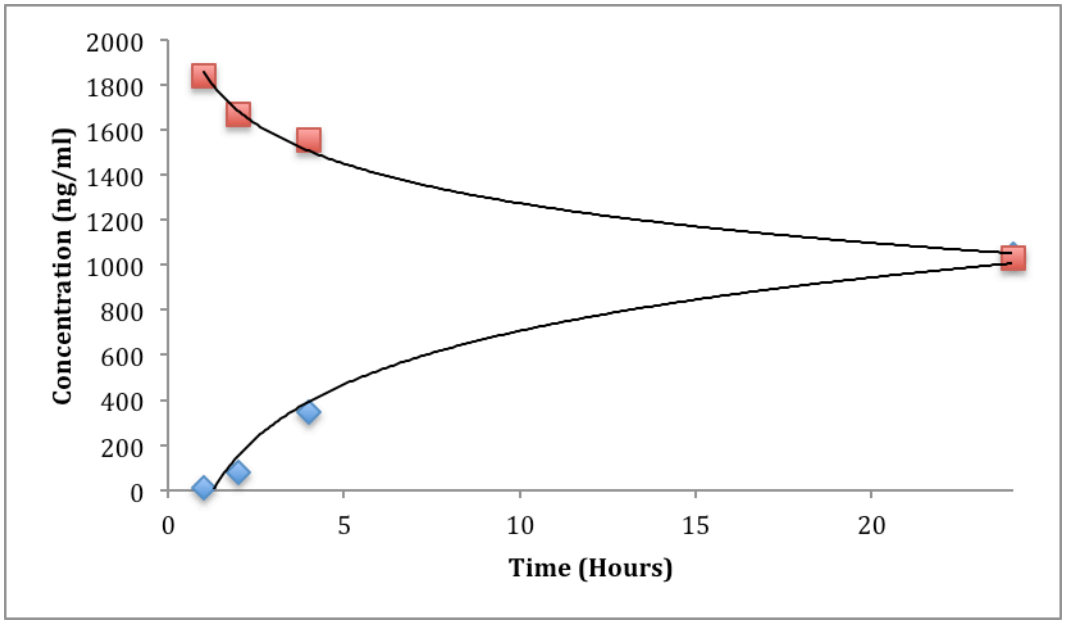


Figure 4.14 Change in apical (blue) and basolateral (red) aqueous EFV concentration measured over the 24-hour period of permeability assay. 10 µM of EFV was added to the basolateral chamber.

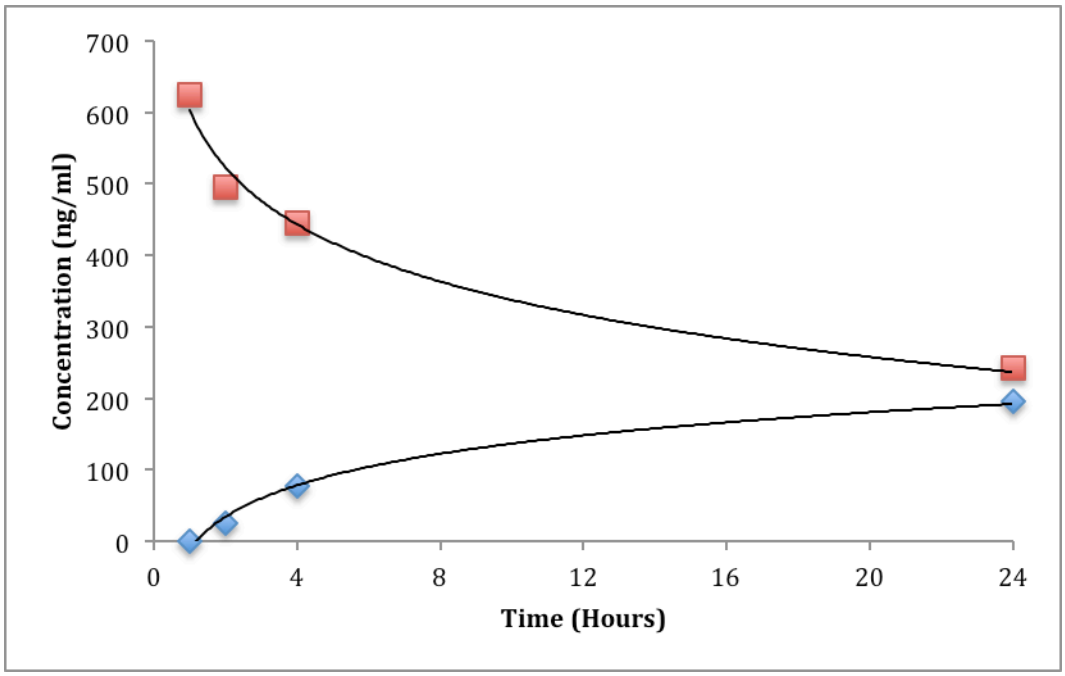


Figure 4.15 Change in apical (blue) and basolateral (red) nanoemulsion EFV concentration measured over the 24-hour period of permeability assay. 10 µM of LPV was added to the basolateral chamber.

### 4.3.8 Cellular Accumulation in Caco-2 Cells

In Caco-2 cell experiments, there was no difference in cellular accumulation ratio (CAR) seen between the aqueous EFV solution and EFV nanoemulsion after both 4 and 24-hour incubations. Reported CAR values at 4 hours were 1.1 for aqueous solution and 6.4 for nanoemulsion ($p = 0.89$), while at 24 hours the CAR values were 1.1 for both aqueous and nanoemulsion EFV ($p = 0.41$) (Figure 4.16).

### 4.3.9 Cellular Accumulation of EFV in HepG2 Cells

There was a difference observed between aqueous EFV solution and EFV nanoemulsion after 4-hour incubation in HepG2 cells, with CAR values of 4.6 and 0.8 respectively. However this could only be viewed as borderline significant as the p value was $p = 0.053$. At 24 hours there was again no difference observed, with CAR values of 0.8 for EFV aqueous solution and 1.6 for EFV nanoemulsion ($p = 0.09$). There was a significant increase in CAR observed between the EFV aqueous solution at 4 and 24 hours ($p = 0.02$) (Figure 4.16).

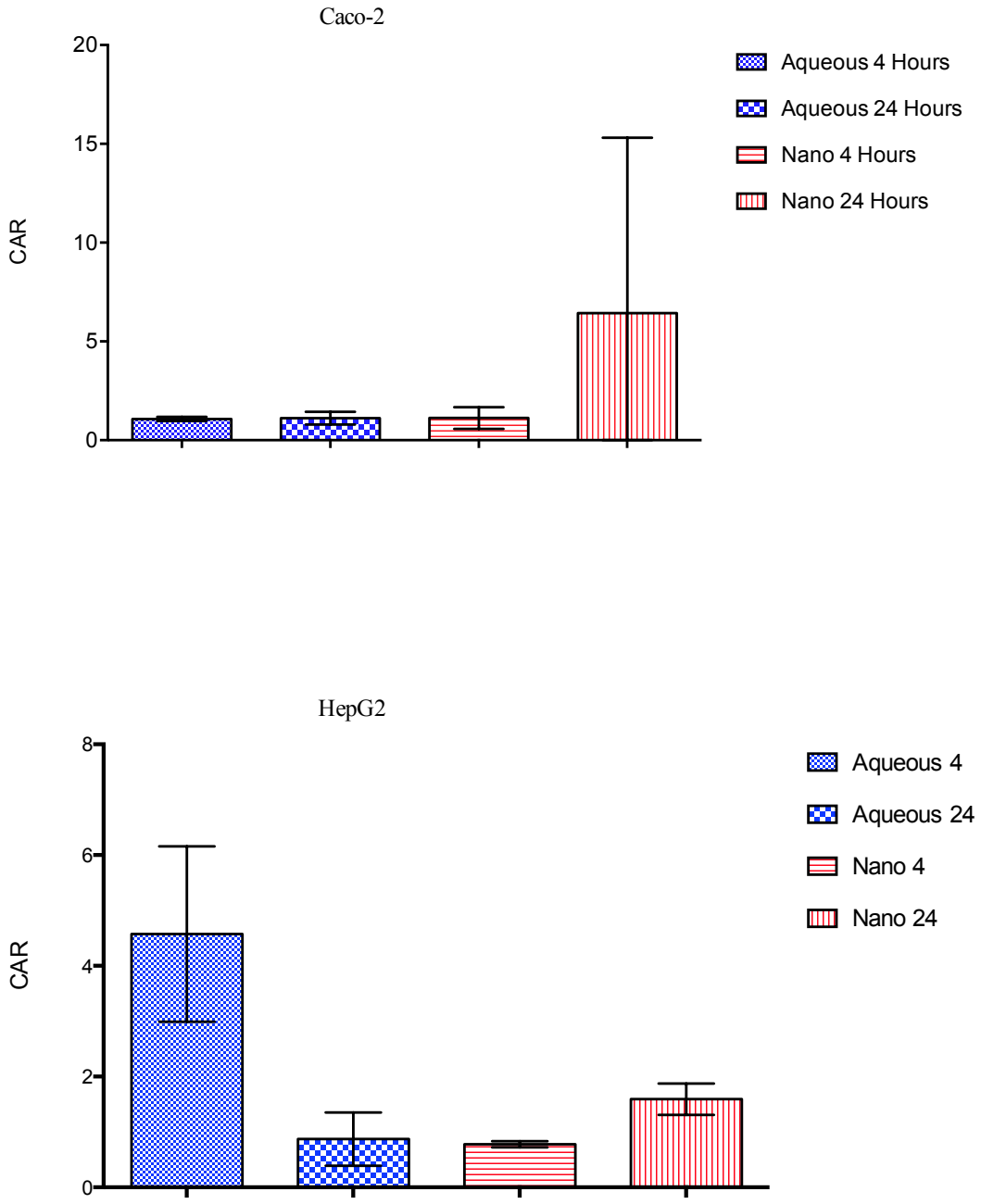


Figure 4.16 Cellular Accumulation Ratio (CAR) of both Aqueous (blue) and nanoemulsion (red) formula of EFV in Caco-2 cells (top) and HepG2 cells (bottom). 1 million cells per well, in a 24 well plate, were incubated with a final concentration of 10 μM drug. Sample concentrations were derived by HPLC analysis Data is shown as +/- standard deviation of N=3.

### 4.3.10 Cellular Accumulation of EFV in Raji-B Cells

Cellular accumulation in Raji B cells showed that there was no difference between the EFV aqueous solution and the EFV nanoemulsion ($p = 0.10$) (Figure 4.17).

### 4.3.11 Cellular Accumulation of EFV in CEM Cells

Cellular accumulation in CEM cells showed that there was no difference between the EFV aqueous solution and the EFV nanoemulsion ($p = 0.70$) (Figure 4.17).

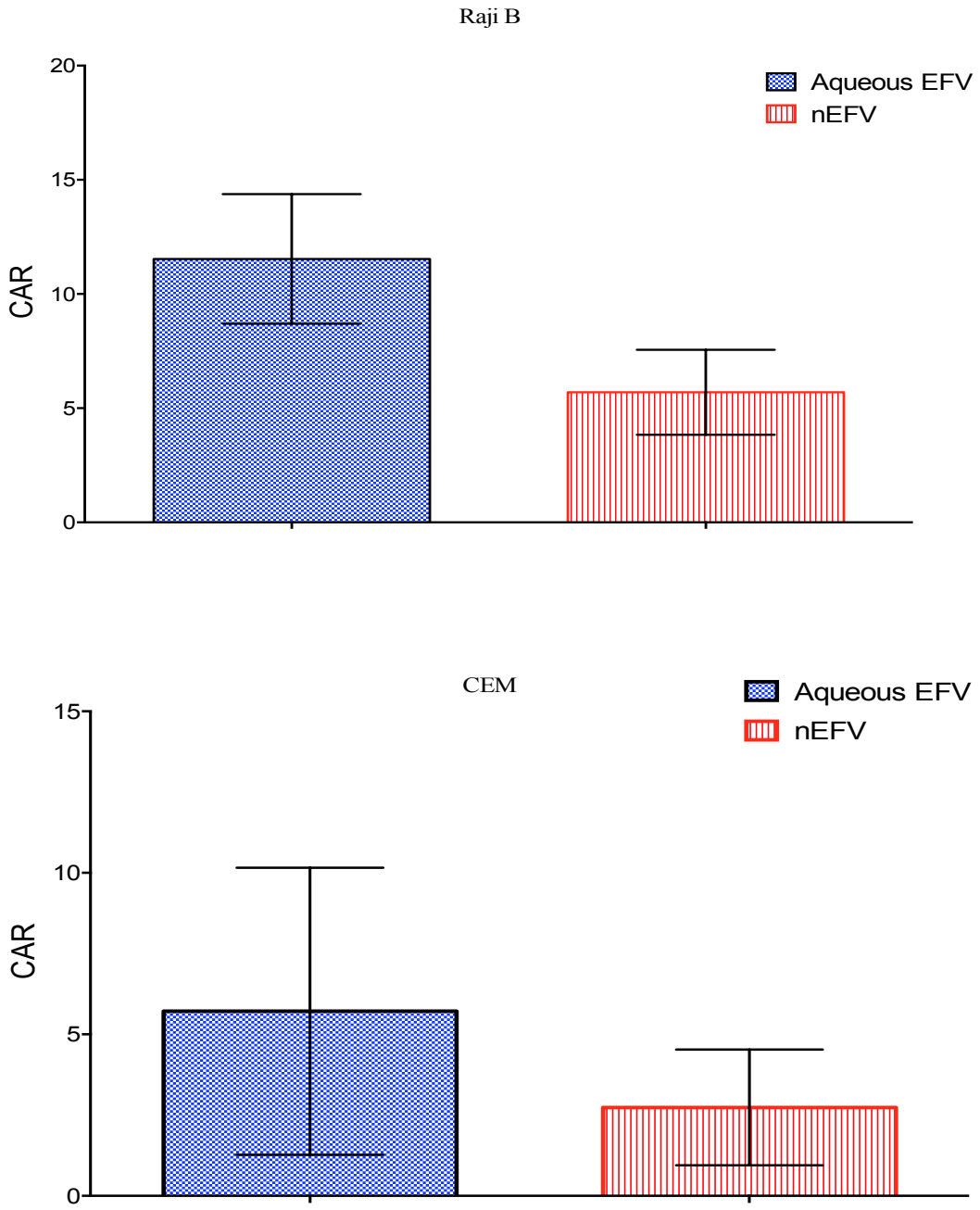


Figure 4.17 Cellular accumulation ratios of 10 μM aqueous (blue) and nanoemulsion (red) formulations of EFV in Raji-B cells (top) and CEM cells (bottom). All samples were taken at 4-hour time point. 1 million cells per well, in a 24 well plate, were incubated with a final concentration of 10 μM drug. Sample concentrations were derived by HPLC analysis Data is shown as +/- standard deviation of N=3.

**4.4 Discussion**

The Papp data for aqueous and nanoemulsion LPV initially showed that the apical to basolateral permeation was improved for the nanoemulsion at the 1-hour time point. However it is also observed that the permeation in the opposite direction, that is basolateral to apical, is also much higher than the aqueous value. LPV is a known p-gp substrate [399], which would make it likely to undergo efflux back out of the Caco-2 cells in the B-A direction. However, the conditions of the transwell assay system do not ideally match those that would be found in an animal model or indeed the human body, as the drug would not accumulate and build up in the basolateral compartment, instead being carried away by the systemic circulation. Additionally caco-2 cells do not form as tight monolayers as those found *in vivo,* which has been cited as a source for the underestimation of compounds that permeate via paracellular routes, as opposed to transport [400]. For this reason it is very promising that the large increase in permeation in the A-B direction at 1 hour would likely result in more drug crossing the intestinal barrier.

The data for the 2-hour time point again showed there was an increase in the permeation from apical to basolateral for the nanoemulsion compared to the aqueous solution of LPV. However, in this instance the same increase in the basolateral to apical direction was not observed, suggestive that the permeation of LPV nanoemulsions is superior to LPV aqueous solution.

The difference in permeation between the aqueous and nanoemulsion formulations could suggest that the drug is being transported across the monolayer by different mechanisms. As the nanoemulsion would be unlikely to be transported across the monolayer via transport proteins, it would infer that the nanoemulsion droplets permeate across the monolayer via paracellular transport, which has been seen in previous studies of nanoparticle permeation [401-404]. This could also explain why there is such a large increase in B-A permeation of the nanoemulsion over the aqueous, as the formulation allows for the movement of drug between the small gaps in the monolayer as it is entrapped within the emulsion droplet. A possible explanation for the reduction in B-A permeation at 2 hours as compared with at 1 hour for the nanoemulsion could be that the nanoemulsions have begun to aggregate and can no longer pass through the monolayer via paracellular means.

By the 24-hour time point, the amount of permeation from A-B and B-A had reached similar levels for both aqueous and nanoemulsion LPV. This could have been due to the nanoemulsion formulation no longer holding the LPV within the oil droplet, due to the LPV leaching out and entering into the aqueous environment. This would be in contrast to studies which have shown a sustained and slow release of drug from within an oil-in-water nanoemulsion [405, 406], but it would be in agreement with a study by Bali *et al* in which oil-in-water nanoemulsions released >60% of loaded drug within 1 hour [407]. It would not be expected that the nanoemulsion had broken down and thus released its payload due to the data observed in Chapter 3 showing that the nanoemulsions remained stable for in excess

of 2 years when dispersed into water, and at least 3 months when dispersed into cell culture medium, as used in the permeation studies.

The data for nanoemulsion EFV permeation was initially less promising, as after 1 hour there was no increase observed in apparent permeability. However after both 2 and 24 hours, the EFV nanoemulsion had significantly increased permeability. At 1 and 2 hours the B-A permeability of EFV aqueous solution was increased compared to EFV nanoemulsion, but again it should be noted that in a static system like the transwell assay, B-A permeability is a less useful measure than A-B. It is still promising to see a reduction in B-A permeability. Another issue of the Caco-2 transwell system is that Caco-2 cells do not express cytochrome P450 2B6 [408, 409], and as this is the main route of metabolism for EFV, there will be an underestimation as to the protective effects that having the drug within the emulsion droplet could have, if it is protected from metabolism. It should also be noted that EFV already shows good intestinal permeability, as it has class 2 status with the FDA (poor solubility, high intestinal permeability) [410, 411], so to have seen further improvements suggests the nanoemulsion formulation has inherently good permeability characteristics.

The role of efflux transporter p-gp (ABCB1, MRP1) is not fully understood for EFV, in a study by Janneh *et al* it was shown that EFV was not a substrate for p-gp, as accumulation was not affected by p-gp [412]. However, other studies have presented conflicting results [413-416], and as such it is hard to put the results for B-A permeability for EFV into context with the transport proteins that would be present in the assay.

The benefit of the nanoemulsion formulation was shown in that it could be directly diluted into aqueous culture media and used in the assay, without need for prior dissolution into a solvent. This could be highly attractive for making more tolerable and safe oral formulations that are easily dose adjustable, especially as in a paediatric setting where the use of solvents such as ethanol is a concern [393], and where there is limited availability to appropriate dosage forms and unknown bioavailability [377, 417, 418].

Monitoring the concentration between the apical and basolateral chambers when one or the other was given media with aqueous or nanoemulsion EFV at 10 μM, showed that the drug was able to permeate through the monolayer and that the concentrations reached equilibrium between the two chambers. Where the final 24 hour time point showed a slight deviation from equal concentrations in both chambers, this could be attributed to the concentration of drug that could have been accumulated within the caco-2 cells in the monolayer, or potentially interacting with

the membrane of the transwells if the nanoemulsions had aggregated and prevented the total release of the encapsulated drug.

Accumulation of EFV in HepG2 cells and Caco-2 cells showed a small difference only at the 4 hour time point in HepG2, suggesting that the ability of the nanoemulsion formulation to accumulate into cells is at least as good as the aqueous solution. Taken one way, these data suggested that there had been no increase in the pharmacological properties of EFV as a nanoemulsion formulation. However, it must be remembered that in order to achieve the equivalent concentrations of 10 μM of LPV and EFV, the aqueous powders were initially dissolved in solvent and then diluted to the appropriate concentration, whereas the nanoemulsion was dispersed in an aqueous phase of water. This is due to the very low aqueous solubility attributed to EFV powder, at approximately 4 μg/ml [419] and LPV is practically insoluble in water [420]. This opens up the possibility of being able to formulate EFV into a liquid solution that does not require an undesirable solvent, such as ethanol [393]. Again, this would be particularly beneficial in paediatric settings, especially considering that 90% of HIV positive children are found in developing countries [419] and these countries do not have access to adequate dosage formulations for children or in those patients that find it difficult to swallow tablets [377]. Having an appropriate adjustable dosage would remove the need to cut up or crush tablets, which has been shown to affect dosage accuracy [421, 422].

This ability to disperse the EFV in oil-in-water nanoemulsions is due to the highly lipophilic nature of the drug (LogP 3.89 as determined by ALOGPS [423]) and that the stock solution of the drug can be made by directly dissolving into the castor oil, which makes up the oil phase of the nanoemulsion. The logP of a compound refers to the ratio of that compound in the aqueous or oil phase of a mixture of two immiscible liquids.

Castor oil is made up of long chain triglycerides, of which 90% are ricinoleate [339], and as such provides an ideal environment to obtain high dissolution and loading of highly lipophilic drugs such as EFV. The maximum concentration of EFV in the oil phase of the nanoemulsion was 50 mg/ ml and for LPV it was 25 mg/ml, which correlates with other studies in the literature in which castor oil based nanoparticles have been used to achieve delivery vehicles with good drug loading [424-426].

The nanoemulsion accumulating to a lesser degree after 4 hours incubation in HepG2 cells is potentially a beneficial outcome, considering that HepG2 cells are a human hepatic cell line, and it is in the liver where the majority of the first pass metabolism of EFV occurs by cytochrome P450s and in particular the 2B6 isoform [427, 428]. These metabolites are ineffective against HIV [429, 430] and thus preventing or delaying metabolism is key to prolonging the circulation of the active drug.

Reducing the amount of drug that accumulates in hepatic tissue would potentially result in an increased circulation time of the drug, due to the fact it is evading metabolism for longer. However, these data are for HepG2 cell lines only, which are not a like-for-like environment that would be found within the liver itself, particularly when it comes to the expression levels of the important metabolic enzymes as shown in previous studies that compared levels of expression of important metabolic genes between human liver and HepG2 cells [431-433]. A further study by Guo *et al* showed that HepG2 cells did not express CYP2B6 or the expression of CYP2B6 was lower than could be detected [434].

As with the HepG2 and Caco-2 data, when accumulation studies were performed in the immune cell lines CEM and Raji-B there was no significant difference observed in the accumulation ratios between the aqueous and nanoemulsion formulations.

EFV binds readily to proteins, with data suggesting that it can be >97% protein bound in the systemic circulation [435], so it is possible that the EFV could also interact with the hydrophilic poly ethylene glycol chains which stabilise the nanoemulsion droplets. This could potentially be investigated by the use of Isothermal Titration Calorimetric analysis, which would give a clearer answer as to whether the polymer and drug molecules could interact [436]. Another hypothesis would be that the nanoemulsion droplets interact with, and again possibly bind to the surface of the cells being used in the assay. With the cell surface covered, either

partially or completely, then the ability of EFV to enter into the cell via passive diffusion would be reduced.

In summary the data presented here has shown that the nanoemulsions are able to accumulate and permeate at least as well as the standard aqueous solutions of EFV and LPV. This is particularly promising, as the nanoemulsion formulations require no addition of solvent to achieve the appropriate concentrations.

# CHAPTER 5

# Assessment of Antiviral Activity of Optimised Oil-in-Water Nanoemulsion (E65) Against HIV-1 IIIB

**Table of Contents**

## 5.1 Introduction

Nanomaterials have the potential to improve the activity of certain drugs, primarily by improving their bioavailability, targeting to diseased cells, or interacting with targets. A number of examples have already been reported in the literature [437-441] and many are in use clinically at present with more in development. In the case of the antiretroviral drugs EFV and LPV, their primary site of action is located inside cells infected with HIV as they target the HIV reverse transcriptase and protease respectively [245, 442]. This is also the case for a number of other therapies that have intracellular targets or mode of action [443-445]. Therefore, by increasing the intracellular accumulation of the API in relevant target cells it may be possible to improve the activity of API without altering their inherent chemical structure.

As highlighted in Chapter 1, EFV is a non-nucleoside reverse transcriptase inhibitor (NNRTI) and impacts HIV replication by inhibiting the viral reverse transcriptase enzyme [442]. This inhibition disrupts the formation of new copies of viral RNA being formed by binding to a distinct site away from the active site on the viral reverse transcriptase enzyme, and as a result new viral particles cannot be created [446]. LPV is a protease inhibitor [245] and works by inhibiting the viral protease enzyme, which is vital for the cleavage of the gag-pol polyprotein, which consists of the viral group antigens (gag) [447] and the viral reverse transcriptase enzyme (pol) [448]. Preventing the cleavage of the polyprotein results in the formation of immature viral particles that are non-infectious [449].

As both of the drugs being used in this thesis have intracellular targets, it was vital for the nanoemulsion formulations to be able to either; permeate the drug molecules inside of the cell as an intact nanostructure and then be broken down to release the drug, or for the nanoemulsion to release the drug prior to entering the cell itself, allowing for the drug molecules to then enter the cells. This could occur as a result of the drug molecules leaching out of the emulsion droplets or from the emulsion droplets associating with the cellular membranes and then the drug diffusing out of the oil phase and into the cell.

There are a number of methods available to assess *in vitro* the antiviral activity of a compound, including enzyme-linked immunosorbant assay (ELISA) for HIV p24 antigen, MTT assay and real time polymerise chain reaction (RT-PCR) techniques.

The method utilised in this Chapter was via MTT viability assay and was used due to its ability to determine the direct effect of the virus on cell viability, and not just to determine number of viral particles, as well as it being a higher throughput assay. Cells that become infected with the virus and are subsequently exposed to viral replication within them will become non viable and have metabolic dysfunction [450]. As the MTT assay is a measure of metabolic function, it is appropriate for the assessment of HIV impact of cellular viability. The MTT assay has also been used previously in the literature to assess the antiviral activity of novel compounds targeting HIV [451].

The aims of the work presented within this Chapter were to assess the viral activity of both LPV and EFV nanoemulsion formulations, and compare that activity with aqueous solutions of these agents. Cytotoxicity against MT4 cells was initially assessed in order to ensure no interference with antiviral activity assays. It was hypothesised that following on from the data presented for cellular accumulation in chapter 4, that there would be no increase in antiviral activity as a result of formulation into a nanoemulsion.

## 5.2 Materials and Methods

### 5.2.1 Materials

In addition to sections 2.21, 3.2.1, and 4.2, the following materials were purchased: HIV-1 IIIB was acquired from the National Institute of Biological Standards and Control (Potters Bar, UK) and MT4 human T-Cell leukaemia cell line was purchased from Public Health England General Cell Collection (Porton Down, UK).

### 5.2.2 Containment Level 3 Protocols

Containment Level 3 (CL3) safety and viral handling training was undertaken before commencement of viral activity assays and all associated work carried out in the CL3 laboratory in the Department of Molecular and Clinical Pharmacology.

### 5.2.3 MT4 Cell Culture

MT4 cells were cultured by seeding a starter culture vial of approximately 5 x $10^6$ in a Nunc T25 flask, containing 10 ml of pre-warmed RPMI media supplemented with 15% FBS. The FBS was sterile filtered before addition to media using 0.2 μm syringe filters. Cells were placed at 37°C in an atmosphere containing 5% $CO_2$ overnight. After this time, cell media was changed to remove residual DMSO from the starting culture vial by pelleting the cells at 2000 RPM for 5 minutes at 4°C, and re-suspended in fresh culture media containing 10% FBS. DMSO at a concentration of 10% had been used as a cryopreserving agent whilst cells were stored at -80°C.

### 5.2.4 MT4 Cell Passage

The cell suspension was transferred from culture flasks into 50 ml falcon tubes and centrifuged for 5 minutes at 2000 RPM in order to pellet cells. Media was aspirated and fresh complete culture media used to re-suspend the cell pellet. The cell suspension was then transferred to fresh culture flasks at a 1 in 4 ratio, such that cells would continue to divide and grow. Cells were passaged in this way every 3 days or sooner depending on indicators from media (phenol red). Cells were counted in the same way as described in section 2.2.8.

### 5.2.5 Viral Replication and Isolation

The lab adapted HIV-1 IIIB strain was added to CD4+ MT4 cells in T-75 cell culture flasks containing 20 mL of pre-warmed RPMI cell culture media, supplemented with 10% sterile filtered FBS. HIV-1 IIIB replicates within the MT4 cells before budding out into the culture media. Viral particles were extracted and frozen at -80°C for future use. The multiplicity of infection (MOI) for the virus was 0.01.

### 5.2.6 MTT Cytotoxicity Assay

Cytotoxicity of EFV and LPV nanoemulsion and aqueous solutions was assessed using MTT assay as described in section 3.2.7

### 5.2.7 Assessing the Activity of Aqueous solution and Nanoemulsion Antiretrovirals Against HIV-1 IIIB

1 vial of HIV-1 IIIB per 1 x $10^6$ MT4 cells suspended in cell culture medium was defrosted and added to MT4 cells in a 50 ml falcon tube. This was centrifuged for 90 minutes at 5000 rpm and 4°C such that the viral particles were able to be in proximity to the MT4 cells and encourage infection of those cells. The supernatant was discarded and the cell-virus pellet re-suspended in fresh culture media to give a concentration of 20,000 cells per 80 μL.

80 μL of cell and virus suspension was plated into individual wells of a 96 well cell culture plate. To this, 20 μL of a 5x concentrated stock solution of candidate drug (aqueous solution or nanoemulsion formulations) was added, giving a final maximal concentration of 10 μM, reducing in a 1:1 dilution series to 0.00512 nM. Negative controls consisted of wells containing only cells and media, whereas positive controls consisted of wells containing cells, media and HIV-1 IIIB without the antiretroviral drug. Plates were incubated for 5 days at 37°C and 5% $CO_2$. Activity of both aqueous and nanoformulations against HIV-1 IIIB was determined by quantifying the amount of live cells in each condition by means of an MTT cell viability assay. Concentrations of LPV and EFV used were below that which showed cytotoxicity, ensuring that any observed cell death was due solely to HIV infection.

The assay worked on the principle that cellular viability could be used as a proxy for viral activity of the aqueous and nanoemulsion formulations. Using the MTT assay to determine cellular viability as previously described in chapters 2 and 3, it was possible to quantify an IC50 value for both LPV and EFV. Higher levels of cellular metabolism would be indicative of increased cell viability, which in turn would suggest that there had been an increase in viral kill

### 5.2.8 Data Analysis

Data were analysed using a non-linear regression curve fit model to generate dose response graphs using Prism for Macintosh computers version 6. Statistical analysis was performed using SPSS version 21 for Macintosh computers. Where data were normally distributed an independent samples t-test was performed to obtain p values. Where data were non normally distributed a non-parametric Mann-Whitney U test was performed. P values are stated throughout.

## 5.3 Results

### 5.3.1 LPV Cellular Cytotoxicity

The data showed that both aqueous solution and nanoemulsion LPV exhibited no cytotoxicity towards MT4 cells at the concentrations used in the assay, as shown by the lack of convergence of sigmoidal dose response curves in Figure 5.1. Analysis of the data was unable to produce an $IC_{50}$ value at this concentration range (10 - 5 x $10^{-6}$ μM), confirming that at the highest concentration used for the activity assay there would be no skewing of the data due to a cytotoxic effect of either the aqueous solutions or nanoformulations.

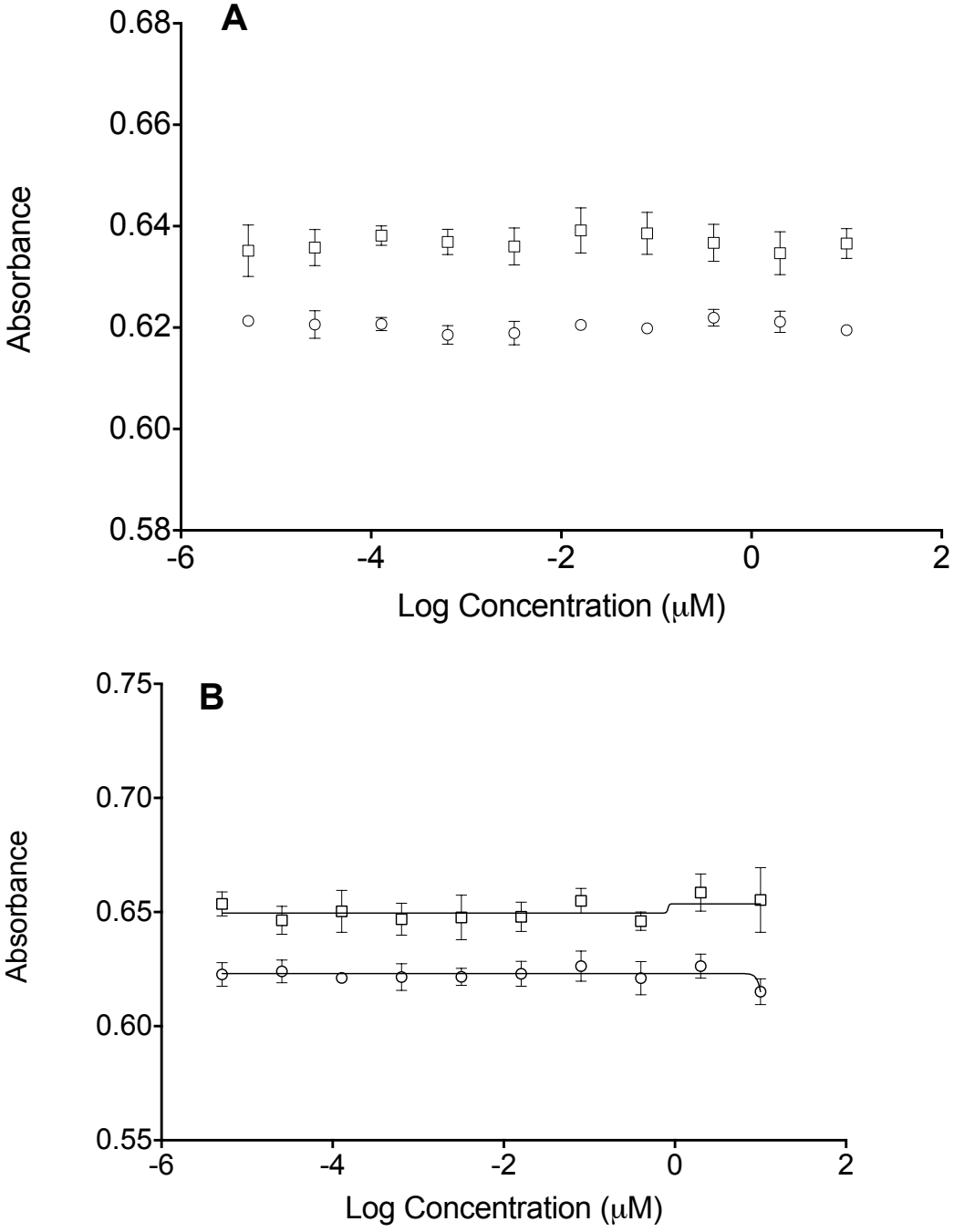


Figure 5.1 Metabolic activity of 100,000 MT4 cells per well in a 96 well plate. Cells were exposed to a concentration range of aqueous (circles) and nanoemulsion (squares) LPV after 24 hours incubation (A) and 5 days incubation (B). Data represented as +/- standard deviation, N=4. As a proxy for cellular viability.

### 5.3.2 EFV Cellular Cytotoxicity

As with the LPV samples, the data for EFV showed that both aqueous and nanoemulsion formulations exhibited no cytotoxicity towards MT4 cells except for at the highest concentration used in the assay, as shown by the lack of convergence of sigmoidal dose response curves in Figure 5.2. Analysis of the data was unable to produce an $IC_{50}$ value at this concentration range (10 - 5 x $10^{-6}$ μM), suggesting that at the highest concentration used for the activity assay there would potentially be a loss in viability due to the concentration of the drug as opposed to the virus, but at all other concentrations in the activity assay this would not be the case.

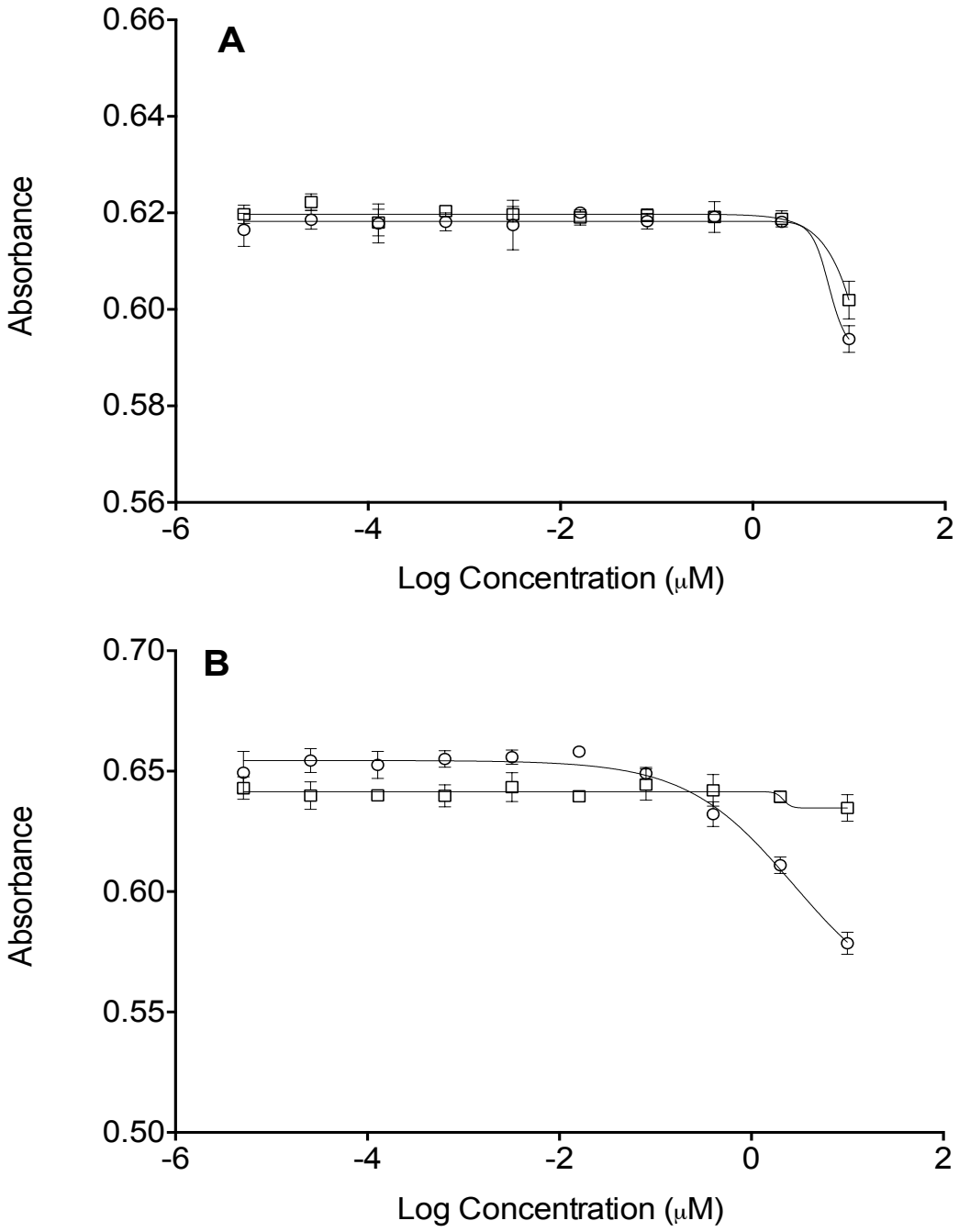


Figure 5.2 Metabolic activity of 100,000 MT4 cells per well in a 96 well plate. Cells were exposed to a concentration range of aqueous (circles) and nanoemulsion (squares) EFV after 24 hours incubation (A) and 5 days incubation (B). Data represented as +/- standard deviation, N=4. As a proxy for cellular viability.

### 5.3.3 Antiviral Activity of LPV

The antiviral activity of aqueous LPV was slightly lower than that of the nanoemulsion LPV with $IC_{50}$ values of 0.9 μM and 1.1 μM, respectively. Figure 3 shows the % viral kill of both aqueous and nanoemulsion LPV, and it was seen that the activity of both formulations were equal, despite the small difference observed in overall $IC_{50}$ values.

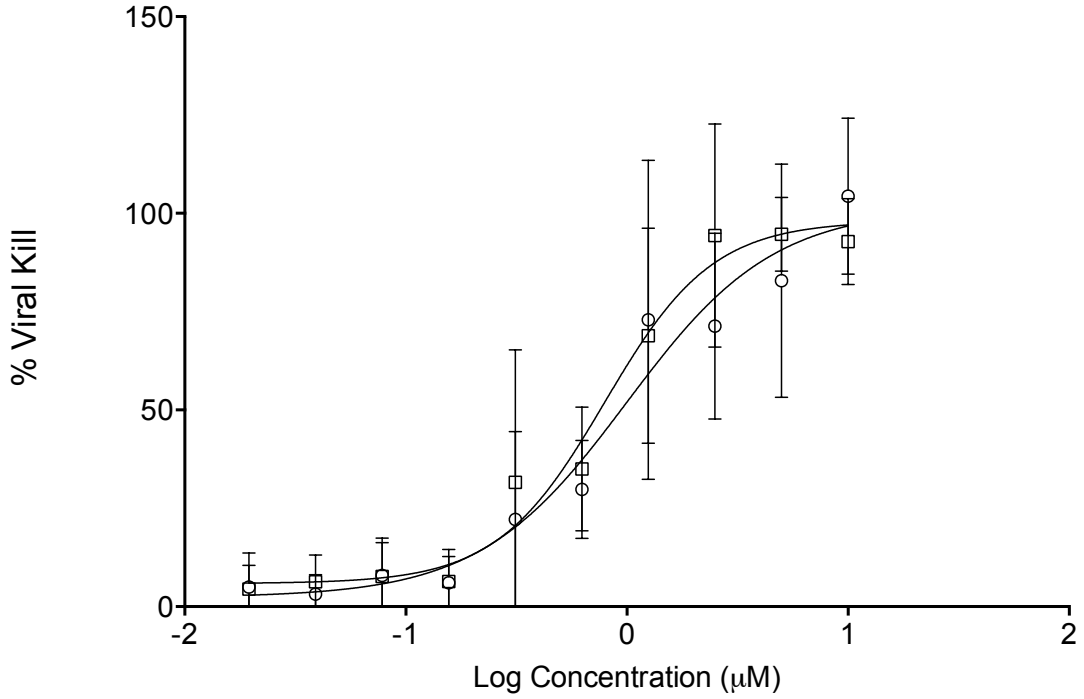


Figure 5.3 Antiviral activity of aqueous LPV (circles) and nanoemulsion LPV (squares) after 5 days incubation with MT4 cells and HIV-1 IIIB. Viral kill was derived by using MTT assay to quantify the metabolic activity of the MT4 cells, using this a proxy of cellular viability. Increased viability indicated an increased viral kill, as compared to control untreated MT4 cells, exposed only to HIV-1 IIIB. Data expressed as +/- standard deviation, N=8.

### 5.3.4 Antiviral Activity of EFV

The antiviral activity of aqueous EFV solution and EFV nanoemulsion was identical with $IC_{50}$ value of 0.6. Figure 4 shows the % viral kill of both aqueous EFV solution and EFV nanoemulsion, and it was again seen that the activity of both formulations were equipotent despite the small difference observed in overall $IC_{50}$ values.

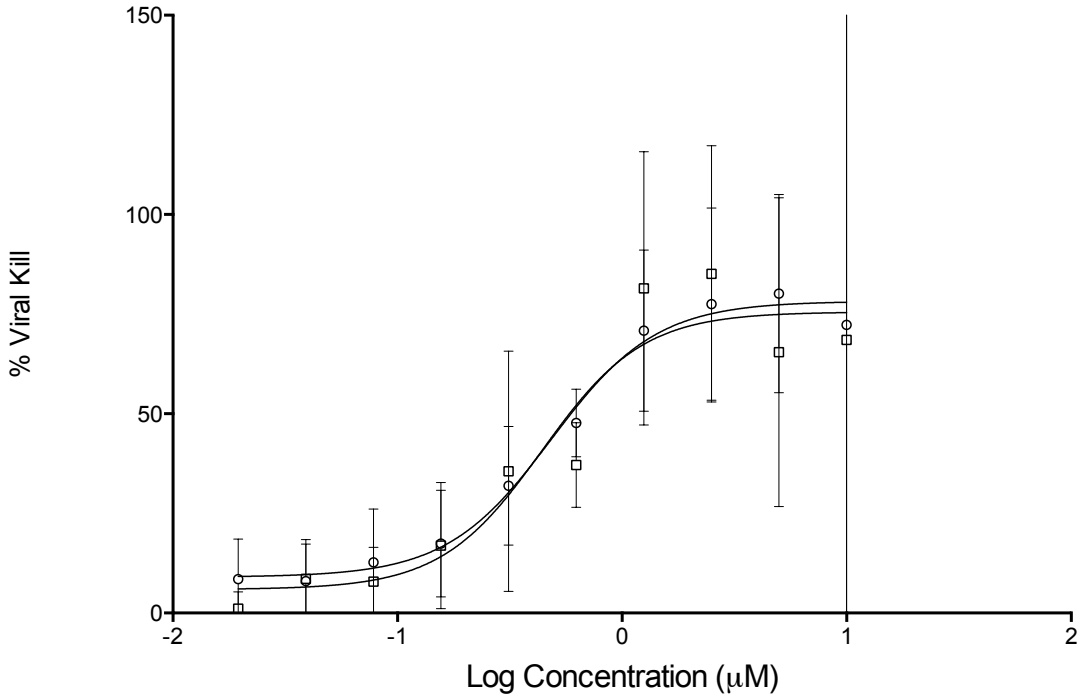


Figure 5.4 Antiviral activity of aqueous EFV (circles) and nanoemulsion EFV (squares) after 5 days incubation with MT4 cells and HIV-1 IIIB. Viral kill was derived by using MTT assay to quantify the metabolic activity of the MT4 cells, using this a proxy of cellular viability. Increased viability indicated an increased viral kill, as compared to control untreated MT4 cells, exposed only to HIV-1 IIIB. Data expressed as +/- standard deviation, N=8.

### 5.3.5 Antiviral Activity of Unloaded Nanoemulsion

As the data in Figure 5 shows, when unloaded nanoemulsion was incubated with MT4 cells and HIV-1 there was no antiviral activity observed. This confirms the nanoemulsion delivery vehicle itself had no inherent antiviral properties, and the activity seen in 5.3.4 and 5.3.3 was due to the entrapped LPV and EFV.

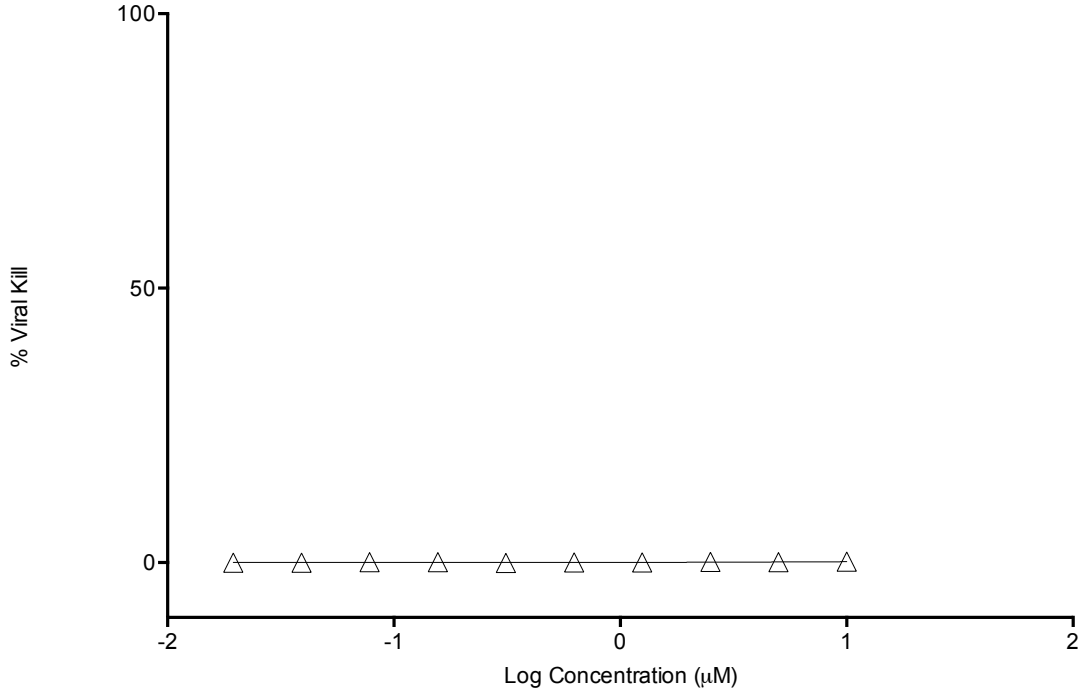


Figure 5.5 Antiviral activity of unloaded nanoemulsion after 5 days incubation with MT4 cells and HIV-1 IIIB. Viral kill was derived by using MTT assay to quantify the metabolic activity of the MT4 cells, using this a proxy of cellular viability. Increased viability indicated an increased viral kill, as compared to control untreated MT4 cells, exposed only to HIV-1 IIIB. Data expressed as +/- standard deviation, N=4.

### 5.3.6 Statistical Summary of Antiviral Activity

Table 5.1 Summary of $IC_{50}$ values for all formulations tested

| **Formulation** | **$IC_{50}$ (µM, +/- SD)** |
|---|---|
| Aqueous LPV | 0.9 (+/- 0.32) |
| Nanoemulsion LPV | 1.1 (+/- 0.59) |
| Aqueous EFV | 0.6 (+/- 0.01) |
| Nanoemulsion EFV | 0.6 (+/- 0.22) |

Statistical analysis showed that there was no difference between the IC50 of LPV aqueous solution and LPV nanoemulsion with values of 0.9 µM and 1.1 µM respectively, ($p = 0.4$). The same was seen for EFV aqueous solution and EFV nanoemulsion with a value of 0.6 µM for both ($p = 0.1$) (Figure 5.6).

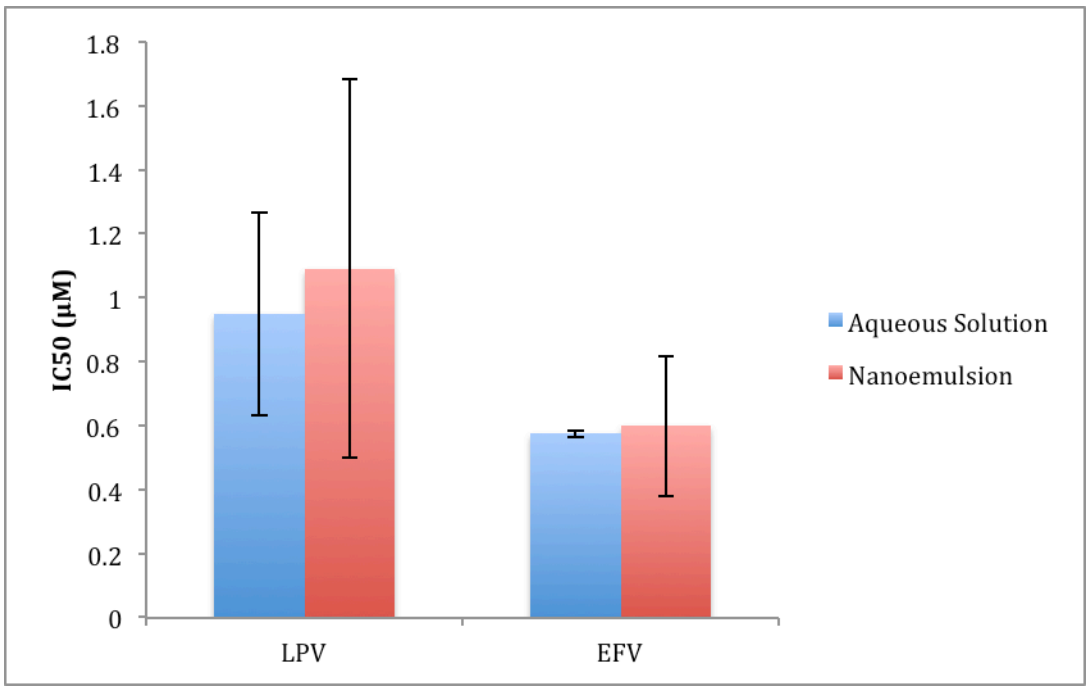


Figure 5.6 Summary of $IC_{50}$ values for viral kill of HIV-1 IIIB after exposure to EFV and LPV aqueous solutions and nanoemulsions. Viral kill was derived by using MTT assay to quantify the metabolic activity of the MT4 cells, using this a proxy of cellular viability. Increased viability indicated an increased viral kill, as compared to control untreated MT4 cells, exposed only to HIV-1 IIIB. Data is represented as +/- standard deviation N=8.

**5.4 Discussion**

The data for cytotoxicity showed that both the LPV aqueous solution and LPV nanoemulsion formulations had no cytotoxic effect towards the MT4 cells after 5 days, this is in agreement with the data presented in Chapter 3, in which both showed no cytotoxicity towards a range of human cell lines. There was a cytotoxic effect seen for both EFV aqueous solution and EFV nanoemulsion at the highest concentration used, but again, no $IC_{50}$ value was determined at the concentration range used, so in order to determine an $IC_{50}$ value for cytotoxicity an increased range of drug concentrations would be needed. This was however not necessary in this study, as only the highest concentration of drug used for the activity testing showed a slight cytotoxicity, and as such it reassures that the activity data was not overtly skewed by the loss of MT4 cells due to overt cellular cytotoxicity, although this doesn't necessarily mean that the materials are not cytotoxic at higher concentrations.

The data for viral activity was very promising as it showed that the nanoemulsion formulations had equal activity against the laboratory strain HIV-1 IIIB. This was highly suggestive that the incorporation of antiviral drugs into nanoemulsion formulations would not have a detrimental effect on the effectiveness of those drugs, at least in the case for drugs whose targets lie within the cell. As equal activity was shown for both LPV and EFV, this inferred that the formulation of the drugs into a nanoemulsion did not affect the activity, despite LPV and EFV having different

target sites and modes of action. Nanoemulsions have previously been reported as having controlled drug release profiles [405, 452-454].

There are no literature reports that show nanoemulsions as enhancing the antiretroviral activity of HIV drugs. There are however reports on polymer based nanoformulations. Work by das Neves *et al* has shown that dapivirine (also known as TMC120) when formulated into poly(epsilon-caprolactone) based nanoparticles has an increase antiviral activity. The increase in antiviral activity correlated with increased intracellular accumulation [455]. In other work by Balkundi *et al* it was shown that nanoformulations of EFV, indinavir (IDV), RTV, and atazanavir (ATV) produced by wet milling techniques had varying antiretroviral activities. This variance correlated with the drug being used, and potentially due to the milling technique used, as the drug would be a core part of the nanoparticle structure [456].

The data for the unloaded nanoemulsion droplets showed there was no antiviral effect and as such the activity of the nanoemulsion formulations of EFV and LPV was solely due to the drug molecules. This would also explain why there was no increase in activity shown when the drugs were in nanoemulsion form and also supports the hypothesis that the drug molecules were prevented from leaving the emulsion droplet. It was not possible from this data however to determine when the drug molecules left the nanoemulsion droplets, or how they left, be it by leaching or breakdown of the entire nanoemulsion. It was also not possible to determine if any intact nanoemulsions, or constituents of those nanoemulsions (polymer, initiator, oil)

had entered into the cells. This could be explored further in the future by the incorporation of radioisotope tracer to the constituent parts of the nanoemulsions.

In summary, the nanoemulsions produced in this thesis have been shown to have equal activity against HIV-1 IIIB. Added to the findings in the previous Chapter 4, suggest that the nanoemulsion formulation is a valid vehicle for the delivery of ARVs and does not affect the antiviral activity. The data presented in Chapter 6 will finally explore the safety of these nanoemulsion formulations in respect to the human immune system.

# CHAPTER 6

# Immunological and Haematological Safety Assessment of Optimised Oil-in-Water Nanoemulsion (E65)

**Table of Contents**

## 6.1 Introduction

Chapters 2 and 3 provided evidence to demonstrate that the formulated nanoemulsions are stable and have good, reproducible, physicochemical characteristics. Additionally, there was no overt cytotoxicity of either the unloaded nanoemulsion or the drug-loaded nanoemulsions in the cells assessed. However, it is possible that nanoemulsions, and nanoparticles in general, may have other deleterious effects. The aim of this Chapter was to investigate the interaction of these nanoemulsions with human immunological and haematological systems using *in vitro* and *ex vivo* assays that have been shown to have good correlation with *in vivo* effects [457]. There is an increasing body of evidence of these kinds of interactions by nanoparticles and suggestions that their investigation should form a part of any preclinical assessment of novel nanomaterials.

Currently there is a relative lack of guidance on the preclinical assessment of nanomaterials compared to small molecules and biotherapuetics. The view of the regulatory agencies is generally that each new material should be investigated on a case-by-case basis [458-460]. Additionally, due to their inherent physicochemical properties, many nanomaterials can directly interfere with the assays being used to assess them [461, 462]. The heterogeneity of nanomaterials being produced is perhaps the biggest advantage and disadvantage of the field. Whilst nanomaterials can be engineered to produce a number of desired effects, this heterogeneity makes determining structure-activity relationships difficult. Additionally, differences in experimental approach and the relative lack of reporting negative effects of

nanomaterials makes their safety/compatibility assessment challenging. In 2008 a workshop was held at the National Cancer Institute, USA, in an effort to begin to address these challenges, with the recommendations being published by Dobrovolskaia *et al* [463].

For the purposes of this Chapter, immunotoxicity will be used as a term not only for direct cytotoxicity of nanomaterials to cells of the immune system, but also their impact on immune function. There have been a number of cases reported in the literature where apparent immunotoxicity of nanomaterials has been shown to be caused by chemical or biological contaminants in the samples used rather than the material itself [464]. Biological contamination may come from endotoxin (lipopolysaccharide; LPS), mycoplasma or bacteria. Endotoxin can be present in a material and not cause any problems, but there have been cases in the literature in which endotoxin was detected alongside nanomaterials at levels that usually cause no response, but the presence of the nanomaterial exacerbated the effects [465]. The presence of these contaminants must be screened for, as there is the potential hazard to health, as well as published guidelines on the amount of endotoxin that can be present in administered materials. Currently the accepted levels are set at 5 endotoxin units (EU) per kg for any route of administration and 0.2 EU/kg for intrathecal, as stipulated in the US Pharmacopeia. For reference, the current endotoxin limit for pure water is 0.25 EU/kg. Additionally, these biological contaminants can provide potential false positive results in immunological assays

[462, 466] and it is therefore important to measure contamination prior to studies of immune interference.

In this Chapter the interaction of nanoemulsions with various immunological and haematological targets was investigated. The choice of these targets is based on the disease context i.e. HIV infection as well as evidence from the literature on previous undesirable interactions.

Macrophages are a very important component of the immune system in regards to HIV therapy, as they are sites for infection and sanctuary for the HIV particles [467], allowing continual replication with sub-optimal concentrations of current therapeutic agents [468, 469]. Macrophages can be split into two types; M1 macrophages [470] that are usually responsible for the engulfing and subsequent removal of cellular debris and pathogenic materials; and M2 macrophages [471] that are used in cellular repair [472]. It is important to assess any interaction with macrophages due to their vital role in maintaining host defence mechanisms. Macrophages also have the potential to alter the biodistribution of nanoparticle-based delivery systems as they may engulf the particles and transfer them elsewhere [473], including routing them to the lymph nodes. The lymph nodes are heavily populated with T cells and as such exposure to macrophages may increase nanoparticle exposure to T cells via the lymphatic system.

For immunotoxicity, T-cells are also important due to their role in the immune response. T helper cells [474] are responsible for the activation of the immune response after being presented with an antigen. T helper cells can secrete cytokines [475], which can then go on to activate other immune cells including cytotoxic CD8+ T cells [476]. After activation T helper cells can differentiate into either type 1 T Helper cells (Th1) or type 2 T Helper cells (Th2) [477], each with its own cytokine profile, allowing for the activation and regulation of distinct immune responses [478]. Previously nanoparticles have been shown to interact with and affect the differentiation and response of T cells after exposure [479-482].

CD8+ T cells are responsible for the destruction of virally infected cells, and as such play a vital role in the immune response [483, 484]. Assessments must be made on new nanomaterials to determine any interactions with CD8+ T cells, as any stimulating effect could lead to problems with autoimmune related conditions and an inhibitory effect could lead to compromised immune responses and a lack of protection towards infective entities, particularly in the case of a disease like HIV. This is particularly relevant for nanoemulsions as, depending on their route of administration, they may come directly into contact with immune cells in the blood as well as being taken up into the cells and having an intracellular effect. In the context of HIV therapy, CD4+ T-cells are a desirable target for a nanoformulation due to the fact that HIV can reside within these cells, and drug penetration into these cells can be low for standard HIV drugs [468, 485, 486]. This highlights the

importance of this cellular target for immunotoxicity studies where an increased uptake of material needs to be balanced for desirability versus safety.

Nanomaterials can also interact directly with red blood cells, particularly those formulations that are to be injected [487, 488]. This can cause haemolysis: the process in which red blood cells are damaged by biological or mechanical means [489], resulting in the leakage of haemoglobin into the blood stream and subsequent binding to haptoglobin [490]. It is therefore important to assess any interaction a nanomaterial may have on red blood cells, particularly as there is the chance for serious complications, such as anaemia, to arise [348, 460, 491, 492].

Aside from the destruction of red blood cells, nanomaterials should also be assessed for their propensity to induce or prevent coagulation of blood via clotting or in the formation of a thrombus; a mixture of red blood cells, platelets and fibrin [352]. Coagulation is essential not only for the prevention of bleeding in response to a wound, but it also plays a role in the immune response, specifically when pathogens are present in the blood stream [493]. Maintaining homeostasis between procoagulant and anticoagulant states is controlled by a combination of cells (such as platelets), blood proteins and the flow of blood itself, collectively known as Virchow's triad [494]. Nanomaterials have the potential to interact at all stages of the coagulation system, and as such investigations into the effect of the nanoemulsion formulations on coagulation were essential to predict any potential

effects, particularly as nanoparticles have been previously shown to interact with blood coagulation [495-498].

Exposing a patient to a material that has shown an ability to induce clotting carries an inherent risk, but it would not necessarily signal the end of development for a formulation as if the effect on clotting was only small and well documented, then appropriate precautions and the administration of an anticoagulant may mitigate the risk. This would however only be a viable option if the benefits of that particular formulation outweighed the added risk.

Natural killer (NK) cells are a type of lymphocyte that play a cytotoxic role in the body's immune response to virally infected and cancerous cells [499-501], but they differ from cytotoxic CD8+ T cells in that they are involved in innate immunity and early defence [502]. NK cells are also involved in the secretion of cytokines when activated [503, 504], further adding to the immune response and in particular against viral infections. As such it was important to assess the effect nanomaterials may have on NK cells due to their vital role in viral suppression, as well as their ability to initiate further immune responses.

The complement system, a part of the innate immune system, is an aid to antibodies and phagocytic cells, helping them to remove pathogens from the body [505]. In mammals there are around 30-40 proteins that have been associated with the complement system and they are found in the blood plasma, body fluids and

associated on surfaces [506]. A material that had the effect of activating the complement system would be undesirable because of the chance of activation leading to inflammatory and autoimmune reactions, and the recruitment of complement molecules to the nanomaterial may also lead to a decrease in the levels of complement in the systemic circulation and potential for pathogens to avoid the immune response. Activation of the complement system can also have a pro-coagulant effect that may lead to clotting via disseminated intravascular coagulopathy [507]. There have been reports in the literature of nanomaterials that have activated the complement system [508-510].

The work presented in this Chapter aims to evaluate the safety of the nanoemulsion system with respect to the different areas of the immune system outlined previously. Nanoemulsions were compared with aqueous solutions of EFV in order to give a comparison with the currently approved pharmaceutical agent. It was hypothesised that the formulation of EFV into the nanoemulsion carrier would not have a significant impact on immunological safety, as compared to the aqueous solution of EFV. This would be due to the polymer stabilisers consisting of relatively inert poly PEG chains, which has been used in other forms previously, in pharmaceutical products.

## 6.2 Materials and Methods

In addition to sections 2.21, 3.2.1, 4.2, and 5.2.1 the following materials were purchased:

Ficoll-Paque was purchased from Fisher Scientific (Loughborough, UK), Buffy coats were obtained from the National Health Service Blood and Transplant Special Health Authority (Liverpool, UK). FITC fluorescently labelled CD4 and CD8 antibodies, APC fluorescently labelled CD44 and CD69 antibodies and PE fluorescently labelled CD25 and CD95 were all bought from Miltenyi Biotec GmbH (Bergisch Gladbach, Germany). Miltenyi also supplied MACSQuant® running buffer, MACSQuant® calibration beads, MACS separation beads (human CD8, CD56 and CD4), QuadroMACS$^{TM}$ magnetic separator, MACS LS separation columns, and human T-cell activation/expansion kit containing: Anti-Biotin MACSiBead$^{TM}$ particles cell culture grade, human CD2-Biotin, human CD3-Biotin, and human CD28-Biotin. $H^3$ thymidine was supplied by Moravek Biochemicals (California, USA).

All reagents for cytokine secretion studies were supplied by Bio-Rad Laboratories LTD (Hemel Hempstead, UK) in the form of a Bio-Plex Pro kit, containing: coupled magnetic beads, detection antibodies (for IL-1b, IL-2, IL-6, IL-8 IL-10, TNF-α and IFN-γ), cytokine standards, standard diluent, sample diluent, assay buffer, wash buffer, detection antibody diluent, streptavidin-PE and a 96 well filter plate. Bio-Plex calibration and validation kits, along with Bio-Plex sheath fluid were also purchased from Bio-Rad Laboratories LTD.

For NK cell studies, phosphate buffered saline, horse serum, fetal bovine serum, MEM alpha modification, RPMI-1640 and L-glutamine were purchased from GE Healthcare HyClone (Logan, USA), Myo-inositol and folic acid were purchased from Sigma-Aldrich (St Louis, USA), while 2-mercaptoethanol and trypan blue solution were bought from Invitrogen (Life Technologies, New York, USA). NK92 cells were purchased from the American Tissue Culture Collection (ATCC) (Manassas, US).

For LAL studies, sodium hydroxide and hydrochloric acid were bought from Sigma-Aldrich (St Louis, USA) while control endotoxin standard, LAL reagent and LAL water were purchased from Associates of Cape Cod (East Falmouth, USA).

### 6.2.1 Adherent Cell Culture

As described in 2.2.8

### 6.2.2 NK92 Cell Culture

NK92 cells were cultured in Alpha Minimum Essential medium without ribonucleosides and deoxyribonucleosides but with 2 mM L-glutamine, 1.5 g/L sodium bicarbonate, 0.2 mM inositol, 0.1 mM 2-mercaptoethanol, 0.02 mM folic acid, 200 U/ml recombinant IL-2 and adjusted to a final concentration of 12.5% horse serum and 12.5% fetal bovine serum. Viability of NK92 following treatment with nanomaterials was assessed via trypan blue exclusion.

### 6.2.3 Suspension Cell Culture

As described in 2.2.9

### 6.2.4 Peripheral Blood Mononuclear Cell Isolation and Culture

Peripheral Blood Mononuclear Cells (PBMCs) were isolated from buffy coats that had been separated from whole blood via Ficoll-Paque density centrifugation. Whole blood was layered on top of the Ficoll reagent in a 50 mL falcon tube at a ratio of 2 parts blood to 1 part Ficoll. This was then centrifuged for 30 minutes at 2000 rpm and 4°C and importantly the brakes of the centrifuge were not applied, instead allowing the rotor to come to a natural stop so as to prevent disruption to the PBMC layer. The PBMC layer was present between the top layer of plasma and the bottom layer of red blood cells; PBMCs were carefully removing using a transfer pipette and placed into a 50 mL falcon tube. This was topped up with HBSS and further centrifuged for 5 minutes at 2000 rpm and 4°C in order to wash the cells. The supernatant was discarded and cell pellet re-suspended in fresh RPMI media supplemented with 10% sterile filtered FBS, before transfer into a T-175 cell culture flask.

PBMCs were placed in T-175 cell culture flasks and left in a cell incubator overnight at 37°C and 5% $CO_2$. For subsequent immune assays fresh PBMCs were again isolated from new batches of buffy coats.

### 6.2.5 Detection and Quantification of Gram Negative Bacterial Endotoxin Contamination in Nanoemulsions by Kinetic Turbidity Limulus Amoebocyte Lysate (LAL) Assay

This assay was conducted by Dr Neill Liptrott while a visiting researcher at the Nanotechnology Characterisation Laboratory based within the National Cancer Institute, Maryland, USA. The assay worked on the principle that the presence of endotoxin in the sample would cause the LAL to coagulate, thus forming a gelled clot. The result of the experiment was a simple clot or no clot read out, therefore providing a non-qualitative measure of any endotoxin present.

Standard lipopolysaccharide (LPS) from *E. coli* was reconstituted to a final concentration of 1000 EU/mL in pyrogen-free LAL water. Further dilutions were then made in pyrogen-free LAL water to produce a standard curve of 1, 0.1, 0.01 and 0.001 EU/mL. LAL was reconstituted in Glucashield buffer to prevent possible interference by β-glucans that may be present in sample materials. Negative control consisted of pyrogen-free LAL water only and positive control 0.05 EU/mL LPS. Samples of EFV aqueous solution and EFV nanoemulsion were prepared in pyrogen-free LAL water at concentrations of 4 μg/mL and 40 μg/mL. Inhibition/enhancement (IEC) controls consisted of test samples containing 0.05 EU/mL LPS. Reactions consisted of standard, sample or control with the addition of LAL (50 μL). Samples were then analysed using a Pyros Kinetic Flex reader (American Associates of Cape Cod). Results from each individual assay run were not considered valid unless the precision and accuracy of the standard curve ($r^2 \geq$

0.98) and quality controls were within 25% and the inhibition/enhancement control exhibited 50–200% spike recovery.

### 6.2.6 Detection and Quantification of Gram Negative Bacterial Endotoxin Contamination in Nanoemulsions by Limulus Amoebocyte Lysate (LAL) analysis (gel-clot)

This assay was conducted by Dr Neill Liptrott while a visiting researcher at the Nanotechnology Characterisation Laboratory based within the National Cancer Institute, Maryland, USA.

Samples were prepared as for kinetic turbidity analysis with the exception of standard curve samples, which were prepared as 0.25 λ to 2 λ (λ is the sensitivity of the lysate provided for each lot of the lysate by the manufacturer). IEC were prepared in 0.25 λ to 2 λ samples to assess interference with the assay. Samples were incubated for 1 hour at 37°C in an unstirred water bath. Following incubation, sample tubes were inverted to assess the formation of a clot.

### 6.2.7 Sterility Testing of Nanoemulsions by LB Agar Plate Streaks

This assay was conducted by Dr Neill Liptrott while a visiting researcher at the Nanotechnology Characterisation Laboratory based within the National Cancer Institute, Maryland, USA.

To determine if microbial contamination was present in sample materials 50 μL (1 mg/mL) of material was streaked onto LB agar plates and incubated in a humidified incubator at 37°C for 48 hours. An *E. coli* stock solution was used as a positive control for microbial growth. Following incubation plates were visually inspected for signs of microbial growth and recorded digitally.

### 6.2.8 Sterility Testing of Nanoemulsions by Mycoplasma Analysis in H460 Cells

This assay was conducted by Dr Neill Liptrott while a visiting researcher at the Nanotechnology Characterisation Laboratory based within the National Cancer Institute, Maryland, USA.

H460 cells were treated with sample materials (4 μg/mL) and passaged every 48 hours in RPMI-1640 media containing 10% FBS. At each passage, a sample of culture supernatant was retained for mycoplasma analysis. After 18 passages the first and last passage samples were analysed for the presence of mycoplasma using endpoint PCR containing specific primer sequences.

### 6.2.9 MACs Separation of Immune Cell Subsets from PBMCs

PBMCs were separated from buffy coats as described in 6.2.4 and cell number determined by trypan blue exclusion (See Section 2.2.8), up to 1 x $10^7$ were used for the following separation conditions. Higher cell numbers would require scale-up of reagents as appropriate. All work was carried out on ice and buffers and solutions had been pre-cooled. Cells were centrifuged at 300 x g for 10 minutes at 4°C. Supernatant fraction was aspirated and discarded, with cell pellet being re-suspended in 80 µL of buffer (PBS at pH 7.2 supplemented with 0.5% bovine serum albumin and 2 mM EDTA). 20 µL of appropriate (CD4 or CD56 or CD8) MicroBeads were added to the cell suspension and mixed well then left in the fridge (2-8 °C) for 15 minutes. After this time, cells were washed by adding 2 mL of buffer and centrifuging for 10 minutes at 300 x g and 4°C, supernatant was discarded and cell pellet re-suspended in 500 µL of buffer. At this point cells were ready to proceed to the separation step.

Miltenyi Biotec LS columns (columns containing ferromagnetic spheres with cell-friendly coating) were placed into a Miltenyi Biotec QuadroMACS™ cell separator and prepared by rinsing with 3 mL of buffer. Magnetically labelled cell suspension was applied to the top of the column and washed through with 3 x 3 mL of buffer, allowing unlabelled cells to pass through the column whilst labelled cells were held in the column under the magnetic field. After the final rinse, 5 mL of buffer was added to the column, and immediately the column was removed from the QuadroMACS™ and labelled cells flushed out of the column into a 15 mL falcon

tube, by applying the LS column plunger and firmly pressing down. Immune subsets were now ready for use directly into cellular assays, or for placing into RPMI media and incubated for use later.

### 6.2.10 Human T-Cell Activation Via Miltenyi T Cell Activation Kit

PBMCs were separated from buffy coats as described in section 6.2.4 and cell number determined by trypan blue exclusion (See section 2.2.8). T cell activation was performed on resting T cells from the PBMCs, but positively selected T Cells (CD4, CD8, etc) could also be processed using the protocol described in section 6.2.9.

Anti-Biotin MACSiBead$^{TM}$ particles were re-suspended by thoroughly vortexing before use in order to obtain a homogenous suspension of particles. 100 µL each of CD2-Biotin, CD3-Biotin and CD28-Biotin was pipetted into a 1.8 mL universal tube, to which 500 µL of Anti-Biotin MACSiBead$^{TM}$ particles were added, giving a total of 1 x $10^8$ particles. Finally, 200 µL of buffer (PBS at pH 7.2 supplemented with 0.5% human serum albumin and 2 mM EDTA) was added to adjust the volume to 1 mL, and this was placed on a gentle roller in a 4°C cold room for 2 hours. After this time the loaded bead particles were ready for use and could be stored for up to 4 months.

The following protocol was used to give a ratio of 1 Anti-Biotin MACSiBead$^{TM}$ particle per 2 PMBC and the volumes were used for up to 5 x $10^6$ cells. When using

higher cell numbers, reagent volumes would be scaled-up appropriately. Loaded Anti-Biotin MACSiBead™ particles were re-suspended thoroughly by vortexing, and 25 µL was transferred to a 15 mL falcon tube. 200 µL of RPMI culture media was added, following which the suspension was centrifuged at 300 x g for 5 minutes at 4°C. Supernatant was aspirated and discarded, with loaded Anti-Biotin MACSiBead™ re-suspended in 100 µL of fresh RPMI culture media. PMBCs were re-suspended to a density of 5 x $10^6$ cells per 900 µL of RPMI culture media, to which the 100 µL of Anti-Biotin loaded MACSiBead™ particles were added. These were then used as the bead activated cells for cytokine secretion studies.

### 6.2.11 Stimulation of Lymphocytes for Cytokine Secretion Studies

PBMCs were separated from buffy coats as described in section 6.2.4 and cell number determined by trypan blue exclusion (See section 2.2.8), 1 x $10^6$ cells were seeded per well in 24 well cell culture plates. The assay was set up separately using both activated PBMCs (See Section 6.2.10) and non-activated PBMCs straight from buffy coats. EFV aqueous solution and EFV nanoemulsion were added to appropriate wells to give a final concentration of 10 µM of drug in 1 mL total of suspension. Negative controls of PBMCs (either bead activated or non-bead activated) were plated without the presence of drug compound to give a background reading of cytokine secretion. All conditions were performed on N=4 buffy coats in duplicate.

The 24 well cell culture plates were then incubated at 37°C with an atmosphere of 5% $CO_2$ for 24 hours, after which time the culture plates were centrifuged at 2000 rpm for 5 minutes and 4°C. The supernatant was collected in 100 µL fractions in 96-well plates and stored at -80°C for analysis later using the Bio-Plex 200 Luminex Plate Reader (Bio-Rad Laboratories LTD, Hemel Hampstead, UK).

### 6.2.12 Cytokine Secretion Studies in Differentiated Monocyte Derived Macrophages

PBMCs were separated from buffy coats as described in section 6.2.4 and then from these, CD14+ cells were isolated using MACs separation as described in section 6.2.9. The CD14+ cells were seeded at a density of 500,000 cells per well in 24-well plates to which 50 ng/ml of macrophage colony-stimulating factor (MCSF) was added. These plates were left for 7 days to allow the CD14+ cells to differentiate into macrophages. The macrophages were then exposed to EFV aqueous solution and EFV nanoemulsion in the same was as for stimulated lymphocytes, described in section 6.2.11.

### 6.2.13 Quantification of Cytokine Concentrations by Bio-Plex 200 Luminex System

An 8-point standard curve was generated by reconstituting the lyophilised standard provided in the Bio-Plex kit (Bio-Plex Pro™ Human Cytokine Standard 27-Plex Group 1). The analytes of interest for PBMCs (IL-2, IL-10, IFN-γ) had top concentrations of 13,690 pg/mL, 26,094 pg/mL and 34,920 pg/ml, respectively. The analytes of interest for macrophage secretion (IL-1b, IL-6, IL-8 and TNF-α) had top concentrations of 31,130 pg/ml, 25,160 pg/ml, 26,160 pg/ml and 107,172 pg/ml, respectively.

50 µL of the coupled beads was added to each well and then the wells washed twice using wash buffer and vacuum filtration. 50 µL of cytokine standard and 50 µL of sample (from section 6.2.11 for T cells or section 6.2.12 for macrophages) was then added to each well and incubated at room temperature on an orbital shaker for 30 minutes.

After the 30 minute incubation the plate was again washed 3 times using wash buffer and vacuum filtration, after which 25 µL of detection antibody was added to each well and incubated on an orbital shaker at room temperature for 30 minutes. After the incubation period the plate was washed 3 times and then 50 µL streptavidin solution added to each well. The streptavidin was incubated on an orbital shaker at room temperature for 10 minutes, after which the cells were washed 3 times. After the final wash, 125 µL of assay buffer was added to each well and shaken for 30

seconds at 1100 rpm. The plate was now ready to run on the Bio-Plex 200 Luminex Plate Reader.

The Bio-Plex 200 was calibrated and validated prior to use by running the in-built calibration and validation protocols, together with Bio-Plex calibration and validation bead kits. The information of the standards and analytes was entered into the software, including the maximum concentration of each standard and the bead region (all provided within the assay kit). Importantly, the data acquisition was set to 50 beads per region, bead map was set to 100 region, sample size was 50 µL and the doublet discriminator (DD) gates were set to 5000 (low) and 25,000 (high).

### 6.2.14 Immune Cell Surface Antibody Expression Studies by Flow Cytometry

PBMCs were separated from buffy coats as described in section 6.2.4 and cell number determined by trypan blue exclusion (see section 2.2.8) and 1 x $10^6$ cells were seeded per well in 1 mL volume in 24 well plates. A further 1 mL of either EFV aqueous solution or EFV nanoemulsion containing media was added to appropriate wells to give a final concentration of 10 µM drug. These plates were then left to incubate at 37°C and 5% $CO_2$ for 24 hours.

After the 24-hour incubation period, cell suspensions were collected into deep welled 96-well plates and cells pelleted by centrifuging at 2000 x g for 5 minutes. Supernatant was aspirated and discarded, while cells were re-suspended in 100 µL of buffer (PBS at pH 7.2, supplemented with 2 mM EDTA and 0.5% BSA). To this, 10

μL of each antibody (anti-CD4, CD8, CD25, CD44, CD69, or CD95) was added as appropriate.

Samples were mixed well and then left in the dark in a fridge (2-8°C) for 10 minutes, after which unbound antibody was washed from the cells by adding 2 mL of buffer and centrifuging at 300 xg for 10 minutes. Supernatant was aspirated and discarded and cells re-suspended in 1 mL of MASCQuant® running buffer, ready for analysis on a MACSQuant® flow cytometer (Miltenyi Biotec GmbH, Bergisch Gladbach, Germany). The PBMC population was gated using linear forward and side scatter and a previously optimised compensation matrix applied, suitable for the antibody conjugates used.

### 6.2.15 T-Cell Proliferation Studies

PBMCs were separated from buffy coats as described in 6.2.4 and cell number determined by trypan blue exclusion (see section 2.2.8). 250,000 cells per well were seeded in 96-well cell culture plates, half of which were spiked with 50 μL of Phytohaemagglutinin (PHA) to deliberately induce T Cell proliferation, the other half were not stimulated with PHA.

50 μL of RPMI media containing either EFV aqueous solution or EFV nanoemulsion was added to both the PHA+ and PHA- plates to give a final concentration of 10 μM and incubated for 72 hours at 37°C and 5% $CO_2$. For the last 16 hours of the incubation period, 1 μL of a 1 mCi/ml stock solution of $H^3$ labelled

thymidine was added to each well to give a final concentration of 1 μCi of $H^3$ thymidine per well.

Cells were transferred from 96-well cell culture plates to nitrocellulose membranes using a cell washer and harvester (TomTec Life Sciences, Connecticut, USA). Solid scintillation was added on top of the nitrocellulose membranes and placed into a MicroBeta counter (Perkin Elmer, Ohio, USA) and the level of $H^3$ thymidine incorporation quantified to give a measure of T-Cell proliferation.

### 6.2.16 Plasma Coagulation Studies

This assay was conducted by Dr Neill Liptrott while a visiting researcher at the Nanotechnology Characterisation Laboratory based within the National Cancer Institute, Maryland, USA.

Human blood from three donors was collected by venepuncture into tubes anti-coagulated with sodium citrate; blood was used within one hour of collection. Test plasma was prepared by centrifuging blood at 2500 x g, at 21°C, for 10 minutes with the resultant plasma collected and pooled. Pooled plasma was stable at room temperature for 8 hours. Nanoemulsion samples were prepared at 10x the required final concentration to accommodate dilution when added to test plasma. Concentrations and subsequent dilutions were based on the concentrations of EFV contained within the samples with dilutions of blank nanoemulsion diluted in the same fashion. Final concentrations tested were 40 μg/mL, 4 μg/mL, 0.8 μg/mL and 0.16 μg/mL. Nanoemulsion samples were mixed with test plasma and incubated at

37°C for 30 minutes. Each nanoemulsion preparation was prepared in triplicate. Lyophilised controls representing normal and abnormal plasma (plasma with coagulation delay) were reconstituted with distilled water (2mL) and left to equilibrate to room temperature 30 minutes prior to use. These controls were used as instrumentation controls for the STArt4 coagulometer (Diagnositca Stago).

Cuvettes were placed into A, B, C and D test rows on the coagulometer and one metal ball added into each cuvette (warmed for at least 3 minutes prior to use). 100 µL of either control or test plasma was added to a cuvette when testing PT or thrombine time and 50µL when testing APTT with three duplicate cuvettes for each plasma sample. Additionally, for the APTT assays 50 µL of PTT-A was also added. The timer was started for each of the test rows and cuvettes transferred to PIP row 10 seconds prior to alarm notification. Once incubation time was complete, coagulation reagent was added to each cuvette and coagulation time recorded. Percentage coefficient of variation was calculated for each control and test samples according to the following formula: %CV = SD/Mean X 100%. If %CV was greater than 5% for study samples that sample was reanalysed. Data was expressed as a percentage of the coagulation time recorded for plasma with no nanomaterial present (plasma only control).

### 6.2.17 Platelet Aggregation Studies

This assay was conducted by Dr Neill Liptrott while a visiting researcher at the Nanotechnology Characterisation Laboratory based within the National Cancer Institute, Maryland, USA.

Platelet rich plasma (PRP) was prepared from healthy volunteer whole blood in sodium citrate by centrifugation at 250 x g for 8 minutes. Platelet poor plasma (PPP) was prepared by centrifugation of whole blood at 2500 x g for 10 minutes. PRP was treated with either 4 μg/mL or 40 μg/mL of sample materials for 15 minutes at 37°C. PPP was used as a background control and also treated with the same concentrations of sample materials. Samples were analysed using a Chrono-log aggregometer, gain was set to 0.005 and optical baseline established using PPP controls. Platelet aggregation (turbidity) and ATP release (luminescence) were recorded as area under the curve for treated and untreated samples. Collagen (1 μg/mL) was used as a positive control for platelet aggregation and materials were also tested in the presence of collagen to ensure inhibition of aggregation did not occur.

### 6.2.18 Haemolysis Studies

This assay was conducted by Dr Neill Liptrott while a visiting researcher at the Nanotechnology Characterisation Laboratory based within the National Cancer Institute, Maryland, USA.

Haemolysis was determined using cyanomethaemoglobin (CMH) reagent and a haemoglobin standard. A standard curve of known haemoglobin concentrations was created (range 0.025-0.8 mg/mL) with low (0.0625 mg/mL), medium (0.125 mg/mL) and high (0.625 mg/mL) quality control samples. Triton X100 was included as a positive control. Sample materials were tested at a range of concentrations (0.16, 0.8, 4 and 40 μg/mL). Whole blood was collected from healthy volunteers in Li-heparin tubes and pooled blood prepared by mixing equal volumes of blood from each donor. An aliquot of pooled whole blood was taken and centrifuged at 800 x g for 15mins to determine plasma free haemoglobin (PFH). Briefly, 200 μL of calibration standard, quality controls and blanks were added to respective wells of a 96 well plate. TBH (200 μL, prepared by combining 20 μL of pooled whole blood and 5 mL of cyanomethaemoglobin) was added to each well. 100 μL of plasma (for PFH) was added per well. Finally, 100 μL of CMH reagent was added to each well containing samples. Plates were covered with a plate sealer and gently shaken for 1-2 minutes. Absorbance at 540 nm was measured to determine haemoglobin concentration. Remaining pooled whole blood was diluted with $Ca^{2+}$/$Mg^{2+}$ Dulbeccos Phosphate Buffered Saline (DPBS) to adjust total blood haemoglobin concentration to 10 ±2 mg/mL (TBHd). In a separate universal tube, 100 μL of test

sample, blank or positive/negative control was added. $Ca^{2+}/Mg^{2+}$ DPBS (700 µL) was then added to each tube and 100 µL of TBHd to each test sample. In parallel, 100 µL of $Ca^{2+}/Mg^{2+}$ DPBS was added to separate tubes to represent a "no blood" control to evaluate potential interference of the sample materials with the assay. Tubes were covered and mixed gently avoiding vortexing which may damage erythrocytes. Tubes were then placed in an incubator at 37°C for 3 hours (±15mins) and samples were mixed every 30mins. Following incubation, tubes were centrifuged at 800 x g for 15 minutes. A fresh set of calibrators and controls were prepared previously. To a fresh 96-well plate, 200 µL of blank reagent, calibrators, and quality controls of TBHd were added to each well. 100 µL of test samples, positive and negative controls were also added to the plate followed by 100 µL of CMH reagent to every well. The plate was covered with a plate sealer and shaken gently on a plate shaker for 1-2 minutes. Absorbance at 540 nm was measured spectrophotometrically and the %CV and percentage difference from theoretical (PDFT) were calculated. Assays were accepted if %CV and PDFT were within 20%.

### 6.2.19 Complement Activation Studies

This assay was conducted by Dr Neill Liptrott while a visiting researcher at the Nanotechnology Characterisation Laboratory based within the National Cancer Institute, Maryland, USA.

Blood was collected from healthy volunteers in tubes containing sodium citrate as anticoagulant. Plasma was prepared by centrifugation of blood samples at 2500 x g

for 10 minutes. Plasma was evaluated visually for haemolysis; plasma deemed to be haemolysed was not used to prepare the plasma pool. Plasma was used for complement testing within 1 hour of collection. Pooled plasma was combined with either test material (at concentrations of 0.16, 0.8, 4 and 40 μg/mL) or positive control (cobra venom factor) or negative control (0.9% saline). Plasma was also treated with a generic form of Taxol as a clinically relevant example of a licensed drug with known complement activation. Samples were incubated for 30mins at 37°C. Following incubation the manufacturers guidelines were then followed for completion of the iC3b ELISA. Optical density of the samples was measured at 405nm.

The assay worked on a 3-step principle, in which in the first step, the samples were added to assay well that contained iC3b antibody. This antibody would bind only the iC3b, and a washing step ensured removal of any other material. The second step added a HRP bound iC3B antibody, which would bind to the previously trapped human iC3b. The final step added a HRP specific enzyme substrate, which produced a green colour, the intensity of which was proportional to the amount of iC3b present.

### 6.2.20 Assessment of Nanoemulsion Effect on Natural Killer Cells

This assay was conducted by Dr Neill Liptrott while a visiting researcher at the Nanotechnology Characterisation Laboratory based within the National Cancer Institute, Maryland, USA.

Effector cells (NK92) were prepared at 1 x $10^6$ cells/mL and treated with test nanoparticles for 24 hours. Target cell (HepG2) density was adjusted to 0.5 x $10^6$ cells/mL. Media (50µL RPMI-1640) was added to all wells and plate attached to real time-cell electronic sensing (RT-CES) system (ACEA Biosciences, San Diego, USA), starting the appropriate program. Following background measurement, HepG2 (50µL) were added per well of the RT-CES plate and data acquisition started. HepG2 cells were left in culture for approximately 16-20 hours prior to the addition of NK92 cells. On the second day, NK92 cell viability was determined via trypan blue exclusion and cells readjusted to a density of 25 x $10^6$ viable cells/mL resulting in an effector to target (E:T) ratio of 5:1. The RT-CES program was paused for the addition of NK92 cells and then returned to the incubator to resume data acquisition for a further 24 hours. On day 3, data acquisition was stopped and the data analysed by assessing the area under the curve (AUC) for each sample.

### 6.2.21 Statistical Analysis

Statistical analysis was performed using SPSS version 21 for Macintosh computers, where data was normally distributed an independent samples t-test was performed to obtain p values. Where data was non normally distributed a non-parametric Mann-Whitney U test was performed. P values are stated throughout.

## 6.3 Results

### 6.3.1 Gram Negative Bacterial Endotoxin Analysis by Kinetic Turbidity LAL Assay

Results from the turbidimetric endotoxin analysis showed that there were 0.8 endotoxin units per mL (EU/mL) of blank emulsion sample and 0.1 endotoxin units per mL of EFV loaded nanoemulsion (Figure 6.1). These were well below the regulatory guideline concentration of 5 EU/ml as set out in the US Pharmacopeia.

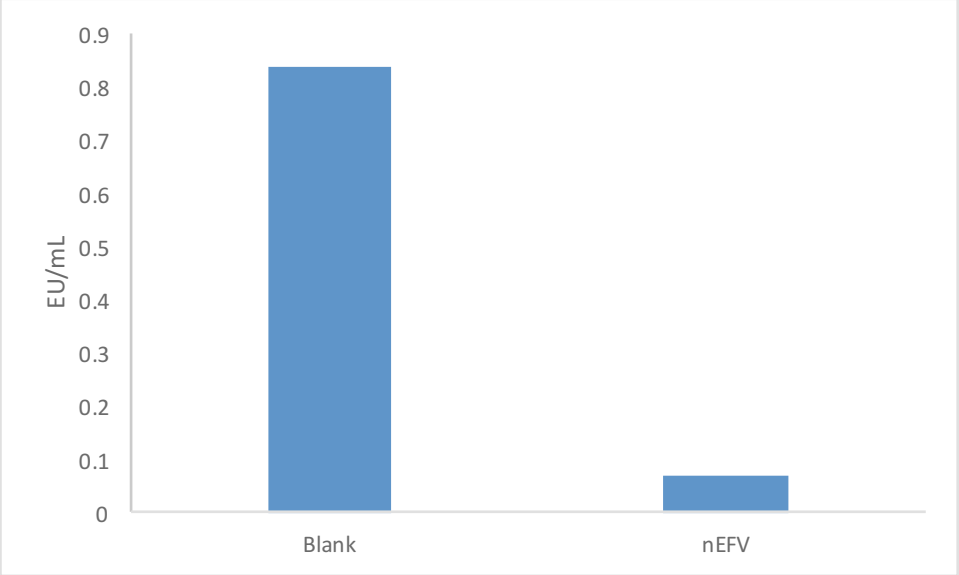


Figure 6.1. Amount of endotoxin detected in Blank and EFV (nEFV) loaded nanoemulsions . Data derived from kinetic turbidity LAL Assay and expressed in endotoxin units per mL (EU/mL). For reference, the limit of endotoxin permitted in a sample, as defined by the US Pharmacopeia was 5 EU/mL.

### 6.3.2 Gram Negative Bacterial Endotoxin Analysis by Gel-Clot Assay

Results from gel clot assay confirmed the results obtained in section 6.3.1 in that there was no significant amount of endotoxin present, as no clot was formed.

### 6.3.3 Nanoemulsion Sterility Testing by LB Agar Plate Streaks

Visual analysis of the LB agar plates that had been streaked with blank and EFV loaded nanoemulsion samples showed that there was no bacterial growth after 2 days incubation (Figure 6.2).

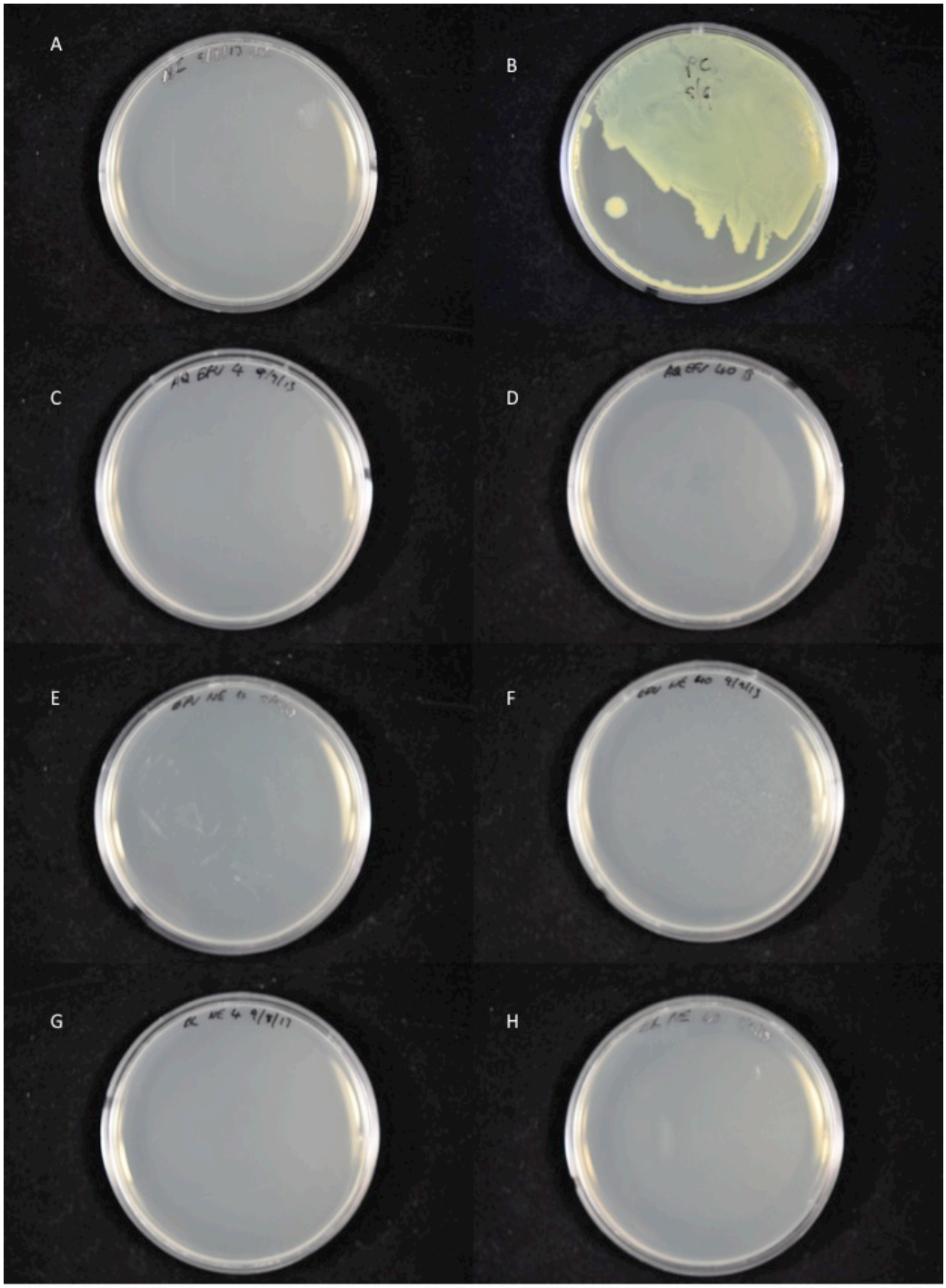


Figure 6.2 Agar plates after streaking with either Negative control (A), positive control (B), aqueous EFV solution at 4 μg/ml (C) and 40 μg/ml (D), EFV loaded nanoemulsion at 4 μg/ml (E) and 40 μg/ml (F), or blank nanoemulsion at 4 μg/ml (G) and 40 μg/ml (H).

### 6.3.4 Nanoemulsion Sterility Testing Mycoplasma Analysis in H460 Cells

Samples from H460 cells that had been exposed to 4 μg/mL of nanoemulsion sample, both blank and EFV loaded were sent to the Fredrick National Laboratory for Cancer Research (Fredrick, USA). The results from that analysis showed that there was no mycoplasma present in the nanoemulsion samples.

### 6.3.5 Cytokine Secretion Studies in T-Cells

The extracellular media of the expression assay (see section 6.3.7) was isolated and analysed for the secretion levels of cytokines IL-2, IL-10 and IFN-γ using a Bioplex 200 system and assay kit (Bio-Rad). Data for cells that were pre-stimulated with a T-cell activation kit showed that the levels of IL-10 were the same between control cells, EFV aqueous solution and nanoemulsion EFV ($p > 0.05$). For IL-2, there was no difference observed between the control cells and either EFV aqueous solution or EFV nanoemulsion ($p > 0.1$ for all conditions) and the same was true for IFN-γ ($p > 0.2$) (Figure 6.3).

The same experiment was conducted on un-stimulated cells, with the results showing undetectable levels of cytokines across all conditions (data not shown).

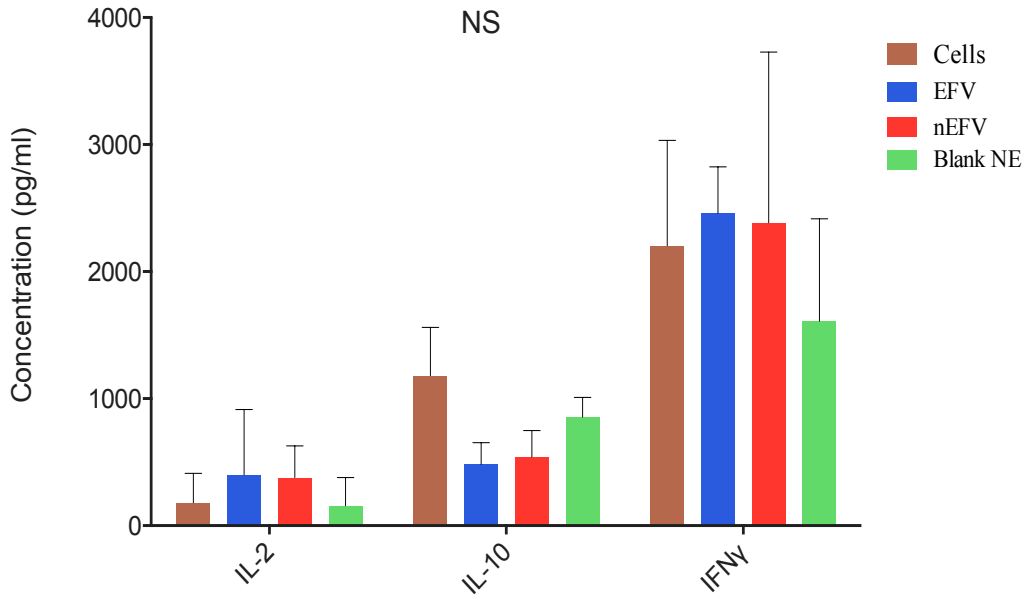


Figure 6.3. Levels of secretion of cytokines IL-2, IL-10 and IFN-γ from $1x10^6$ T-Cells per well in a 24 well plate. Cells were separated from PBMCs and incubated with 10 μM of either aqueous EFV solution or EFV nanoemulsion sample for 24 hours prior to analysis. Data shown as +/- standard deviation N=4.

### 6.3.6 Cytokine Secretion Studies in Macrophages

The level of cytokine secretion from monocyte-derived macrophages is shown in Figure 6.4. For both TNF-α and IL-1b the error in the values suggested that there was no secretion detected within the limits of the assay. The secretion of IL-6 showed no difference from the control cells for both EFV aqueous solution and EFV nanoemulsion ($p > 0.4$), whilst IL-8 also showed no difference between the EFV aqueous solution and EFV nanoemulsion as compared with the cellular control ($p = 1.000$).

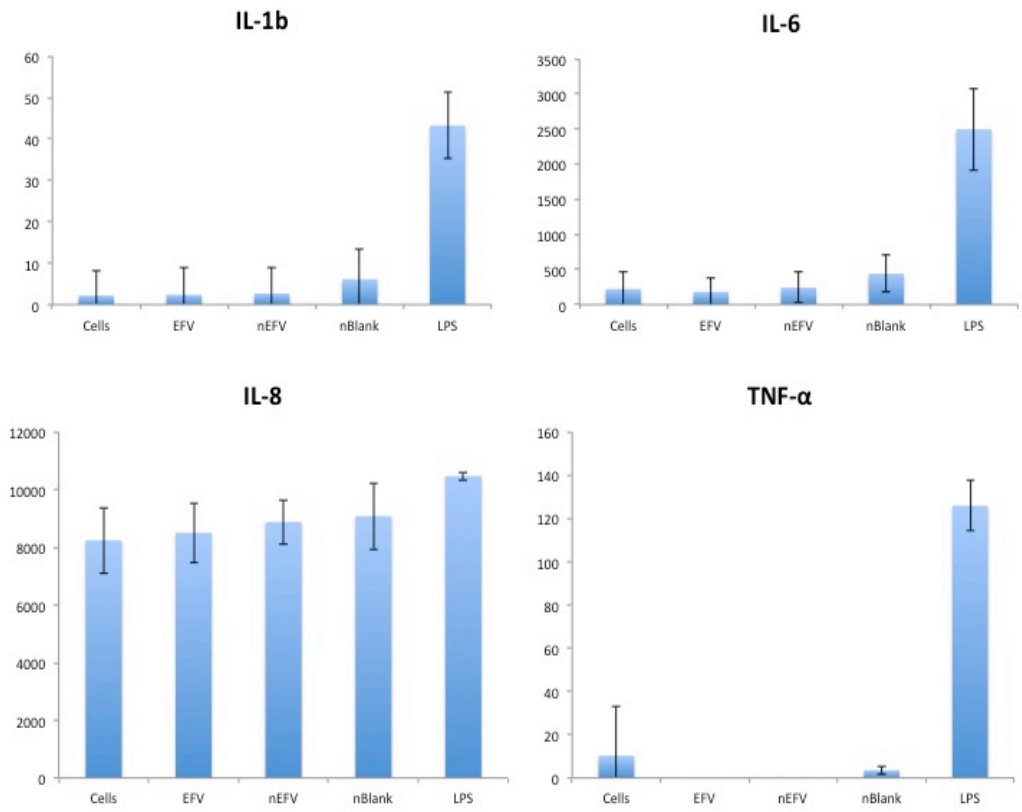


Figure 6.4 Levels of secretion of cytokines IL-1b, IL-6, IL-8 and TNF-α from $0.5x10^6$ monocyte derived macrophages per well in a 24 well plate. Cells were incubated either aqueous EFV solution or EFV nanoemulsion sample for 24 hours prior to analysis. Data shown as +/- standard deviation N=4.

### 6.3.7 Effect of Nanoemulsion on Immune Cell Surface Maker Expression

The expression of cell surface activation markers (CD25, CD44, CD69 and CD95) were determined using both CD4+ and CD8+ cells separated from the PBMC's. The data for the un-activated PBMC set showed that there was no difference in the expression of the activation markers as a result of exposure to the nanoemulsion formulation of EFV or EFV aqueous solution, when compared to untreated control cells (Figure 6.5). The data for the activated PBMC set again showed no difference in the levels of expression of these surface markers, and showed that neither EFV nanoemulsion nor EFV aqueous solution impacted the expression by either stimulating or supressing the surface markers (Figure 6.5).

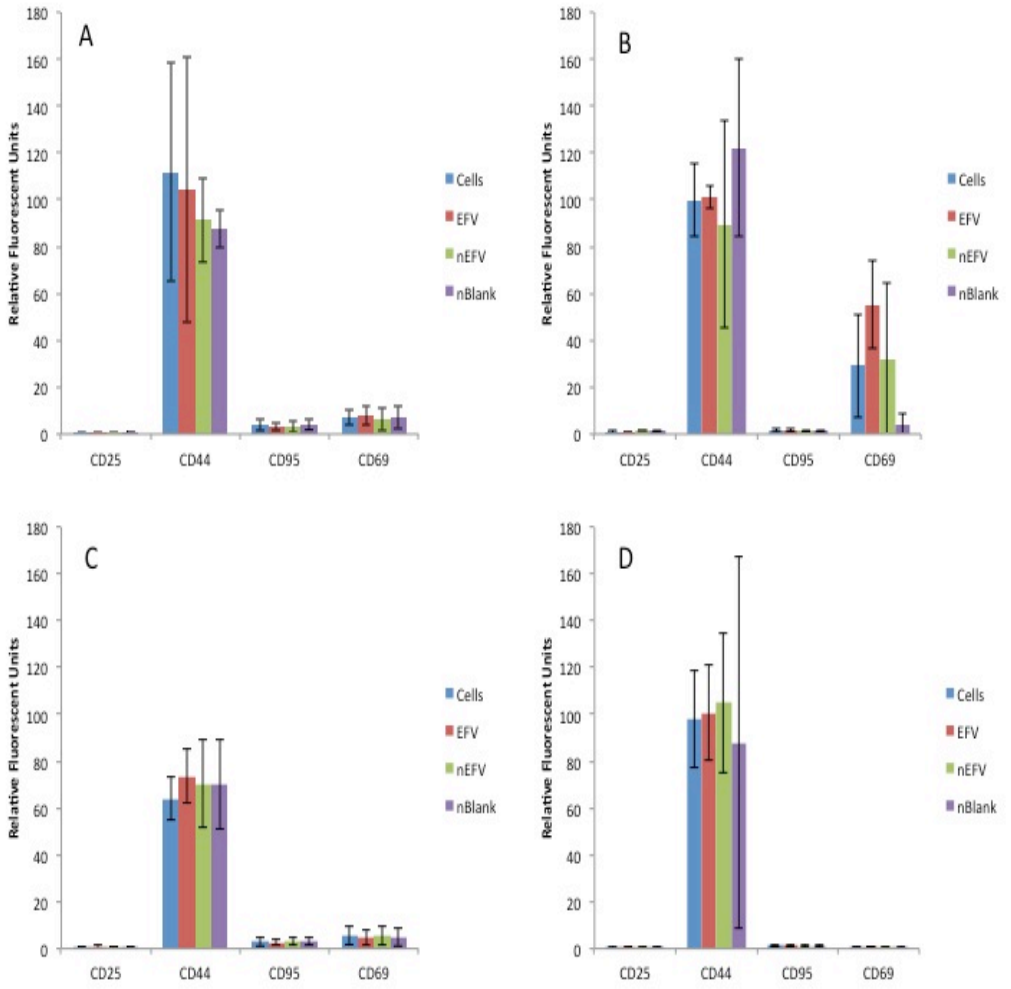


Figure 6.5 Levels of expression of cell surface markers on stimulated CD4+ (A) and CD8+ (C) PBMCs, and also unstimulated CD4+ (B) and CD8+ (D) PBMCs after exposure to EFV aqueous solution, EFV nanoemulsion and blank nanoemulsion. Cells were seeded at a density of $1x10^6$ cells per well in a 24-plate, and sample incubated for 24 hours prior to analysis. Cell population was gated on the flow cytometer using linear forward and side scatter, and a previously optimised compensation matrix. Data is showed as +/- standard deviation, N=4.

### 6.3.8 Nanoemulsion Effect on Primary lymphocyte Proliferation

No significant difference in the incorporation of $^{3}$H-thymidine was observed for PBMC samples treated with either EFV aqueous solution or EFV nanoemulsion ($p > 0.2$). Similarly the aqueous solution and nanoemulsion had no significant inhibitory effect on the proliferation caused by addition of PHA ($p > 0.3$) (Figure 6.6).

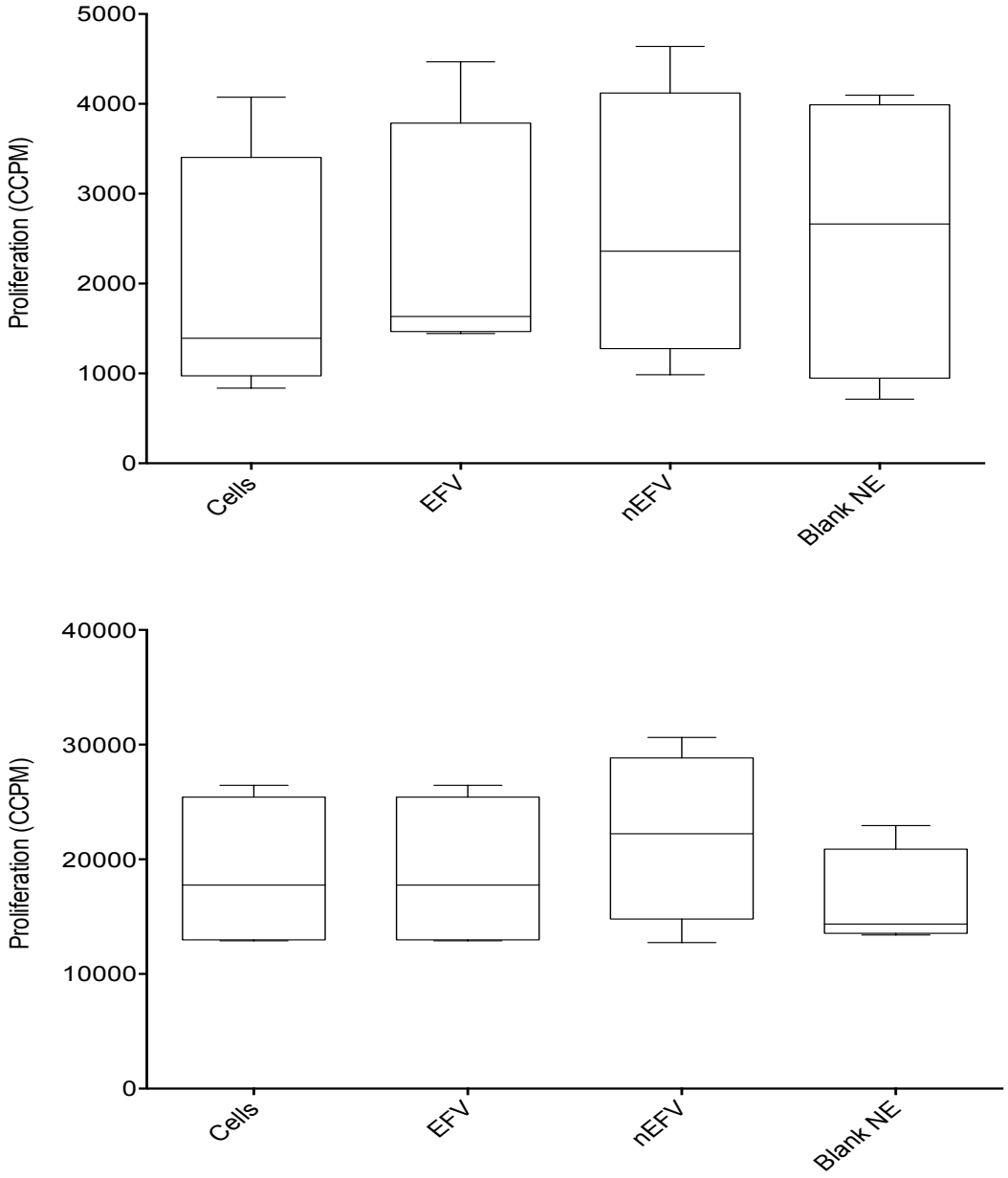


Figure 6.6 Proliferation of primary T-Cells after exposure to EFV aqueous solution and EFV nanoemulsion. Cells previously stimulated with PHA to induce proliferation are shown (bottom), and non-PHA stimulated cells shown in top figure. Data is expressed as a box and whisker figure, showing the maximum and minimum values +/- standard deviation, N=4.

### 6.3.9 Nanoemulsion Effect on the Coagulation of Plasma

The data for coagulation of plasma was separated into 3 areas in order to assess 3 major pathways to coagulation. In both the prothrombin time (PT) and thrombin time (TT) data sets, there was no difference observed between aqueous EFV solution, blank nanoemulsion and EFV-loaded nanoemulsion, in the time taken for plasma coagulation to occur. All of the test formulations had coagulation times that were identical to the control (Figures 6.7 and 6.8).

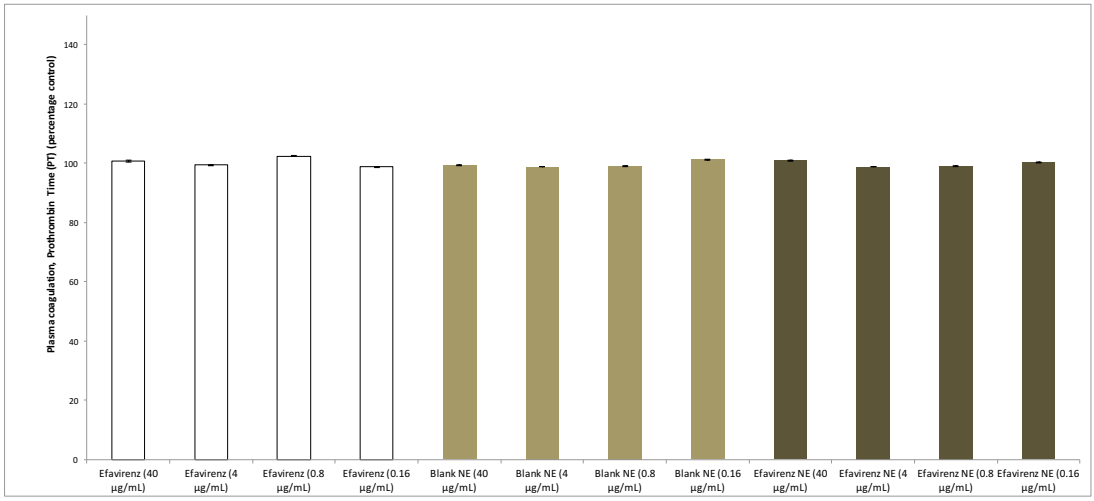


Figure 6.7 Prothrombin time (induced by neoplastine) in healthy volunteer plasma in response to aqueous EFV solution (white), unloaded blank nanoemulsions (gold) and EFV-loaded nanoemulsions (brown). Data is expressed as percentage difference in time taken for coagulation, as compared to control values.

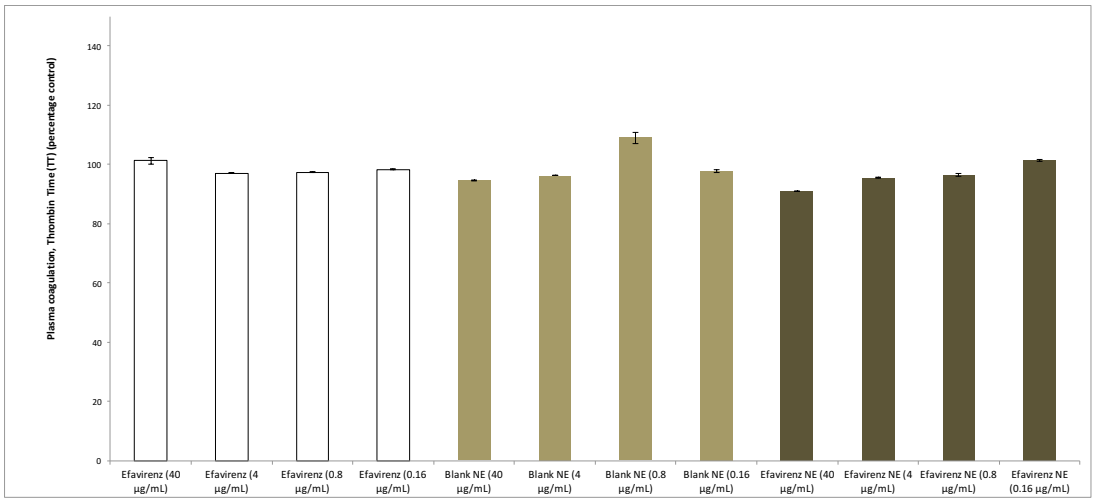


Figure 6.8 Thrombin time (induced by thrombine) in healthy volunteer plasma in response to aqueous EFV solution (white), unloaded blank nanoemulsions (gold) and EFV loaded nanoemulsions (brown). Data is expressed as percentage difference in time taken for coagulation, as compared to control values.

A significant prolongation in activated partial thromboplastin time (APTT) was observed for the EFV loaded nanoemulsions at 40 and 4 µg/ml, which demonstrated a 147% and 88% increase in coagulation time as compared to test plasma respectively ($p < 0.001$). Similarly for the unloaded nanoemulsions, significant increases in APTT were observed at both 4 µg/ml (52 % increase) and 40 µg/ml (159% increase) ($p < 0.001$) (Figure 6.9).

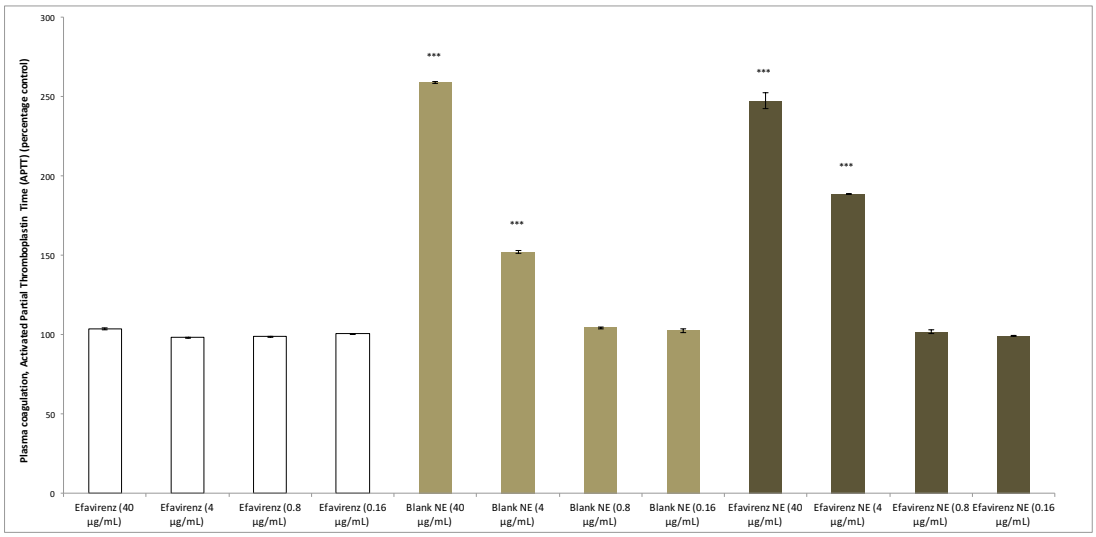


Figure 6.9 Activated Partial Thromboplastine time (induced by $CaCl_2$) in healthy volunteer plasma in response to aqueous EFV solution (white), blank nanoemulsion (gold) and EFV loaded nanoemulsion (brown). Data is expressed as percentage difference in time taken for coagulation, as compared to control values.

### 6.3.10 Nanoemulsion Effect on the Aggregation of Platelets

The data showed that there was no aggregation of platelets after exposure to both the aqueous solution of EFV and the nanoemulsion formulation of EFV, at 4 µg/ml and 40 µg/ml concentrations. These two conditions had the same values as for the negative control of 0.9% saline solution and significantly lower than the collagen spiked positive control sample (Figure 6.10).

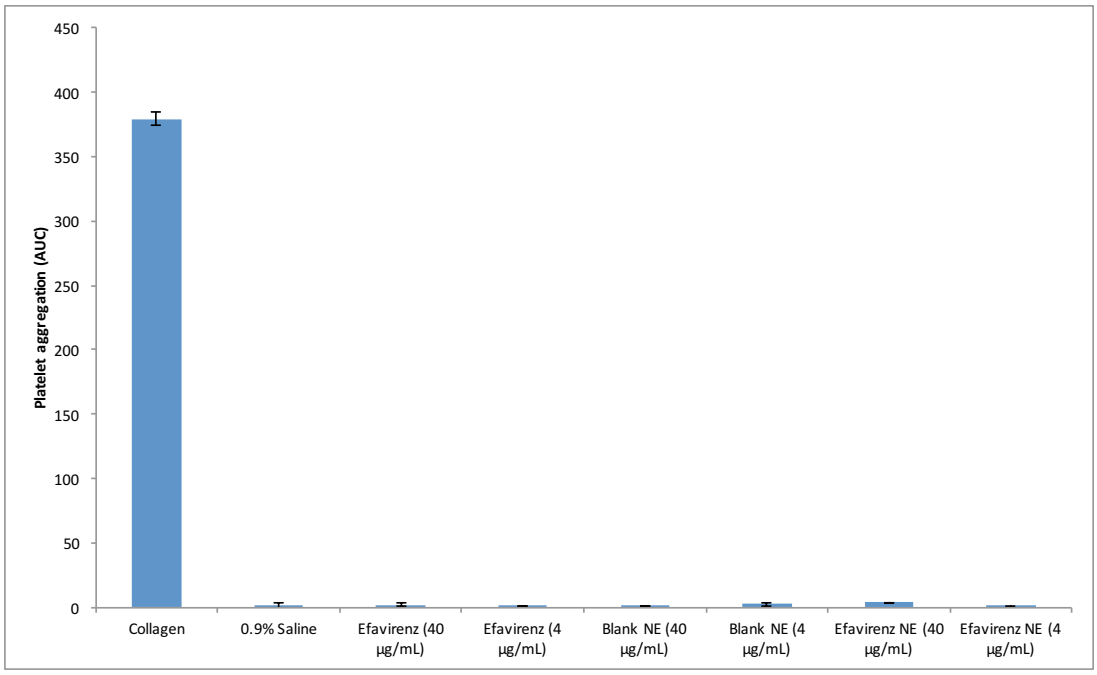


Figure 6.10 Amount of platelet aggregation after 15 exposure to collagen (positive control), saline (negative control), aqueous EFV solution, blank nanoemulsion and EFV nanoemulsion at 37°C. Data is shown as area under the curve (AUC) plus and minus standard deviation.

When the collagen positive control was also added to the aqueous and nanoformulations there was no effect seen on aggregation, with both aqueous EFV and nanoemulsion EFV showing the same levels of aggregation as the positive control, showing that aggregation was not being prevented when stimulated (Figure 6.11).

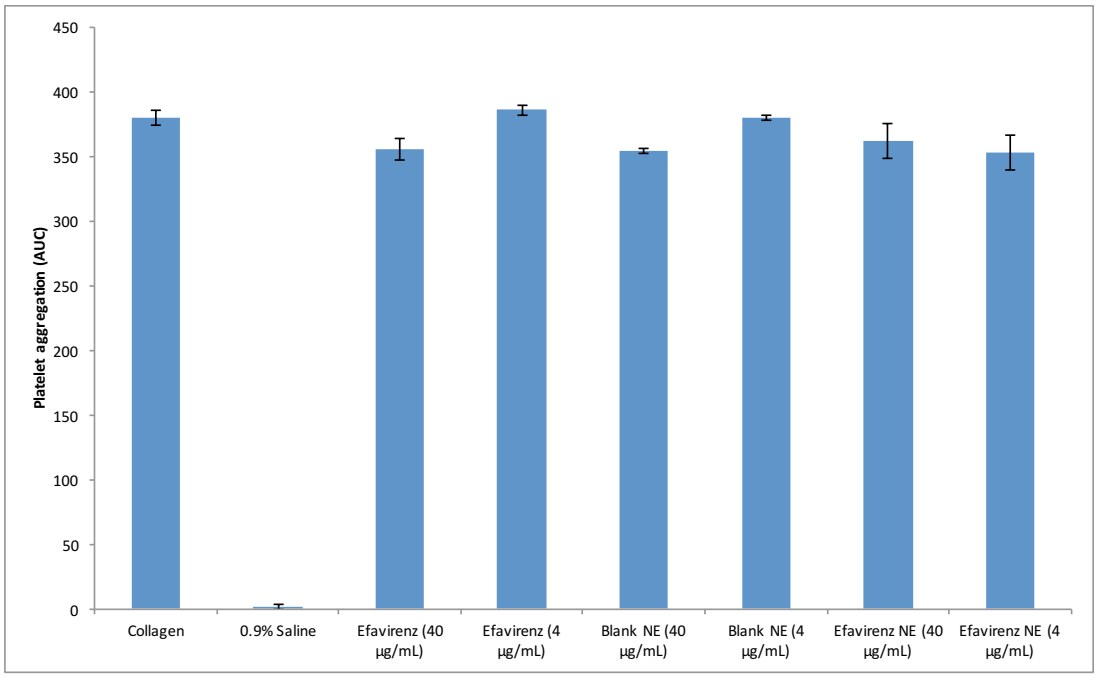


Figure 6.11 Amount of platelet aggregation after 15 minute exposure to collagen (positive control), saline (negative control), aqueous EFV solution plus collagen, blank nanoemulsion plus collagen and EFV nanoemulsion plus collagen at 37°C. Data is shown as area under the curve (AUC) plus and minus standard deviation.

The data for ATP release from platelets mirrored that of the aggregation data in that both formulations at both concentrations had no effect on causing aggregation to occur (Figure 6.12), or from preventing it when stimulated to aggregate (Figure 6.13).

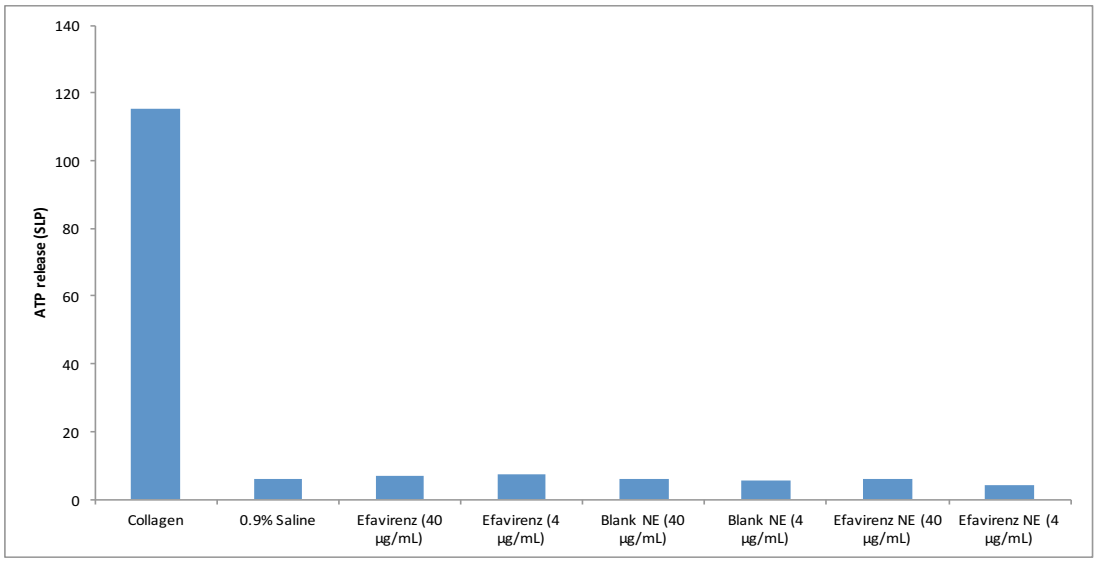


Figure 6.12 Amount of ATP release from platelets after 15 minute exposure to collagen (positive control), saline (negative control), aqueous EFV solution, blank nanoemulsion and EFV nanoemulsion, at 37°C.

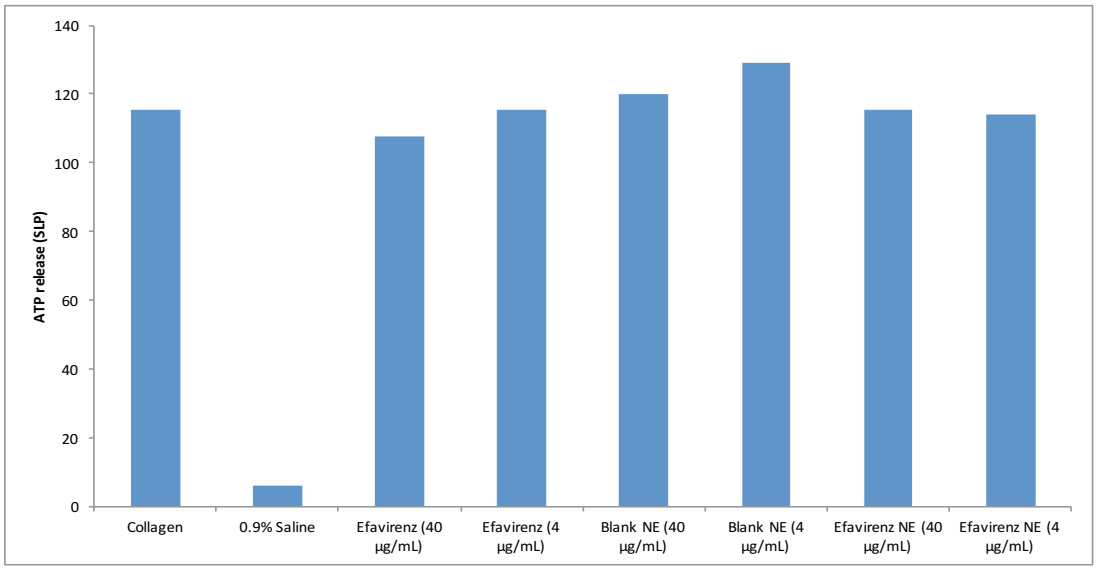


Figure 6.13 Amount of ATP release from platelets after 15 minute exposure to collagen (positive control), saline (negative control), aqueous EFV solution plus collagen, blank nanoemulsion plus collagen and EFV nanoemulsion plus collagen 37°C.

### 6.3.11 Nanoemulsion Effect on the Activation of Complement

The data showed that the levels of complement receptor iCb3 detected for all test conditions were the same as for that of the negative control 0.9% saline solution. Both the blank nanoemulsion and the EFV loaded nanoemulsion showed lower levels of complement activation than the clinically approved nanoformulation of paclitaxel, Abraxane (Figure 6.14).

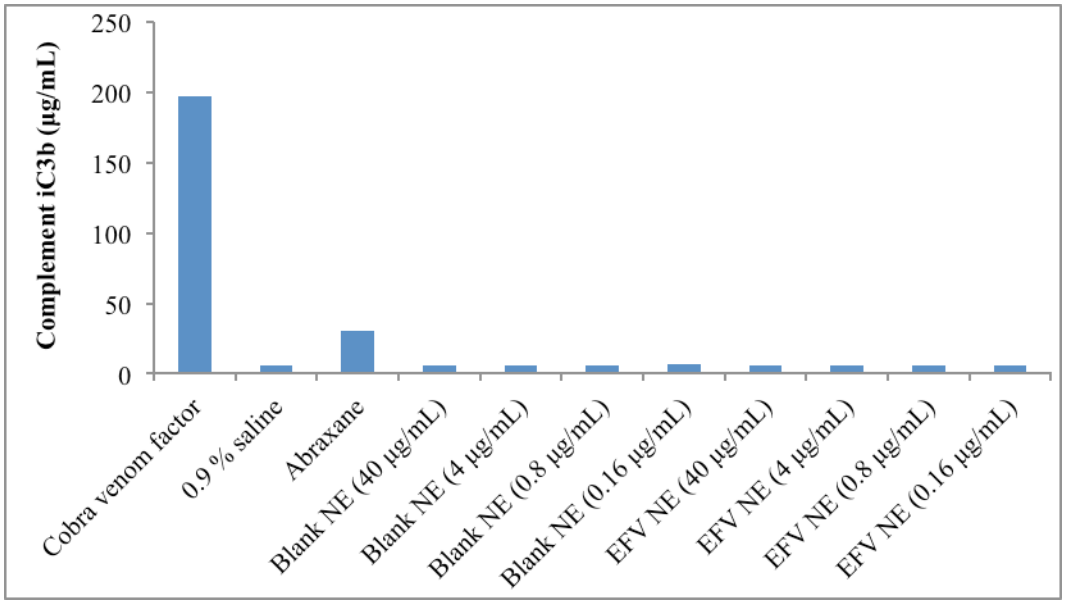


Figure 6.14 The amount of compliment iC3b detected by ELISA assay after exposure of blood plasma to positive (combra venom factor) and negative (0.9% saline) controls, and aqueous and nanoemulsion formulations of EFV. Abraxane was used as an indicator of acceptable compliment activation, as it was a clinically approved formulation, regarded as having a safe complement profile.

### 6.3.12 Nanoemulsion Effect on Haemolysis of Red Blood Cells

The data showed that for the aqueous solution of EFV at 40 µg/ml there was a significant increase in the percentage of haemolysis observed as compared to the negative control, with values of 86% and 3% respectively ($p = < 0.001$). At the lower concentrations the percentage haemolysis was similar to that of the negative control ($p = > 0.05$) (Figure 6.15).

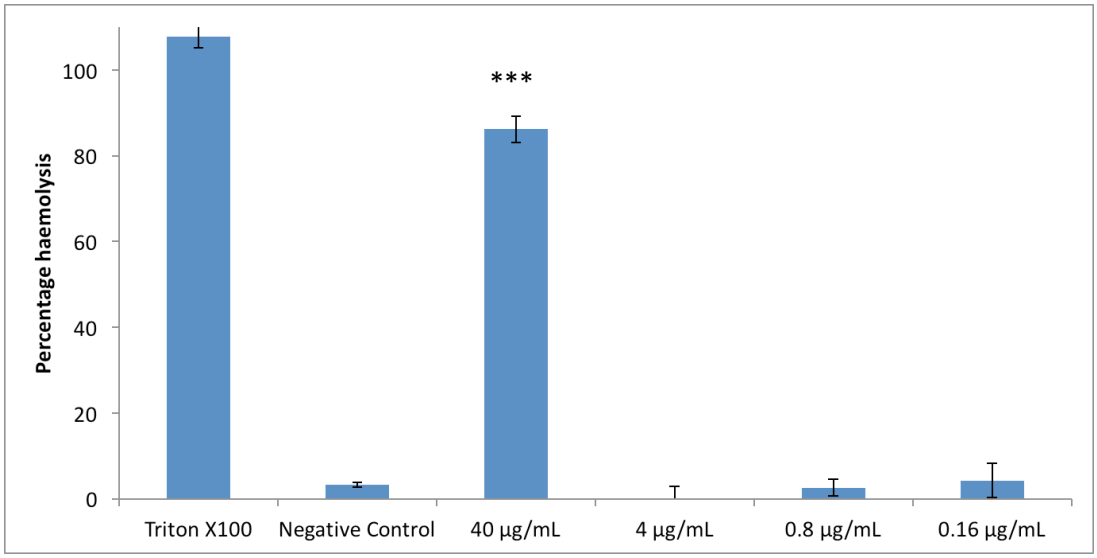


Figure 6.15 Haemolysis of erythrocytes following addition of aqueous EFV solution. Samples were incubated for 3 hours at 37°C, and were mixed every 30 minutes. Data expressed as percentage haemolysis as compared to positive control, plus and minus standard deviation.

There was no haemolysis observed for the blank nanoemulsion formulation at any of the concentrations tested ($p > 0.8$) (Figure 6.16). For the EFV loaded nanoemulsion there was an increase observed in the haemolysis at 40 µg/ml with values of 17% compared with 3% for the negative control, but this was not significant ($p = 0.96$) (Figure 6.17). There was no haemolysis observed for the EFV loaded nanoemulsion at 4.0, 0.8 and 0.16 µg/ml concentrations (Figure 6.17).

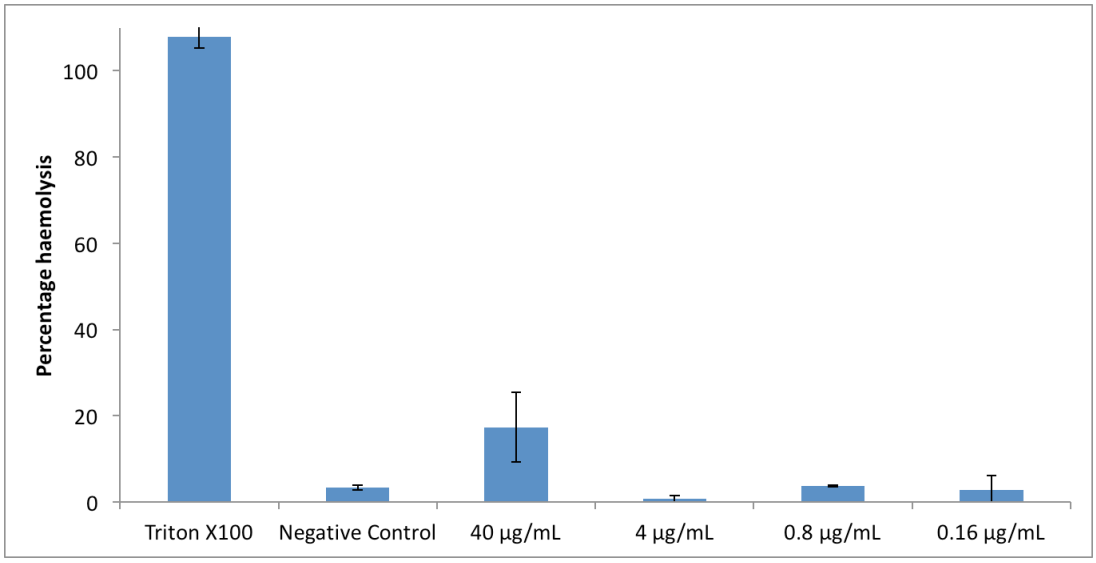


Figure 6.16 Haemolysis of erythrocytes following addition of blank nanoemulsion. Samples were incubated for 3 hours at 37°C, and were mixed every 30 minutes. Data expressed as percentage haemolysis as compared to positive control, plus and minus standard deviation.

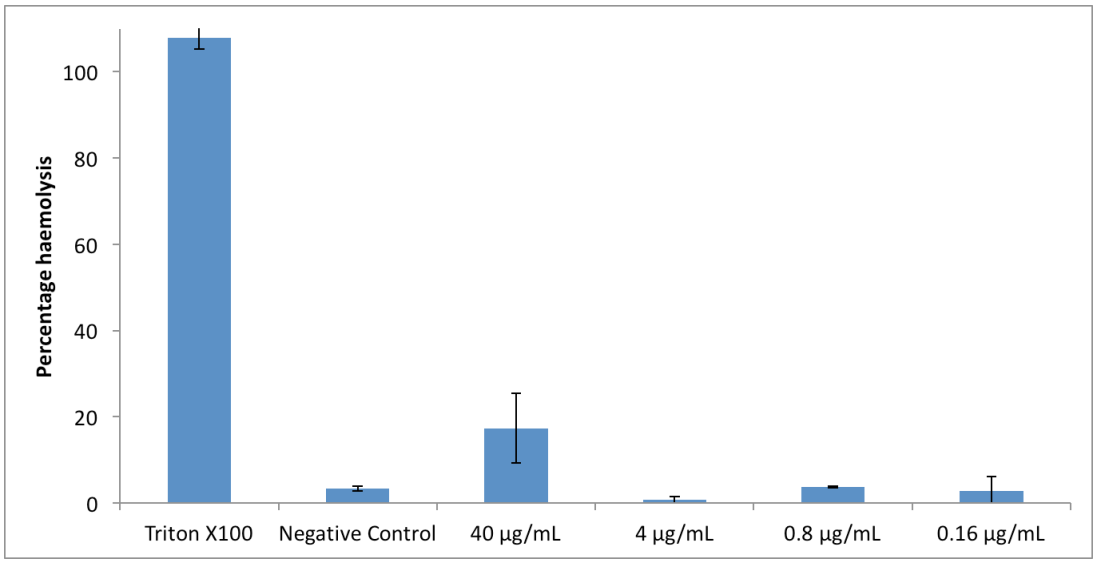


Figure 6.17. Haemolysis of erythrocytes following addition EFV nanoemulsion. Samples were incubated for 3 hours at 37°C, and were mixed every 30 minutes. Data expressed as percentage haemolysis as compared to positive control, plus and minus standard deviation.

### 6.3.13 Nanoemulsion Effect on NK Cells

Treatment of NK cells with both blank nanoemulsion (Figure 6.18) and EFV loaded nanoemulsion (Figure 6.19) did not affect the cytotoxic ability of the NK cells against HepG2 target cells.

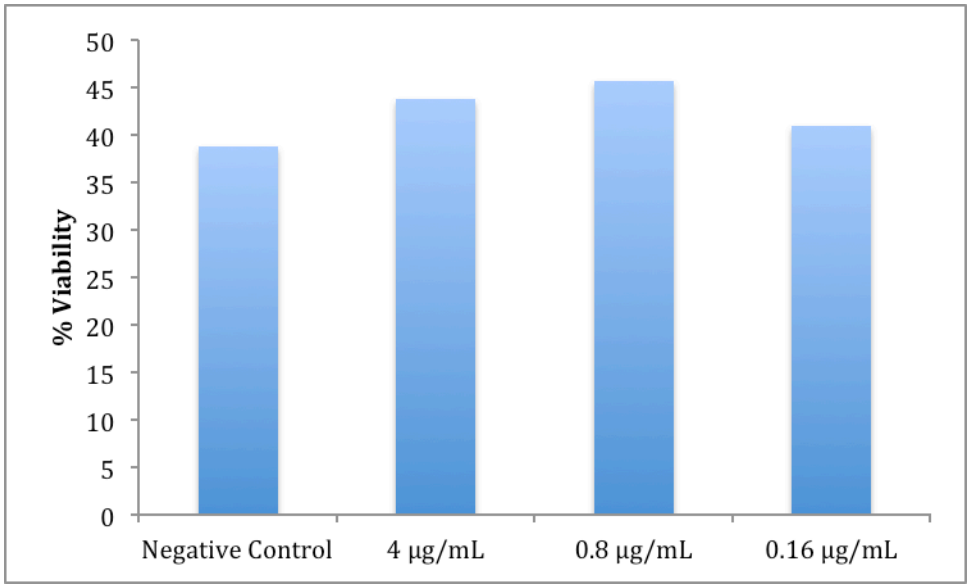


Figure 6.18 % viability of $1x10^6$ NK cells after 24-hour exposure to blank nanoemulsion. Viability of NK cells was calculated by determining the amount of target HepG2 cells that had been destroyed by the NK cells, using RT-CES system. Increased removal of HepG2 cells correlated with increased viability of the NK cells.

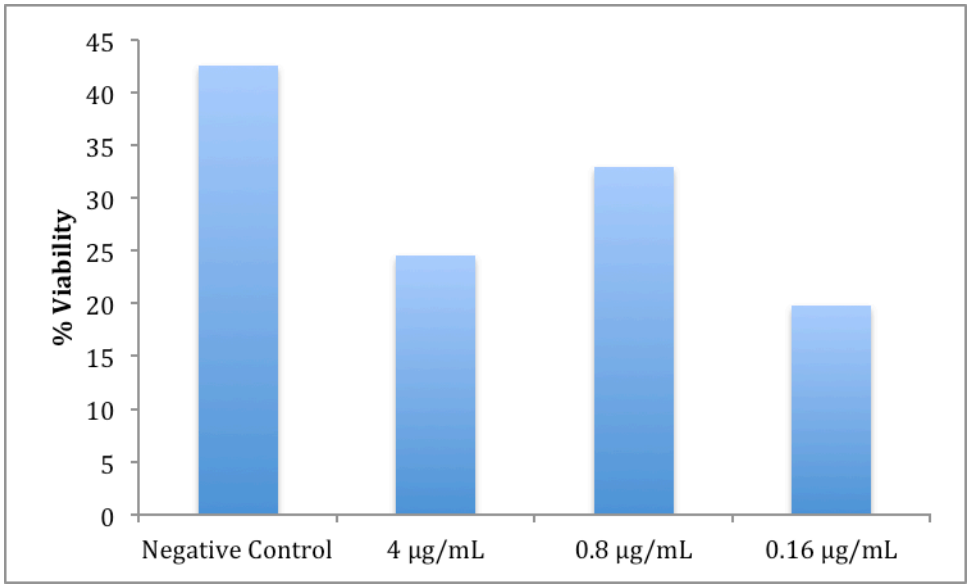


Figure 6.19 % viability of $1x10^6$ NK cells after 24-hour exposure to EFV nanoemulsion. Viability of NK cells was calculated by determining the amount of target HepG2 cells that had been destroyed by the NK cells, using RT-CES system. Increased removal of HepG2 cells correlated with increased viability of the NK cells.

## 6.4 Discussion

The focus of this Chapter was to perform a preliminary, preclinical assessment of the immunological compatibility of the nanoemulsions. The data showed that the amount of endotoxin present in nanoemulsion samples was below that of the USP and FDA limit of 5 EU/ml [511], which suggests the synthesis protocol and subsequent handling and storage of the nanoemulsions is appropriate to prevent contamination. The low concentrations of endotoxin not only means that the synthesis method appears to be relatively free of endotoxin (as compared to guideline amounts) but also that the subsequent immunological assays carried out were not affected by the presence of endotoxin, which has been shown to interfere and skew the results of some immunological tests [512].

There was also no detectable presence of either mycoplasma or bacteria in any of the samples, which again suggests that the method of synthesis of the nanoemulsions did not introduce contamination into the final product, and that there was no interference with the assays subsequently used, as has previously been demonstrated for other materials [513, 514].

As cytokines have such a wide-ranging effect on the immune system, it has been suggested that they would act as a good marker for investigating the immunotoxicity of nanomaterials [515]. To this end, the data from the cytokine secretion assays is very promising as it clearly shows that the nanoemulsion formulation of EFV had neither an inhibitory nor enhancing effect on the secretion of cytokines from primary

immune cells. The levels of all three cytokines assayed (IL-2, IL-10 and IFN-γ) were identical to those of the untreated control cells, showing that the nanoemulsions do not have an effect on the immune cells in terms of secretion. A number of reports have shown a range of nanomaterials that have been produced having no effect on the secretion profiles of cytokines [516, 517], a trend which the nanoemulsions in this study follow.

Previously published work by Villiers *et al* showed gold nanoparticles significantly modified the secretion of cytokines, suggesting a disruption to the immune system [518]. Furthermore, De Jong *et al* showed that silver nanoparticles could affect the immune system of rats [519]. Further work by Liptrott *et al* demonstrated that modified and unmodified gold nanoparticles augmented the release of cytokines from PBMCs [520].

A lack of immune stimulation in response to nanoemulsions was also seen when looking at the secretion of cytokines from macrophages. When LPS was used as a positive control, a clear increase in the secretion of IL-1b, IL-6 and TNF-α was observed. Previously nanoparticles have been shown to interact with macrophages, affecting their function and cytokine secretion [521-524].

In addition to cytokine secretion, data for the expression of cell surface markers on PBMCs revealed no apparent interaction or activation of T cells. The levels of expression were not significantly different when comparing activation markers to

untreated PBMCs. These markers were selected for analysis for individual reasons; CD25 is the alpha chain of the IL-2 receptor [525] and as such is used for measuring the increase in IL-2, CD44 is involved in cell-to-cell interactions and also in cell adhesion, thus is used to assess cell migration due to chemoattraction [526]. CD69 has been shown as one of the earliest cell surface markers for lymphocyte proliferation [527] and CD95 is the FAS receptor, involved in apoptosis [528].

As this data was produced using primary immune cells from 4 separate blood donors, it showed some of the variability that can occur across the population, as evidenced by the size of the error bars. However, using primary immune cells as opposed to immune cell lines, such as CEM or THP-1 is much more representative of what will occur *in vivo* due to the primary cells having the appropriate expression profiles [529]. It is well documented that immortalised cell lines, although convenient, are lacking in expression of certain important enzymes and proteins when compared to primary cells [530].

As mentioned previously in the introduction (see section 6.1), T-Cells play a vital role in the immune response and any alteration in the expression or proliferation of these cells can have profound effects on the body. The effect of T-Cell exposure to nanoemulsions was shown to be minimal. As with all of the data discussed thus far, levels of T-cell proliferation were seen to be equal to that of untreated control T-cells for all of the formulations tested. This was true regardless of whether the T-cells have been previously stimulated with PHA, showing that the nanoemulsions

had neither a stimulatory nor suppressive effect. As this data is for primary T-cells it would suggest that the nanoemulsions would not produce a T-cell response in humans, but as the assay was conducted on isolated T-cells it should only be taken as a guidance, as the interplay between cells of the immune system is complex.

The data for the coagulation study takes into consideration the three main routes from which coagulation can be triggered, the intrinsic [531], extrinsic [532], and common pathways. The extrinsic pathway was assessed by inducing coagulation using neoplastine and then measuring the prothrombin time, and as seen from the data there were no difference observed between the aqueous or nanoemulsion formulations. The same was true for the common pathway, which was assessed by triggering coagulation using thrombine and then measuring the thrombin time. There was no difference observed in the thrombin time between aqueous solution and the nanoemulsion formulation.

Differences were seen when assessing the intrinsic pathway, which was measured by inducing coagulation with $CaCl_2$ and recording the activated partial thromboplastine time (APTT). The data showed a prolongation in APTT for both the blank nanoemulsion and the EFV loaded nanoemulsion at 40 μg/ml and 4 μg/ml. One explanation for the prolonged APTT of the nanoemulsions might lie in the potential for the nanoemulsion to be interacting with the various factors (FVIII for example [533]) and possibly sequestering them, leading to a prolonged time taken to coagulate.

The increase in APTT time may not necessarily mean that the nanoemulsion formulations are not suitable, as if the exact mode in which they cause prolongation can be derived then it would be possible to manage the situation with additional treatments to cancel out the anticoagulant effect (although clearly this is not ideal). There are also some disease states, cancers for example, that produce procoagulant effects [534], so a nanoemulsion formulation of an anti-cancer therapeutic that also reduced the procoagulant effect of the cancer itself may be worth pursuing in the future.

The platelet aggregation studies showed no difference in aggregation between the negative control and the nanoemulsion formulations, both blank and EFV loaded. The same was true for the aqueous solution of EFV, giving some confidence the incorporation of EFV into a nanoemulsion would not cause issues with platelet aggregation if the intact nanoemulsion droplets made it into the blood stream. It is currently unknown whether or not the nanoemulsion droplets would enter the blood stream intact after oral administration, but if used in an intravenous setting the data give some indication that there would be no negative effect on platelet aggregation. Clearly, *in vivo* analysis of this would also be required. Nanoemulsions have previously been shown to be good vehicles for the intravenous delivery of therapeutics [535-537].

The nanoemulsions did not cause an increase in the levels of compliment iC3b detected via an ELISA assay. The amount of iC3b detected was in fact lower than that of Abraxane, which is a currently licensed nanoformulation of the anti-cancer drug paclitaxel [538]. Abraxane has previously been shown to have a stimulatory effect on compliment, but despite this, is still safe to use clinically. This data further supports the safety profile of the nanoemulsions.

When looking at the haemolysis of red blood cells it was observed that at 40 μg/ml of aqueous EFV solution there was over 80% haemolysis. When the concentration was 4 μg/ml and lower this haemolytic effect was no longer present. This is in comparison to both the blank and EFV loaded nanoemulsions, which displayed no haemolysis at all concentrations used. These data suggest that the haemolysis was due to the high concentration of EFV aqueous solution present, and this effect is masked when EFV in nanoemulsion formulation due to the encapsulation of the drug. This would be expected due to the poor aqueous solubility of the EFV aqueous solution leading to it potentially not being fully dissolved at the 40 μg/ml concentrations. The data further reinforces the benefits of the nanoemulsion system, at least in respect to its ability to disperse poorly water-soluble therapeutics.

The nanoemulsion had no effect on the cytotoxic activity of NK cells, which is of particular importance to a HIV therapeutic due to the vital role that NK cells play in the host defence against viral infections.

In summary, the nanoemulsion formulations were shown to have no interactions with the main areas of the immune system, with the exception of the intrinsic coagulation pathway. The data suggest that the nanoemulsion formulation of EFV could be used for further experimental testing *in vivo* to progress the formulation further, with studies in humans possible subject to successful in vivo preclinical safety.

# CHAPTER 7

# General Discussion

## 7.1 General Discussion

The work in this thesis set out to explore the use of nanomedicine approaches to tackle the limitations associated with HIV therapies. The work can, however, be applied to other therapies which are poorly water soluble, especially those that utilise lipophilic APIs. With the pharmaceutical industry currently facing an uncertain future in terms of the number of major frontline patented drugs on the market [539], and with a portfolio containing increasing numbers of therapeutic compounds that have both poor solubility and poor permeability, it is likely that reformulation strategies using nanomedicine approaches will become increasingly common [540-542].

The work presented in this thesis has shown a rational and iterative process for the development of novel nanoparticle based drug delivery systems. The close relationship between chemical development, cytotoxicity testing and detailed pharmacological testing, has allowed the project to assess a large number of potential formulations with limited resources [543]. This has mainly been possible due to an early screening approach, which prevented the incorporation of substituents with undesirable profiles.

Large scale cytotoxicity testing is manageable and multiple assays can be run in parallel even in the scope of a single PhD project. However, detailed pharmacological testing, such as transcellular permeability and immunological safety assessments are much more intensive and expensive. By excluding excipients

based upon undesirable cytotoxicity profiles earlier in the development process, it meant less potential for failure downstream [544]. Figure 7.1 details the approach taken to the development of the project and highlights the stages in which information from pharmacological testing was fed back in order to steer the chemical development.

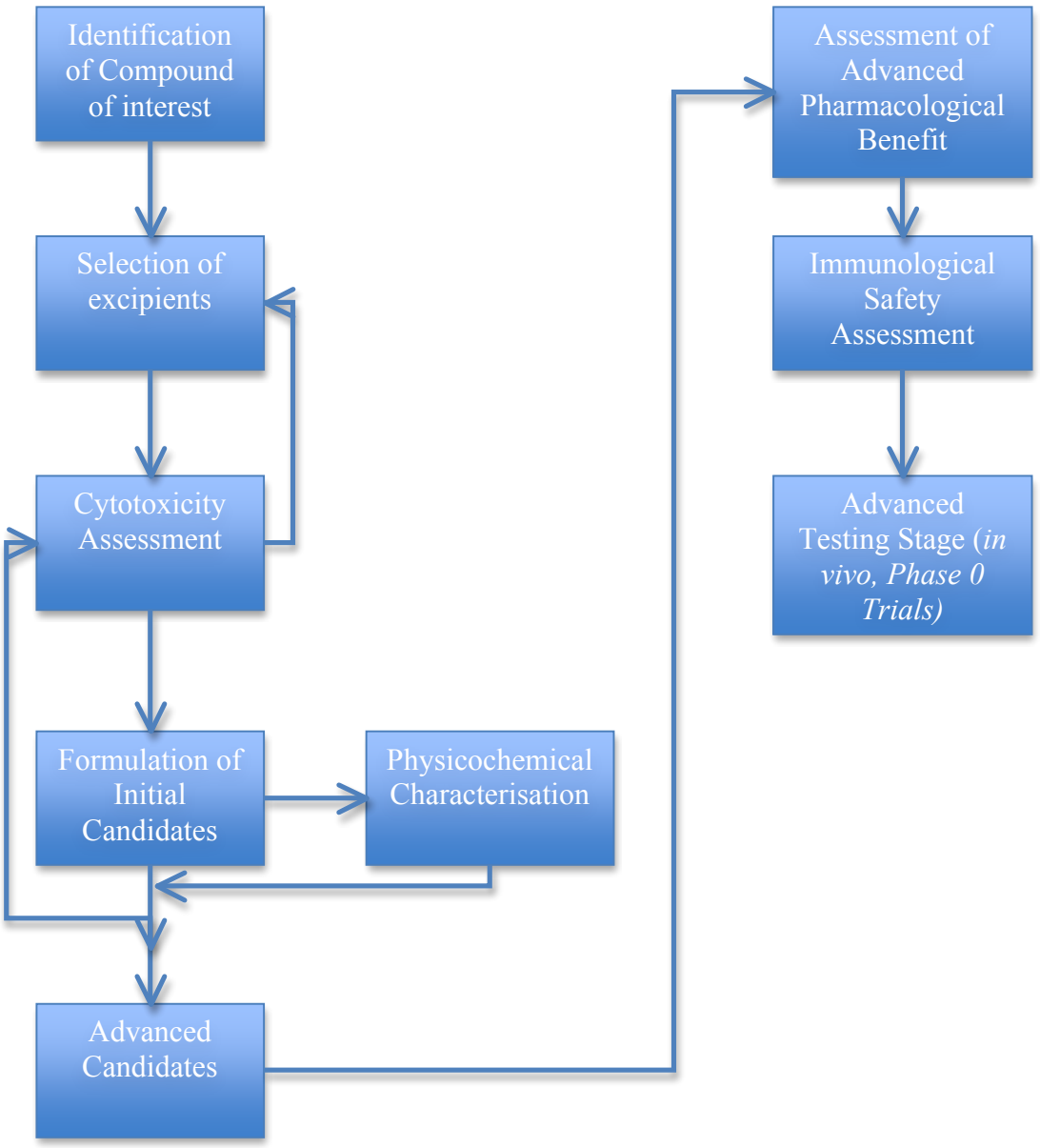


Figure 7.1 Workflow of structure based and iterative development process for novel nanomedicine based drug delivery systems.

The order of experimentation that this work followed was also designed in a rational way. Once lead candidates had been identified it was important to prioritise assessment of pharmacological benefit (Papp, CAR etc.) prior to a more in depth immunological safety assessment. Having this level of pre-assessment assures that only the most promising candidates are subjected to the more intensive assays, which involve expensive reagents and primary cells, as well as considerable time investment to conduct the assays. This approach could be translated to development of novel formulations in settings as small as individual research laboratories, right up to pharmaceutical enterprises. In both situations it may help optimise the efficiency of development and reduce costs.

There was a constant need to assess the physicochemical properties of the samples being produced throughout this project, both in terms of assessing batch-to-batch variability, but also to screen out candidates based upon their size. There are numerous literature reports that demonstrate size-dependent characteristics in nanoparticles, in particular with the likelihood of permeability and accumulation [545, 546]. There is however, an on-going global problem with the validation of physicochemical properties of nanoparticles. This is in part due to there not being a single defined value for nanoemulsion size [547], and because different labs across the world use a variety of different platforms to determine the size of their particles. Measurements are also conducted at different concentrations and in different diluents, which all lead to variation in reported sizes of the same material. There is a need for a recognised definition and agreed standard of measurement, which may

take the form of a validation process across several different size determination platforms [548-551].

The next logical step in the progression of the work presented in this study would be to progress the candidates through to *in vivo* studies [457, 552, 553]. The distribution of EFV and LPV would be assessed in comparison to equivalent aqueous solutions of the drug and/or previously validated preclinical formulations. Previously, nanoemulsions have been shown to increase the distribution of poorly water-soluble drugs in rodent models [554-556]. *In vivo* studies would provide a more robust estimation of the likelihood of any benefits gained by having EFV or LPV in nanoemulsion formulation. The pharmacokinetic profile of EFV and LPV nanoemulsions could also be determined in rodent models, and all of this work would be conducted within the academic setting in the first instance.

For *in vivo* studies, the current scale of production would be sufficient to produce the volume of sample required for the experiments proposed. However, for longer-term progression of the formulations, initial safety trials would need to be conducted in humans. This would require the scale-up in production of the nanoemulsions and production at GMP standards [557]. This stage of development would likely be conducted in collaboration with a contract manufacturing organisation or a commercial partner, as the cost of equipment necessary is not feasible for the academic setting [558-560]. Potential problems could arise when making the move

to large-scale production of the nanoemulsions, particularly in assuring batch-to-batch reproducibility.

The step after *in vivo* studies would be to progress to human trials, initially with a phase 0 "first in man" pharmacokinetic study [561], followed up with a phase 1 initial safety assessment. Currently, there are nanoformulated anticancer therapeutics undergoing phase 1 clinical trials [562]. Both of these trial phases could be conducted in healthy volunteers. The phase 0 trial would be very small, with no more than 10-15 volunteers involved. Phase 0 clinical trials are becoming commonplace, particularly in the development of anticancer therapeutics [563-565]. The dosage received would be sub therapeutic, and deliberately low to ensure there is the least possible chance of any unsafe reactions. This small dose would still allow for the absorption, distribution, metabolism and excretion (ADME) [566] to be assessed, essential if the formulation were to proceed any further in the development process.

It would be here that any unexpected accumulation or distribution would be seen, which would inform on the suitability of the drug formulation for its intended task, but more importantly from a safety point of view. There would also be the opportunity at this stage to examine whether smaller doses of the nanoemulsion could result in greater therapeutic concentrations (i.e. bioequivalence from a lower dose).

The phase 1 trial would be larger in scope (20-100 volunteers), but still focused exclusively on healthy volunteers. The purpose of this phase would be to determine a safe range of concentrations in which the nanoemulsion formulation could be administered. It would be hoped that a therapeutic concentration of LPV or EFV was reached before the dose of the nanoemulsion equalled that of the standard formulation. At this stage of the trial, any side effects would also be monitored carefully. Previous work involving nanoformulations of cancer therapeutics has led to phase 1 trials being conducted [567-569]. A phase 1 trial would involve a considerable amount of resource and investment, and is something that would have to be conducted in partnership with a large charitable organisation or pharmaceutical company. Again, nanoformulations of anticancer therapeutics have gained a lot of attention over the past decade, with a number of clinical trials having already taken place [570].

The issue of scale-up would again be an issue for the clinical trial phases of development. The requirement for all constituents of the nanoemulsion system to be at GMP grade would add significantly to the cost of producing the formulation at large quantities. There would be the need to conduct accelerated stability studies, complete with assessment of any possible degradation products that may be formed. All of this information would need to be detailed in a complete Investigational Medicinal Product Dossier (IMPD) [571] and regulatory approval would be needed before any progression to clinical trials would be allowed. The IMPD would have to include a detailed summary relating to all aspects of the nanoemulsion formulation,

including its production, quality and the manufacturing process. There would also be the need to include all preclinical data generated to date. The IMPD would also contain the relevant certificates of GMP quality for all of the constituents used in making the formulation [571]. This is where a potential hurdle would be encountered, as the production of PolyOEGMA would need to be outsourced. Large scale production and to GMP grade would not be possible within the laboratories at the University of Liverpool.

Every piece of scientific work is not without its limitations and the same applies to the work described in this thesis. The main limitations of a Ph.D. project are time and resources, and although the work presented here was funded by a generous grant from the British Society for Antimicrobial Chemotherapy, there is still much more work to be done.

There are a large number of polymers and copolymers that could have been made and assessed for their ability as emulsion stabilising agents. The project had the advantage of being informed from the work of Weaver *et al* [290-295], and as such there was a solid starting point with lots of background work already complete. Further iteration in this area is certainly worth considering however, in that polymer which could be reacted in such a way as to add signalling molecules or recognition sites to the polymer chain would be highly beneficial. Having a dual stabilising/targeting agent would allow for potentially increased distribution and accumulation to certain tissues types, for example CD4+ T cells, which would have

a direct positive benefit for HIV therapy. To expand further into different APIs, targeting molecules could be used for a variety of tissue types, dependent upon the disease being treated. Previous work in the literature has demonstrated the use of targeting strategies on nanoparticle-based therapies [572-576]. This is of course all assuming that the formulation of different lipophilic APIs translates as well as it did for EFV and LPV.

There were also limitations in the type and numbers of experiments that were conducted. Cytotoxicity, for example, was assessed by two different assays, namely MTT and Cell TiterGlo® assay. These two assays respond to changes in the mitochondrial metabolism of the cells, and it could be argued that using two assays that targeted different aspects of the cell (such as trypan blue for cell membrane integrity) would have been more informative. It would also have been informative to assess the effect of the drugs on the growth rates of the cells, as there may not have been any overt cytotoxicity observed, but potentially the growth of the cells over time could be affected. This is tricky to assess in cell lines however, as changes in the morphology of cell lines can occur dependent upon passage number [577, 578].

The experimentation to assess the level of pharmaceutical benefit (accumulation, Papp) was conducted solely on model cell lines. Although these are well developed and accepted models, they still deviate significantly from primary human cells and tissues. To expand this investigation, it would be necessary to repeat the tests in

primary human tissues [579, 580], although this would have added significantly to the cost of the project.

The use of animal models would provide a significant increase in the confidence of the level of benefit seen. Animal models of drug distribution and plasma concentrations would provide an indication as to how the nanoemulsion would perform in a whole body situation. Again this was not possible in this study due to financial and time constraints, as well as the issues of strict licensing and control of animal testing. As stated previously above, *in vivo* animal testing is certainly the next step to take in the continuation of development of this project.

Although there was a large set of immunological safety assays conducted, in part due to the collaboration with the Nanotechnology Characterisation Laboratory, there are many other aspects that can be assessed. It would be unrealistic to conduct every possible type of immune assay available, but the assays used in this project do cover a wide range of scenarios and represent an in depth first assessment of potential immunological side effects. There is room for further investigation into the coagulation effect of the nanoemulsions, as this was the only assay conducted that showed significant effect. It would be important to follow up this result in order to ascertain why the prolonged APTT coagulation was seen, and to work out a mechanism for it. Potential detrimental effects can be predicted and possibly prevented. This may perhaps be achieved by avoiding dosage to patients already

identified as having impaired coagulation functions or by co administration with a compound to offset the effect seen by the nanoemulsion.

In summary, the work presented in this thesis has shown a successful and cosrt effective approach to developing a nanoformulation of an existing first line drug. The data suggest that the nanoemulsion formulations have good potential to be beneficial over the existing aqueous formulation. The data also justifies the further investigation into the nanoemulsion formulations in order to further characterise and quantify the effect that this formulation may have in a drug delivery setting. Dependant upon the results of further investigation, particularly that which addresses the limitations of this study, nanoemulsions could be a viable platform for achieving improvements in the effectiveness of poorly water soluble therapeutics.

**References**


1. UNAIDS, *2012 Report on the Global AIDS Epidemic.* 2012.
2. UNAIDS, *Global update on HIV treatment 2013: results, impact and opportunities*. 2013.
3. Ferguson, M.R., et al., *HIV-1 replication cycle.* Clinics in Laboratory Medicine, 2002. **22**(3): p. 611-+.
4. Huet, T., et al., *Genetic organization of a chimpanzee lentivirus related to HIV-1.* Nature, 1990. **345**(6273): p. 356-359.
5. Hirsch, V.M., et al., *An African primate lentivirus (SIVsmclosely related to HIV-2.* Nature, 1989. **339**(6223): p. 389-392.
6. Hahn, B.H., et al., *AIDS as a Zoonosis: Scientific and Public Health Implications.* Science, 2000. **287**(5453): p. 607-614.
7. de Silva, T.I., M. Cotten, and S.L. Rowland-Jones, *HIV-2: the forgotten AIDS virus.* Trends in Microbiology, 2008. **16**(12): p. 588-595.
8. Popper, S.J., et al., *Low plasma human immunodeficiency virus type 2 viral load is independent of proviral load: low virus production in vivo.* J Virol, 2000. **74**(3): p. 1554-7.
9. Berry, N., et al., *Low level viremia and high CD4% predict normal survival in a cohort of HIV type-2-infected villagers.* Aids Research and Human Retroviruses, 2002. **18**(16): p. 1167-1173.
10. Rowland-Jones, S.L. and H.C. Whittle, *Out of Africa: what can we learn from HIV-2 about protective immunity to HIV-1?* Nat Immunol, 2007. **8**(4): p. 329-31.

11. Kopko, P.M., et al., *HIV transmissions from a window-period platelet donation.* American Journal of Clinical Pathology, 2001. **116**(4): p. 562-566.

12. Matebeni, Z., et al., *"I thought we are safe": Southern African lesbians' experiences of living with HIV.* Culture Health & Sexuality, 2013. **15**: p. 34-47.

13. Quinn, T.C., et al., *Viral load and heterosexual transmission of human immunodeficiency virus type 1.* New England Journal of Medicine, 2000. **342**(13): p. 921-929.

14. Mathers, B.M., et al., *Global epidemiology of injecting drug use and HIV among people who inject drugs: a systematic review.* Lancet, 2008. **372**(9651): p. 1733-1745.

15. Ezeanolue, E.E. and C. Schenauer, *Challenges to the elimination of mother-to-child transmission of HIV infection: Four case reports.* Aids Reader, 2007. **17**(1): p. 33-38.

16. Coutsoudis, A., *Breast-feeding and HIV transmission.* Nutrition Research Reviews, 2001. **14**(2): p. 191-206.

17. Smed-Sorensen, A. and K. Lore, *Dendritic cells at the interface of innate and adaptive immunity to HIV-1.* Current Opinion in Hiv and Aids, 2011. **6**(5): p. 405-410.

18. Douek, D.C., et al., *HIV preferentially infects HIV-specific CD4(+) T cells.* Nature, 2002. **417**(6884): p. 95-98.

19. He, J.L., et al., *Human-immunodeficiency-virus type-1 viral-protein-r (vpr) arrests cells in the g(2) phase of the cell-cycle by inhibiting p34(cdc2) activity.* Journal of Virology, 1995. **69**(11): p. 6705-6711.

20. Alimonti, J.B., T.B. Ball, and K.R. Fowke, *Mechanisms of CD4(+) T lymphocyte cell death in human immunodeficiency virus infection and AIDS.* Journal of General Virology, 2003. **84**: p. 1649-1661.

21. Fauci, A.S., *The human immunodeficiency virus - infectivity and mechanisms of pathogenesis.* Science, 1988. **239**(4840): p. 617-622.

22. Nie, Z., et al., *HIV-1 protease processes procaspase 8 to cause mitochondrial release of cytochrome c, caspase cleavage and nuclear fragmentation.* Cell Death and Differentiation, 2002. **9**(11): p. 1172-1184.

23. Korant, B.D., et al., *A cellular anti-apoptosis protein is cleaved by the HIV-1 protease.* Adv Exp Med Biol, 1998. **436**: p. 27-9.

24. Espert, L., et al., *Autophagy and CD4(+) T lymphocyte destruction by HIV-1.* Autophagy, 2007. **3**(1): p. 32-34.

25. Wren, L.H., et al., *Specific antibody-dependent cellular cytotoxicity responses associated with slow progression of HIV infection.* Immunology, 2013. **138**(2): p. 116-123.

26. Zagury, D., et al., *Interferon alpha and Tat involvement in the immunosuppression of uninfected T cells and C-C chemokine decline in AIDS.* Proceedings of the National Academy of Sciences of the United States of America, 1998. **95**(7): p. 3851-3856.

27. Mann, D.A. and A.D. Frankel, *Endocytosis and targeting of exogenous HIV-1 tat protein.* Embo Journal, 1991. **10**(7): p. 1733-1739.

28. Ensoli, B., et al., *Tat protein of HIV-1 stimulates growth of cells derived from kaposis-sarcoma lesions of AIDS patients.* Nature, 1990. **345**(6270): p. 84-86.

29. Gulzar, N. and K.F.T. Copeland, *CD8+T-cells: Function and response to HIV infection.* Current Hiv Research, 2004. **2**(1): p. 23-37.

30. Okoye, A.A. and L.J. Picker, *CD4+T-cell depletion in HIV infection: mechanisms of immunological failure.* Immunological Reviews, 2013. **254**: p. 54-64.

31. Garg, H., J. Mohl, and A. Joshi, *HIV-1 induced bystander apoptosis.* Viruses, 2012. **4**(11): p. 3020-43.

32. Crowe, S.M. and S. Sonza, *HIV-1 can be recovered from a variety of cells including peripheral blood monocytes of patients receiving highly active antiretroviral therapy: a further obstacle to eradication.* Journal of Leukocyte Biology, 2000. **68**(3): p. 345-350.

33. Schnittman, S.M., et al., *The reservoir for HIV-1 in human peripheral-blood is a T-cell that maintains expression of CD4.* Science, 1989. **245**(4915): p. 305-308.

34. Embretson, J., et al., *Massive covert infection of helper T-lymphocytes and macrophages by HIV during the incubation period of AIDS.* Nature, 1993. **362**(6418): p. 359-362.

35. Hoetelmans, R.M.W., *Sanctuary sites in HIV-1 infection.* Antiviral Therapy, 1998. **3**: p. 13-17.

36. Cory, T.J., et al., *Overcoming pharmacologic sanctuaries.* Current Opinion in Hiv and Aids, 2013. **8**(3): p. 190-195.

37. Chan, D.C., et al., *Core structure of gp41 from the HIV envelope glycoprotein.* Cell, 1997. **89**(2): p. 263-273.

38. Wu, L.J., et al., *CD4-induced interaction of primary HIV-1 gp120 glycoproteins with the chemokine receptor CCR-5.* Nature, 1996. **384**(6605): p. 179-183.

39. Svicher, V., et al., *HIV-1 dual/mixed tropic isolates show different genetic and phenotypic characteristics and response to maraviroc in vitro.* Antiviral Research, 2011. **90**(1): p. 42-53.

40. Moore, J.P., et al., *The CCR5 and CXCR4 coreceptors - Central to understanding the transmission and pathogenesis of human immunodeficiency virus type 1 infection.* Aids Research and Human Retroviruses, 2004. **20**(1): p. 111-126.

41. Vandekerckhove, L., C. Verhofstede, and D. Vogelaers, *Maraviroc: integration of a new antiretroviral drug class into clinical practice.* Journal of Antimicrobial Chemotherapy, 2008. **61**(6): p. 1187-1190.

42. Edo-Matas, D., et al., *Comparison of in vivo and in vitro evolution of CCR5 to CXCR4 coreceptor use of primary human immunodeficiency virus type 1 variants.* Virology, 2011. **412**(2): p. 269-277.

43. Stein, B.S., et al., *pH-independent HIV entry into CD4-positive T cells via virus envelope fusion to the plasma membrane.* Cell, 1987. **49**(5): p. 659-668.

44. Hernandez, L.D., et al., *Virus-cell and cell-cell fusion.* Annual Review of Cell and Developmental Biology, 1996. **12**: p. 627-661.

45. Doms, R.W. and J.P. Moore, *HIV-1 Membrane Fusion: Targets of Opportunity.* The Journal of Cell Biology, 2000. **151**(2): p. F9-F13.

46. Preston, B., B. Poiesz, and L. Loeb, *Fidelity of HIV-1 reverse transcriptase.* Science, 1988. **242**(4882): p. 1168-1171.

47. Roberts, J., K. Bebenek, and T. Kunkel, *The accuracy of reverse transcriptase from HIV-1.* Science, 1988. **242**(4882): p. 1171-1173.

48. Kati, W.M., et al., *Mechanism and fidelity of HIV reverse-transcriptase.* Journal of Biological Chemistry, 1992. **267**(36): p. 25988-25997.

49. Hindmarsh, P. and J. Leis, *Retroviral DNA integration.* Microbiology and Molecular Biology Reviews, 1999. **63**(4): p. 836-+.

50. Schroder, A.R.W., et al., *HIV-1 integration in the human genome favors active genes and local hotspots.* Cell, 2002. **110**(4): p. 521-529.

51. Finzi, D., et al., *Latent infection of CD4(+) T cells provides a mechanism for lifelong persistence of HIV-1, even in patients on effective combination therapy.* Nature Medicine, 1999. **5**(5): p. 512-517.

52. Marciniak, R.A. and P.A. Sharp, *HIV-1 tat protein promotes formation of more-processive elongation complexes.* Embo Journal, 1991. **10**(13): p. 4189-4196.

53. Marciniak, R.A., et al., *HIV-1 tat protein trans-activates transcription in vitro.* Cell, 1990. **63**(4): p. 791-802.

54. Mancebo, H.S.Y., et al., *P-TEFb kinase is required for HIV Tat transcriptional activation in vivo and in vitro.* Genes & Development, 1997. **11**(20): p. 2633-2644.

55. Tahirov, T.H., et al., *Crystal structure of HIV-1 Tat complexed with human P-TEFb.* Nature, 2010. **465**(7299): p. 747-U2.

56. Kohl, N.E., et al., *Active human immunodeficiency virus protease is required for viral infectivity.* Proceedings of the National Academy of Sciences of the United States of America, 1988. **85**(13): p. 4686-4690.

57. Morita, E. and W.I. Sundquist, *Retrovirus budding.* Annual Review of Cell and Developmental Biology, 2004. **20**: p. 395-425.

58. Clark, S.J., et al., *High titers of cytopathic virus in plasma of patients with symptomatic primary HIV-1 infection.* New England Journal of Medicine, 1991. **324**(14): p. 954-960.

59. Daar, E.S., et al., *Transient high-levels of viremia in patients with primary human-immunodeficiency-virus type-1 infection.* New England Journal of Medicine, 1991. **324**(14): p. 961-964.

60. Chun, T.W., et al., *Quantification of latent tissue reservoirs and total body viral load in HIV-1 Infection.* Nature, 1997. **387**(6629): p. 183-188.

61. Blankson, J.N., D. Persaud, and R.F. Siliciano, *The challenge of viral reservoirs in HIV-1 infection.* Annual Review of Medicine, 2002. **53**: p. 557-593.

62. Richman, D.D., et al., *Rapid evolution of the neutralizing antibody response to HIV type 1 infection.* Proceedings of the National Academy of Sciences of the United States of America, 2003. **100**(7): p. 4144-4149.

63. Wei, X.P., et al., *Antibody neutralization and escape by HIV-1.* Nature, 2003. **422**(6929): p. 307-312.

64. Walker, B.D., et al., *HIV-specific cytotoxic T-lymphocytes in seropositive individuals.* Nature, 1987. **328**(6128): p. 345-348.

65. Rosenberg, E.S., et al., *Immune control of HIV-1 after early treatment of acute infection.* Nature, 2000. **407**(6803): p. 523-526.

66. Ogg, G.S., et al., *Quantitation of HIV-1-specific cytotoxic T lymphocytes and plasma load of viral RNA.* Science, 1998. **279**(5359): p. 2103-2106.

67. Lassen, K., et al., *The multifactorial nature of HIV-1 latency.* Trends in Molecular Medicine, 2004. **10**(11): p. 525-531.

68. Han, Y.F., et al., *Experimental approaches to the study of HIV-1 latency.* Nature Reviews Microbiology, 2007. **5**(2): p. 95-106.

69. Coiras, M., et al., *Understanding HIV-1 latency provides clues for the eradication of long-term reservoirs.* Nature Reviews Microbiology, 2009. **7**(11): p. 798-812.

70. Pratt, R.D., et al., *Virologic characterization of primary human immunodeficiency virus type 1 infection in a health care worker following needlestick injury.* Journal of Infectious Diseases, 1995. **172**(3): p. 851-854.

71. Pantaleo, G., et al., *HIV-infection is active and progressive in lymphoid-tissue during the clinically latent stage of disease.* Nature, 1993. **362**(6418): p. 355-358.

72. Brooks, D.G., et al., *Identification of T cell-signaling pathways that stimulate latent HIV in primary cells.* Proceedings of the National Academy of Sciences of the United States of America, 2003. **100**(22): p. 12955-12960.

73. McCune, J.M., *The dynamics of CD4(+) T-cell depletion in HIV disease.* Nature, 2001. **410**(6831): p. 974-979.

74. Narain, J.P. and Y.R. Lo, *Epidemiology of HIV-TB in Asia.* Indian Journal of Medical Research, 2004. **120**(4): p. 277-289.

75. Fine, A.D., et al., *Influenza A among patients with human immunodeficiency virus: An outbreak of infection at a residential facility in New York City.* Clinical Infectious Diseases, 2001. **32**(12): p. 1784-1791.

76. Godet, C., G. Beraud, and J. Cadranel, *Bacterial pneumonia in HIV-infected patients (excluding mycobacterial infection).* Revue Des Maladies Respiratoires, 2012. **29**(8): p. 1058-1066.

77. NIAID. *Biology of HIV*. 2012 April 2012 [cited 2013 25th October]; Available from: http://www.niaid.nih.gov/topics/hivaids/understanding/biology/Pages/biology.aspx.

78. Fang, C.T., et al., *Life expectancy of patients with newly-diagnosed HIV infection in the era of highly active antiretroviral therapy.* Qjm-an International Journal of Medicine, 2007. **100**(2): p. 97-105.

79. Ammassari, A., et al., *Beyond virological suppression: the role of adherence in the late HAART era.* Antiviral Therapy, 2012. **17**(5): p. 785-792.

80. Martin, M.T., et al., *Adverse side effects of antiretroviral therapy: relationship between patients perception and adherence.* Medicina Clinica, 2007. **129**(4): p. 127-133.

81. Cihlar, T. and A.S. Ray, *Nucleoside and nucleotide HIV reverse transcriptase inhibitors: 25 years after zidovudine.* Antiviral Research, 2010. **85**(1): p. 39-58.

82. Khan, A.K.R., S.A. Khan, and M. Ansari, *Quantum chemical-based drug-receptor interaction of tetrahydroimidobenzodiazepinones (HIV-1-NNRTIs) with receptor (HIV-1-NNRTI-binding pocket).* Medicinal Chemistry Research, 2011. **20**(2): p. 231-238.

83. Usach, I., V. Melis, and J.E. Peris, *Non-nucleoside reverse transcriptase inhibitors: a review on pharmacokinetics, pharmacodynamics, safety and tolerability.* Journal of the International Aids Society, 2013. **16**.

84. van 't Klooster, G., et al., *Pharmacokinetics and Disposition of Rilpivirine (TMC278) Nanosuspension as a Long-Acting Injectable Antiretroviral Formulation.* Antimicrobial Agents and Chemotherapy, 2010. **54**(5): p. 2042-2050.

85. Maurin, C., F. Bailly, and P. Cotelle, *Structure-activity relationships of HIV-1 integrase inhibitors - Enzyme-ligand interactions.* Current Medicinal Chemistry, 2003. **10**(18): p. 1795-1810.

86. Cocohoba, J. and B.J. Dong, *Raltegravir: The First HIV Integrase Inhibitor.* Clinical Therapeutics, 2008. **30**(10): p. 1747-1765.

87. Wainberg, M.A., P.K. Quashie, and T. Mesplede, *Dolutegravir HIV integrase inhibitor treatment of HIV infection.* Drugs of the Future, 2012. **37**(10): p. 697-707.

88. Andrews, C.D., et al., *Long-Acting Integrase Inhibitor Protects Macaques from Intrarectal Simian/Human Immunodeficiency Virus.* Science, 2014. **343**(6175): p. 1151-1154.

89. Dorr, P., et al., *Maraviroc (UK-427,857), a potent, orally bioavailable, and selective small-molecule inhibitor of chemokine receptor CCR5 with broad-spectrum anti-human immunodeficiency virus type 1 activity.* Antimicrobial Agents and Chemotherapy, 2005. **49**(11): p. 4721-4732.

90. Matthews, T., et al., *Enfuvirtide: The first therapy to inhibit the entry of HIV-1 into host CD4 lymphocytes.* Nature Reviews Drug Discovery, 2004. **3**(3): p. 215-225.

91. Lieberman-Blum, S.S., H.B. Fung, and J.C. Bandres, *Maraviroc: A CCR5-receptor antagonist for the treatment of HIV-1 infection.* Clinical Therapeutics, 2008. **30**(7): p. 1228-1250.

92. Sattentau, Q.J. and J.P. Moore, *Conformational-changes induced in the human-immunodeficiency-virus envelope glycoprotein by soluble CD4 binding.* Journal of Experimental Medicine, 1991. **174**(2): p. 407-415.

93. Bottaro, E.G., *Enfuvirtide: The first step for a new strategy of antiretroviral therapy.* Medicina-Buenos Aires, 2007. **67**(2): p. 195-205.

94. Eggink, D., B. Berkhout, and R.W. Sanders, *Inhibition of HIV-1 by Fusion Inhibitors.* Current Pharmaceutical Design, 2010. **16**(33): p. 3716-3728.

95. Zha, W.B., et al., *The Cellular Pharmacokinetics of HIV Protease Inhibitors: Current Knowledge and Future Perspectives.* Current Drug Metabolism, 2012. **13**(8): p. 1174-1183.

96. Kempf, D.J., et al., *Pharmacokinetic enhancement of inhibitors of the human immunodeficiency virus protease by coadministration with ritonavir.* Antimicrobial Agents and Chemotherapy, 1997. **41**(3): p. 654-660.

97. Ferreira, C., et al., *Representation of illness and of treatment side effects as determinants of adherence to treatment of HIV patients.* Annales Medico-Psychologiques, 2010. **168**(1): p. 25-33.

98. Feeney, E., E. Muldoon, and W.G. Powderly, *Management of antiretroviral drug toxicity.* Current Opinion in Hiv and Aids, 2006. **1**(5): p. 430-436.

99. Kasim, N.A., et al., *Molecular properties of WHO essential drugs and provisional biopharmaceutical classification.* Mol Pharm, 2004. **1**(1): p. 85-96.

100. Ammassari, A., et al., *Self-reported symptoms and medication side effects influence adherence to highly active antiretroviral therapy in persons with HIV infection.* Journal of Acquired Immune Deficiency Syndromes, 2001. **28**(5): p. 445-449.

101. Shirasaka, T., *Adverse effects of antiretroviral agents, and their treatment.* Nihon rinsho. Japanese journal of clinical medicine, 2010. **68**(3): p. 480-5.

102. Martin, A.M., et al., *Predisposition to abacavir hypersensitivity conferred by HLA-B*5701 and a haplotypic Hsp70-Hom variant.* Proceedings of the National Academy of Sciences of the United States of America, 2004. **101**(12): p. 4180-4185.

103. Mallal, S., et al., *Association between presence of HLA-B*5701, HLA-DR7, and HLA-DQ3 and hypersensitivity to HIV-1 reverse-transcriptase inhibitor abacavir.* Lancet, 2002. **359**(9308): p. 727-732.

104. Hetherington, S., et al., *Genetic variations in HLA-B region and hypersensitivity reactions to abacavir.* Lancet, 2002. **359**(9312): p. 1121-1122.

105. Martin, A.M., et al., *Predisposition to nevirapine hypersensitivity associated with HLA-DRB1*0101 and abrogated by low CD4 T-cell counts.* Aids, 2005. **19**(1): p. 97-99.

106. Stevens, A.M. and F.C. Johnson, *A new eruptive fever associated with stomatitis and ophthalmia - Report of two cases in children.* American Journal of Diseases of Children, 1922. **24**(6): p. 526-533.

107. Lyell, A., *Toxic epidermal necrolysis - an eruption resembling scalding of the skin.* British Journal of Dermatology, 1956. **68**(11): p. 355-361.

108. Reust, C.E., *Common Adverse Effects of Antiretroviral Therapy for HIV Disease.* American Family Physician, 2011. **83**(12): p. 1443-1451.

109. Soliman, E.Z., et al., *Boosted protease inhibitors and the electrocardiographic measures of QT and PR durations.* Aids, 2011. **25**(3): p. 367-377.

110. Boesecke, C. and D.A. Cooper, *Toxicity of HIV protease inhibitors: clinical considerations.* Current Opinion in Hiv and Aids, 2008. **3**(6): p. 653-659.

111. Hsu, A., G.R. Granneman, and R.J. Bertz, *Ritonavir - Clinical pharmacokinetics and interactions with other anti-HIV agents.* Clinical Pharmacokinetics, 1998. **35**(4): p. 275-291.

112. Foisy, M.M., E.M. Yakiwchuk, and C.A. Hughes, *Induction effects of ritonavir: Implications for drug interactions.* Annals of Pharmacotherapy, 2008. **42**(7-8): p. 1048-1059.

113. Roberts, J.D., K. Bebenek, and T.A. Kunkel, *The accuracy of reverse-transcriptase from hiv-1.* Science, 1988. **242**(4882): p. 1171-1173.

114. Huang, K.J. and D.P. Wooley, *A new cell-based assay for measuring the forward mutation rate of HIV-1.* Journal of Virological Methods, 2005. **124**(1-2): p. 95-104.

115. Alizon, S. and C. Fraser, *Within-host and between-host evolutionary rates across the HIV-1 genome.* Retrovirology, 2013. **10**: p. 10.

116. Richman, D.D., et al., *Nevirapine resistance mutations of human-immunodeficiency-virus type-1 selected during therapy.* Journal of Virology, 1994. **68**(3): p. 1660-1666.

117. Little, S.J., et al., *Antiretroviral-drug resistance among patients recently infected with HIV.* New England Journal of Medicine, 2002. **347**(6): p. 385-394.

118. Larder, B.A. and S.D. Kemp, *Multiple mutations in HIV-1 reverse-transcriptase confer high-level resistance to zidovudine (AZT).* Science, 1989. **246**(4934): p. 1155-1158.

119. Condra, J.H., et al., *In-vivo emergence of HIV-1 variants resistant to multiple protease inhibitors.* Nature, 1995. **374**(6522): p. 569-571.

120. Clavel, F. and A.J. Hance, *Medical progress: HIV drug resistance.* New England Journal of Medicine, 2004. **350**(10): p. 1023-1035.

121. Asahchop, E.L., et al., *Antiviral Drug Resistance and the Need for Development of New HIV-1 Reverse Transcriptase Inhibitors.* Antimicrobial Agents and Chemotherapy, 2012. **56**(10): p. 5000-5008.

122. Anta, L., et al., *Resistance to the most recent protease and non-nucleoside reverse transcriptase inhibitors across HIV-1 non-B subtypes.* Journal of Antimicrobial Chemotherapy, 2013. **68**(9): p. 1994-2002.

123. Menéndez-Arias, L., *Molecular basis of human immunodeficiency virus type 1 drug resistance: Overview and recent developments.* Antiviral Research, 2013. **98**(1): p. 93-120.

124. Shafer, R.W. and J.M. Schapiro, *HIV-1 drug resistance mutations: an updated framework for the second decade of HAART.* Aids Reviews, 2008. **10**(2): p. 67-84.

125. Wagner, V., et al., *The emerging nanomedicine landscape.* Nature Biotechnology, 2006. **24**(10): p. 1211-1217.

126. Riehemann, K., et al., *Nanomedicine-Challenge and Perspectives.* Angewandte Chemie-International Edition, 2009. **48**(5): p. 872-897.

127. Lammers, T., et al., *Theranostic Nanomedicine.* Accounts of Chemical Research, 2011. **44**(10): p. 1029-1038.

128. Kim, B.Y.S., J.T. Rutka, and W.C.W. Chan, *Current Concepts: Nanomedicine.* New England Journal of Medicine, 2010. **363**(25): p. 2434-2443.

129. Gogtay, J.A. and G. Malhotra, *Reformulation of existing antiretroviral drugs.* Current Opinion in Hiv and Aids, 2013. **8**(6): p. 550-555.

130. Brewster, M.E., *Biopharmaceutics Classification System.* Third Annual Congress on Strategies to Enhance Solubility & Drug Absorption, 2008.

131. Keller, T., *Nanomaterials: A realistic business case for Pharma*. Nsti Nanotech 2008, Vol 2, Technical Proceedings, ed. M. Laudon and B. Romanowicz. 2008. 190-193.

132. Crawford, K.W., et al., *Optimising the manufacture, formulation, and dose of antiretroviral drugs for more cost-efficient delivery in resource-limited settings: a consensus statement.* The Lancet Infectious Diseases, 2012. **12**(7): p. 550-560.

133. Tyner, K. and N. Sadrieh, *Considerations When Submitting Nanotherapeutics to FDA/CDER for Regulatory Review*, in *Characterization of Nanoparticles Intended for Drug Delivery*, S.E. McNeil, Editor. 2011, Humana Press Inc: Totowa. p. 17-31.

134. Hoet, P., et al., *Do Nanomedicines Require Novel Safety Assessments to Ensure their Safety for Long-Term Human Use?* Drug Safety, 2009. **32**(8): p. 625-636.

135. Steinbach, O.C., *Industry Update: The latest developments in therapeutic delivery.* Therapeutic delivery, 2013. **4**(9): p. 1087-92.

136. Ventola, C.L., *The nanomedicine revolution: part 2: current and future clinical applications.* P T, 2012. **37**(10): p. 582-91.

137. Tian, X., M. Zhu, and G. Nie, *How can nanotechnology help membrane vesicle-based cancer immunotherapy development?* Human Vaccines & Immunotherapeutics, 2013. **9**(1): p. 228-231.

138. Pantic, I., *Nanoparticles and modulation of immune responses.* Science Progress, 2011. **94**(1): p. 97-107.

139. Look, M., et al., *Application of nanotechnologies for improved immune response against infectious diseases in the developing world.* Advanced Drug Delivery Reviews, 2010. **62**(4-5): p. 378-393.

140. Starmans, L.W.E., et al., *Iron Oxide Nanoparticle-Micelles (ION-Micelles) for Sensitive (Molecular) Magnetic Particle Imaging and Magnetic Resonance Imaging.* Plos One, 2013. **8**(2).

141. Neumaier, C.E., et al., *MR and iron magnetic nanoparticles. Imaging opportunities in preclinical and translational research.* Tumori, 2008. **94**(2): p. 226-233.

142. Li, M., et al., *Comparison of Two Ultrasmall Superparamagnetic Iron Oxides on Cytotoxicity and MR Imaging of Tumors.* Theranostics, 2012. **2**(1): p. 76-85.

143. Petersen, A., et al., *Nanotechnologies, risk and society.* Health Risk & Society, 2007. **9**(2): p. 117-124.

144. Keller, K.H., *Nanotechnology and society.* Journal of Nanoparticle Research, 2007. **9**(1): p. 5-10.

145. Nowack, B. and T.D. Bucheli, *Occurrence, behavior and effects of nanoparticles in the environment.* Environmental Pollution, 2007. **150**(1): p. 5-22.

146. Mueller, N.C. and B. Nowack, *Exposure modeling of engineered nanoparticles in the environment.* Environmental Science & Technology, 2008. **42**(12): p. 4447-4453.

147. Yanamala, N., et al., *Biodiesel versus diesel exposure: Enhanced pulmonary inflammation, oxidative stress, and differential morphological changes in the mouse lung.* Toxicology and applied pharmacology, 2013. **272**(2): p. 373-83.

148. Kovats, N., et al., *Ecotoxicity and genotoxicity assessment of exhaust particulates from diesel-powered buses.* Environmental Monitoring and Assessment, 2013. **185**(10): p. 8707-8713.

149. Verma, S., A.J. Domb, and N. Kumar, *Nanomaterials for regenerative medicine.* Nanomedicine, 2011. **6**(1): p. 157-181.

150. Zarbin, M.A., et al., *Regenerative nanomedicine and the treatment of degenerative retinal diseases.* Wiley Interdisciplinary Reviews-Nanomedicine and Nanobiotechnology, 2012. **4**(1): p. 113-137.

151. Chen, J., et al., *Rare earth nanoparticles prevent retinal degeneration induced by intracellular peroxides.* Nature Nanotechnology, 2006. **1**(2): p. 142-150.

152. Glover, D.J., H.J. Lipps, and D.A. Jans, *Towards safe, non-viral therapeutic gene expression in humans.* Nature Reviews Genetics, 2005. **6**(4): p. 299-U29.

153. Prow, T., et al., *Nanoparticle tethered antioxidant response element as a biosensor for oxygen induced toxicity in retinal endothelial cells.* Molecular Vision, 2006. **12**(67-69): p. 616-625.

154. Mo, Y., et al., *Human serum albumin nanoparticles for efficient delivery of Cu, Zn superoxide dismutase gene.* Molecular Vision, 2007. **13**(80-85): p. 746-757.

155. Farjo, R., et al., *Efficient Non-Viral Ocular Gene Transfer with Compacted DNA Nanoparticles.* Plos One, 2006. **1**(1).

156. Cai, X., S. Conley, and M. Naash, *Nanoparticle applications in ocular gene therapy.* Vision Research, 2008. **48**(3): p. 319-324.

157. Mooney, D.J. and H. Vandenburgh, *Cell delivery mechanisms for tissue repair.* Cell Stem Cell, 2008. **2**(3): p. 205-213.

158. Reddi, A.H., J. Becerra, and J.A. Andrades, *Nanomaterials and Hydrogel Scaffolds for Articular Cartilage Regeneration.* Tissue Engineering Part B-Reviews, 2011. **17**(5): p. 301-305.

159. Zhou, J., et al., *Engineering the heart: Evaluation of conductive nanomaterials for improving implant integration and cardiac function.* Scientific Reports, 2014. **4**: p. 11.

160. Weissleder, R., M. Nahrendorf, and M.J. Pittet, *Imaging macrophages with nanoparticles.* Nature Materials, 2014. **13**(2): p. 125-138.

161. Smith, A.M., et al., *Bioconjugated quantum dots for in vivo molecular and cellular imaging.* Advanced Drug Delivery Reviews, 2008. **60**(11): p. 1226-1240.

162. Ruemenapp, C., B. Gleich, and A. Haase, *Magnetic Nanoparticles in Magnetic Resonance Imaging and Diagnostics.* Pharmaceutical Research, 2012. **29**(5): p. 1165-1179.

163. Probst, J., et al., *Luminescent nanoparticles and their use for in vitro and in vivo diagnostics.* Expert Review of Molecular Diagnostics, 2012. **12**(1): p. 49-64.

164. Pandey, A.P., et al., *Graphene Based Nanomaterials: Diagnostic Applications.* Journal of Biomedical Nanotechnology, 2014. **10**(2): p. 179-204.

165. Larguinho, M. and P.V. Baptista, *Gold and silver nanoparticles for clinical diagnostics - From genomics to proteomics.* Journal of Proteomics, 2012. **75**(10): p. 2811-2823.

166. Doria, G., et al., *Noble Metal Nanoparticles for Biosensing Applications.* Sensors, 2012. **12**(2): p. 1657-1687.

167. McDonald, T.O., et al., *Antiretroviral Solid Drug Nanoparticles with Enhanced Oral Bioavailability: Production, Characterization, and In Vitro-In Vivo Correlation.* Adv Healthc Mater, 2013.

168. Khrenov, V., et al., *The formation of hydrophobic inorganic nanoparticles in the presence of amphiphilic copolymers.* Colloid and Polymer Science, 2006. **284**(8): p. 927-934.

169. Ding, G.B., et al., *A double-targeted magnetic nanocarrier with potential application in hydrophobic drug delivery.* Colloids and Surfaces B-Biointerfaces, 2012. **91**: p. 68-76.

170. Maity, A.R., et al., *Carbohydrate coated, folate functionalized colloidal graphene as a nanocarrier for both hydrophobic and hydrophilic drugs.* Nanoscale, 2014. **6**(5): p. 2752-2758.

171. Abbasian, M., et al., *Synthesis and characterization of amphiphilic methoxypoly(ethylene glycol)-polystyrene diblock copolymer by ATRP and NMRP techniques.* Journal of Elastomers and Plastics, 2012. **44**(2): p. 205-220.

172. Xu, J., et al., *Synthesis of monodisperse gold nanoparticles stabilized by gemini surfactant in reverse micelles.* Journal of Dispersion Science and Technology, 2005. **26**(4): p. 473-476.

173. Lee, J., et al., *Amphiphilic amino acid copolymers as stabilizers for the preparation of nanocrystal dispersion.* European Journal of Pharmaceutical Sciences, 2005. **24**(5): p. 441-449.

174. Pickering, S.U., *CXCVI.-Emulsions.* Journal of the Chemical Society, Transactions, 1907. **91**(0): p. 2001-2021.

175. Nowacek, A.S., et al., *Analyses of nanoformulated antiretroviral drug charge, size, shape and content for uptake, drug release and antiviral activities in human monocyte-derived macrophages.* Journal of Controlled Release, 2011. **150**(2): p. 204-211.

176. Rhee, Y.S. and H.M. Mansour, *Nanopharmaceuticals I: nanocarrier systems in drug delivery.* International Journal of Nanotechnology, 2011. **8**(1-2): p. 84-114.

177. Wong, H.L., et al., *Nanotechnology applications for improved delivery of antiretroviral drugs to the brain.* Advanced Drug Delivery Reviews, 2010. **62**(4-5): p. 503-517.

178. Debbage, P., *Targeted Drugs and Nanomedicine: Present and Future.* Current Pharmaceutical Design, 2009. **15**(2): p. 153-172.

179. Kadam, R.S., D.W.A. Bourne, and U.B. Kompella, *Nano-Advantage in Enhanced Drug Delivery with Biodegradable Nanoparticles: Contribution of Reduced Clearance.* Drug Metabolism and Disposition, 2012. **40**(7): p. 1380-1388.

180. Zhang, Z.W., et al., *Nano-based Drug Delivery System Enhances the Oral Absorption of Lipophilic Drugs with Extensive Presystemic Metabolism.* Current Drug Metabolism, 2012. **13**(8): p. 1110-1118.

181. Xu, Z.P., et al., *Inorganic nanoparticles as carriers for efficient cellular delivery.* Chemical Engineering Science, 2006. **61**(3): p. 1027-1040.

182. Ghosh, P., et al., *Gold nanoparticles in delivery applications.* Advanced Drug Delivery Reviews, 2008. **60**(11): p. 1307-1315.

183. Wu, W., et al., *Smart Core-Shell Hybrid Nanogels with Ag Nanoparticle Core for Cancer Cell Imaging and Gel Shell for pH-Regulated Drug Delivery.* Chemistry of Materials, 2010. **22**(6): p. 1966-1976.

184. Roy, I., et al., *Ceramic-based nanoparticles entrapping water-insoluble photosensitizing anticancer drugs: A novel drug-carrier system for photodynamic therapy.* Journal of the American Chemical Society, 2003. **125**(26): p. 7860-7865.

185. Barbe, C., et al., *Silica particles: A novel drug-delivery system.* Advanced Materials, 2004. **16**(21): p. 1959-1966.

186. Bauer, L.A., N.S. Birenbaum, and G.J. Meyer, *Biological applications of high aspect ratio nanoparticles.* Journal of Materials Chemistry, 2004. **14**(4): p. 517-526.

187. Probst, C.E., et al., *Quantum dots as a platform for nanoparticle drug delivery vehicle design.* Advanced Drug Delivery Reviews, 2013. **65**(5): p. 703-718.

188. Kumar, C. and F. Mohammad, *Magnetic nanomaterials for hyperthermia-based therapy and controlled drug delivery.* Advanced Drug Delivery Reviews, 2011. **63**(9): p. 789-808.

189. Sandhu, K.K., et al., *Gold nanoparticle-mediated Transfection of mammalian cells.* Bioconjugate Chemistry, 2002. **13**(1): p. 3-6.

190. Jen, C.P., et al., *A nonviral transfection approach in vitro: The design of a gold nanoparticle vector joint with microelectromechanical systems.* Langmuir, 2004. **20**(4): p. 1369-1374.

191. Peek, R. and K.R. Reddy, *FDA approves Cimzia to treat Crohn's disease.* Gastroenterology, 2008. **134**(7): p. 1819-1819.

192. Frimat, L., et al., *Anaemia management with CERA in routine clinical practice: OCEANE (Cohorte Mircera patients non-dialyses), a national, multicenter, longitudinal, observational prospective study, in patients with chronic kidney disease not on dialysis.* Bmj Open, 2013. **3**(3): p. 14.

193. Barnard, D.L., *Pegasys (Hoffmann-La Roche).* Current opinion in investigational drugs (London, England : 2000), 2001. **2**(11): p. 1530-8.

194. Rolland, O., et al., *Dendrimers and nanomedicine: multivalency in action.* New Journal of Chemistry, 2009. **33**(9): p. 1809-1824.

195. Hawker, C.J. and J.M.J. Frechet, *Preparation of polymers with controlled molecular architecture. A new convergent approach to dendritic macromolecules.* Journal of the American Chemical Society, 1990. **112**(21): p. 7638-7647.

196. Akagi, T., M. Baba, and M. Akashi, *Development of vaccine adjuvants using polymeric nanoparticles and their potential applications for anti-HIV vaccine.* Yakugaku Zasshi-Journal of the Pharmaceutical Society of Japan, 2007. **127**(2): p. 307-317.

197. Craparo, E.F. and M.L. Bondi, *Application of polymeric nanoparticles in immunotherapy.* Current Opinion in Allergy and Clinical Immunology, 2012. **12**(6): p. 658-664.

198. Zhang, J., et al., *Ternary Polymeric Nanoparticles for Oral siRNA Delivery.* Pharmaceutical Research, 2013. **30**(5): p. 1228-1239.

199. Eerikainen, H. and E.I. Kauppinen, *Preparation of polymeric nanoparticles containing corticosteroid by a novel aerosol flow reactor method.* International Journal of Pharmaceutics, 2003. **263**(1-2): p. 69-83.

200. Grottkau, B.E., et al., *Polymeric Nanoparticles for a Drug Delivery System.* Current Drug Metabolism, 2013. **14**(8): p. 840-846.

201. Wang, X.Q. and Q. Zhang, *pH-sensitive polymeric nanoparticles to improve oral bioavailability of peptide/protein drugs and poorly water-soluble drugs.* European Journal of Pharmaceutics and Biopharmaceutics, 2012. **82**(2): p. 219-229.

202. Malam, Y., M. Loizidou, and A.M. Seifalian, *Liposomes and nanoparticles: nanosized vehicles for drug delivery in cancer.* Trends in Pharmacological Sciences, 2009. **30**(11): p. 592-599.

203. Torchilin, V.P., *Recent advances with liposomes as pharmaceutical carriers.* Nature Reviews Drug Discovery, 2005. **4**(2): p. 145-160.

204. Qin, L., et al., *Polymeric micelles for enhanced lymphatic drug delivery to treat metastatic tumors.* Journal of Controlled Release, 2013. **171**(2): p. 133-142.

205. Nishiyama, N. and K. Kataoka, *Current state, achievements, and future prospects of polymeric micelles as nanocarriers for drug and gene delivery.* Pharmacology & Therapeutics, 2006. **112**(3): p. 630-648.

206. Mukherjee, S., S. Ray, and R.S. Thakur, *Solid Lipid Nanoparticles: A Modern Formulation Approach in Drug Delivery System.* Indian Journal of Pharmaceutical Sciences, 2009. **71**(4): p. 349-358.

207. Gasco, M.R. and S. Morel, *Lipospheres from microemulsions.* Farmaco, 1990. **45**(10): p. 1127-1128.

208. Lee, M.-K., S.-J. Lim, and C.-K. Kim, *Preparation, characterization and in vitro cytotoxicity of paclitaxel-loaded sterically stabilized solid lipid nanoparticles*. Biomaterials, 2007. **28**(12): p. 2137-2146.

209. Koziara, J.M., et al., *In-vivo efficacy of novel paclitaxel nanoparticles in paclitaxel-resistant human colorectal tumors.* Journal of Controlled Release, 2006. **112**(3): p. 312-319.

210. Koziara, J.M., et al., *Paclitaxel nanoparticles for the potential treatment of brain tumors.* Journal of Controlled Release, 2004. **99**(2): p. 259-269.

211. Chen, D.B., et al., *In vitro and in vivo study of two types of long-circulating solid lipid nanoparticles containing paclitaxel.* Chemical & Pharmaceutical Bulletin, 2001. **49**(11): p. 1444-1447.

212. Venkateswarlu, V. and K. Manjunath, *Preparation, characterization and in vitro release kinetics of clozapine solid lipid nanoparticles.* Journal of Controlled Release, 2004. **95**(3): p. 627-638.

213. Friedrich, I., S. Reichl, and C.C. Muller-Goymann, *Drug release and permeation studies of nanosuspensions based on solidified reverse micellar solutions (SRMS).* International Journal of Pharmaceutics, 2005. **305**(1-2): p. 167-175.

214. Schubert, M.A. and C.C. Müller-Goymann, *Solvent injection as a new approach for manufacturing lipid nanoparticles - Evaluation of the method*

*and process parameters.* European Journal of Pharmaceutics and Biopharmaceutics, 2003. **55**(1): p. 125-131.

215. Hu, F.Q., et al., *Preparation of solid lipid nanoparticles with clobetasol propionate by a novel solvent diffusion method in aqueous system and physicochemical characterization.* International Journal of Pharmaceutics, 2002. **239**(1-2): p. 121-128.

216. Zur Mühlen, A., C. Schwarz, and W. Mehnert, *Solid lipid nanoparticles (SLN) for controlled drug delivery - Drug release and release mechanism.* European Journal of Pharmaceutics and Biopharmaceutics, 1998. **45**(2): p. 149-155.

217. Siekmann, B. and K. Westesen, *Investigations on solid lipid nanoparticles prepared by precipitation in o/w emulsions.* European Journal of Pharmaceutics and Biopharmaceutics, 1996. **42**(2): p. 104-109.

218. Sjostrom, B. and B. Bergenstahl, *Preparation of submicron drug particles in lecithin-stabilized o/w emulsions. I. Model studies of the precipitation of cholesteryl acetate.* International Journal of Pharmaceutics, 1992. **88**(1-3): p. 53-62.

219. Muller, R.H., et al., *Solid lipid nanoparticles (SLN) - An alternative colloidal carrier system for controlled drug delivery.* European Journal of Pharmaceutics and Biopharmaceutics, 1995. **41**(1): p. 62-69.

220. Yang, S.C., et al., *Body distribution in mice of intravenously injected camptothecin solid lipid nanoparticles and targeting effect on brain.* Journal of Controlled Release, 1999. **59**(3): p. 299-307.

221. Ugazio, E., R. Cavalli, and M.R. Gasco, *Incorporation of cyclosporin A in solid lipid nanoparticles (SLN).* International Journal of Pharmaceutics, 2002. **241**(2): p. 341-344.

222. Luo, Y., et al., *Solid lipid nanoparticles for enhancing vinpocetine's oral bioavailability.* Journal of Controlled Release, 2006. **114**(1): p. 53-59.

223. Hu, L.D., X. Tang, and F.D. Cui, *Solid lipid namoparticles (SLNs) to improve oral bioavailability of poorly soluble drugs.* Journal of Pharmacy and Pharmacology, 2004. **56**(12): p. 1527-1535.

224. Bunjes, H., *Lipid nanoparticles for the delivery of poorly water-soluble drugs.* Journal of Pharmacy and Pharmacology, 2010. **62**(11): p. 1637-1645.

225. Sarker, D.K., *Engineering of nanoemulsions for drug delivery.* Current Drug Delivery, 2005. **2**(4): p. 297-310.

226. de Campos, V.E.B., E. Ricci-Junior, and C.R.E. Mansur, *Nanoemulsions as delivery systems for lipophilic drugs.* Journal of nanoscience and nanotechnology, 2012. **12**(3): p. 2881-90.

227. Sadurni, N., et al., *Studies on the formation of O/W nano-emulsions, by low-energy emulsification methods, suitable for pharmaceutical applications.* Eur J Pharm Sci, 2005. **26**(5): p. 438-45.

228. Flanagan, J. and H. Singh, *Microemulsions: a potential delivery system for bioactives in food.* Crit Rev Food Sci Nutr, 2006. **46**(3): p. 221-37.

229. Pons, R., et al., *Formation and properties of miniemulsions formed by microemulsions dilution.* Advances in Colloid and Interface Science, 2003. **106**: p. 129-146.

230. Elaasser, M.S., et al., *The miniemulsification process - different form of spontaneous emulsification.* Colloids and Surfaces, 1988. **29**(1): p. 103-118.

231. Benita, S. and M.Y. Levy, *Submicron emulsions as colloidal drug carriers for intravenous administration - comprehensive physicochemical characterization.* Journal of Pharmaceutical Sciences, 1993. **82**(11): p. 1069-1079.

232. Tadros, T., et al., *Formation and stability of nano-emulsions.* Advances in Colloid and Interface Science, 2004. **108**: p. 303-318.

233. Walstra, P., *Principles of emulsion formation.* Chemical Engineering Science, 1993. **48**(2): p. 333-349.

234. Santana, R.C., F.A. Perrechil, and R.L. Cunha, *High- and Low-Energy Emulsifications for Food Applications: A Focus on Process Parameters.* Food Engineering Reviews, 2013. **5**(2): p. 107-122.

235. Yang, Y., et al., *Fabrication of ultrafine edible emulsions: Comparison of high-energy and low-energy homogenization methods.* Food Hydrocolloids, 2012. **29**(2): p. 398-406.

236. Takami, T. and Y. Murakami, *Unexpected and Successful "One-Step" Formation of Porous Polymeric Particles Only by Mixing Organic Solvent and Water under "Low-Energy-Input" Conditions.* Langmuir : the ACS journal of surfaces and colloids, 2014. **30**(12): p. 3329-36.

237. Kaci, M., et al., *Emulsification by high frequency ultrasound using piezoelectric transducer: Formation and stability of emulsifier free emulsion.* Ultrasonics Sonochemistry, 2014. **21**(3): p. 1010-1017.

238. Qian, C. and D.J. McClements, *Formation of nanoemulsions stabilized by model food-grade emulsifiers using high-pressure homogenization: Factors affecting particle size.* Food Hydrocolloids, 2011. **25**(5): p. 1000-1008.

239. Bennet, D. and S. Kim, *A Transdermal Delivery System to Enhance Quercetin Nanoparticle Permeability.* Journal of Biomaterials Science-Polymer Edition, 2013. **24**(2): p. 185-209.

240. O'Connor, J.L., et al., *Factors Associated With Adherence Amongst 5295 People Receiving Antiretroviral Therapy as Part of an International Trial.* Journal of Infectious Diseases, 2013. **208**(1): p. 40-49.

241. Xi, J., et al., *Formulation Development and Bioavailability Evaluation of a Self-Nanoemulsified Drug Delivery System of Oleanolic Acid.* Aaps Pharmscitech, 2009. **10**(1): p. 172-182.

242. Ragelle, H., et al., *Nanoemulsion formulation of fisetin improves bioavailability and antitumour activity in mice.* International Journal of Pharmaceutics, 2012. **427**(2): p. 452-459.

243. Chhabra, G., et al., *Design and development of nanoemulsion drug delivery system of amlodipine besilate for improvement of oral bioavailability.* Drug Development and Industrial Pharmacy, 2011. **37**(8): p. 907-916.

244. Lu, Y., J. Qi, and W. Wu, *Absorption, disposition and pharmacokinetics of nanoemulsions.* Curr Drug Metab, 2012. **13**(4): p. 396-417.

245. Hurst, M. and D. Faulds, *Lopinavir.* Drugs, 2000. **60**(6): p. 1371-1379.

246. Singh, B., et al., *Development of optimized self-nano-emulsifying drug delivery systems (SNEDDS) of carvedilol with enhanced bioavailability potential.* Drug Deliv, 2011. **18**(8): p. 599-612.

247. Sun, M., et al., *Intestinal absorption and intestinal lymphatic transport of sirolimus from self-microemulsifying drug delivery systems assessed using the single-pass intestinal perfusion (SPIP) technique and a chylomicron flow blocking approach: linear correlation with oral bioavailabilities in rats.* Eur J Pharm Sci, 2011. **43**(3): p. 132-40.

248. Li, X., et al., *Development of silymarin self-microemulsifying drug delivery system with enhanced oral bioavailability.* AAPS PharmSciTech, 2010. **11**(2): p. 672-8.

249. Wu, H., et al., *Examination of lymphatic transport of puerarin in unconscious lymph duct-cannulated rats after administration in microemulsion drug delivery systems.* Eur J Pharm Sci, 2011. **42**(4): p. 348-53.

250. Dixit, A.R., S.J. Rajput, and S.G. Patel, *Preparation and bioavailability assessment of SMEDDS containing valsartan.* AAPS PharmSciTech, 2010. **11**(1): p. 314-21.

251. Thakkar, H., et al., *Formulation and characterization of lipid-based drug delivery system of raloxifene-microemulsion and self-microemulsifying drug delivery system.* J Pharm Bioallied Sci, 2011. **3**(3): p. 442-8.

252. Liu, Y., et al., *Optimization and in situ intestinal absorption of self-microemulsifying drug delivery system of oridonin.* Int J Pharm, 2009. **365**(1-2): p. 136-42.

253. Arida, A.I., M.M. Al-Tabakha, and H.A. Hamoury, *Improving the high variable bioavailability of griseofulvin by SEDDS.* Chem Pharm Bull (Tokyo), 2007. **55**(12): p. 1713-9.

254. Cui, J., et al., *Enhancement of oral absorption of curcumin by self-microemulsifying drug delivery systems.* Int J Pharm, 2009. **371**(1-2): p. 148-55.

255. Souza, V.B., et al., *Stability of Orange Oil/Water Nanoemulsions Prepared by the Pit Method.* Journal of Nanoscience and Nanotechnology, 2011. **11**(3): p. 2237-2243.

256. Piriyaprasarth, S., et al., *Effect of Coconut Oil and Surfactants on Stability of Nanoemulsions*, in *Biomaterials and Applications*, T. Tunkasiri, Editor. 2012. p. 429-432.

257. Peng, L.-C., et al., *Optimization of water-in-oil nanoemulsions by mixed surfactants.* Colloids and Surfaces a-Physicochemical and Engineering Aspects, 2010. **370**(1-3): p. 136-142.

258. Howe, A.M. and A.R. Pitt, *Rheology and stability of oil-in-water nanoemulsions stabilised by anionic surfactant and gelatin 2) addition of homologous series of sugar-based co-surfactants.* Advances in Colloid and Interface Science, 2008. **144**(1-2): p. 30-37.

259. Choi, A.-J., et al., *Effects of Surfactants on the Formation and Stability of Capsaicin-loaded Nanoemulsions.* Food Science and Biotechnology, 2009. **18**(5): p. 1161-1172.

260. Schrade, A., K. Landfester, and U. Ziener, *Pickering-type stabilized nanoparticles by heterophase polymerization.* Chemical Society Reviews, 2013. **42**(16): p. 6823-6839.

261. Cui, Y.N., M. Threlfall, and J.S. van Duijneveldt, *Optimizing organoclay stabilized Pickering emulsions.* Journal of Colloid and Interface Science, 2011. **356**(2): p. 665-671.

262. Yin, D.Z., et al., *Covalently bonded polystyrene/SiO2 microspheres via emulsion polymerisation stabilised solely by surface active Pickering stabiliser.* Materials Technology, 2013. **28**(3): p. 138-144.

263. Liu, G.P., et al., *Aqueous Dispersions of MgAl Double Hydroxide Particles of Different Forms and Stabilized Pickering Emulsions.* Chemical Journal of Chinese Universities-Chinese, 2013. **34**(2): p. 386-393.

264. Mehling, A., M. Kleber, and H. Hensen, *Comparative studies on the ocular and dermal irritation potential of surfactants.* Food and Chemical Toxicology, 2007. **45**(5): p. 747-758.

265. Heinze, J.E., P.L. Casterton, and J. Al-Atrash, *Relative eye irritation potential of nonionic surfactants: Correlation to dynamic surface tension.* Journal of Toxicology-Cutaneous and Ocular Toxicology, 1999. **18**(4): p. 359-374.

266. Hall-Manning, T.J., et al., *Skin irritation potential of mixed surfactant systems.* Food and Chemical Toxicology, 1998. **36**(3): p. 233-238.

267. Khan, I.A., et al., *A comparative study of interaction of ibuprofen with biocompatible polymers.* Colloids and Surfaces B-Biointerfaces, 2011. **88**(1): p. 72-77.

268. Moore, T.L., et al., *Multifunctional Polymer-Coated Carbon Nanotubes for Safe Drug Delivery.* Particle & Particle Systems Characterization, 2013. **30**(4): p. 365-373.

269. Schweiger, C., et al., *Novel magnetic iron oxide nanoparticles coated with poly(ethylene imine)-g-poly(ethylene glycol) for potential biomedical application: Synthesis, stability, cytotoxicity and MR imaging.* International Journal of Pharmaceutics, 2011. **408**(1-2): p. 130-137.

270. Saffer, E.M., G.N. Tew, and S.R. Bhatia, *Poly(lactic acid)-poly(ethylene oxide) Block Copolymers: New Directions in Self-Assembly and Biomedical Applications.* Current Medicinal Chemistry, 2011. **18**(36): p. 5676-5686.

271. Park, D., W. Wu, and Y. Wang, *A functionalizable reverse thermal gel based on a polyurethane/PEG block copolymer.* Biomaterials, 2011. **32**(3): p. 777-786.

272. Otsuka, H., Y. Nagasaki, and K. Kataoka, *Self-assembly of poly(ethylene glycol)-based block copolymers for biomedical applications.* Current Opinion in Colloid & Interface Science, 2001. **6**(1): p. 3-10.

273. Li, X. and X. Yuan, *Poly(ethylene glycol)-poly(lactic acid) copolymers for drug carriers.* Progress in Chemistry, 2007. **19**(6): p. 973-981.

274. Shahalom, S., et al., *Poly(DEAEMa-co-PEGMa): A new pH-responsive comb copolymer stabilizer for emulsions and dispersions.* Langmuir, 2006. **22**(20): p. 8311-8317.

275. Saigal, T., et al., *Stable emulsions with thermally responsive microstructure and rheology using poly(ethylene oxide) star polymers as emulsifiers.* Journal of Colloid and Interface Science, 2013. **394**: p. 284-292.

276. Rossi, J., et al., *Long-circulating poly(ethylene glycol)-coated emulsions to target solid tumors.* European Journal of Pharmaceutics and Biopharmaceutics, 2007. **67**(2): p. 329-338.

277. Fu, Z., et al., *Stabilization of water-in-octane nano-emulsion. II Enhanced by amphiphilic graft copolymers based on poly (higher alpha-olefin)-graft-poly(ethylene glycol).* Fuel, 2010. **89**(12): p. 3860-3865.

278. Castellanos, I.J., G. Flores, and K. Griebenow, *Effect of the molecular weight of poly(ethylene glycol) used as emulsifier on alpha-chymotrypsin stability upon encapsulation in PLGA microspheres.* Journal of Pharmacy and Pharmacology, 2005. **57**(10): p. 1261-1269.

279. Castellanos, I.J., R. Crespo, and K. Griebenow, *Poly(ethylene glycol) as stabilizer and emulsifying agent: a novel stabilization approach preventing aggregation and inactivation of proteins upon encapsulation in bioerodible polyester microspheres.* Journal of Controlled Release, 2003. **88**(1): p. 135-145.

280. Moad, G., E. Rizzardo, and S.H. Thang, *Living radical polymerization by the RAFT process.* Australian Journal of Chemistry, 2005. **58**(6): p. 379-410.

281. Hawker, C.J., et al., *Initiating systems for nitroxide-mediated "living" free radical polymerizations: Synthesis and evaluation.* Macromolecules, 1996. **29**(16): p. 5245-5254.

282. Matyjaszewski, K. and J.H. Xia, *Atom transfer radical polymerization.* Chemical Reviews, 2001. **101**(9): p. 2921-2990.

283. Lowe, A.B., *Thiol-ene "click" reactions and recent applications in polymer and materials synthesis.* Polymer Chemistry, 2010. **1**(1): p. 17-36.

284. Decker, C., *Photoinitiated crosslinking polymerisation.* Progress in Polymer Science, 1996. **21**(4): p. 593-650.

285. Liu, P., et al., *Synthesis of well-defined comb-like amphiphilic copolymers with protonizable units in the pendent chains: 1. Preparation of narrow polydispersity copolymers of methyl methacrylate and 2-hydroxyethyl methacrylate by atom-transfer radical polymerization.* Polymer International, 2004. **53**(2): p. 136-141.

286. Jiang, J., X. Lu, and Y. Lu, *Stereospecific preparation of polyacrylamide with low polydispersity by ATRP in the presence of Lewis acid.* Polymer, 2008. **49**(7): p. 1770-1776.

287. Jiang, J., X. Lu, and Y. Lu, *Preparation of carboxyl-end-group polyacrylamide with low polydispersity by ATRP initiated with chloroacetic acid.* Journal of Polymer Science Part a-Polymer Chemistry, 2007. **45**(17): p. 3956-3965.

288. Guha, S., *Dead polyacrylamide of low polydispersity from atom transfer radical polymerization of acrylamide using CuCl/Me6TREN as catalyst.* Journal of the Indian Chemical Society, 2008. **85**(1): p. 64-70.

289. Gao, H., S. Ohno, and K. Matyjaszewski, *Low polydispersity star polymers via cross-linking macromonomers by ATRP.* Journal of the American Chemical Society, 2006. **128**(47): p. 15111-15113.

290. Weaver, J.V.M. and D.J. Adams, *Synthesis and application of pH-responsive branched copolymer nanoparticles (PRBNs): a comparison with pH-responsive shell cross-linked micelles.* Soft Matter, 2010. **6**(12): p. 2575-2582.

291. Woodward, R.T., et al., *Controlling responsive emulsion properties via polymer design.* Chemical Communications, 2009(24): p. 3554-3556.

292. Weaver, J.V.M., et al., *PH-responsive branched polymer nanoparticles.* Soft Matter, 2008. **4**(5): p. 985-992.

293. Weaver, J.V.M., *pH-Responsive Polymer Nanoparticles*. Advanced Polymer Nanoparticles: Synthesis and Surface Modifications, ed. V. Mittal. 2011. 169-196.

294. Woodward, R.T., et al., *Fabrication of large volume, macroscopically defined and responsive engineered emulsions using a homogeneous pH-trigger.* Journal of Materials Chemistry, 2010. **20**(25): p. 5228-5234.

295. Woodward, R.T. and J.V.M. Weaver, *The role of responsive branched copolymer composition in controlling pH-triggered aggregation of*

*"engineered" emulsion droplets: towards selective droplet assembly.* Polymer Chemistry, 2011. **2**(2): p. 403-410.

296. Lin, I.C., et al., *Effect of polymer grafting density on silica nanoparticle toxicity.* Bioorganic & Medicinal Chemistry, 2012. **20**(23): p. 6862-6869.

297. Knetsch, M.L.W., N. Olthof, and L.H. Koole, *Polymers with tunable toxicity: A reference scale for cytotoxicity testing of biomaterial surfaces.* Journal of Biomedical Materials Research Part A, 2007. **82A**(4): p. 947-957.

298. Wang, J.S. and K. Matyjaszewski, *Controlled living radical polymerization - atom-transfer radical polymerization in the presence of transition-metal complexes.* Journal of the American Chemical Society, 1995. **117**(20): p. 5614-5615.

299. Cosmetic Ingredient Review Expert, P., *Final report of the safety assessment of methacrylic acid.* International journal of toxicology, 2005. **24 Suppl 5**: p. 33-51.

300. Kurata, S., et al., *Cytotoxic effects of acrylic acid, methacrylic acid, their corresponding saturated carboxylic acids, HEMA, and hydroquinone on fibroblasts derived from human pulp.* Dental Materials Journal, 2012. **31**(2): p. 219-225.

301. Rogers, J.G., et al., *Methacrylic-acid as a teratogen in rat embryo culture.* Teratology, 1986. **33**(1): p. 113-117.

302. Arpicco, S., et al., *Preparation and characterization of novel poly(ethylene glycol) paclitaxel derivatives.* International Journal of Pharmaceutics, 2013. **454**(2): p. 653-659.

303. Bahmani, B., et al., *Effect of polyethylene glycol coatings on uptake of indocyanine green loaded nanocapsules by human spleen macrophages in vitro.* Journal of Biomedical Optics, 2011. **16**(5).

304. Jiang, X., et al., *Nanoparticles of 2-deoxy-d-glucose functionalized poly(ethylene glycol)-co-poly(trimethylene carbonate) for dual-targeted drug delivery in glioma treatment.* Biomaterials, 2014. **35**(1): p. 518-29.

305. Kobayashi, Y., et al., *In-vivo fluorescence imaging technique using colloid solution of multiple quantum dots/silica/poly(ethylene glycol) nanoparticles.* Journal of Sol-Gel Science and Technology, 2013. **66**(1): p. 31-37.

306. Narayanan, D., et al., *Poly-(ethylene glycol) modified gelatin nanoparticles for sustained delivery of the anti-inflammatory drug Ibuprofen-Sodium: An in vitro and in vivo analysis.* Nanomedicine-Nanotechnology Biology and Medicine, 2013. **9**(6): p. 818-828.

307. Patnaik, A., et al., *Phase I dose-escalation study of EZN-2208 (PEG-SN38), a novel conjugate of poly(ethylene) glycol and SN38, administered weekly in patients with advanced cancer.* Cancer Chemotherapy and Pharmacology, 2013. **71**(6): p. 1499-1506.

308. Rodrigues, C.D., et al., *Amphotericin B-Loaded Poly(Lactide)-Poly(Ethylene Glycol)-Blend Nanoparticles: Characterization and In Vitro Efficacy and Toxicity.* Current Nanoscience, 2013. **9**(5): p. 594-598.

309. Yang, L., et al., *Novel Biodegradable Polylactide/poly(ethylene glycol) Micelles Prepared by Direct Dissolution Method for Controlled Delivery of Anticancer Drugs.* Pharmaceutical Research, 2009. **26**(10): p. 2332-2342.

310. Xu, M., et al., *Reduction/pH dual-sensitive PEGylated hyaluronan nanoparticles for targeted doxorubicin delivery.* Carbohydrate Polymers, 2013. **98**(1): p. 181-188.

311. Wei, X., et al., *Biodegradable poly(epsilon-caprolactone)-poly(ethylene glycol) copolymers as drug delivery system.* International Journal of Pharmaceutics, 2009. **381**(1): p. 1-18.

312. Veronese, F.M. and G. Pasut, *PEGylation, successful approach to drug delivery.* Drug Discovery Today, 2005. **10**(21): p. 1451-1458.

313. Shen, J., et al., *Synthesis, characterization, in vitro and in vivo evaluation of PEGylated oridonin conjugates.* International Journal of Pharmaceutics, 2013. **456**(1): p. 80-86.

314. Otsuka, H., Y. Nagasaki, and K. Kataoka, *PEGylated nanoparticles for biological and pharmaceutical applications.* Advanced Drug Delivery Reviews, 2003. **55**(3): p. 403-419.

315. Lei, Y., et al., *Anticancer drug delivery of PEG based micelles with small lipophilic moieties.* International Journal of Pharmaceutics, 2013. **453**(2): p. 579-586.

316. Kao, H.-W., et al., *A pharmacokinetics study of radiolabeled micelles of a poly(ethylene glycol)-block-poly(caprolactone) copolymer in a colon carcinoma-bearing mouse model.* Applied Radiation and Isotopes, 2013. **80**: p. 88-94.

317. Jeong, B., et al., *Biodegradable block copolymers as injectable drug-delivery systems.* Nature, 1997. **388**(6645): p. 860-862.

318. Greenwald, R.B., et al., *Effective drug delivery by PEGylated drug conjugates.* Advanced Drug Delivery Reviews, 2003. **55**(2): p. 217-250.

319. Fan, M., et al., *Preparation and invitro characterization of dexamethasone-loaded poly(d,l-lactic acid) microspheres embedded in poly(ethylene glycol)-poly(-caprolactone)-poly(ethylene glycol) hydrogel for orthopedic tissue engineering.* Journal of Biomaterials Applications, 2013. **28**(2): p. 288-297.

320. Alconcel, S.N.S., A.S. Baas, and H.D. Maynard, *FDA-approved poly(ethylene glycol)-protein conjugate drugs.* Polymer Chemistry, 2011. **2**(7): p. 1442-1448.

321. Zhang, X.-D., et al., *Size-dependent in vivo toxicity of PEG-coated gold nanoparticles.* International Journal of Nanomedicine, 2011. **6**: p. 2071-2081.

322. Wang, S., et al., *Challenge in understanding size and shape dependent toxicity of gold nanomaterials in human skin keratinocytes.* Chemical Physics Letters, 2008. **463**(1-3): p. 145-149.

323. Song, M., et al., *Size-Dependent Toxicity of Nano-C-60 Aggregates: More Sensitive Indication by Apoptosis-Related Bax Translocation in Cultured Human Cell.* Environmental Science & Technology, 2012. **46**(6): p. 3457-3464.

324. Sohaebuddin, S.K., et al., *Nanomaterial cytotoxicity is composition, size, and cell type dependent.* Particle and Fibre Toxicology, 2010. **7**.

325. Oh, W.-K., et al., *Shape-Dependent Cytotoxicity of Polyaniline Nanomaterials in Human Fibroblast Cells.* Journal of Nanoscience and Nanotechnology, 2011. **11**(5): p. 4254-4260.

326. Inoue, K., et al., *Size effects of nanomaterials on lung inflammation and coagulatory disturbance.* International Journal of Immunopathology and Pharmacology, 2008. **21**(1): p. 197-206.

327. Fifis, T., et al., *Size-dependent immunogenicity: Therapeutic and protective properties of nano-vaccines against tumors.* Journal of Immunology, 2004. **173**(5): p. 3148-3154.

328. Park, J., et al., *Size dependent macrophage responses and toxicological effects of Ag nanoparticles.* Chemical Communications, 2011. **47**(15): p. 4382-4384.

329. Oh, W.-K., et al., *Cellular Uptake, Cytotoxicity, and Innate Immune Response of Silica - Titania Hollow Nanoparticles Based on Size and Surface Functionality.* Acs Nano, 2010. **4**(9): p. 5301-5313.

330. Ma, X., et al., *Gold Nanoparticles Induce Autophagosome Accumulation through Size-Dependent Nanoparticle Uptake and Lysosome Impairment.* Acs Nano, 2011. **5**(11): p. 8629-8639.

331. Herd, H., et al., *Nanoparticle Geometry and Surface Orientation Influence Mode of Cellular Uptake.* Acs Nano, 2013. **7**(3): p. 1961-1973.

332. Rancan, F., et al., *Skin Penetration and Cellular Uptake of Amorphous Silica Nanoparticles with Variable Size, Surface Functionalization, and Colloidal Stability.* Acs Nano, 2012. **6**(8): p. 6829-6842.

333. Zhang, W., et al., *Adsorption of hematite nanoparticles onto Caco-2 cells and the cellular impairments: effect of particle size.* Nanotechnology, 2010. **21**(35): p. 9.

334. Pinnamaneni, S., N.G. Das, and S.K. Das, *Comparison of oil-in-water emulsions manufactured by microfluidization and homogenization.* Pharmazie, 2003. **58**(8): p. 554-558.

335. Marquez, P.L., G.G. Palazolo, and J.R. Wagner, *Cream-like emulsions prepared with soybean milk: Effect of controlled stirring on rheological behaviour.* Grasas Y Aceites, 2005. **56**(2): p. 89-95.

336. Jafari, S.M., Y.H. He, and B. Bhandari, *Nano-emulsion production by sonication and microfluidization - A comparison.* International Journal of Food Properties, 2006. **9**(3): p. 475-485.

337. Burapapadh, K., H. Takeuchi, and P. Sriamornsak, *Pectin-Based Nano-Sized Emulsions Prepared by High-Pressure Homogenization*, in *Biomaterials and Applications*, T. Tunkasiri, Editor. 2012, Trans Tech Publications Ltd: Stafa-Zurich. p. 286-289.

338. Lai, M.K. and R.C.C. Tsiang, *Microencapsulation of acetaminophen into poly(L-lactide) by three different emulsion solvent-evaporation methods.* Journal of Microencapsulation, 2005. **22**(3): p. 261-274.

339. Johnson, W., *Final report on the safety assessment of ricinus communis (castor) seed oil, hydrogenated castor oil, glyceryl ricinoleate, glyceryl ricinoleate SE, ricinoleic acid, potassium ricinoleate, sodium ricinoleate, zinc ricinoleate, cetyl ricinoleate, ethyl ricinoleate, glycol ricinoleate,*

*isopropyl ricinoleate, methyl ricinoleate, and octyldodecyl ricinoleate.* International Journal of Toxicology, 2007. **26**: p. 31-77.

340. Riemenschneider, W. and H.M. Bolt, *Esters, Organic*, in *Ullmann's Encyclopedia of Industrial Chemistry*. 2000, Wiley-VCH Verlag GmbH & Co. KGaA.

341. Pietroiusti, A., L. Campagnolo, and B. Fadeel, *Interactions of Engineered Nanoparticles with Organs Protected by Internal Biological Barriers.* Small, 2013. **9**(9-10): p. 1557-1572.

342. Coyuco, J.C., et al., *Functionalized carbon nanomaterials: exploring the interactions with Caco-2 cells for potential oral drug delivery.* International Journal of Nanomedicine, 2011. **6**: p. 2253-2263.

343. Wick, P., et al., *Barrier Capacity of Human Placenta for Nanosized Materials.* Environmental Health Perspectives, 2010. **118**(3): p. 432-436.

344. Ragnaill, M.N., et al., *Internal benchmarking of a human blood-brain barrier cell model for screening of nanoparticle uptake and transcytosis.* European Journal of Pharmaceutics and Biopharmaceutics, 2011. **77**(3): p. 360-367.

345. Syed, S., A. Zubair, and M. Frieri, *Immune Response to Nanomaterials: Implications for Medicine and Literature Review.* Current Allergy and Asthma Reports, 2013. **13**(1): p. 50-57.

346. Moghimi, S.M. and Z.S. Farhangrazi, *Nanomedicine and the complement paradigm.* Nanomedicine-Nanotechnology Biology and Medicine, 2013. **9**(4): p. 458-460.

347. Mizrahy, S., et al., *Hyaluronan-coated nanoparticles: The influence of the molecular weight on CD44-hyaluronan interactions and on the immune response.* Journal of Controlled Release, 2011. **156**(2): p. 231-238.

348. Mayer, A., et al., *The role of nanoparticle size in hemocompatibility.* Toxicology, 2009. **258**(2-3): p. 139-147.

349. Landesman-Milo, D. and D. Peer, *Altering the immune response with lipid-based nanoparticles.* Journal of Controlled Release, 2012. **161**(2): p. 600-608.

350. Kim, H.G., et al., *Pluronic nanoparticles do not modulate immune responses mounted by macrophages.* Macromolecular Research, 2013. **21**(12): p. 1355-1359.

351. Dobrovolskaia, M.A. and S.E. McNeil, *Immunological properties of engineered nanomaterials.* Nature Nanotechnology, 2007. **2**(8): p. 469-478.

352. Dobrovolskaia, M.A., et al., *Preclinical studies to understand nanoparticle interaction with the immune system and its potential effects on nanoparticle biodistribution.* Molecular Pharmaceutics, 2008. **5**(4): p. 487-495.

353. Pierige, F., et al., *Cell-based drug delivery.* Advanced Drug Delivery Reviews, 2008. **60**(2): p. 286-295.

354. Moghimi, S.M., A.C. Hunter, and J.C. Murray, *Nanomedicine: current status and future prospects.* Faseb Journal, 2005. **19**(3): p. 311-330.

355. Mukonzo, J.K., et al., *HIV/AIDS Patients Display Lower Relative Bioavailability of Efavirenz than Healthy Subjects.* Clinical Pharmacokinetics, 2011. **50**(8): p. 531-540.

356. Desai, M.P., et al., *The mechanism of uptake of biodegradable microparticles in Caco-2 cells is size dependent.* Pharmaceutical Research, 1997. **14**(11): p. 1568-1573.

357. Sonavane, G., et al., *In vitro permeation of gold nanoparticles through rat skin and rat intestine: Effect of particle size.* Colloids and Surfaces B-Biointerfaces, 2008. **65**(1): p. 1-10.

358. Ye, D., et al., *Nanoparticle accumulation and transcytosis in brain endothelial cell layers.* Nanoscale, 2013. **5**(22): p. 11153-11165.

359. Sahay, G., D.Y. Alakhova, and A.V. Kabanov, *Endocytosis of nanomedicines.* Journal of Controlled Release, 2010. **145**(3): p. 182-195.

360. Akinc, A. and G. Battaglia, *Exploiting endocytosis for nanomedicines.* Cold Spring Harbor perspectives in biology, 2013. **5**(11).

361. Banerjee, A., A. Berezhkovskii, and R. Nossal, *On the Size Dependence of Cellular Uptake of Nanoparticle via Clathrin-Mediated Endocytosis.* Biophysical Journal, 2013. **104**(2, Supplement 1): p. 622a.

362. Vacha, R., F.J. Martinez-Veracoechea, and D. Frenkel, *Receptor-Mediated Endocytosis of Nanoparticles of Various Shapes.* Nano Letters, 2011. **11**(12): p. 5391-5395.

363. Panyam, J. and V. Labhasetwar, *Dynamics of endocytosis and exocytosis of poly(D,L-lactide-co-glycolide) nanoparticles in vascular smooth muscle cells.* Pharmaceutical Research, 2003. **20**(2): p. 212-220.

364. Li, Y., et al., *Molecular modeling of the relationship between nanoparticle shape anisotropy and endocytosis kinetics.* Biomaterials, 2012. **33**(19): p. 4965-4973.

365. Kim, J.-S., et al., *Cellular uptake of magnetic nanoparticle is mediated through energy-dependent endocytosis in A549 cells.* Journal of Veterinary Science, 2006. **7**(4): p. 321-326.

366. Huang, C., et al., *Role of nanoparticle geometry in endocytosis: laying down to stand up.* Nano letters, 2013. **13**(9): p. 4546-50.

367. Delmas, T., et al., *How To Prepare and Stabilize Very Small Nanoemulsions.* Langmuir, 2011. **27**(5): p. 1683-1692.

368. Shakeel, F., et al., *Accelerated stability testing of celecoxib nanoemulsion containing Cremophor-EL.* African Journal of Pharmacy and Pharmacology, 2008. **2**(8): p. 179-183.

369. Voorhees, P.W., *The theory of ostwald ripening.* Journal of Statistical Physics, 1985. **38**(1-2): p. 231-252.

370. Clogston, J.D. and A.K. Patri, *Zeta potential measurement.* Methods Mol Biol, 2011. **697**: p. 63-70.

371. Romer, I., et al., *Aggregation and dispersion of silver nanoparticles in exposure media for aquatic toxicity tests.* Journal of Chromatography A, 2011. **1218**(27): p. 4226-4233.

372. Pavlin, M. and V.B. Bregar, *Stability of nanoparticle suspensions in different biologically relevant media.* Digest Journal of Nanomaterials and Biostructures, 2012. **7**(4): p. 1389-1400.

373. Stebounova, L.V., E. Guio, and V.H. Grassian, *Silver nanoparticles in simulated biological media: a study of aggregation, sedimentation, and dissolution.* Journal of Nanoparticle Research, 2011. **13**(1): p. 233-244.

374. Velikov, K.P., et al., *Effect of the surfactant concentration on the kinetic stability of thin foam and emulsion films.* Journal of the Chemical Society-Faraday Transactions, 1997. **93**(11): p. 2069-2075.

375. Helgason, T., et al., *Effect of surfactant surface coverage on formation of solid lipid nanoparticles (SLN).* Journal of Colloid and Interface Science, 2009. **334**(1): p. 75-81.

376. Adeyeye, C.M. and J.C. Price, *Effect of nonionic surfactant concentration and type on the formation and stability of w/o/w multiple emulsions - microscopic and conductometric evaluations.* Drug Development and Industrial Pharmacy, 1991. **17**(5): p. 725-736.

377. Standing, J.F. and C. Tuleu, *Paediatric formulations - Getting to the heart of the problem.* International Journal of Pharmaceutics, 2005. **300**(1-2): p. 56-66.

378. Nahata, M.C. and L.V. Allen, *Extemporaneous Drug Formulations.* Clinical Therapeutics, 2008. **30**(11): p. 2112-2119.

379. Brion, F., A.J. Nunn, and A. Rieutord, *Extemporaneous (magistral) preparation of oral medicines for children in European hospitals.* Acta Paediatrica, 2003. **92**(4): p. 486-490.

380. Best, B.M., et al., *Pharmacokinetics of Lopinavir/Ritonavir Crushed Versus Whole Tablets in Children.* Jaids-Journal of Acquired Immune Deficiency Syndromes, 2011. **58**(4): p. 385-391.

381. Jain, S., et al., *Surface-stabilized lopinavir nanoparticles enhance oral bioavailability without coadministration of ritonavir.* Nanomedicine (London, England), 2013. **8**(10): p. 1639-55.

382. Madhavi, B.B., et al., *Dissolution enhancement of efavirenz by solid dispersion and PEGylation techniques.* International journal of pharmaceutical investigation, 2011. **1**(1): p. 29-34.

383. Sathigari, S., et al., *Physicochemical Characterization of Efavirenz-Cyclodextrin Inclusion Complexes.* Aaps Pharmscitech, 2009. **10**(1): p. 81-87.

384. Krampe, B. and M. Al-Rubeai, *Cell death in mammalian cell culture: molecular mechanisms and cell line engineering strategies.* Cytotechnology, 2010. **62**(3): p. 175-188.

385. Mendonca, R.Z., S.J. Arrozio, and M.M. Antoniazzi, *Morphological characterization of vero cell death induced by nutrient depletion.* Acta Microscopica, 2009. **18**(3): p. 204-219.

386. Sheridan, J.W. and R.J. Simmons, *Studies on a human-melanoma cell-line - effect of cell crowding and nutrient depletion on the biophysical and kinetic characteristics of the cells.* Journal of Cellular Physiology, 1981. **107**(1): p. 85-100.

387. Tracqui, P., et al., *Global analysis of endothelial cell line proliferation patterns based on nutrient-depletion models: implications for a standardization of cell proliferation assays.* Cell Proliferation, 2005. **38**(3): p. 119-135.

388. Yu, H.L. and Q.R. Huang, *Investigation of the cytotoxicity of food-grade nanoemulsions in Caco-2 cell monolayers and HepG2 cells.* Food Chemistry, 2013. **141**(1): p. 29-33.

389. Yang, H., et al., *In Vitro Study of Silica Nanoparticle-Induced Cytotoxicity Based on Real-Time Cell Electronic Sensing System.* Journal of Nanoscience and Nanotechnology, 2010. **10**(1): p. 561-568.

390. Thomassen, L.C.J., et al., *Synthesis and Characterization of Stable Monodisperse Silica Nanoparticle Sols for in Vitro Cytotoxicity Testing.* Langmuir, 2010. **26**(1): p. 328-335.

391. Studer, A.M., et al., *Nanoparticle cytotoxicity depends on intracellular solubility: Comparison of stabilized copper metal and degradable copper oxide nanoparticles.* Toxicology Letters, 2010. **197**(3): p. 169-174.

392. Mukherjee, S.G., et al., *Comparative in vitro cytotoxicity study of silver nanoparticle on two mammalian cell lines.* Toxicology in Vitro, 2012. **26**(2): p. 238-251.

393. Svirskis, D., M. Toh, and S. Ram, *The use of ethanol in paediatric formulations in New Zealand.* European Journal of Pediatrics, 2013. **172**(7): p. 919-926.

394. Marquis, J., et al., *Swallowing difficulties with oral drugs among polypharmacy patients attending community pharmacies.* International Journal of Clinical Pharmacy, 2013. **35**(6): p. 1130-1136.

395. Schiele, J.T., et al., *Difficulties swallowing solid oral dosage forms in a general practice population: prevalence, causes, and relationship to dosage forms.* European Journal of Clinical Pharmacology, 2013. **69**(4): p. 937-948.

396. Park, B.K., et al., *The role of metabolic activation in drug-induced hepatotoxicity*, in *Annual Review of Pharmacology and Toxicology*. 2005, Annual Reviews: Palo Alto. p. 177-202.

397. Decloedt, E.H. and G. Maartens, *Neuronal toxicity of efavirenz: a systematic review.* Expert Opinion on Drug Safety, 2013. **12**(6): p. 841-846.

398. Elsby, R., et al., *Validation and application of Caco-2 assays for the in vitro evaluation of development candidate drugs as substrates or inhibitors of P-glycoprotein to support regulatory submissions.* Xenobiotica, 2008. **38**(7-8): p. 1140-1164.

399. Agarwal, S., D. Pal, and A.K. Mitra, *Both P-gp and MRP2 mediate transport of Lopinavir, a protease inhibitor.* International Journal of Pharmaceutics, 2007. **339**(1-2): p. 139-147.

400. Yee, S., *In vitro permeability across Caco-2 cells (colonic) can predict in vivo (small intestinal) absorption in man--fact or myth.* Pharm Res, 1997. **14**(6): p. 763-6.

401. Wang, M., et al., *Permeability of Exendin-4-Loaded Chitosan Nanoparticles across MDCK Cell Mono layers and Rat Small Intestine.* Biological & Pharmaceutical Bulletin, 2014. **37**(5): p. 740-747.

402. Kim, J.-E., et al., *Emulsion-based colloidal nanosystems for oral delivery of doxorubicin: Improved intestinal paracellular absorption and alleviated cardiotoxicity.* International Journal of Pharmaceutics, 2014. **464**(1-2): p. 117-126.

403. Guri, A., I. Guelseren, and M. Corredig, *Utilization of solid lipid nanoparticles for enhanced delivery of curcumin in cocultures of HT29-MTX and Caco-2 cells.* Food & Function, 2013. **4**(9): p. 1410-1419.

404. Foraker, A.B., et al., *Microfabricated porous silicon particles enhance paracellular delivery of insulin across intestinal Caco-2 cell monolayers.* Pharmaceutical Research, 2003. **20**(1): p. 110-116.

405. Choudhury, H., et al., *Improvement of cellular uptake, in vitro antitumor activity and sustained release profile with increased bioavailability from a nanoemulsion platform.* International Journal of Pharmaceutics, 2014. **460**(1-2): p. 131-143.

406. Moura, J.A., et al., *Novel formulation of a methotrexate derivative with a lipid nanoemulsion.* International Journal of Nanomedicine, 2011. **6**: p. 2285-2295.

407. Bali, V., M. Ali, and J. Ali, *Novel nanoemulsion for minimizing variations in bioavailability of ezetimibe.* Journal of Drug Targeting, 2010. **18**(7): p. 506-519.

408. van de Kerkhof, E.G., I.A.M. de Graaf, and G.M.M. Groothuis, *In vitro methods to study intestinal drug metabolism.* Current Drug Metabolism, 2007. **8**(7): p. 658-675.

409. Lau, Y.Y., et al., *Evaluation of a novel in vitro caco-2 hepatocyte hybrid system for predicting in vivo oral bioavailability.* Drug Metabolism and Disposition, 2004. **32**(9): p. 937-942.

410. Kasim, N.A., et al., *Molecular properties of WHO essential drugs and provisional biopharmaceutical classification.* Molecular Pharmaceutics, 2004. **1**(1): p. 85-96.

411. Takano, R., et al., *Oral absorption of poorly water-soluble drugs: Computer simulation of fraction absorbed in humans from a miniscale dissolution test.* Pharmaceutical Research, 2006. **23**(6): p. 1144-1156.

412. Janneh, O., et al., *Intracellular accumulation of efavirenz and nevirapine is independent of P-glycoprotein activity in cultured CD4 T cells and primary human lymphocytes.* Journal of Antimicrobial Chemotherapy, 2009. **64**(5): p. 1002-1007.

413. Fellay, J., et al., *Response to antiretroviral treatment in HIV-1-infected individuals with allelic variants of the multidrug resistance transporter 1: A pharmacogenetics study.* Lancet, 2002. **359**(9300): p. 30-36.

414. Mukonzo, J.K., et al., *A novel polymorphism in ABCB1 gene, CYP2B6*6 and sex predict single-dose efavirenz population pharmacokinetics in Ugandans.* British Journal of Clinical Pharmacology, 2009. **68**(5): p. 690-699.

415. Nasi, M., et al., *MDR1 C3435T genetic polymorphism does not influence the response to antiretroviral therapy in drug-naive HIV-positive patients.* AIDS, 2003. **17**(11): p. 1696-1698.

416. Winzer, R., et al., *No influence of the P-glycoprotein genotype (MDR1 C3435T) on plasma levels of lopinavir and efavirenz during antiretroviral treatment.* European journal of medical research, 2003. **8**(12): p. 531-534.

417. Charkoftaki, G., G. Valsami, and P. Macheras, *From Supersaturated Drug Delivery Systems to the Rising Era of Pediatric Formulations.* Chemical and Biochemical Engineering Quarterly, 2012. **26**(4): p. 427-434.

418. Walsh, J., et al., *Delivery devices for the administration of paediatric formulations: Overview of current practice, challenges and recent developments.* International Journal of Pharmaceutics, 2011. **415**(1-2): p. 221-231.

419. Chiappetta, D.A., C. Hocht, and A. Sosnik, *A Highly Concentrated and Taste-Improved Aqueous Formulation of Efavirenz for a More Appropriate Pediatric Management of the Anti-HIV Therapy.* Current Hiv Research, 2010. **8**(3): p. 223-231.

420. Donato, E.M., et al., *Development and validation of dissolution test for lopinavir, a poorly water-soluble drug, in soft gel capsules, based on in vivo data.* Journal of Pharmaceutical and Biomedical Analysis, 2008. **47**(3): p. 547-552.

421. Rosenberg, J.M., J.P. Nathan, and F. Plakogiannis, *Weight variability of pharmacist-dispensed split tablets.* Journal of the American Pharmaceutical Association (Washington,D.C. : 1996), 2002. **42**(2): p. 200-205.

422. Teng, J., et al., *Lack of medication dose uniformity in commonly split tablets.* Journal of the American Pharmaceutical Association (Washington,D.C. : 1996), 2002. **42**(2): p. 195-199.

423. Kujawski, J., et al., *Prediction of log P: ALOGPS Application in Medicinal Chemistry Education.* Journal of Chemical Education, 2012. **89**(1): p. 64-67.

424. Han, C., et al., *Hydrogenated castor oil nanoparticles as carriers for the subcutaneous administration of tilmicosin: in vitro and in vivo studies.* Journal of Veterinary Pharmacology and Therapeutics, 2009. **32**(2): p. 116-123.

425. Shelke, N.B., et al., *Development of transdermal drug-delivery films with castor-oil-based polyurethanes.* Journal of Applied Polymer Science, 2007. **103**(2): p. 779-788.

426. Xie, S., et al., *Formulation, characterization and pharmacokinetics of praziquantel-loaded hydrogenated castor oil solid lipid nanoparticles.* Nanomedicine, 2010. **5**(5): p. 693-701.

427. Ogburn, E.T., et al., *Efavirenz Primary and Secondary Metabolism In Vitro and In Vivo: Identification of Novel Metabolic Pathways and Cytochrome P450 2A6 as the Principal Catalyst of Efavirenz 7-Hydroxylation.* Drug Metabolism and Disposition, 2010. **38**(7): p. 1218-1229.

428. Desta, Z., et al., *Impact of CYP2B6 polymorphism on hepatic efavirenz metabolism in vitro.* Pharmacogenomics, 2007. **8**(6): p. 547-558.

429. Mutlib, A.E., et al., *Identification and characterization of efavirenz metabolites by liquid chromatography/mass spectrometry and high field NMR: species differences in the metabolism of efavirenz.* Drug Metab Dispos, 1999. **27**(11): p. 1319-33.

430. Ward, B.A., et al., *The Cytochrome P450 2B6 (CYP2B6) Is the Main Catalyst of Efavirenz Primary and Secondary Metabolism: Implication for HIV/AIDS Therapy and Utility of Efavirenz as a Substrate Marker of CYP2B6 Catalytic Activity.* Journal of Pharmacology and Experimental Therapeutics, 2003. **306**(1): p. 287-300.

431. Hart, S.N., et al., *A Comparison of Whole Genome Gene Expression Profiles of HepaRG Cells and HepG2 Cells to Primary Human Hepatocytes and Human Liver Tissues.* Drug Metabolism and Disposition, 2010. **38**(6): p. 988-994.

432. Jetten, M.J.A., et al., *Baseline and genotoxic compound induced gene expression profiles in HepG2 and HepaRG compared to primary human hepatocytes.* Toxicology in Vitro, 2013. **27**(7): p. 2031-2040.

433. Wilkening, S., F. Stahl, and A. Bader, *Comparison of primary human hepatocytes and hepatoma cell line HEPG2 with regard to their biotransformation properties.* Drug Metabolism and Disposition, 2003. **31**(8): p. 1035-1042.

434. Guo, L., et al., *Similarities and Differences in the Expression of Drug-Metabolizing Enzymes between Human Hepatic Cell Lines and Primary Human Hepatocytes.* Drug Metabolism and Disposition, 2011. **39**(3): p. 528-538.

435. Cavalcante, G.I.T., et al., *Implications of efavirenz for neuropsychiatry: a review.* The International Journal Of Neuroscience, 2010. **120**(12): p. 739-745.

436. Santos, H.A., et al., *Thermodynamic analysis of binding between drugs and glycosaminoglycans by isothermal titration calorimetry and fluorescence spectroscopy.* European Journal of Pharmaceutical Sciences, 2007. **32**(2): p. 105-114.

437. Babu, A., et al., *Gelatin Nanocarrier Enables Efficient Delivery and Phototoxicity of Hypocrellin B Against a Mice Tumour Model.* Journal of Biomedical Nanotechnology, 2012. **8**(1): p. 43-56.

438. Manandhar, K.D., et al., *Nanonization increases the antileishmanial efficacy of amphotericin B: an ex vivo approach.* Advances in experimental medicine and biology, 2014. **808**: p. 77-91.

439. Senkiv, Y., et al., *Enhanced Anticancer Activity and Circumvention of Resistance Mechanisms by Novel Polymeric/Phospholipidic Nanocarriers of Doxorubicin.* Journal of Biomedical Nanotechnology, 2014. **10**(7): p. 1369-1381.

440. Wang, H., et al., *Nanoparticle formulations of decoquinate increase antimalarial efficacy against liver stage Plasmodium infections in mice.*

Nanomedicine-Nanotechnology Biology and Medicine, 2014. **10**(1): p. 57-65.

441. Zykova, M.G., et al., *Influence of doxorubicin inclusion into phospholipid nanoformulation on its antitumor activity in mice: Increased efficiency for resistant tumor model.* Experimental Oncology, 2012. **34**(4): p. 323-326.

442. Adkins, J.C. and S. Noble, *Efavirenz.* Drugs, 1998. **56**(6): p. 1055-1064.

443. Baltch, A.L., et al., *Antibacterial activities of gemifloxacin, levofloxacin, gatifloxacin, moxifloxacin and erythromycin against intracellular Legionella pneumophila and Legionella micdadei in human monocytes.* Journal of Antimicrobial Chemotherapy, 2005. **56**(1): p. 104-109.

444. Hammerschlag, M.R., P.M. Roblin, and C.M. Bebear, *Activity of telithromycin, a new ketolide antibacterial, against atypical and intracellular respiratory tract pathogens.* Journal of Antimicrobial Chemotherapy, 2001. **48**: p. 25-31.

445. Heffeter, P., et al., *Intracellular protein binding patterns of the anticancer ruthenium drugs KP1019 and KP1339.* Journal of Biological Inorganic Chemistry, 2010. **15**(5): p. 737-748.

446. De Clercq, E., *The role of non-nucleoside reverse transcriptase inhibitors (NNRTIs) in the therapy of HIV-1 infection.* Antiviral Research, 1998. **38**(3): p. 153-179.

447. Spearman, P., et al., *Identification of human-immunodeficiency-virus type-1 gag protein domains essential to membrane-binding and particle assembly.* Journal of Virology, 1994. **68**(5): p. 3232-3242.

448. Quillent, C., et al., *Extensive regions of pol are required for efficient human immunodeficiency virus polyprotein processing and particle maturation.* Virology, 1996. **219**(1): p. 29-36.

449. Konnyu, B., et al., *Gag-Pol Processing during HIV-1 Virion Maturation: A Systems Biology Approach.* Plos Computational Biology, 2013. **9**(6): p. 15.

450. Miró, Ò., et al., *Mitochondrial Effects of HIV Infection on the Peripheral Blood Mononuclear Cells of HIV-Infected Patients Who Were Never Treated with Antiretrovirals.* Clinical Infectious Diseases, 2004. **39**(5): p. 710-716.

451. Hazen, R., et al., *In Vitro Antiviral Activity of the Novel, Tyrosyl-Based Human Immunodeficiency Virus (HIV) Type 1 Protease Inhibitor Brecanavir (GW640385) in Combination with Other Antiretrovirals and against a Panel of Protease Inhibitor-Resistant HIV.* Antimicrobial Agents and Chemotherapy, 2007. **51**(9): p. 3147-3154.

452. Jerobin, J., et al., *Biodegradable polymer based encapsulation of neem oil nanoemulsion for controlled release of Aza-A.* Carbohydrate Polymers, 2012. **90**(4): p. 1750-1756.

453. Macedo, A.S., et al., *Nanoemulsions for delivery of flavonoids: formulation and in vitro release of rutin as model drug.* Pharmaceutical Development and Technology, 2014. **19**(6): p. 677-680.

454. Morais, J.M. and D.J. Burgess, *Micro-and Nanoemulsions (Controlled Release Parenteral Drug Delivery Systems)*, in *Long Acting Injections and Implants*, J.C. Wright and D.J. Burgess, Editors. 2012. p. 221-238.

455. das Neves, J., et al., *Polymeric Nanoparticles Affect the Intracellular Delivery, Antiretroviral Activity and Cytotoxicity of the Microbicide Drug Candidate Dapivirine.* Pharmaceutical Research, 2012. **29**(6): p. 1468-1484.

456. Balkundi, S., et al., *Comparative manufacture and cell-based delivery of antiretroviral nanoformulations.* International Journal of Nanomedicine, 2011. **6**: p. 3393-3404.

457. Dobrovolskaia, M.A. and S.E. McNeil, *Understanding the correlation between in vitro and in vivo immunotoxicity tests for nanomedicines.* Journal of Controlled Release, 2013. **172**(2): p. 456-466.

458. FDA. *Nanotechnology Fact Sheet*. 2014 26/6/2014 [cited 2014 July 21st]; Available from: http://www.fda.gov/ScienceResearch/SpecialTopics/Nanotechnology/ucm402230.htm.

459. MHRA. *How we regulate nanotechnology*. 2013 [cited 21/7/2014]; Available from: http://www.mhra.gov.uk/Howweregulate/Nanotechnology/.

460. Dobrovoiskaia, M.A., et al., *Method for analysis of nanoparticle hemolytic properties in vitro.* Nano Letters, 2008. **8**(8): p. 2180-2187.

461. Manke, A., L. Wang, and Y. Rojanasakul, *Mechanisms of Nanoparticle-Induced Oxidative Stress and Toxicity.* Biomed Research International, 2013.

462. Kucki, M., C. Cavelius, and A. Kraegeloh, *Interference of silica nanoparticles with the traditional Limulus amebocyte lysate gel clot assay.* Innate Immunity, 2014. **20**(3): p. 327-336.

463. Dobrovolskaia, M.A., D.R. Germolec, and J.L. Weaver, *Evaluation of nanoparticle immunotoxicity.* Nature Nanotechnology, 2009. **4**(7): p. 411-414.

464. Liu, X., et al., *Targeted removal of bioavailable metal as a detoxification strategy for carbon nanotubes.* Carbon, 2008. **46**(3): p. 489-500.

465. Inoue, K.-i., *Promoting effects of nanoparticles/materials on sensitive lung inflammatory diseases.* Environmental Health and Preventive Medicine, 2011. **16**(3): p. 139-143.

466. Lin, I.C. and C.D. Kuo, *Pro-inflammatory effects of commercial alpha-lactalbumin on RAW 264.7 macrophages is due to endotoxin contamination.* Food and Chemical Toxicology, 2010. **48**(10): p. 2642-2649.

467. Brown, A., et al., *In vitro modeling of the HIV-macrophage reservoir.* Journal of Leukocyte Biology, 2006. **80**(5): p. 1127-1135.

468. Shehu-Xhilaga, M., et al., *Antiretroviral compounds: Mechanisms underlying failure of HAART to eradicate HIV-1.* Current Medicinal Chemistry, 2005. **12**(15): p. 1705-1719.

469. Devi, K.V. and R.S. Pai, *Antiretrovirals: Need for an effective drug delivery.* Indian Journal of Pharmaceutical Sciences, 2006. **68**(1): p. 1-6.

470. Martinez, F.O., et al., *Macrophage activation and polarization.* Frontiers in Bioscience-Landmark, 2008. **13**: p. 453-461.

471. Mantovani, A., et al., *Macrophage polarization: tumor-associated macrophages as a paradigm for polarized M2 mononuclear phagocytes.* Trends in Immunology, 2002. **23**(11): p. 549-555.

472. Mills, C.D., *M1 and M2 Macrophages: Oracles of Health and Disease.* Crit Rev Immunol, 2012. **32**(6): p. 463-88.

473. Jain, N.K., V. Mishra, and N.K. Mehra, *Targeted drug delivery to macrophages.* Expert Opinion on Drug Delivery, 2013. **10**(3): p. 353-367.

474. Abbas, A.K., K.M. Murphy, and A. Sher, *Functional diversity of helper T lymphocytes.* Nature, 1996. **383**(6603): p. 787-793.

475. Luckheeram, R.V., et al., *CD4(+)T Cells: Differentiation and Functions.* Clinical & Developmental Immunology, 2012: p. 12.

476. Ramanathan, S., et al., *Cytokine Synergy in Antigen-Independent Activation and Priming of Naive CD8(+) T Lymphocytes.* Critical Reviews in Immunology, 2009. **29**(3): p. 219-239.

477. Dong, C. and R.A. Flavell, *Th1 and Th2 cells.* Current Opinion in Hematology, 2001. **8**(1): p. 47-51.

478. Mosmann, T.R. and R.L. Coffman, *Th1-cell and Th2-cell - different patterns of lymphokine secretion lead to different functional-properties.* Annual Review of Immunology, 1989. **7**: p. 145-173.

479. Fallarini, S., et al., *Factors affecting T cell responses induced by fully synthetic glyco-gold-nanoparticles.* Nanoscale, 2013. **5**(1): p. 390-400.

480. Huang, L., et al., *Engineering DNA Nanoparticles as Immunomodulatory Reagents that Activate Regulatory T Cells.* Journal of Immunology, 2012. **188**(10): p. 4913-4920.

481. Schanen, B.C., et al., *Immunomodulation and T Helper TH1/TH2 Response Polarization by CeO2 and TiO2 Nanoparticles.* Plos One, 2013. **8**(5).

482. Shen, C.-C., et al., *Iron oxide nanoparticles suppressed T helper 1 cell-mediated immunity in a murine model of delayed-type hypersensitivity.* International Journal of Nanomedicine, 2012. **7**: p. 2729-2737.

483. Saez-Cirion, A., et al., *Heterogeneity in HIV Suppression by CD8 T Cells from HIV Controllers: Association with Gag-Specific CD8 T Cell Responses.* Journal of Immunology, 2009. **182**(12): p. 7828-7837.

484. Blackbourn, D.J., et al., *Suppression of HIV replication by lymphoid tissue CD8(+) cells correlates with the clinical state of HIV-infected individuals.* Proceedings of the National Academy of Sciences of the United States of America, 1996. **93**(23): p. 13125-13130.

485. Lafeuillade, A., et al., *Diffusion of HIV-1 Protease inhibitors in sanctuary sites: Implications for therapy.* Abstracts of the Interscience Conference on Antimicrobial Agents and Chemotherapy, 2001. **41**: p. 329.

486. Iglesias-Ussel, M.D. and F. Romerio, *HIV Reservoirs: The New Frontier.* Aids Reviews, 2011. **13**(1): p. 13-29.

487. Ramreddy, S., P. Kandadi, and K. Veerabrahma, *Formulation and pharmacokinetics of diclofenac lipid nanoemulsions for parenteral application.* PDA journal of pharmaceutical science and technology / PDA, 2012. **66**(1): p. 28-37.

488. Muller, R.H., D. Harden, and C.M. Keck, *Development of industrially feasible concentrated 30% and 40% nanoemulsions for intravenous drug delivery.* Drug Development and Industrial Pharmacy, 2012. **38**(4): p. 420-430.

489. Dhaliwal, G., P.A. Cornett, and L.M. Tierney, Jr., *Hemolytic anemia.* American Family Physician, 2004. **69**(11): p. 2599-2606.

490. Lim, S.K., *Consequences of haemolysis without haptoglobin.* Redox Report, 2001. **6**(6): p. 375-378.

491. Kim, D., et al., *Interaction of PLGA nanoparticles with human blood constituents.* Colloids Surf B Biointerfaces, 2005. **40**(2): p. 83-91.

492. Lin, Y.-S. and C.L. Haynes, *Impacts of Mesoporous Silica Nanoparticle Size, Pore Ordering, and Pore Integrity on Hemolytic Activity.* Journal of the American Chemical Society, 2010. **132**(13): p. 4834-4842.

493. Esmon, C.T., J. Xu, and F. Lupu, *Innate immunity and coagulation.* Journal of Thrombosis and Haemostasis, 2011. **9**: p. 182-188.

494. Chung, I. and G.Y.H. Lip, *Virchow's triad revisited: Blood constituents.* Pathophysiology of Haemostasis and Thrombosis, 2003. **33**(5-6): p. 449-454.

495. Liu, X. and J. Sun, *Time-Course Effects of Intravenously Administrated Silica Nanoparticles on Blood Coagulation and Endothelial Function in Rats.* Journal of Nanoscience and Nanotechnology, 2013. **13**(1): p. 222-228.

496. Oslakovic, C., et al., *Polystyrene nanoparticles affecting blood coagulation.* Nanomedicine-Nanotechnology Biology and Medicine, 2012. **8**(6): p. 981-986.

497. Steuer, H., R. Krastev, and N. Lembert, *Metallic oxide nanoparticles stimulate blood coagulation independent of their surface charge.* Journal of Biomedical Materials Research Part B-Applied Biomaterials, 2014. **102**(5): p. 897-902.

498. Stevens, K.N.J., et al., *The relationship between the antimicrobial effect of catheter coatings containing silver nanoparticles and the coagulation of contacting blood.* Biomaterials, 2009. **30**(22): p. 3682-3690.

499. Berger, C.T. and G. Alter, *Natural killer cells in spontaneous control of HIV infection.* Current Opinion in Hiv and Aids, 2011. **6**(3): p. 208-213.

500. Brandstadter, J.D. and Y. Yang, *Natural Killer Cell Responses to Viral Infection.* Journal of Innate Immunity, 2011. **3**(3): p. 274-279.

501. Koh, J., et al., *Susceptibility of CD24(+) ovarian cancer cells to anti-cancer drugs and natural killer cells.* Biochemical and Biophysical Research Communications, 2012. **427**(2): p. 373-378.

502. Biron, C.A., et al., *Natural killer cells in antiviral defense: Function and regulation by innate cytokines.* Annual Review of Immunology, 1999. **17**: p. 189-220.

503. Lee, C.L., et al., *Glycodelin-A modulates cytokine production of peripheral blood natural killer cells.* Fertility and Sterility, 2010. **94**(2): p. 769-771.

504. Kadowaki, N., et al., *Distinct cytokine profiles of neonatal natural killer T cells after expansion with subsets of dendritic cells.* Journal of Experimental Medicine, 2001. **193**(10): p. 1221-1226.

505. Rus, H., C. Cudrici, and F. Niculescu, *The role of the complement system in innate immunity.* Immunologic Research, 2005. **33**(2): p. 103-112.

506. Mayflyan, K.R., et al., *The complement system in innate immunity*, in *Innate Immunity of Plants, Animals, and Humans*, H. Heine, Editor. 2008, Springer-Verlag Berlin, Heidelberger Platz 3, D-14197 Berlin, Germany. p. 219-236.

507. Mosad, E., K.I. Elsayh, and A.A. Eltayeb, *Tissue Factor Pathway Inhibitor and P-Selectin as Markers of Sepsis-Induced Non-overt Disseminated Intravascular Coagulopathy.* Clinical and Applied Thrombosis-Hemostasis, 2011. **17**(1): p. 80-87.

508. Bertholon, I., C. Vauthier, and D. Labarre, *Complement activation by core-shell poly(isobutylcyanoacrylate)-polysaccharide nanoparticles: Influences of surface morphology, length, and type of polysaccharide.* Pharmaceutical Research, 2006. **23**(6): p. 1313-1323.

509. Rybak-Smith, M.J. and R.B. Sim, *Complement activation by carbon nanotubes.* Advanced Drug Delivery Reviews, 2011. **63**(12): p. 1031-1041.

510. Talaei, F., et al., *Core shell methyl methacrylate chitosan nanoparticles: In vitro mucoadhesion and complement activation.* Daru-Journal of Pharmaceutical Sciences, 2011. **19**(4): p. 257-265.

511. Malyala, P. and M. Singh, *Endotoxin limits in formulations for preclinical research.* Journal of Pharmaceutical Sciences, 2008. **97**(6): p. 2041-2044.

512. Oostingh, G.J., et al., *Problems and challenges in the development and validation of human cell-based assays to determine nanoparticle-induced immunomodulatory effects.* Particle and Fibre Toxicology, 2011. **8**: p. 21.

513. Souza, F.T.S., et al., *Comparison of the measurement of lysosomal hydrolase activity in mycoplasma-contaminated and non-contaminated human fibroblast cultures treated with mycoplasma removal agent.* Clinical Biochemistry, 2007. **40**(8): p. 521-525.

514. Romero-Rojas, A., et al., *Immunomodulatory properties of Mycoplasma pulmonis. III. Lymphocyte stimulation and cytokine production Mycoplasma pulmonis products.* International Immunopharmacology, 2001. **1**(9-10): p. 1699-1707.

515. Elsabahy, M. and K.L. Wooley, *Cytokines as biomarkers of nanoparticle immunotoxicity.* Chemical Society Reviews, 2013. **42**(12): p. 5552-5576.

516. Hussain, S., et al., *Cerium dioxide nanoparticles do not modulate the lipopolysaccharide-induced inflammatory response in human monocytes.* International Journal of Nanomedicine, 2012. **7**: p. 1387-1397.

517. Ziady, A.G., et al., *Minimal toxicity of stabilized compacted DNA nanoparticles in the murine lung.* Molecular Therapy, 2003. **8**(6): p. 948-956.

518. Villiers, C.L., et al., *Analysis of the toxicity of gold nano particles on the immune system: effect on dendritic cell functions.* Journal of Nanoparticle Research, 2010. **12**(1): p. 55-60.

519. De Jong, W.H., et al., *Systemic and immunotoxicity of silver nanoparticles in an intravenous 28 days repeated dose toxicity study in rats.* Biomaterials, 2013. **34**(33): p. 8333-8343.

520. Liptrott, N.J., et al., *Partial mitigation of gold nanoparticle interactions with human lymphocytes by surface functionalization with a 'mixed matrix'.* Nanomedicine (Lond), 2014: p. 1-13.

521. Castillo, P.M., et al., *Tiopronin monolayer-protected silver nanoparticles modulate IL-6 secretion mediated by Toll-like receptor ligands.* Nanomedicine, 2008. **3**(5): p. 627-635.

522. Qu, G., et al., *Cytotoxicity of quantum dots and graphene oxide to erythroid cells and macrophages.* Nanoscale Research Letters, 2013. **8**.

523. Scholer, N., et al., *Surfactant, but not the size of solid lipid nanoparticles (SLN) influences viability and cytokine production of macrophages.* International Journal of Pharmaceutics, 2001. **221**(1-2): p. 57-67.

524. Ufkin, M. and D. Hall, *Immunological impact on macrophages exposed to nanoparticles.* Faseb Journal, 2006. **20**(5): p. A978-A978.

525. Thornton, A.M., *Signal transduction in CD4(+)CD25(+) regulatory T cells: CD25 and IL-2.* Frontiers in Bioscience, 2006. **11**: p. 921-927.

526. Iczkowski, K.A., *Cell adhesion molecule CD44: its functional roles in prostate cancer.* American Journal of Translational Research, 2011. **3**(1): p. 1-7.

527. Lindsey, W.B., et al., *CD69 expression as an index of T-cell function: assay standardization, validation and use in monitoring immune recovery.* Cytotherapy, 2007. **9**(2): p. 123-132.

528. Ciusani, E., et al., *Fas/CD95-mediated apoptosis in human glioblastoma cells: a target for sensitisation to topoisomerase I inhibitors.* Biochemical Pharmacology, 2002. **63**(5): p. 881-887.

529. Schildberger, A., et al., *Monocytes, Peripheral Blood Mononuclear Cells, and THP-1 Cells Exhibit Different Cytokine Expression Patterns following Stimulation with Lipopolysaccharide.* Mediators of Inflammation, 2013.

530. Schildberger, A., et al., *Monocytes, Peripheral Blood Mononuclear Cells, and THP-1 Cells Exhibit Different Cytokine Expression Patterns following Stimulation with Lipopolysaccharide.* Mediators of Inflammation, 2013: p. 10.

531. Chatterjee, K., et al., *Contributions of contact activation pathways of coagulation factor XII in plasma.* Journal of Biomedical Materials Research Part A, 2009. **90A**(1): p. 27-34.

532. Chu, A.J., *Tissue factor, blood coagulation, and beyond: an overview.* International journal of inflammation, 2011. **2011**: p. 367284-367284.

533. Mehmedagic, A., et al., *In vitro modeling of the influence of FVIII activity and heparin induced prolongation of APTT.* Bosnian journal of basic medical sciences / Udruzenje basicnih mediciniskih znanosti = Association of Basic Medical Sciences, 2005. **5**(3): p. 26-9.

534. ten Cate, H. and A. Falanga, *Overview of the postulated mechanisms linking cancer and thrombosis.* Pathophysiology of haemostasis and thrombosis, 2008. **36**(3-4): p. 122-30.

535. Ahmed, M., et al., *Potential of nanoemulsions for intravenous delivery of rifampicin.* Pharmazie, 2008. **63**(11): p. 806-811.

536. Madhusudhan, B., et al., *1-O-alkylglycerol stabilized carbamazepine intravenous o/w nanoemulsions for drug targeting in mice.* Journal of Drug Targeting, 2007. **15**(2): p. 154-161.

537. Mueller, R.H., D. Harden, and C.M. Keck, *Development of industrially feasible concentrated 30% and 40% nanoemulsions for intravenous drug delivery.* Drug Development and Industrial Pharmacy, 2012. **38**(4): p. 420-430.

538. Gradishar, W.J., et al., *Phase III trial of nanoparticle albumin-bound paclitaxel compared with polyethylated castor oil-based paclitaxel in women with breast cancer.* Journal of Clinical Oncology, 2005. **23**(31): p. 7794-7803.

539. Janero, D.R., *The future of drug discovery: enabling technologies for enhancing lead characterization and profiling therapeutic potential.* Expert Opinion on Drug Discovery, 2014. **9**(8): p. 847-858.

540. Etheridge, M.L., et al., *The big picture on nanomedicine: the state of investigational and approved nanomedicine products.* Nanomedicine-Nanotechnology Biology and Medicine, 2013. **9**(1): p. 1-14.

541. Juliano, R.L., *The future of nanomedicine: Promises and limitations.* Science and Public Policy, 2012. **39**(1): p. 99-104.

542. Nel, A., et al., *Nanomedicine and the fight against HIV/AIDS.* Nanomedicine, 2014. **9**(2): p. 193-206.

543. Silber, B.M., *Driving Drug Discovery: The Fundamental Role of Academic Labs.* Science Translational Medicine, 2010. **2**(30): p. 6.

544. Phatak, S.S., C.C. Stephan, and C.N. Cavasotto, *High-throughput and in silico screenings in drug discovery.* Expert Opinion on Drug Discovery, 2009. **4**(9): p. 947-959.

545. Hirn, S., et al., *Particle size-dependent and surface charge-dependent biodistribution of gold nanoparticles after intravenous administration.* European Journal of Pharmaceutics and Biopharmaceutics, 2011. **77**(3): p. 407-416.

546. Schaedlich, A., et al., *Tumor Accumulation of NIR Fluorescent PEG PLA Nanoparticles: Impact of Particle Size and Human Xenograft Tumor Model.* Acs Nano, 2011. **5**(11): p. 8710-8720.

547. McClements, D.J., *Nanoemulsions versus microemulsions: terminology, differences, and similarities.* Soft Matter, 2012. **8**(6): p. 1719-1729.

548. Braun, A., et al., *Validation of dynamic light scattering and centrifugal liquid sedimentation methods for nanoparticle characterisation.* Advanced Powder Technology, 2011. **22**(6): p. 766-770.

549. Hagendorfer, H., et al., *Characterization of Silver Nanoparticle Products Using Asymmetric Flow Field Flow Fractionation with a Multidetector Approach - a Comparison to Transmission Electron Microscopy and Batch Dynamic Light Scattering.* Analytical Chemistry, 2012. **84**(6): p. 2678-2685.

550. Hagendorfer, H., et al., *Application of an asymmetric flow field flow fractionation multi-detector approach for metallic engineered nanoparticle characterization - Prospects and limitations demonstrated on Au nanoparticles.* Analytica Chimica Acta, 2011. **706**(2): p. 367-378.

551. Taurozzi, J.S., V.A. Hackley, and M.R. Wiesner, *A standardised approach for the dispersion of titanium dioxide nanoparticles in biological media.* Nanotoxicology, 2013. **7**(4): p. 389-401.

552. Liu, S.Y., et al., *Toxicology studies of a superparamagnetic iron oxide nanoparticle in vivo*, in *Multi-Functional Materials and Structures, Pts 1 and 2*, A.K.T. Lau, et al., Editors. 2008, Trans Tech Publications Ltd: Stafa-Zurich. p. 1097-1100.

553. Rytting, E., et al., *In vitro and in vivo performance of biocompatible negatively-charged salbutamol-loaded nanoparticles.* Journal of Controlled Release, 2010. **141**(1): p. 101-107.

554. Choi, A.Y., et al., *Pharmacokinetic Characteristics of Capsaicin-Loaded Nanoemulsions Fabricated with Alginate and Chitosan.* Journal of Agricultural and Food Chemistry, 2013. **61**(9): p. 2096-2102.

555. Li, X., et al., *Nanoemulsions coated with alginate/chitosan as oral insulin delivery systems: preparation, characterization, and hypoglycemic effect in rats.* International Journal of Nanomedicine, 2013. **8**: p. 23-32.

556. Sun, D., et al., *Enhanced oral absorption and therapeutic effect of acetylpuerarin based on D-alpha-tocopheryl polyethylene glycol 1000 succinate nanoemulsions.* International Journal of Nanomedicine, 2014. **9**: p. 3413-3423.

557. Food and H.H.S. Drug Administration, *Amendment to the current good manufacturing practice regulations for finished pharmaceuticals. Direct final rule.* Federal register, 2007. **72**(232): p. 68064-70.

558. Shegokar, R., K.K. Singh, and R.H. Muller, *Production & stability of stavudine solid lipid nanoparticles-From lab to industrial scale.* International Journal of Pharmaceutics, 2011. **416**(2): p. 461-470.

559. Laouini, A., et al., *Preparation of liposomes: A novel application of microengineered membranes-From laboratory scale to large scale.* Colloids and Surfaces B-Biointerfaces, 2013. **112**: p. 272-278.

560. Galindo-Rodriguez, S.A., et al., *Comparative scale-up of three methods for producing ibuprofen-loaded nanoparticles.* European Journal of Pharmaceutical Sciences, 2005. **25**(4-5): p. 357-367.

561. Fuloria, N.K., S. Fuloria, and S. Vakiloddin, *Phase zero trials: a novel approach in drug development process.* Renal Failure, 2013. **35**(7): p. 1044-1053.

562. Libutti, S.K., et al., *Phase I and Pharmacokinetic Studies of CYT-6091, a Novel PEGylated Colloidal Gold-rhTNF Nanomedicine.* Clinical Cancer Research, 2010. **16**(24): p. 6139-6149.

563. Picat, M.Q., et al., *Phase 0 exploratory clinical trials: literature review 2006-2009.* Bulletin Du Cancer, 2011. **98**(7): p. 753-759.

564. Kummar, S., et al., *Phase 0 clinical trials: Conceptions and misconceptions.* Cancer Journal, 2008. **14**(3): p. 133-137.

565. Murgo, A.J., et al., *Designing phase 0 cancer clinical trials.* Clinical Cancer Research, 2008. **14**(12): p. 3675-3682.

566. Pellegatti, M., *Preclinical in vivo ADME studies in drug development: a critical review.* Expert Opinion on Drug Metabolism & Toxicology, 2012. **8**(2): p. 161-172.

567. Bapsy, P.P., et al., *Phase 1 study to determine tolerability and pharmacokinetics (PK) of D0/NDR/02, a novel nanoparticle paclitaxel in patients with locally advanced or metastatic breast cancer (MBC).* Ejc Supplements, 2005. **3**(2): p. 433-433.

568. Hamaguchi, T., et al., *Phase I Study of NK012, a Novel SN-38-Incorporating Micellar Nanoparticle, in Adult Patients with Solid Tumors.* Clinical Cancer Research, 2010. **16**(20): p. 5058-5066.

569. McKiernan, J.M., et al., *A Phase I Trial of Intravesical Nanoparticle Albumin-Bound Paclitaxel in the Treatment of Bacillus Calmette-Guerin Refractory Nonmuscle Invasive Bladder Cancer.* Journal of Urology, 2011. **186**(2): p. 448-451.

570. Hedgire, S., S. McDermott, and M. Harisinghani, *Nanoparticles in Clinical Trials*, in *Nanomedicine - Basic and Clinical Applications in Diagnostics and Therapy*, C. Alexiou, Editor. 2011, Karger: Basel. p. 96-105.

571. Lettani, D. and T.J. DiFeo, *The European Clinical Trials Directive - A regulatory approach for filing drug substance information.* Drug Development and Industrial Pharmacy, 2005. **31**(8): p. 709-718.

572. Deshayes, S., et al., *"Click" Conjugation of Peptide on the Surface of Polymeric Nanoparticles for Targeting Tumor Angiogenesis.* Pharmaceutical Research, 2011. **28**(7): p. 1631-1642.

573. Dinauer, N., et al., *Selective targeting of antibody-conjugated nanoparticles to leukemic cells and primary T-lymphocytes.* Biomaterials, 2005. **26**(29): p. 5898-5906.

574. Jin, C., et al., *Paclitaxel-loaded nanoparticles decorated with anti-CD133 antibody: a targeted therapy for liver cancer stem cells.* Journal of Nanoparticle Research, 2013. **16**(1).

575. Manoochehri, S., et al., *Surface modification of PLGA nanoparticles via human serum albumin conjugation for controlled delivery of docetaxel.* Daru-Journal of Pharmaceutical Sciences, 2013. **21**.

576. Sun, W.Q., et al., *Specific role of polysorbate 80 coating on the targeting of nanoparticles to the brain.* Biomaterials, 2004. **25**(15): p. 3065-3071.

577. Briske-Anderson, M.J., J.W. Finley, and S.M. Newman, *The Influence of Culture Time and Passage Number on the Morphological and Physiological Development of Caco-2 Cells.* Experimental Biology and Medicine, 1997. **214**(3): p. 248-257.

578. Sambuy, Y., et al., *The Caco-2 cell line as a model of the intestinal barrier: influence of cell and culture-related factors on Caco-2 cell functional characteristics.* Cell Biology and Toxicology, 2005. **21**(1): p. 1-26.

579. Eglen, R. and T. Reisine, *Primary Cells and Stem Cells in Drug Discovery: Emerging Tools for High-Throughput Screening.* Assay and Drug Development Technologies, 2011. **9**(2): p. 108-124.

580. Goldbard, S., *Bringing primary cells to mainstream drug development and drug testing.* Current Opinion in Drug Discovery & Development, 2006. **9**(1): p. 110-116.